Contrasting Effects of Overexpressing the Neurotrophin Receptors TrkA and TrkB During Development

Laura Eve Cassels

A thesis submitted to Cardiff University in accordance with the requirements for the degree of Doctor of Philosophy in the discipline of Neuroscience

School of Biosciences, Cardiff University

December 2018

In memory of John, Pat and Gil.

Declaration

This work has not been submitted in substance for any other degree or award at this or any other university or place of learning, nor is being submitted concurrently in candidature for any degree or other award.

Signed .... Date ....

STATEMENT 1

This thesis is being submitted in partial fulfilment of the requirements for the degree of PhD.

Signed .... Date ....

STATEMENT 2

This thesis is the result of my own independent work/investigation, except where otherwise stated, and the thesis has not been edited by a third party beyond what is permitted by Cardiff University's Policy on the Use of Third Party Editors by Research Degree Students. Other sources are acknowledged by explicit references. The views expressed are my own.

Signed .... Date ....

STATEMENT 3

I hereby give consent for my thesis, if accepted, to be available online in the University's Open Access repository and for inter-library loan, and for the title and summary to be made available to outside organisations.

Signed .... Date ....

Acknowledgements

I would like to firstly thank my supervisor, Professor Yves Barde, for the immeasurable advice, interesting anecdotes, and for the opportunity to work in such a diverse and exciting lab. I also am grateful to Dr. Xinsheng Nan for his technical guidance, and most crucially for generating the TrkA animals, with the corresponding TrkB constructs. Thank you to Dr. Hayley Dingsdale, not just for being a wonderful friend and human, but also for the useful advice and support with writing this thesis. Additional thanks to Dr. Isabel Martinez-Garay and Dr. Stephane Baudouin for their feedback, and general words of wisdom over the past few years.

Thanks also to Professor Alun Davies, Dr. Sean Wyatt, Dr. Laura Howard, and Dr. Anthony Horton for providing their expertise and knowledge on the neurotrophins, dissections, and iDISCO. I am especially grateful to Derek Scarborough of the Cardiff University Bioimaging Hub, for completing the H&E stains on such an industrial scale. Likewise, this work would not have been possible without the generous funding and support of the Wellcome Trust.

I am extremely appreciative of having such a wonderful, supportive lab family; Pedro, Katharina, Kate, Spyros, Jess, Shireene, Natalia, Ellen, Erin, Sylvia and Sarah. Thank you for all of the laughter, and for making the rubbish moments less rubbish. I am also so grateful to my friends, particularly; Katy, James, and Lucy for their words of encouragement and being so patient. I am furthermore blessed to have a large family of incredible people, Mum and Dad Cassels, and the rest of the Cassels, Baker, Reynolds and Regin clans. It is not possible to thank you all individually for what you have done, but please know you are cherished.

Finally, I have to thank my four best friends; Mum, Dad, my sister Aimie, and the love of my life, Jamie. I have re-written this section so many times, but the truth is that words cannot convey how grateful I am for all of your support and unconditional love. Thank you for the cuddles, pep-talks, belly-bursting laughter, and adventures. Thank you for teaching me everything I know, for sharing the burden, for believing in me, and for helping me reach this point. I am just constantly in awe of how inspiring you each are, and am so, so proud of you all.

Abstract

Neurotrophins and their cognate receptors are part of an important signalling system in the vertebrate nervous system. This includes the control of cell survival during the development of the peripheral nervous system. Whilst the neurotrophins and their respective tyrosine kinase receptors are closely related in structure, unexpected differences have begun to appear with regard to their function. In particular, the tropomyosin receptor kinase A (TrkA) has been reported to cause the death of neurons in the absence of its neurotrophin ligand, nerve growth factor (NGF). By contrast, there have been no indications as of yet that the expression of the closely related brain-derived neurotrophic factor (BDNF) and neurotrophin-4 (NT4) receptor TrkB induces the death of neurons during development. A better understanding of the function of these receptors has important implications as unlike TrkA in the peripheral nervous system, TrkB is widely expressed in the central nervous system where BDNF does not seem to play a significant role as a survival factor. To further explore the role of these receptors, novel *in vitro* and *in vivo* models were generated that allowed the conditional overexpression of TrkA and TrkB. It was found that the ubiquitous overexpression of TrkA from the earliest stages of mouse gestation led to a perinatal death phenotype, whilst mice overexpressing TrkB were viable and fertile. Detailed histological examination indicated that the overexpression of TrkA led to the loss of neurons known to depend on NGF for their survival during development. Indeed TrkA-overexpressing mice phenocopy mutants lacking both *Ngf* alleles. By contrast, the postnatal survival of TrkB-overexpressing mice was unimpaired, despite a loss of cranial sensory neurons approaching what has been reported for mice lacking the genes encoding BDNF and NT4. Potential explanations for these surprising observations are discussed.

Abbreviations

°C	Degrees celcius
3D	Three-dimensional
5FdU	5-flouro2'-deoxyuridin
Akt	Protein kinase B
ANOVA	Analysis of variance
APAF-1	Apoptotic protease activating factor-1
APP	Amyloid precursor protein
Ara-C	Cytosine arabinoside
ASPA	Animals (Scientific Procedures) Act 1986
ATP	Adenosine triphosphate
Bad	B-cell lymphoma 2-associated death promoter
Bak	B-cell lymphoma 2 homologous antagonist/killer
Bax	B-cell lymphoma 2-associated X protein
Bcl-2	B-cell lymphoma 2
Bcl-XL	B-cell lymphoma-extra large
BDNF	Brain-derived neurotrophic factor
Bdnf$^{-/-}$	Brain-derived neurotrophic factor knockout mouse
BH3	B-cell lymphoma 2 homology domain 3
Bid	B-cell lymphoma 2 homology 3 interacting-domain death agonist
Bik	B-cell lymphoma 2-interacting killer
BLBP	Brain lipid binding protein
bp	Base pair
BSA	Bovine serum albumin
C. elegans	*Caenorhabditis elegans*
C1/C2	Cysteine-rich clusters
CA	Cellular aggregate
CaCl$_2$	Calcium chloride
Cas9	CRISPR associated protein 9
Caspase	Cysteine-aspartic proteases
CED-3	Cell death abnormal-3

CED-4	Cell death abnormal-4
CED-9	Cell-death abnormal-9
ChAT	Choline acetyltransferase
CMV	Cytomegalovirus
CNS	Central nervous system
CO_2	Carbon dioxide
CR1-4	Cysteine rich domains
Cre	Calcium responsive element
CreER^{T2}	Cre recombinase fused with triple mutated oestrogen receptor
CRISPR	Clustered regularly interspaced short palindromic repeats
D	Day
D. melanogaster	*Drosophila melanogaster*
DAPI	4',6-diamidino-2-phenylindole
DBE	Dibenzyl ether
DCC	Deleted in colorectal cancer gene
DCM	Dichloromethane
ddH_2O	Double-distilled water
DFF40/CAD	DNA fragmentation factor-45/inhibitor of caspase-activated deoxyribonuclease
DFF45/ICAD	DNA fragmentation factor-40/caspase-activated DNase
DIC	Differential interference contrast
DIV	Days in vitro (neuronal)
DMEM	Dulbecco modified eagle medium
DMEM-F12	Dulbecco's modified eagle medium: nutrient mixture F-12
DMSO	Dimethyl sulfoxide
DNA	Deoxyribonucleic acid
DNase	Deoxyribonuclease
dNTPs	Deoxynucleotide triphosphates
DRG	Dorsal root ganglion
DTT	Dithiothreitol
E	Embryonic Day
E. coli	*Escherichia coli*
EB buffer	Elution buffer

EDTA	Ethylenediaminetetraacetic acid
EGFP	Enhanced green fluorescent protein
EGL-1	Egg-laying defective-1
EpiSCs	Epiblast stem cells
ER	Estrogen receptor
ERK 1-2	Extracellular signal related kinases 1 and 2
ES Media	Embryonic stem cell media
ESCs	Embryonic stem cells
FBS	Fetal bovine serum
g	Gram
GABA	Gamma-aminobutyric acid
GAPDH	Glyceraldehyde 3-phosphate dehydrogenase
GFAP	Glial fibrillary acid protein
GFP	Green fluorescent protein
GSK-3	Glycogen synthase kinase-3
H_2O_2	Hydrogen peroxide
HA	Hemagglutinin
HCl	Hydrochloric acid
HEK293T	Human embryonic kidney 283
H3K9ac	Histone H3 lysine 9 acetylation
Hsp90	Heat-shock protein 90
HTNC	Cell permeable cre
iDISCO	Immunolabelling-enabled three-dimensional imaging of solvent-cleared organs
Igl 1-2	Immunoglobulin-like domain 1-2
IRES	Internal ribosome entry site
Kb	Kilobase
KCl	Potassium chloride
Kd	Dissociation constant
kDa	Kilodaltons
LDS	Lithium dodecyl sulfate
LIF	Leukemia inhibitory factor
LRR1-3	Leucine-rich repeat 1-3

M	Molar
M	Mean
MAPK	Mitogen-activated protein kinases
Mapt	Microtubule associated protein gene
MEFs	Mouse embryonic fibroblasts
MEK	Mitogen-activated protein kinase kinase
MeOH	Methanol
MES	2-(N-morpholino)ethanesulfonic acid
μg	Microgram
μL	Microliter
μM	Micromolar
μm	Micrometer
mg	Milligram
min.	Minutes
mL	Milliliter
mm	Millimeter
mM	Millimolar
MOMP	Mitochrondrial outer membrane permeabilisation
mRNA	Messenger ribonucleic acid
N	Number of samples
NaCl	Sodium chloride
NaOAc	Sodium acetate
NEAA	Non-essential amino acids
Ng	Nanogram
NGF	Nerve growth factor
Ngf$^{-/-}$	Nerve growth factor knockout mouse
NLS	Nuclear localisation signal
nm	Nanometer
NPG	Nodose-petrosal ganglia
NS	Not-significant
NT3	Neurotrophin 3
NT4	Neurotrophin 4
Ntf3$^{-/-}$	Neurotrophin 3 knockout mouse

Ntf4^{-/-}	Neurotrophin 4 knockout mouse
O.C.T.	Optimum cutting temperature
ORF	Open reading frame
P	Postnatal day
p	Probability value
p75^{NTR}	p75 neurotrophin receptor
PAM	Protospacer adjacent motif
PBS	Phosphate-buffered saline
PBST	Phosphate-buffered saline with 0.1% Triton X-100
PBST-S	Phosphate-buffered saline with 0.1% Triton X-100 + 10% donkey serum
pc	*post coitum*
PCD	Programmed cell death
PCR	Polymerase chain reaction
Pen-strep	Penicillin-streptomycin
PFA	Paraformaldehyde
PI3K	Phosphoinositide 3-kinase
PLCγ	Phospholipase C gamma
PNS	Peripheral nervous system
PORN	Poly-DL-ornithine hydrobromide
PrP	Prion protein fragment
PtWH	Heparin solution
RA	Retinoic acid
rcf	Relative centrifugal force
RNA	Ribonucleic acid
RT	Room temperature
S.O.C Media	Super optimal broth with catabolite repression
SCG	Superior cervical ganglia
SD	Standard deviation
SDS	Sodium dodecyl sulfate
sgRNA	Single-guide ribonucleic acid
Shc	Src homologous and collagen-like
s-p75^{NTR}	Short p75^{NTR}

TAE	Tris-acetate-EDTA buffer
Tamoxifen	4-hydroxytamoxifen
TE buffer	Tris-EDTA buffer
TG	Trigeminal ganglia
TGFβ	Transforming growth factor beta
THF	Tetrahydrofuran
TK	Tyrosine kinase
TNF	Tumour necrosis factor
TRAF	Tumour necrosis factor receptor-associated factor
Trk	Tropomyosin receptor kinase
TrkA$^{-/-}$	Tropomyosin receptor kinase A knockout mouse
TrkB.T1	Truncated TrkB T1
TrkB.T2	Truncated TrkB T2
TrkB$^{-/-}$	Tropomyosin receptor kinase B knockout mouse
TrkC$^{-/-}$	Tropomyosin receptor kinase C knockout mouse
TrkC-KF	TrkC killer fragment
TTX	Tetrodotoxin
TX	Triton X-100
UNC5H	Uncoordinated-5 homolog gene
UTR	Untranslated region
V	Volts
VG	Vestibular ganglia
vs.	*Versus*
WT	Wild type
Xm	Maternal X chromosome
Xp	Paternal X chromosome
ZFN	Zinc finger nuclease
zVAD-fmk	Carbobenzoxy-valyl-alanyl-aspartyl-[O-methyl]-flouromethylketone

Table of Contents

List of Figures

List of Tables

1. Introduction

Neurons are the core unit of the nervous system and as a result, their number impacts the output of the brain, spinal cord and peripheral nerves. For this reason, the number of neurons needs to be tightly controlled to maintain appropriate functionality of the nervous system (Dekkers et al., 2013). In vertebrates, the number of neurons is, in part, regulated by the availability of growth factors that prevent cell death. The best characterised family of such growth factors comprises the neurotrophins, a small family of four related genes (Dekkers et al., 2013). Whilst it has long been established that neurotrophins exert their pro-survival effects by interactions with tropomyosin receptor kinases (Trk), it was only recently that the Trk receptors had been found to have an additional role in determining the fate of neurons by actively inducing cell death in the absence of their neurotrophic ligands (Nikoletopoulou et al., 2010). As very little is known about the biological functions of the Trk receptors in the absence of their ligands, the main objective of this thesis was to test possible functions of these receptors in development by expressing them from the earliest stages of embryogenesis (before significant ligand expression), at times and in tissues where the receptor is not normally expressed.

1.1. Cell death

1.1.1. Cell death in development

During development, entire organisms are generated from a single fertilised oocyte. To achieve this, there is a rapid proliferation of cells, leading to growth and expansion of the organism. However strict regulation of the number of cells is essential for proper development and thus proliferation is balanced with developmental cell death (Vaux and Korsmeyer, 1999). The first recording of developmental cell death is attributed to Carl Vogt in 1842 when he noted the "destruction of embryonic cells" during development of the notochord in toads (Zakeri and Lockshin, 2008). Cell death was later characterised as being a highly conserved process present in all Metazoans (Bender et al., 2012; Cikala et al., 1999). In 1964 Lockshin and Williams noted that the death of muscles in American silk moths followed a biological plan which they

termed programmed cell death (PCD; also referred to as apoptosis) (Lockshin and Williams, 1964). These apoptotic cells resembled each other in that they demonstrated DNA fragmentation, shrinkage of the cell, chromatin condensation and zeiosis (rapid bleb formation that gives the cell an appearance of boiling) (Kerr et al., 1972). In contrast, cells that had encountered stress or injury, such as mechanical stress or heat, had different death characteristics; the plasma membranes ruptured and led to inflammation of surrounding tissues (Sun and Wang, 2014). Indeed, it is now established that these observed differences are due to the fact that there are three different types of cell death in the developing embryo; necrosis as a response to injury, apoptosis as a developmental programme, and autophagocytosis, a catabolic process that results in removal of cell organelles (Doherty and Baehrecke, 2018). However, what has been lacking for a long time was a mechanistic understanding of PCD until the results of studies with the nematode worm, *Caenorhabditis elegans (C. elegans),* revolutionised the field of cell death.

1.1.2. *C. elegans* as a model of apoptosis

C. elegans was introduced as a model organism by Nobel prize winner Sydney Brenner to allow study of a simple nervous system, and used to great effect by co-laureates John Sulston and Robert Horvitz to advance the understanding of the mechanisms of apoptosis (Nobel Media Ab, 2018a). The *C. elegans*, comprised of only 1090 cells, has a short generation time (3.5 days) that makes it ideally suited for genetic studies. Furthermore its transparency made it possible to directly observe cell division utilising differential interference contrast (DIC) microscopy (Sulston et al., 1983). Utilising this method, Sulston was able to map the cell lineage of the *C. elegans* from fertilisation up to the adult organism, and noted that the cells followed a remarkably predictable programme of division and differentiation (Sulston et al., 1983), with 113 cells always being eliminated during development, and the same 18 cells being eliminated post-embryonically (Sulston et al., 1983). The fact that cell fate could be mapped so precisely indicated that the process of apoptosis was intrinsically determined, i.e. cell autonomous (Sulston and White, 1980). The *C. elegans* could also be genetically modified to test fundamental questions about development that were more time consuming, expensive and complex in larger organisms (Brenner, 1974).

In a continuation of the work initiated by Brenner (Brenner, 1974), Horvitz began to define several of the key apoptotic genes in *C. elegans* that were later found to have homologs in mammals (Conradt and Horvitz, 1998; Hengartner and Horvitz, 1994; Trent et al., 1983; Yuan et al., 1993). The key observation, that the identified genes were active within the dying cells themselves, led to the notion that cell death is part of a "cell-suicide" mechanism. In other words, that cells activate an intrinsic cell death programme which leads to their elimination (Yuan and Horvitz, 1990).

1.1.3. Genetic regulators of apoptosis

The key genes involved in apoptosis in *C. elegans*, identified by Robert Horvitz, were identified as: *egg-laying defective-1 (egl-1), cell-death abnormal-9 (ced-9), ced-4* and *ced-3* (Hengartner and Horvitz, 1994; Trent et al., 1983; Yuan et al., 1993). It was revealed that these genes encode proteins that interact with each other to regulate apoptosis (Figure 1.1), and have homologs in mammals that interact in a similar manner.

The *Ced-9* mammalian homolog is B cell lymphoma 2 (*Bcl-2*) (Hengartner and Horvitz, 1994), an intracellular protein that was originally discovered due to its role as a proto-oncogene in human follicular lymphoma (Bakhshi et al., 1985; Tsujimoto et al., 1985). Mutations to *ced-9* led to embryonic lethality of the *C. elegans* larvae, and it was discovered that CED-9 protein, or BCL-2 in mammals, actually act in an anti-apoptotic manner, protecting cells from cell death (Hengartner et al., 1992; Vaux et al., 1988). Due to sequence similarities in BCL-2 homology (BH) domains (BH1-4), fourteen other BCL-2 family members have been identified in mammals, all of which are located in the outer membrane of the mitochondria (Adams and Cory, 2001). The BCL-2 family can be subdivided based on whether they are anti- or pro-apoptotic. Anti-apoptotic BCL-2 family members such as BCL-2, and BCL-XL, which contain BH domains 1-4, act to prevent cell death (Adams and Cory, 2001). BCL-2 pro-apoptotic family members are further divided depending on presence or absence of particular BH domains. For example, BAX and BAK contain BH1-3, while BH3-only pro-apoptotic proteins include BIK, BID and BAD (Chittenden et al., 1995; Korsmeyer, 1999). Similarly, *Egl-1* in *C. elegans* was found to be pro-apoptotic, and have homology with the mammalian BH3 domain, indicating that it may act in a

similar way to BIK and BAD (Conradt and Horvitz, 1998; Del Peso et al., 1998). Interactions of the pro- and anti-apoptotic BCL-2 family members (such as BCL-2 and BAX) determines the sensitivity of a cell to apoptosis by modulating mitochondrial outer membrane permeabilisation (MOMP), resulting in the release of a normally sequestered protein called cytochrome c from the mitochondrial membrane (Kluck et al., 1997; Narita et al., 1998; Yang et al., 1997) (Figure 1.1).

Finally the mammalian *ced-4* homolog was identified as apoptotic protease activating factor-1 (*Apaf-1*) (Liu et al., 1996; Zou et al., 1997), and *ced-3* as homologous to cysteine-aspartic protease (caspase)-3 (Xue et al., 1996; Yuan et al., 1993). The caspases are a family of fourteen cysteine proteases that cleave at specific aspartic acid residues (Cohen, 1997; Howard et al., 1991). They are ubiquitously expressed zymogens, inactive enzymes that first require cleavage themselves to be active, and upon activation they initiate a protease cascade that amplifies the apoptotic signal which leads to rapid cell death (Hengartner, 2000). The caspase family is separated into three groups of enzymes; 1) initiator caspases (caspase-2, -8, -9 and -10) that bind to adaptor molecules that promote further caspase-activation, 2) executioner caspases (caspase-3, -6 and -7) that activate various proteases and nucleases that leads to the breakdown of the cell, and 3) the inflammatory caspases (caspase-1, -4, -5, -11, and -12) that inhibit pyroptosis during infection and stress (McIlwain et al., 2013). In *C. elegans,* CED-4 activates CED-3 processing to induce apoptosis (Seshagiri and Miller, 1997), however in mammals, the situation is a little more complex. In mammals, the CED-4 homolog APAF-1 binds released cytochrome c (Figure 1.1), and undergoes a conformational change to recruit caspase-9, forming a multimeric complex called the apoptosome. Upon recruitment to the apoptosome caspase-9 is autocatalytically cleaved to its active form (Li et al., 1997; Saleh et al., 1999; Zou et al., 1999). This in turn leads to activation by cleavage of the zymogen executioner caspases that ultimately result in apoptosis, such as caspase-3 or caspase-7. Caspase-3 and -7 are thought to initiate apoptosis by cleaving cellular substrates that lead to apoptosis. For example, active caspase-3 and -7 induces DNA fragmentation through proteolytic inactivation of DNA fragmentation factor-45/inhibitor of caspase-activated deoxyribonuclease (DFF45/ICAD) which normally inhibits the endonuclease DNA fragmentation factor-40/caspase-activated DNase (DFF40/CAD). Upon unbinding of DFF45/ICAD and DFF40/CAD, the endonuclease can cleave DNA, leading to

fragmentation (Enari et al., 1998; Liu et al., 1998; Liu, Zou, et al., 1997; Sakahira et al., 1998; Wolf et al., 1999). Similarly, caspase-3 can cleave gelsolin, an actin binding protein, which results in membrane blebbing and nuclear fragmentation (Kothakota et al., 1997).
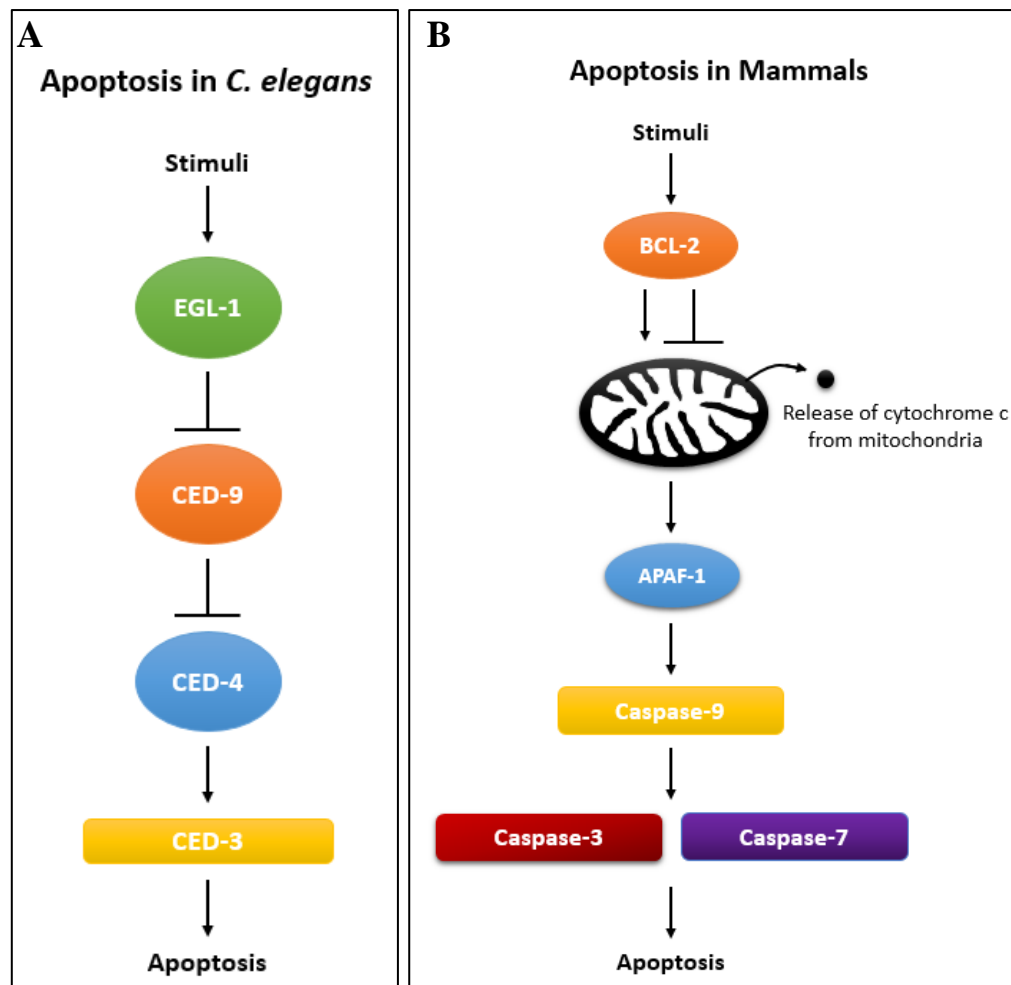
Figure 1.1 Comparison of apoptotic pathways in *C. elegans* and mammals.
A) In the *C. elegans,* EGL-1 (green) is pro-apoptotic, and inhibits anti-apoptotic CED-9 (orange) which results in CED-4 (blue) activating CED-3 (yellow). CED-3 is then able to induce apoptosis. B) In mammals the CED-9 homolog BCL-2 (orange) modulates the mitochondrial outer membrane permeability by interacting with related proteins. Under normal conditions BCL-2 is anti-apoptotic, but upon pro-apoptotic stimuli BCL-2 is inhibited and cytochrome c can be released from the mitochondria (black). Cytochrome c binds to the CED-4 homolog APAF-1 (blue), resulting in conformational changes that lead to recruitment and activation of the CED-3 homolog caspase-9 (yellow) in the apoptosome. In turn the apoptosome activates the executioner caspases, caspase-3 (red) and caspase-7 (purple) to induce apoptosis.

1.1.4. The role of apoptosis in the mammalian nervous system

The fact that 80% of apoptotic cells in the *C. elegans* were neurons quantitatively illustrates the significance of cell death in regulating the development of the nervous system. Remarkably however, inhibiting apoptosis in the *C. elegans* did not cause any overt phenotype in terms of lifespan or behaviour (Ellis, 1986). By contrast, in larger organisms including the *Drosophila melanogaster (D. melanogaster)* (White et al., 1994) and the mouse (Kuida et al., 1996), ablation of apoptosis turned out to be lethal embryonically. This suggests that the dependence of an organism on apoptosis increases with the size, and complexity of the nervous system. This was supported by the observation that, in addition to the intrinsic apoptotic pathway outlined in section 1.1.3 , mammals have evolved an additional, extrinsic pathway of apoptosis that is not found in the *C. elegans* (Aravind et al. 2001*,* see review (Flusberg and Sorger, 2015)). The observation that around half of newly generated neurons are eliminated during mammalian development, led to the hypothesis that there is an initial overabundance of neurons as a mechanism to ensure that distal target tissues are appropriately innervated (Oppenheim, 1991). Indeed, this was not a really novel thought, as it had already been suggested in the early 1900s that the number of peripheral nervous system (PNS) neurons was regulated by the size of peripheral tissues (Shorey, 1909). However the question remained as to how the superfluous neurons were triggered to undergo apoptosis.

1.2. Neurotrophins

1.2.1. Discovery of the neurotrophins

The discovery of never growth factor (NGF) by Rita Levi-Montalcini and Stanley Cohen led to the first mechanistic explanation as to how neuronal number could be regulated by the size of the target to be innervated. Their work, which in 1986 led to them being awarded the Nobel Prize in Physiology and Medicine (Nobel Media Ab, 2018b), began with delicate manipulations of chick embryos. The transplantation of mouse sarcoma 180 into the body wall of chick embryos by Elmer Bueker led to the unexpected observation of substantial innervation by sensory and sympathetic nerves into the transplanted tumour (Bueker, 1948), more so than could be observed by transplantation of homologous tissues from the chick (Levi-Montalcini and Hamburger, 1951). On the other hand, removal of developing chick limb buds resulted in a reduction of the number of motor and sensory neurons in the spinal cord and dorsal root ganglia, respectively (Hamburger, 1934; Hamburger and Levi-Montalcini, 1949). The observation that the hyper-innervated transplants were, in some cases, remotely located from the innervating neurons led to the hypothesis that the sarcoma cells may secrete a diffusible agent. This was confirmed through the use of an *in vitro* culture of chick sensory and sympathetic ganglia supplemented with mouse sarcoma 180, or mouse sarcoma 37 extracts, which showed a significant increase in axonal outgrowth (Cohen et al., 1954; Levi-Montalcini et al., 1954). Ultimately the factor, named NGF, was isolated (Cohen, 1960; Cohen et al., 1954; Levi-Montalcini and Cohen, 1956), and an antiserum was developed against the protein. Daily injections of this antiserum into newborn mice led to massive loss of sympathetic neurons such as those in the superior cervical ganglia (SCG) (Cohen, 1960; Levi-Montalcini et al., 1969; Levi-Montalcini and Cohen, 1960). The discovery of NGF supported the idea that excess neurons are generated during development to ensure adequate innervation of the target tissue, and that the presence of a limited amount of the diffusible factor is a mechanism by which to control the number of surviving neurons; cells that would not come into contact with NGF would undergo intrinsically programmed apoptosis (Raff, 1992).

NGFs effects on survival of PNS sensory neurons sparked a concentrated effort to find a comparable growth factor in the central nervous system (CNS) that would support

the growth and survival of developing neurons. This led to the discovery of brain-derived neurotrophic factor (BDNF) in 1982, initially isolated from pig brains (Barde et al., 1982). Analysis of the sequence similarities between NGF and BDNF revealed substantial comparative sequences (Leibrock et al., 1989), that led to the thought that NGF and BDNF were part of a larger gene family, now called the neurotrophins. By generating polymerase chain reaction (PCR) primers against the homologous sequences, two additional neurotrophins, neurotrophin-3 (NT3) (Hohn et al., 1990; Jones and Reichardt, 1990; Maisonpierre, Belluscio, Squinto, et al., 1990; Rosenthal et al., 1990) and neurotrophin-4 (NT4) (Berkemeier et al., 1991; Hallbook et al., 1991; Ip et al., 1992) were subsequently identified in various mammals. There are no neurotrophin-related genes in *C. elegans* (Zlotkowski et al., 2013)*,* suggesting that evolution of this gene family accompanied that of more complex nervous systems.

1.2.2. Biosynthesis of the neurotrophins

The four neurotrophins are synthesised as pre-proneurotrophins which consist of a pre-prodomain on the N-terminus, and the mature neurotrophin domain on the C-terminus (Berkemeier et al., 1991; Ernfors et al., 1990; Leibrock et al., 1989; Scott et al., 1983; Suter et al., 1991). The N-terminus pre-protein directs nascent polypeptide synthesis to the rough endoplasmic reticulum, following which the pre-sequence is cleaved, to produce the proneurotrophin (Seidah et al., 1996). The proneurotrophins form non-covalent homodimers, in which disulphide bridges form a "cystine knot", a feature also found in other secreted growth factors (Bradshaw et al., 1993). The function of the prodomain is to ensure effective folding. Indeed, studies have shown that disrupting the proneurotrophin sequence prevents the formation of biologically active mature neurotrophins (Suter et al., 1991). The proneurotrophins are then trafficked through the Golgi apparatus to the Golgi network vesicles, where post-translational modifications such as N-glycosylation and possibly cleavage of proneurotrophins occur (Mowla et al., 2001). In neurons the resulting mature neurotrophins, together with the cleaved prodomain, are stored in large, dense-core vesicles in pre-synaptic terminals.

Much less is known about the biosynthesis of neurotrophins in non-neuronal tissues, although it is thought that unprocessed proneurotrophins can also be trafficked, via

interactions with sortilin, to vesicles for secretion (Chen, 2005; Evans et al., 2011; Matsumoto et al., 2008; Skaper et al., 2001). Upon release, proneurotrophins can either undergo extracellular cleavage by matrix metalloproteases, or plasmin to produce a mature neurotrophin (Bradshaw et al., 1993; Bruno and Cuello, 2006; Lee et al., 2001), or may function without any further processing (Teng et al., 2010). The release of proneurotrophins from healthy neurons has historically been a point of controversy. Some studies have indicated that proneurotrophins can be released from neurons, but the majority of this work has utilised *in vitro* neuronal models (Hasan et al., 2003), either using antimitotic agents that may have compromised the health of the neurons, or overexpression paradigms. The use of overexpression paradigms for testing this hypothesis is questionable due to the fact that neurons seem to have a limited capacity to process pro-neurotrophins, as following injury proneurotrophins appear to escape neuronal processing and can be secreted (Dicou, 2008).

1.2.3. Localisation of the neurotrophins

NGF is found both in neuronal and non-neuronal cells, but most notably in the peripheral target tissues of sensory and sympathetic neurons, including the dermal layers (Wheeler and Bothwell, 1992), the whisker pad (Ernfors et al., 1992; Leon et al., 1994; Selby et al., 1987), salivary gland (Levi-Montalcini and Cohen, 1960), heart (Selby et al., 1987), retina and iris (Ernfors et al., 1992; Selby et al., 1987). The areas of the CNS where NGF is secreted at the highest quantities are the hippocampus (Pascual et al., 1998; Rocamora et al., 1996), and cortex (Selby et al., 1987).

As a point of comparison, the levels of BDNF mRNA in the hippocampus are around 50-fold higher than those of NGF mRNA. In the CNS *Bdnf* is primarily expressed by neurons with the highest levels in the hippocampus, neocortex (Hofer et al., 1990; Timmusk, Palm, et al., 1993), cerebellum, and pituitary gland (Timmusk, Belluardo, et al., 1993). BDNF mRNA and protein has also been localised in the cochlea, vestibule macula (Ernfors et al., 1992; Pirvola et al., 1992), heart (Ibáñez et al., 1993), lung (Timmusk, Belluardo, et al., 1993), and kidney (Timmusk, Belluardo, et al., 1993).

*Ntf4 (*the gene encoding NT4 in mice), like *Bdnf*, is expressed in the hippocampus, cortex, cerebellum, and striatum. NT4 can also be detected in non-neuronal tissues

such as the heart, lung, and kidney. However in contrast to BDNF, NT4 can also be found in the testis, skeletal muscle, and thymus (Timmusk, Belluardo, et al., 1993).

Ntf3, the gene for NT3 in mice, has a more restricted expression pattern in the adult CNS than other neurotrophins; and is located in the hippocampus, and cerebellum (Ernfors et al., 1992; Maisonpierre, Belluscio, Friedman, et al., 1990). During development *Ntf3* is the most highly expressed neurotrophin, and expression decreases as cells undergo mitosis. One such example of this is the cortex. NT3 can also be detected in non-neuronal tissues such as the whisker pad, muscle spindles, epithelium, iris, cochlea and heart (Maisonpierre, Belluscio, Friedman, et al., 1990; Pirvola et al., 1992).

1.2.4. The neurotrophin receptors

The neurotrophins interact with two different classes of receptors; tropomyosin receptor kinase (Trk) receptors and the p75 neurotrophin receptor (p75^{NTR}) (Figure 1.2). p75^{NTR} shares a similar affinity for all four mature neurotrophins ($K_d = 10^{-9}$ M) (Esposito et al., 2001; Hempstead et al., 1991; Rodriguez-Tebar et al., 1990), but binds proneurotrophins with higher affinity ($K_d = 10^{-11}$ M) (Lee et al., 2001). The three Trk receptors, designated TrkA, TrkB and TrkC, bind mature neurotrophins with a similar affinity to that of p75^{NTR} ($K_d = 10^{-9}$ M) (Esposito et al., 2001; Hempstead et al., 1991), but with significantly more selectivity; while NGF preferentially binds TrkA (Kaplan et al., 1991; Klein, Jing, et al., 1991), BDNF and NT4 bind TrkB (Klein et al., 1992; Klein, Nanduri, et al., 1991; Soppet et al., 1991; Squinto et al., 1991), and NT3 to TrkC (Lamballe et al., 1991) (Figure 1.2). However NT3 has been found to also bind to both TrkA and TrkB *in vitro* (Cordon-Cardo et al., 1991; Klein, Nanduri, et al., 1991; Soppet et al., 1991; Squinto et al., 1991). Interaction of p75^{NTR} and the Trk receptors leads to high affinity binding sites for the neurotrophins ($K_d = 10^{-11}$ M) (Esposito et al., 2001).
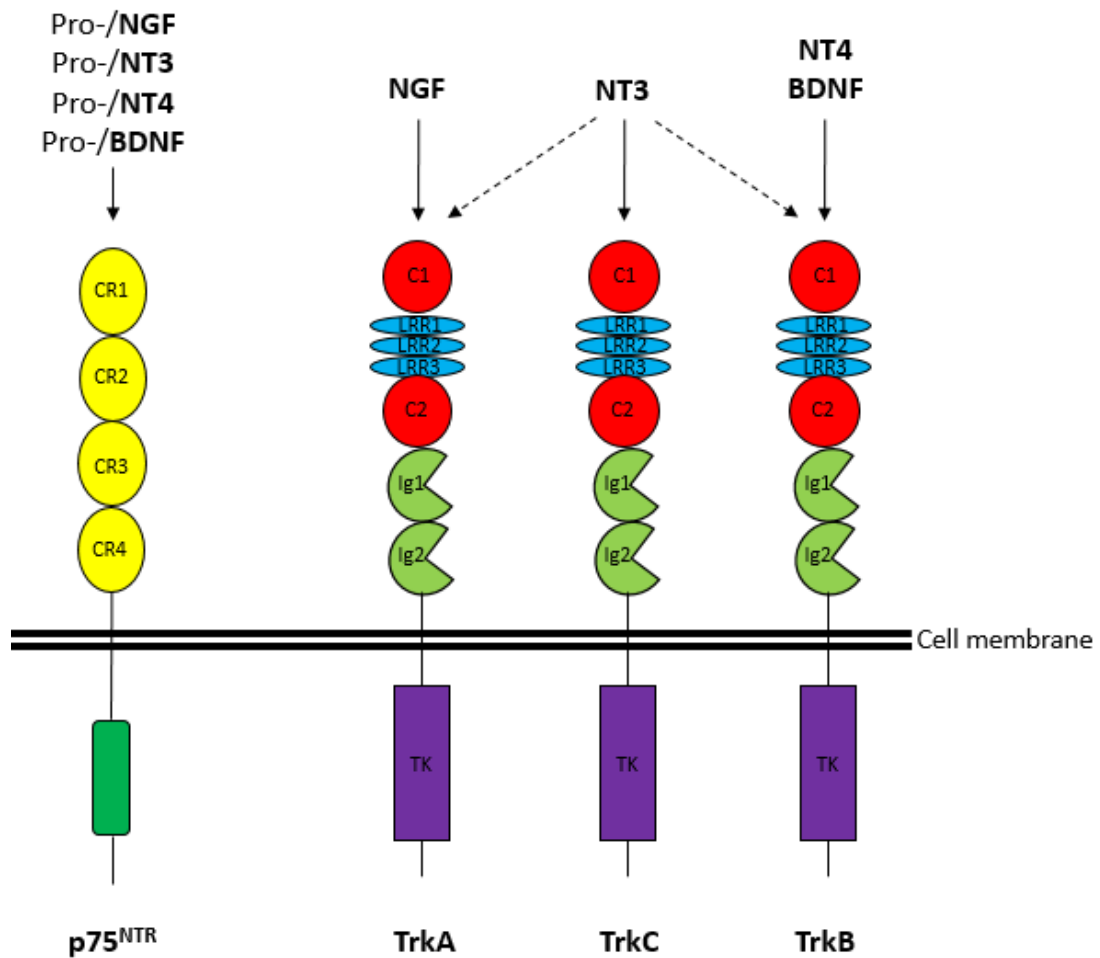
Figure 1.2 Binding of the neurotrophins to the Trk and p75^{NTR} receptors. The mature neurotrophins selectively bind to one of three Trk receptors, although NT3 can bind to TrkA or TrkB *in vitro* (dotted arrows). p75^{NTR} can be bound by all four neurotrophins in both mature and proneurotrophin form. The Trk receptors share a similar structure, with an extracellular domain consisting of two cysteine-rich clusters (C1, C2; red), three leucine-rich repeats (LRR1-3; blue), and two immunoglobulin-like domains (Ig1, Ig2; green). Each Trk has a single transmembrane domain, and a single cytoplasmic tyrosine kinase domain (TK; purple). p75^{NTR} has four cysteine-rich domains (CR1-4; yellow) that are responsible for ligand binding, a single transmembrane domain, and an intracellular death domain (green).

1.2.4.1. p75^{NTR}

p75^{NTR} was the first identified neurotrophin receptor, and first identified member of the tumour necrosis factor (TNF) superfamily (Chao et al., 1986; Johnson et al., 1986; Radeke et al., 1987). The gene encoding p75^{NTR}, named *Ngfr,* is located on chromosome 11 in mice (17q12-17q22 in humans (Huebner et al., 1986; Sehgal et al., 1988)). The p75^{NTR} receptor is a 75 kDa transmembrane glycoprotein with an extracellular domain (consisting of four cysteine-rich (CR) domains responsible for interactions with the neurotrophins (Baldwin et al., 1992; He and Garcia, 2004; Yan and Chao, 1991)), a transmembrane domain, and an intracellular domain. The intracellular domain contains a palmitoylation site which is involved in subcellular trafficking of the receptor (Barker et al., 1994), two potential sites of binding for TNF receptor-associated factor (TRAF) that modulate intracellular signalling (Zotti et al., 2017), and a type II death domain that regulates downstream apoptotic signalling via p75^{NTR} (Lin et al., 2015). p75^{NTR} can bind both mature and pro-neurotrophins, and other ligands, such as prion protein fragment PrP (106-206) (Della-Bianca et al., 2001), and the amyloid precursor protein (APP) Aβ-peptide (Yaar et al., 1997). Alternative splicing of exon III produces an isoform of p75^{NTR} that lacks the cysteine rich domains 2-4 (referred to as s-p75^{NTR}) and consequently, is unable to bind neurotrophins (Figure 1.3). The function of this isoform is still unknown, although it has been found to be expressed in mice, rats and humans (Von Schack et al., 2001).

Several studies have implicated the expression of p75^{NTR} in many CNS and PNS neuronal types across different species (Ernfors et al., 1988; Schatteman et al., 1988; Shelton and Reichardt, 1986; Yan et al., 1988), however recent comparison of p75^{NTR} mRNA levels between chick and murine samples have shown that some regions with high p75^{NTR} expression in the chick, do not show any expression in the mouse, and *vice versa*, indicating that cell-specific comparisons regarding p75^{NTR} expression levels cannot be drawn between these species (S. Wyatt and A. Davies, by communication). Within the mouse, p75^{NTR} is expressed in several CNS populations such as the hippocampus during development, and decreases postnatally (Bernabeu and Longo, 2010).

1.2.4.2. *TrkA, TrkB and TrkC*

The Trk receptors are members of a family of fifty eight enzyme-linked transmembrane glycoproteins called the receptor tyrosine kinases (RTKs). The RTKs share a common structure; with an extracellular ligand binding domain, transmembrane domain, and intracellular tyrosine kinase domain (Hubbard and Miller, 2007). There are three Trk receptors; TrkA, TrkB and TrkC, that share ~40-45% pairwise sequence homology (Ultsch et al., 1999).

All three Trk receptors have an extracellular domain which is comprised of two cysteine-rich clusters (C1, C2), three leucine-rich repeats (LRR1-3), and two immunoglobulin-like domains (Ig1, Ig2) (Schneider and Schweiger, 1991; Windisch et al., 1995). The immunoglobulin-like (Ig) domains are the main site of neurotrophin binding (Holden et al., 1997; Ultsch et al., 1999; Urfer et al., 1995), and the leucine-rich domains seem to also play a role in binding (Windisch et al., 1995). Indeed, TrkC chimeras where the immunoglobulin domains had been replaced by TrkB or TrkA Ig sequences allowed binding of BDNF and NGF (Urfer et al., 1995). The extracellular domain of the Trk receptors are also subject to post-translational glycosylation of the N-terminus which serves to prevent ligand-independent activation of the receptor, and for localisation in the cell membrane (Watson et al., 1999). The intracellular domain consists of a tyrosine kinase domain which recruits various intracellular signalling proteins through phosphorylation (section 1.2.5 for more details) (Obermeier et al., 1994; Obermeier, Halfter, et al., 1993; Obermeier, Lammers, et al., 1993; Stephens et al., 1994) (Figure 1.3).

Each of the Trk receptors have several isoforms in the mouse due to differential splicing of exons that encode the receptors: two splice variants exist for TrkA (Clary and Reichardt, 1994), three for TrkB (Klein, Conway, et al., 1990; Kumanogoh et al., 2008) and six for TrkC (Tessarollo et al., 1997), including full-length and truncated proteins (Figure 1.3). These splicing events can lead to either minor, or major changes in the function of the receptor. An example of a minor alteration are changes to short amino acid sequences in the extracellular, juxtamembrane regions. Lack of the juxtamembrane insert in TrkA or TrkB leads to activation only by NGF and BDNF, respectively (Clary and Reichardt, 1994; Strohmaier et al., 1996; Urfer et al., 1995),

however with the juxtamembrane inserts both receptors can be activated by NT3, and additional activation of TrkB by NT4 can occur (Boeshore et al., 1999; Clary and Reichardt, 1994; Meakin, 1997; Strohmaier et al., 1996).

TrkC also has an isoform with a small insert in the tyrosine kinase domains which affects the substrate specificity, thus altering the intracellular signalling pathways (Garner and Larget, 1994; Guiton et al., 1995; Valenzuela et al., 1993). TrkB receptor splice variants result in truncated receptors that lack the intracellular kinase domain. Two truncated isoforms of TrkB exist in the CNS, TrkB.T1 and TrkB.T2 which differ only by the existence of an Shc-binding site in TrkB.T2 (Klein, Conway, et al., 1990). TrkC splice variants also include four truncated receptors that resemble the previously described truncated TrkB variants (Lamballe et al., 1991; Valenzuela et al., 1993) (Figure 1.3). The predominant theory for the function of these truncated receptors is that they regulate full length Trk receptor function, and are thought to act via a dominant-negative mechanism, forming non-functional heterodimers with full length receptors (Eide et al., 1996).

Whilst both p75^{NTR} and the Trk receptors bind neurotrophins, their extracellular domains are unrelated. Whereas the neurotrophins interact with the Ig2 domains within the Trk receptors (Holden et al., 1997; Ultsch et al., 1999; Urfer et al., 1995), they interact with the cysteine-rich domains in the p75^{NTR} receptor (Baldwin et al., 1992; Wiesmann and de Vos, 2001; Yan and Chao, 1991) (Figure 1.3). Furthermore, the intracellular domain of p75^{NTR} does not contain a tyrosine kinase domain, and are unable to induce ligand-induced activation of intracellular signalling proteins (Roux and Barker, 2002).
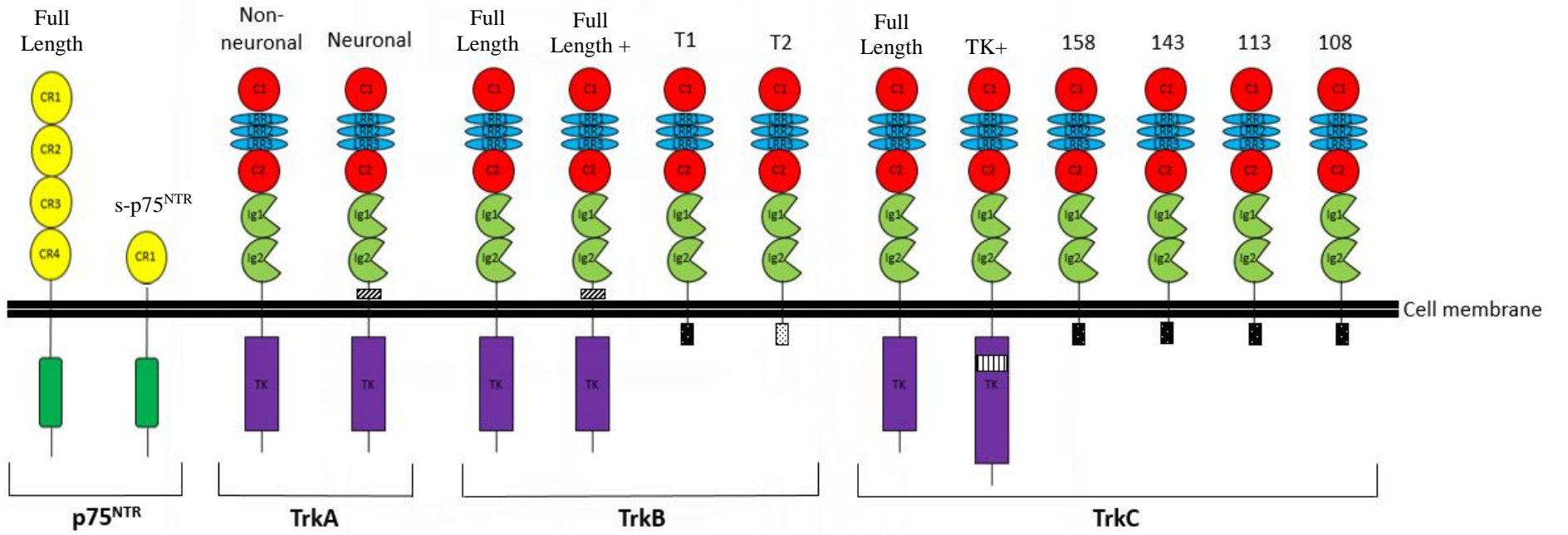
Key

▨	Juxtamembrane insert
▥	Tyrosine Kinase insert
▦	Truncated intracellular domain (1)
▦	Truncated intracellular domain (2)

Figure 1.3 Alternative splicing produces different sizes of neurotrophin receptors. Schematic of the known splice variants for the neurotrophin receptors. Full length p75^{NTR} consists of four extracellular cysteine-rich domains (yellow) while the splice variant, s-p75^{NTR}, only has one CR domain. Both variants of p75^{NTR} contain an intracellular death domain (dark green). TrkA, TrkB and TrkC splice variants have similar extracellular domains with cysteine-rich clusters (C1, C2; red), three leucine-rich repeats (LRR1-3; blue), and two immunoglobulin-like domains (Ig1, Ig2; green), with the exceptions of one splice variant for TrkA (neuronal) and one for TrkB (full-length +) which contain a juxtamembrane insert. TrkB also has two truncated receptors; TrkB.T1 and TrkB.T2 that lack the tyrosine kinase (TK, purple) but have a small intracellular domain which is different between T1 and T2. Finally TrkC has five splice variants; one with a tyrosine kinase insert (TK+), and four truncated receptors.

1.2.5. Signalling via Trk receptors

Binding of the mature neurotrophins to the Trk receptors results in receptor dimerization (Jing et al., 1992), allowing transphosphorylation of the receptors tyrosine kinase domains within the activation loop (Cunningham et al., 1997; Cunningham and Greene, 1998). This results in further phosphorylation of tyrosine sites within the tyrosine kinase domain that then act as docking sites for intracellular adaptor proteins such as Src homologous and collagen-like (Shc) and phospholipase-C (PLC) that are also phosphorylated by the Trk receptor intracellular domain (Obermeier et al., 1994; Obermeier, Halfter, et al., 1993; Obermeier, Lammers, et al., 1993; Stephens et al., 1994). These adaptor proteins activate further signalling cascades such as RAS/mitogen-activated protein kinases (MAPKs), phosphoinositide 3-kinase (PI3K) and phospholipase C γ (PLCγ) (Mitre et al., 2017).

As the locations of neurotrophin expression can be far from the cell soma of Trk-expressing neurons (discussed in section 1.2.3), it is important to note that ligand-bound Trk receptors can be internalised through clathrin-mediated endocytosis (Grimes et al., 1996; Howe et al., 2001; Jullien et al., 2003). Application of monodansylcadaverine, a drug that inhibits clathrin-mediated endocytosis, results in an inhibition of Trk receptor internalisation (Du et al., 2003; Zheng et al., 2008). It is thought that macropinocytic endocytosis of the Trk receptors occurs, but only when there is an excess of the respective neurotrophin or Trk receptor, such as in the cases of genetically-modified animals or *in vitro* experiments, and is therefore not thought to occur under physiological conditions (Philippidou et al., 2011; Shao et al., 2002; Valdez et al., 2007).Within the endosomes, ligand-bound Trk receptors continue signalling (Grimes et al., 1996, 1997), and can also be retrogradely transported along microtubules to the cell soma (Ginty and Segal, 2002; Hendry, Stach, et al., 1974; Hendry, Stockel, et al., 1974). Trk receptors can also be trafficked into late endosomes for degradation into lysosomes.

1.3. Mechanisms of neurotrophin cell survival/cell death

1.3.1. Evidence of cell death caused by neurotrophin-withdrawal

Following the identification of the four neurotrophins and their receptors, their role in supporting the survival of specific populations of sensory neurons has been investigated in considerable detail. *In vitro* studies demonstrated that cultured TrkA, TrkB or TrkC-expressing sympathetic or sensory neurons died within forty-eight hours of neurotrophin withdrawal (Deckwerth and Johnson, 1993; Edwards and Tolkovsky, 1994; Martin et al., 1988). During death the cells had key morphological indicators of apoptosis; around twenty hours after neurotrophin withdrawal the DNA started to fragment (Deckwerth and Johnson, 1993; Edwards et al., 1991), and between eighteen to twenty-four hours, the nuclei shrunk and showed DNA condensation (Deshmukh and Johnson, 1997; Levi-Montalcini et al., 1969; Martin et al., 1988; Mesner et al., 1992). At this stage, microinjection of the prosurvival protein BCL-2 rescued neurotrophin-dependent neurons that had undergone neurotrophin withdrawal (Allsopp et al., 1993; Batistatou et al., 1993; Garcia et al., 1992; Greenlund et al., 1995; Mah et al., 1993; Troy et al., 1996). Neurons reach a commitment point twenty-two hours after neurotrophin withdrawal, and the application of the respective neurotrophin could no longer rescue half of the cells (Deckwerth and Johnson, 1993; Edwards and Tolkovsky, 1994). Observations of morphological apoptosis were matched by biochemical analysis that demonstrated increased caspase activity, and cytochrome c release, after neurotrophin-withdrawal (Deshmukh et al., 1996; Neame et al., 1998; Stefanis et al., 1996; Troy et al., 1996) (discussed in section 1.1.3), supporting that neurotrophin withdrawal results in cell death via the intrinsic apoptotic pathway. Similarly, ablation of APAF-1, caspase-9 or caspase-3 prevented neurotrophin-withdrawal induced apoptosis in sensory and sympathetic neurons (Wright et al., 2007). Although overall RNA and protein synthesis levels dropped by 30% twelve hours after neurotrophin withdrawal (Deckwerth and Johnson, 1993), key apoptotic genes, such as c-Jun that interacts with BCL-2 family proteins to regulate apoptosis (Lei and Davis, 2003), showed a marked increase from five hours after withdrawal (Estus et al., 1994; Freeman et al., 1994). Indeed, inhibiting RNA and protein synthesis, by application of inhibitors such as cycloxheximide, prevented neurotrophin-withdrawal induced death of neurons *in vitro* and *in vivo* (Martin et al.,

1988; Milligan et al., 1994; Oppenheim et al., 1990; Scott and Davies, 1990). Thus, the loss of specific populations of neurons as a result of neurotrophin withdrawal seems to be an *active* process requiring transcription and protein synthesis.

1.3.2. Neurotrophin/Trk knockout studies

The *in vivo* relevance of the neurotrophin signalling system in cell survival during development has been convincingly established in homozygous loss-of-function mouse models (discussed below).

1.3.2.1. NGF and TrkA

Animals lacking NGF ($Ngf^{-/-}$) die within the first few days after birth with no obvious abnormalities in any major organs, but with marked reduction in the size of sympathetic ganglia. This included innervation from the superior cervical ganglia (SCG) to the eye (Crowley et al., 1994). Similar results were obtained in $TrkA^{-/-}$ pups, where the SCG was completely absent (Fagan et al., 1996; Smeyne et al., 1994). The loss of neurons correlated with the finding that >95% of the cells in the SCG are TrkA positive (NGF dependent) (Dixon and McKinnon, 1994).

In the same way, there was a 70-90% loss of sensory dorsal root ganglia (DRG) neurons in the *Ngf* and *TrkA* knockouts (Crowley et al., 1994; Smeyne et al., 1994). The DRG are a collection of sensory neuron cell bodies that lie bilaterally at each vertebral level of the spinal cord. The DRG are made up of several different sub-types of neurons including three main sub-divisions: Aδ, or peptidergic C-fibre, nociceptive neurons that express *TrkA,* Aβ mechanoceptors that express *TrkB,* and Aα and Aβ proprioceptive neurons that express *TrkC* (Duce and Keen, 1977; Harper and Lawson, 1985; Lawson et al., 1974; Lawson, 1979; Mu et al., 1993). The DRG neurons lost in NGF homozygous knockout mice were the nociceptive neurons (Crowley et al., 1994; Smeyne et al., 1994), and as a consequence $Ngf^{-/-}$ or $TrkA^{-/-}$ mice demonstrated increased latency to respond to heat-induced pain, or pin-pricks (Crowley et al., 1994; Smeyne et al., 1994). As there was no loss of the DRG mechanoceptive or proprioceptive neurons in $Ngf^{-/-}$ and $TrkA^{-/-}$, they exhibited normal motor activity and

placing reflexes (Crowley et al., 1994; Smeyne et al., 1994). Similar to the DRG, the trigeminal ganglia (TG) is a heterogeneous collection of sensory neuron cell bodies that differentially express Trk receptors (Mu et al., 1993). *TrkA*$^{-/-}$ and *Ngf*$^{-/-}$ mice showed loss of 70-90% of the small-diameter, nociceptive neurons in the trigeminal ganglia, resulting in a behavioural phenotype where there is loss of pain sensation in response to whisker pad pin-pricks (Smeyne et al., 1994).

Other neuronal populations have also been demonstrated to be modestly affected by loss of NGF/TrkA signalling. There was a small, but non-significant reduction in the nodose ganglia neurons (Crowley et al., 1994), which contains the cell bodies of neurons that project to visceral organs such as the lungs (Conover et al., 1995; Hertzberg et al., 1994). Disruption of NGF/TrkA signalling led to a 20% reduction in the number of *TrkA*-expressing neurons in the CNS, such as the basal forebrain cholinergic neurons (Chen et al., 1997; Fagan et al., 1997; Sanchez-Ortiz et al., 2012; Smeyne et al., 1994; Svendsen et al., 1994) that project to the cerebral cortex, hippocampus and amygdala (Dreyfus, 1989). These changes occur during postnatal development, and so were not initially observed. The loss of this population of cells has been linked to memory deficits in heterozygous *Ngf* knockouts that survived postnatally (Chen et al., 1997). Other ganglia for the facial, acoustic and glossopharyngeal nerves appeared to not be affected by the loss of NGF/TrkA signalling (Smeyne et al., 1994).

1.3.2.1.1. BDNF/NT4 and TrkB

The effects of *Bdnf, Ntf4, TrkB* knockouts differ from those of *Ngf/TrkA* due to the differential pattern of expression of the ligands and their corresponding receptors. For example, as there is no detectable TrkB in the SCG, *Ntf4*$^{-/-}$ or *Bdnf*$^{-/-}$ knockouts did not demonstrate any loss of these neurons (Jones et al., 1994; Liu et al., 1995). What is striking is that *Bdnf*$^{-/-}$ and *Ntf4*$^{-/-}$ mice have clear differences in their phenotypes, despite both binding to TrkB. For example, *Ntf4*$^{-/-}$ mice could survive into adulthood with no obvious behavioural phenotypes (Conover et al., 1995), whilst *Bdnf*$^{-/-}$ or *TrkB*$^{-/-}$ pups died within the first few days of birth, with only a few surviving into the first postnatal week. *Bdnf*$^{-/-}$ or *TrkB*$^{-/-}$ knockout mice displayed no obvious physical deformities, and were a similar size to their littermates at birth, although those that

survive later showed retarded growth compared to their littermates (Erickson et al., 1996; Ernfors, Lee and Jaenisch, 1994; Jones et al., 1994; Klein et al., 1993). *Bdnf*^{-/-} or *TrkB*^{-/-} mice had similar behavioural phenotypes in that they suffered from severe movement deficits such as difficulty righting and spinning, hunched stance, and ataxia, along with breathing abnormalities (Erickson et al., 1996; Ernfors, Lee and Jaenisch, 1994; Jones et al., 1994; Klein et al., 1993). *TrkB*^{-/-} pups were unable to feed as a result of these movement deficits, despite having normal gastrointestinal tracts (Klein et al., 1993).

Over 95% of nodose-petrosal ganglia (NPG) neurons express *TrkB* (Huang et al., 1999). *Ntf4*^{-/-} or *Bdnf*^{-/-} knockout mice demonstrated a loss of 50-60% of the NPG (Conover et al., 1995; Erickson et al., 1996; Ernfors, Lee and Jaenisch, 1994; Liu et al., 1995), whilst double knockouts of both *Bdnf* and *Ntf4* demonstrate a 90% reduction in the number, and size of NPG (Conover et al., 1995; Erickson et al., 1996; Liu et al., 1995). The loss of NPG neurons in the *Bdnf/Ntf4* double knockout matched that of *TrkB*^{-/-} mice (Erickson et al., 1996). Similarly, the geniculate ganglia, containing cell bodies responsible for taste that innervate the gustatory epithelium, demonstrated a 40-50% reduction in the number of neurons in either *Bdnf*^{-/-} or *Ntf4*^{-/-} pups (Conover et al., 1995; Erickson et al., 1996; Jones et al., 1994; Liu et al., 1995), in the *Bdnf/Ntf4* double knockout showed a loss of 95% of the geniculate ganglia cells (Conover et al., 1995; Erickson et al., 1996; Fei and Krimm, 2013; Liu et al., 1995), which corresponds to the reduction of the geniculate ganglia in *TrkB*^{-/-} pups (Fritzsch et al., 1997). This indicates that the NPG and geniculate contain different subpopulations of ganglia that are BDNF or NT4-dependent alone, and the double knockout suggests there is little redundancy between the two ligands. The loss of a similar number of NPG or geniculate ganglia neurons in the double knockout, compared to the TrkB knockout, indicates that these differential effects are still mediated by TrkB in these different subsets of the ganglia. Specific subsets of dopaminergic neurons are lost in the NPG of BDNF knockout mice innervate the carotid body, and they are important for effective ventilation, and cardiorespiratory reflexes (Erickson et al., 1996). This seems to be the main explanation for the severe respiratory abnormalities, and ultimately the lethality, observed in *Bdnf* or *TrkB*, but not *Ntf4* knockouts.

On the other hand, DRG neurons appear to be dependent upon both BDNF (Ernfors, Lee and Jaenisch, 1994), and NT4 (Liu et al., 1995), demonstrating a 30% vs a 15%

reduction in knockouts, respectively, while there is a 20-30% reduction in the number of DRG neurons in $TrkB^{-/-}$ mice. This indicates that there is overlap between NT4 and BDNF responsive neurons in the DRG. The neurons that were lost in these knockouts were found to correspond to the $TrkB$-expressing, large-diameter mechanoceptive neurons (Klein et al., 1993; Minichiello et al., 1995; Perez-Pinera et al., 2008).

The vestibular ganglia, a collection of TrkB-expressing sensory neurons required for balance and locomotion (Ernfors et al., 1992; Robinson, 1996), appeared to only be dependent on BDNF, with reports of 80-90% reduction in the number of vestibular ganglia neurons in $Bdnf^{-/-}$ mice (Conover et al., 1995; Ernfors, Lee and Jaenisch, 1994; Jones et al., 1994). These neurons failed to innervate vestibular sensory epithelia (Ernfors, Lee and Jaenisch, 1994). However the vestibular ganglia were not affected in $Ntf4^{-/-}$ mice (Conover et al., 1995). Similarly there is no additive effect in the $Bdnf/Ntf4$ double knockout (Conover et al., 1995; Liu et al., 1995). This may be an explanation as to the severe movement deficits observed in $Bdnf^{-/-}$ and $TrkB^{-/-}$ mice, but not $Ntf4^{-/-}$ mice. Counter-intuitively, there has been only a reported loss of 60% of vestibular neurons in $TrkB$ knockout mice (Minichiello et al., 1995; Schimmang et al., 1995). There are also differential effects between NT4 and BDNF on survival of trigeminal ganglia. While NT4 doesn't seem to be important in the survival of trigeminal ganglia neurons in knockout mice (Conover et al., 1995), $Bdnf^{-/-}$ mice exhibited a 30-40% reduction in the number of trigeminal neurons (Conover et al., 1995; Ernfors, Lee and Jaenisch, 1994; Jones et al., 1994) that is matched in the $Bdnf/Ntf4$ double knockout (Conover et al., 1995; Liu et al., 1995). Similarly, $TrkB$ knockouts demonstrate a 60% reduction in the number of trigeminal neurons (Klein et al., 1993)

In vitro, and *in vivo* lesion experiments initially suggested that BDNF was important for the survival of CNS neurons, including motor neurons in particular (Alderson et al., 1990; Lindsay et al., 1985; Oppenheim et al., 1992; Sendtner et al., 1992). Given the widespread expression of BDNF across the CNS (Rauskolb et al., 2010), it was expected that BDNF would be responsible for the survival of CNS neurons. However knockout studies have indicated that there are few developmental deficits in the CNS of $Bdnf^{-/-}$ or $Ntf4^{-/-}$ mice (Jones et al., 1994). There appears to be delayed, but normal migration of cerebellar granule neurons in $Bdnf^{-/-}$ or $Ntf4^{-/-}$ animals, while the cortex, basal forebrain, substantia nigra and hippocampus appear normal (Jones et al., 1994;

Liu et al., 1995). Similarly, the loss of *TrkB* has not been found to link to obvious CNS abnormalities (Klein et al., 1993). However studies have found that in *TrkB*$^{-/-}$ mice that can survive for a few weeks postnatally, there is an increase in the number of pyknotic nuclei in the neocortex, striatum, thalamus and dentate gyrus (Alcantara et al., 1997). However, as these effects only occur late and in animals with compromised health status causality is difficult to establish with certainty.

1.3.2.2.   NT3 and TrkC

Ntf3$^{-/-}$ and *TrkC*$^{-/-}$ mice usually die within the first few days of life, although some *TrkC* knockout pups can survive up to three weeks (Klein et al., 1994; Tessarollo et al., 1994, 1997). Both *TrkC* and *Ntf3* knockouts take nourishment from their mothers unlike the *Ngf/TrkA*, or *Bdnf/Ntf4/TrkB* knockouts outlined above, although *TrkC*$^{-/-}$ pups that survive are 25-50% of the body weight of their wild type littermates (Klein et al., 1994). Also unlike the other neurotrophins, both *Ntf3*$^{-/-}$ or *TrkC*$^{-/-}$ mice exhibit severe cardiac deficits such as defects in the atrial and ventricular septum, and pulmonic stenosis (Donovan et al., 1996; Tessarollo et al., 1994, 1997), which could account for the perinatal lethality observed. Later studies have shown that NT3/TrkC signalling via the tyrosine kinase domain is important for the proliferation of cardiac myocytes (Donovan et al., 1996; Lin et al., 2000; Tessarollo et al., 1997).

In the *Ntf3*$^{-/-}$ and *TrkC*$^{-/-}$ mice, there is a loss of specific subsets of sensory and sympathetic neurons. Importantly, the *Ntf3* knockout consistently shows a more severe phenotype compared with *TrkC*$^{-/-}$ animals. For example, within the NPG, 30-50% of neurons are lost in *Ntf3*$^{-/-}$ pups (Ernfors, Lee, Kucera, et al., 1994; Farinas et al., 1994; Tessarollo et al., 1997), compared to 15% in *TrkC*$^{-/-}$ pups (Tessarollo et al., 1997). The number of neurons lost in the NPG in *Ntf3*$^{-/-}$ and *TrkC*$^{-/-}$ mice is not enough to result in any obvious breathing deficits. Similarly there is a 25-35% reduction in the number of neurons in the geniculate nucleus of *Ntf3*$^{-/-}$ pups, but only a modest, non-statistically significant reduction of 10% in *TrkC*$^{-/-}$ pups (Farinas et al., 1994; Tessarollo et al., 1997). Along these lines, *Ntf3*$^{-/-}$ exhibit a 60-70% and a 20% reduction in the number of trigeminal and vestibular ganglia neuronal cell bodies, respectively (Ernfors, Lee, Kucera, et al., 1994; Farinas et al., 1994; Tessarollo et al., 1997; Tojo et al., 1995), versus 20% and 15% in *TrkC*$^{-/-}$ knockouts, respectively (Farinas et al., 1994;

Tessarollo et al., 1997). Finally, the severe abnormal posture and limb movement in *Ntf3*^{-/-} and *TrkC*^{-/-} mice (Klein et al., 1994; Tessarollo et al., 1994) seems to be the result of the loss of large-diameter, TrkC-expressing proprioceptive neurons in the DRG (Klein et al., 1994; Matsuo et al., 1999; Tessarollo et al., 1997). In *Ntf3*^{-/-} mice this is around 55-70% of DRG neurons (Ernfors, Lee, Kucera, et al., 1994; Fariñas et al., 1998; Tessarollo et al., 1997; Tojo et al., 1995), and 20% in *TrkC* knockouts (Klein et al., 1994; Tessarollo et al., 1997). The discrepancy between the phenotype of animals lacking *Ntf3* or *TrkC* is particularly obvious in sympathetic ganglia. For example in the SCG, *TrkC* knockouts show no significant differences in the number of SCG neurons, but there is a 50-80% reduction in *Ntf3* knockouts (ElShamy and Ernfors, 1996; Ernfors, Lee, Kucera, et al., 1994; Fagan et al., 1996; Farinas et al., 1994). As *in vitro* NT3 can also activate the TrkA and TrkB receptors, it was initially proposed that the discrepancy between the phenotype of animals lacking either *Ntf3* or *TrkC* may reflect the activation of heterologous receptors by NT3 in the absence of TrkC (Davies et al., 1995). However, this possibility does not seem to hold true for all ganglia where detailed comparisons have been made using gene substitution experiments. For example, replacing BDNF by NT3 fails to rescue TrkB-expressing vestibular neurons suggesting a failure of NT3 to activate TrkB *in vivo* (Tessarollo, 2004).

1.3.3. Dependence receptors

The observations summarised in section 1.3.2 further added weight to the notion that neurons are intrinsically programmed to die during development unless a diffusible survival factor, such as the neurotrophins, blocks their death (Jacobson et al., 1997; Oppenheim, 1991). Indeed, studies have detailed the pro-survival signalling of the ligand-bound Trk receptors via PI3K/Akt and Ras/MEK/MAPK pathways (Borasio et al., 1993; Crowder and Freeman, 1998; Nobes and Tolkovsky, 1995; Yao and Cooper, 1995). However, there was a struggle to underpin this theory with a pathway for the default apoptotic state, and the question remained; what causes neurons to die in the first place and how could the selectivity of this phenomenon be explained?

In 1998 the concept of dependence receptors was proposed (Bredesen et al., 1998). The term refers to receptors endowed with non-classical signal transduction in that

they signal both when ligand-bound and in the absence of the ligand. When ligand bound the receptors transduce positive signals to support cell survival, and in the absence of the cognate ligand the receptors actively transduce signals to initiate cell death. This new concept was initially developed in the context of tumour biology with the identification of the receptors deleted in colorectal cancer (DCC) and uncoordinated-5 homolog (UNC5H) (Llambi et al., 2001; Mehlen et al., 1998) that kill dividing cells in the absence of the corresponding ligand.

1.3.4. TrkC as a dependence receptor

In 2007, Servane Tauszig-Delamasure and colleagues demonstrated, using *in vitro* cells transfected with Trk receptors, that TrkC acts a dependence receptor. Their experiments involved transient transfection of full length rat *TrkC* (*rTrkC*) in human embryonic kidney 293 (HEK293T), and immortalised olfactory neuroblast 13.S.24 cells (Tauszig-Delamasure et al., 2007). Transfected cells had increased levels of apoptosis, exhibited by increased levels of active caspase-3 and DNA condensation, and the addition of NT3 prevented this cell death in a dose-dependent manner. The authors determined that TrkC-induced apoptosis did not seem to involve the kinase activity of the receptor, as a kinase-dead mutant of TrkC (D679N) elicited similar pro-apoptotic activity, indicating that other mechanisms were involved. Intriguingly, they also observed that TrkC-induced apoptosis was correlated with double cleavage of the TrkC intracellular domain by active caspase 3, and apoptosis could be blocked by preventing cleavage using the pan-caspase inhibitor carbobenzoxy-valyl-alanyl-aspartyl-[O-methyl]-flouromethylketone (zVAD-fmk). To determine if the cleaved TrkC domain would cause cell death, they performed microinjections of the "dependence domain" released by cleavage (mapped as TrkC 496-641 in rat TrkC) into primary DRG neurons, and observed increased apoptosis (Tauszig-Delamasure et al., 2007).

These results provided a novel explanation for how developing sensory and sympathetic neurons undergo apoptosis during development; the mere expression of the Trk receptors causes cell death when the ligand is not present. In this way, the number of cells innervating a target tissue can be controlled by secreting limited amounts of neurotrophins as superfluous neurons that do not get enough neurotrophin

die. This is referred to as the "neurotrophic hypothesis". However, these new observations added to the neurotrophic hypothesis by demonstrating that it is the expression of the Trk receptors in the first place that causes neurons to be susceptible to cell death. These findings neatly explained the neuronal selectivity of neurotrophins as pro-survival factors, and also clarified *in vivo* observations discussed in section 1.3.2 that *Ntf3* knockout mice have an increased loss of sensory and sympathetic cells compared to *TrkC* knockouts.

While around twenty dependence receptors have been identified, these receptors do not share obvious structural similarities, so knowledge of the mechanisms of one receptor cannot inform predictions about related receptors. However in 2013, Tauszig-Delamasure's group reported that the cleaved, intracellular, death domain of TrkC (termed TrkC-KF) is shuttled to the mitochondrial membrane by Cobra1, a cofactor for BRCA1 that relatively little is known about (Figure 1.4). TrkC-KF was then suggested to promote the activation of Bax, which resulted in the release of cytochrome c from the mitochondria, triggering the intrinsic pathway of apoptosis (Ichim et al., 2013). Altogether the findings by Tauszig-Delamasure et al. (2007) and Ichim et al. (2013) fit with the previous observations, for example that apoptosis induced by neurotrophin-withdrawal can be blocked by caspase inhibitors as this would be predicted to prevent caspase-mediated cleavage of TrkC.
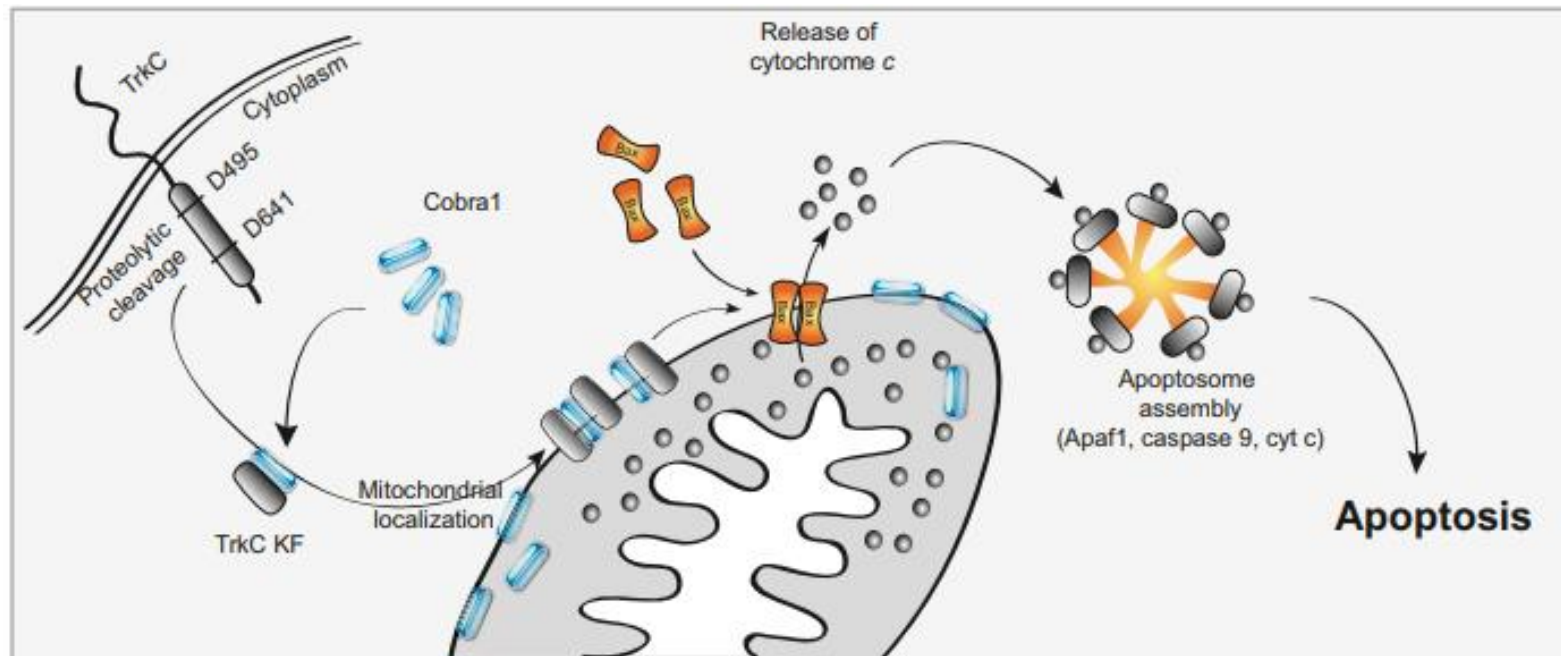
Figure 1.4 Suggested model of TrkC-induced cell death. Unbound TrkC intracellular domain is cleaved by caspase-3 at sites D495 and D641 to produce the TrkC killer fragment (TrkC-KF). Cobra-1 shuttles TrkC-KF to the mitochondrial membrane which allows the release of cytochrome c to induce apoptosis. Taken from (Ichim et al., 2013).

1.3.5. TrkA as a dependence receptor

In the same set of experiments leading to the identification of TrkC as a dependence receptor, Tauszig-Delamasure reported that TrkA or TrkB did not behave as dependence receptors. However, a later study by Nikoletopoulou et al. (2010) identified TrkA, along with TrkC, as a dependence receptor using genetically-modified mouse embryonic stem cells (ESCs). The benefit of ESCs over the HEK293T cells used by Tauszig-Delamasure is that these cells can readily be differentiated into homogenous populations of post-mitotic neurons in which to study neuron-specific processes in a more relevant system. In their experiments Nikoletopoulou et al. (2010) generated mouse ESCs expressing full length rat *TrkA*, *TrkB* or *TrkC* under the neuron-specific promoter microtubule associated protein tau (*Mapt)*. A green fluorescent protein (GFP) cDNA was inserted in the second *Mapt* locus for ease of visualisation of targeted ESCs. In this model, the three Trk sequences were also terminally tagged with a hemagglutinin (HA) epitope, a nine amino acid-long sequence that has been widely used and has not been reported to interrupt the activity of the protein it is tagged to (Jiang et al., 1996; Takeuchi et al., 2002). By having an HA tag on TrkA-C it was possible for Nikoletopoulou and colleagues to discriminate between endogenous and exogenous protein.

Their genetically modified *Mapt-HA-rTrkA, -rTrkB, -rTrkC* and control (*Mapt-EGFP)* ESCs were differentiated into cortical-like neurons following a well-established protocol. In brief, ESCs were cultured for several passages before being placed on a non-adherent dish for eight days where they formed cellular aggregates (Bibel et al., 2004, 2007). Retinoic acid was applied for the final four days of aggregation, and the aggregates dissociated and plated on the eighth day. Upon plating, the cells had a radial glial like morphology and were positive for radial glial markers such as brain lipid binding protein (BLBP), nectin-2 and PAX6. The presence of these markers decreased with time in culture, as these progenitors matured into a culture of 90-95% post-mitotic, glutamatergic neurons. Less than 1% of neurons were positive for other neurotransmitters such as Isl-1, gamma-aminobutyric acid (GABA), tyrosine hydroxylase and choline acetyltransferase (ChAT), with the other 1% of cells being positive for non-neuronal glial-fibrillary acid (GFAP). The resulting neurons were shown to be similar to cortical neurons, and demonstrated both spontaneous and

depolarisation-induced action potentials after twelve days that could be blocked by tetrodotoxin (TTX) and bicuculline, alongside increased activity after the addition of glutamate. Maturation could also be marked by the appearance of spines 21 days after dissociation (referred to as day in vitro; DIV). Western blot analysis of wild type neurons using a pan-Trk antibody indicated that Trk protein could be detected from DIV7 onwards, and was later characterised as endogenous TrkB expression, similar to what is observed in the cortex (Bibel et al., 2004, 2007).

The key observation by Nikoletopoulou and colleagues was that TrkA- and TrkC-expressing ESC-derived neurons formed normally for the first few days *in vitro*, but were completely ablated between DIV 4-6. On the other hand TrkB-expressing neurons survived, even in the complete absence of BDNF. The death of neurons was marked by significantly increased levels of cleaved caspase-3 in the TrkA, and TrkC-expressing neurons, while caspase activity remained unchanged in TrkB-expressing neuronal cultures. As predicted for a candidate dependence receptor, the death of TrkA- (and TrkC-) expressing neurons could be prevented by the addition of the cognate ligand NGF (and NT3 for TrkC). In addition to these *in vitro* experiments, the dependence receptor character of TrkA and TrkC could be verified *in vivo* using a method called tetraploid complementation. In this method tetraploid (4n) mouse blastomeres are combined with the *Mapt-HA-rTrkA, -rTrkB* or *–rTrkC* ESCs, which have a stronger lineage potency and therefore form the entire epiblast (Wang et al., 1997). They noted that similar to their *in vitro* observations, expression of TrkA and TrkC led to massive loss of the nervous system in the embryos by 13.5 days *post-coitum* (E13.5), despite no obvious loss of the nervous system at E11.5. Again, expression of TrkB did not result in cell death. Investigation of potential mechanisms of TrkA and TrkC-induced neuronal death indicated that kinase activity of the Trk intracellular domain was not required for neurotrophin-withdrawal induced death, although kinase activity was required for neurotrophin-induced survival (Nikoletopoulou et al., 2010).

In addition to the generation of neurons to test for potential novel activities of the Trk receptors, the benefit of the system used by Nikoletopoulou and colleagues, is that by comparison with acute, transient transfection of HEK293T cells, the levels of Trk expression are controlled by an endogenous promoter and are much less likely to differ

widely between acutely transfected cells. This is a potentially serious problem with tyrosine kinase receptors as their autoactivation is well-documented when they are over-expressed in transfected cells (Nikoletopoulou et al., 2010), a possible reason why the death-inducing activity of TrkA was missed in the previous publication (Tauszig-Delamasure et al., 2007). In contrast, by virtue of using the HA tag, Nikoletopoulou et al. could demonstrate identical levels of Trk expression across the cultures.

1.4. Aims

Beyond previous work by Tauszig-Delamasure (2007) and Nikoletopoulou et al. (2010), very little is currently known about possible functions of the Trk receptors during development in the absence of activation by their ligands. Given that TrkA, but not TrkB, was identified as a dependence receptor when overexpressed in the nervous system (Nikoletopoulou et al., 2010), this thesis aimed to further investigate the roles, and possible differences between TrkA and TrkB during development. To achieve this, these receptors were overexpressed in all cells from the earliest stages of mouse development. TrkC was not included as there is already a heavy focus on the activity of TrkC by the groups of Servane Tauszig-Delamasure and Patrick Mehlen. To elucidate the mechanisms of TrkA and TrkB functions potentially identified *in vivo*, *in vitro* models were also generated that overexpressed TrkA and TrkB in neurons.

2   Methods

2.1   Culturing mouse embryonic stem cells

2.1.1   Mycoplasma testing

Mycoplasma are a form of bacteria that can contaminate cell cultures. Contamination with these bacteria affects the growth rate of cultured cells; degrading host cell DNA, and outcompeting the host cells for nutrients (Nikfarjam and Farzaneh, 2012; Sokolova et al., 1998). As a consequence, mycoplasma contamination can affect the reliability of data derived from *in vitro* experiments. However, unlike other common cell culture contaminants, mycoplasma cannot be easily observed by an obvious increase in media turbidity (Young et al., 2010), and are difficult to identify through light microscopy due to their small size (0.2-0.3 µm), pleomorphism, and lack of cell wall (Razin, 2006). Due to these physical characteristics, mycoplasma are also able to pass through most filters, and are not sensitive to common antibiotics that act by disrupting bacterial wall synthesis. Therefore preventing, and detecting mycoplasma contamination is not trivial. As such there are estimates that anything from fifteen, and up to seventy percent (Coronato and Coto, 1991; Drexler and Uphoff, 2002; Olarerin-George and Hogenesch, 2015; Rottem and Barile, 1993) of cell lines worldwide are contaminated with mycoplasma. Whilst some anti-mycoplasma antibiotics do exist, there are reports of re-infection shortly after treatment, and these drugs can be cytotoxic to the host cells (Molla Kazemiha et al., 2011). For this reason all cell lines used in this thesis were routinely tested for mycoplasma contamination using a mycoplasma polymerase chain reaction (PCR) detection kit (Sigma-Aldrich) following the manufacturer protocol (Dobrovolny and Bess, 2011).

2.1.2   Preparing gelatine-coated dishes

2% stock solution of gelatine (Sigma-Aldrich) diluted in distilled water was prepared, and autoclaved. Whilst at 50°C, the solution was aliquoted into falcon tubes and stored at 4°C. When required, 2% gelatine was warmed at 37°C until liquid, and diluted in

double distilled water (ddH$_2$O, Thermo Fisher Scientific) to create a 0.2% solution. Required culture dishes were covered in 0.2% gelatine, and incubated for a minimum of fifteen minutes at 37°C before use.

2.1.3   Producing LIF

Leukemia inhibitory factor (LIF) is a cytokine used as a media supplement in mouse embryonic stem cell (ESC) cultures to maintain mouse ESCs in a pluripotent, proliferative state; preventing spontaneous differentiation (Smith et al., 1988; Smith and Hooper, 1987; Williams et al., 1988).

2.1.3.1   Culturing COS-7 cells

COS-7 cells were quickly thawed in a 37°C water bath, and added to fresh cellular aggregate (CA) media (Dulbecco's modified eagle media (DMEM; Thermo Fisher Scientific), 10% fetal bovine serum (FBS; BioSera), Glutamax (Thermo Fisher Scientific), non-essential amino acids (NEAA; Thermo Fisher Scientific), 2-mercaptoethanol (Sigma-Aldrich)) in a 50 mL falcon tube (Corning). Cells were then centrifuged (Eppendorf 5810) at 180 relative centrifugal force (rcf) for three minutes. The supernatant was removed, and cells resuspended in CA media. Cells were then seeded onto 0.2% gelatine-coated 10 cm^2 Nunc dishes (VWR) in 10 mL CA media and incubated at 37°C/7% CO$_2$ until the cells reached around 70-80% confluency.

COS-7 cells were passaged by washing with phosphate-buffered saline (PBS; Thermo Fisher Scientific), and incubated with 0.05% trypsin (Thermo Fisher Scientific) for three minutes at 37°C. Fresh CA media was then added, and the cells transferred to a falcon tube. Cells were centrifuged at 180 rcf for three minutes before aspiration of the supernatant, and the cell pellet was resuspended in fresh CA media. COS-7 cells were then seeded at a low density onto 0.2%-gelatine coated 10 cm^2 Nunc dishes, and incubated at 37°C/7% CO$_2$ until the cells reached 70-80% confluency. The day before transfection, cells were passaged again (as detailed above), and plated at a 1:10 split ratio.

2.1.3.2   Transfection of COS-7 cells with pLIF

The next day a master mix of a LIF plasmid (10 μg per dish; plasmid gifted by Professor Meng Li, Cardiff University) and Lipofectamine 2000 reagent (20 μg per dish, Thermo Fisher Scientific) was made up in Opti-MEM (1 mL per dish, Thermo Fisher Scientific) and left at room temperature for fifteen minutes to allow the lipofectamine and plasmid to form nucleic acid-lipid complexes. Media was then removed from the dishes of COS-7 cells, and replaced with 5 mL Opti-MEM, and 1 mL master mix, and incubated at 37°C/7% CO_2 for 4-6 hours. After this time the transfection mixture was aspirated and replaced with 12 mL CA media, and the transfected cells incubated at 37°C/7% CO_2 for four days to allow secretion of LIF into the media. The media was then pooled into 50 mL falcon tubes, and centrifuged for three minutes at 180 rcf. The supernatant was filtered through 20 μm minisart filters (Sigma-Aldrich) to remove any cellular debris, collected, and stored in 0.5 mL aliquots at -80°C until required.

2.1.3.3   Testing LIF potency

To test the potency of the produced LIF, wild type E14 mouse ESCs were plated at a density of one thousand cells per well in 0.2% gelatine-coated, 12-well Nunc plates (VWR). These were plated in CA media with 15% FBS. Cells were treated with a serial dilution ($1:500-1:6.5 \times 10^6$) of LIF, and incubated at 37°C/7% CO_2. The resulting quality of ESC culture was observed over a period of five days and compared to a no-LIF control, and old LIF stock at 1:1000 dilution. If the new LIF at 1:1000 dilution resulted in a similar quality of ESC culture than the previous batch, and better than the no-LIF control, it was deemed suitable for use and tested for mycoplasma as outlined in section 2.1.1.

2.1.4   Culturing mouse embryonic fibroblasts

2.1.4.1   Background

Some mouse ESC lines, such as J1 ESCs, require culturing on mouse embryonic fibroblasts (MEFs) to prevent spontaneous differentiation. The mechanism by which MEFs improve ESC pluripotency is still undefined. However it is suspected that MEFs not only improve attachment of ESCs to the culture dish, but also that MEFs secrete various growth factors and molecules that support the survival, proliferation and pluripotency of mouse ESCs. Examples of identified secreted molecules from MEFs are transforming growth factor beta-1 (TGFβ) and Activin-A (Eiselleova et al., 2008; Tamm et al., 2013).

2.1.4.2   Wild type MEFS

C57BL/6J mice were time-mated, and plug checked the following morning. 13.5-14 days *post coitum (pc)*, pregnant females were culled by cervical dislocation, dissected, and embryos removed from the placenta. Embryos were washed in PBS, and the head, limbs, tail and organs removed and discarded. The remaining embryonic tissue was pooled in a 50 mL falcon tube, and washed twice with DMEM before transfer to a 10 cm^2 petri dish (VWR) on ice, and chopped using a sterile razor blade. Cut tissue was transferred into a fresh 50 mL tube, and incubated at 37°C with 20 mL 0.05% trypsin and DNase (20 µg/mL; Roche) for thirty minutes to dissociate the tissue. An additional 20 mL 0.05% trypsin was added, and the mixture incubated for a further thirty minutes at 37°C. Trypsin was inactivated by the addition of 10 mL FBS, and the tissue triturated with a 1 mL pipette before centrifugation at 180 rcf for fifteen minutes. The cell pellet was kept, whilst the supernatant was transferred to a separate 50 mL tube and centrifuged again to ensure that all cells had been collected. After aspirating the media, both cell pellets were resuspended in CA media supplemented with 1X penicillin-streptomycin (Thermo Fisher Scientific) to prevent bacterial contamination. The pooled cell suspension was passed through a 40 µm cell strainer (VWR) to remove any intact tissue. The cells were then seeded on 0.2% gelatine-coated 10 cm^2 Nunc dishes at a ratio of 1.5 embryos per dish, and incubated

at 37°C/7% CO_2. CA media was fully changed on alternate days. After reaching ~90% confluency, MEFs were passaged as outlined in section 2.1.4.5, and seeded at a 1:5 split ratio onto 0.2% gelatine-coated 10 cm^2 Nunc dishes. When confluent, MEFs were passaged again and resuspended in CA media with 10% dimethyl sulfoxide (DMSO; Sigma-Aldrich), and frozen to -80°C in a Mr. Frosty freezing container (Thermo Fisher Scientific). After freezing, MEFs were stored in liquid nitrogen until required.

2.1.4.3   Antibiotic-resistant MEFs

Antibiotic-resistant MEFs were required when growing ESCs with antibiotics (see section 2.2.5), which would otherwise result in the death of wild type MEFs. Geneticin-resistant MEFs were purchased from ATCC, whilst immortalised puromycin-resistant MEFs were purchased from Stem Cell Technologies.

2.1.4.4   Thawing MEFs

Stock wild type, or antibiotic-resistant MEFs were quickly thawed in a 37°C water bath. Thawed MEFs were added to CA media before centrifugation at 180 rcf for three minutes. The supernatant was removed, and the cell pellet resuspended in fresh CA media. MEFs were then seeded onto 0.2% gelatine-coated T25 or T75 flasks (VWR) and incubated at 37°C/7% CO_2. Cells were checked on a daily basis, and the media changed every 1-2 days.

2.1.4.5   Passaging MEFs

When confluent, MEFs were washed with PBS before incubation with 0.05% trypsin for three minutes at 37°C. MEFs were then resuspended in CA media, and transferred to 50 mL falcon tubes for centrifugation at 180 rcf for three minutes. After aspirating the supernatant, the cell pellet was resuspended in fresh CA media and MEFs plated on 0.2% gelatine-coated dishes.

2.1.4.6 Inactivating MEFs

To prevent MEFs over-proliferating when used as a substrate for ESC culture, they were inactivated prior to use. To do this, MEFs were incubated with 10 µg/mL mitomycin (Sigma-Aldrich) for two hours, and subsequently washed twice with PBS. MEFs were left to recover in CA media at 37°C/7% CO_2 for a minimum of one hour, and a maximum of three days. Before plating ESCs, CA media was replaced with fresh ES media (see section 2.1.5.2).

2.1.5 Culturing J1 and E14 ESCs

2.1.5.1 Background

ESC lines exist that originated from different mice, and therefore have alternative genetic backgrounds. As a result, these lines can have different requirements for efficient culture. For example, two commonly used wild type ESC lines are J1 (129S4/SvJae background) and E14 (129/Ola background) cells. Whereas J1 ESCs need to be cultured on MEFs to maintain their pluripotency, E14 ESCs can be cultured without MEFs on 0.2% gelatine-coated dishes (Smith, 1991).

2.1.5.2 Thawing ESCs

When culturing J1 ESCs, media from inactivated MEFs (section 2.1.4.6) was replaced with ES media (DMEM, NEAA, Glutamax, 2-mercaptoethanol, 15% FBS and LIF (produced in house, see section 2.1.3)). Wild type (ATCC), or genetically-modified J1 or E14 ESCs were thawed quickly at 37°C and added to ES media in a 50 mL tube. The ESCs were then centrifuged at 180 rcf for three minutes, and the supernatant aspirated. The cell pellet was resuspended in ES media and three million cells seeded into either a T25 flask of inactivated MEFs for J1 ESCs, or 0.2%-gelatine coated T25 flasks for E14 ESCs. Cells were then incubated at 37 °C/7% CO_2 until confluent, and the media changed every 1-2 days.

2.1.5.3 Passaging ESCs

When ESCs reached 70% confluency, they were passaged following a well-established protocol (Bibel et al., 2004, 2007). In brief, ESCs were washed with PBS before incubation with 0.05% trypsin for three minutes at 37°C. Following this, ESCs were resuspended in ES media, and transferred to a 50 mL tube, before centrifugation at 180 rcf for three minutes. The supernatant was removed, and the cell pellet resuspended in fresh ES media before plating onto a new flask of inactivated MEFS, or 0.2%-gelatine coated flasks for J1s and E14s, respectively. Whilst J1 ESCs were passaged at a 1:8-1:12 split ratio, E14 ESCs were passaged at a 1:3-1:6 split ratio.

2.1.5.4 Freezing ESCs

To store ESCs long term, stocks were frozen at early passages. To achieve this, ESCs were passaged as outlined in section 2.1.5.3, but after centrifugation, the cell pellet was instead resuspended in ES media with 10% DMSO. Cells were frozen down to -80°C in a Mr. Frosty freezing container and stored in liquid nitrogen until use.

2.1.5.5 Alternative ESC culture media

In this thesis the effects of different culture media on ESC quality was compared. Where stated, ESCs were passaged and maintained as above, but cultured in either 2I+LIF media (100 mL Neurobasal (Thermo Fisher Scientific), 100 mL DMEM-F12 (Thermo Fisher Scientific), 1 mL N2/BSA stock (1 mL 7.5% bovine serum albumin (BSA, Sigma-Aldrich) and 5 mL N2 supplement (Thermo Fisher Scientific)), 2 mL B27 without retinoic acid (Thermo Fisher Scientific), 2 mL Glutamax, 50 μM 2-mercaptoethanol (Thermo Fisher Scientific), 1 μM PD0325901 (Axon MedChem), 3 μM Chir99201 (Axon MedChem), 100 ng/mL recombinant LIF (Millipore)) or 2I+LIF media supplemented with 15% FBS (2I LIF + FBS). Where targeted E14 cells were cultured on feeders, the protocol outlined in section 2.1.5.3 was followed.

2.1.6 Sub-cloning ESCs

Where stated, ESCs were sub-cloned to isolate a population of ESCs with the desired characteristics, such as ESC cultures with less spontaneously differentiating cells. To do this, ESCs were thawed and expanded as outlined in sections 2.1.5.2 and 2.1.5.3. ESCs were then seeded onto 0.2%-gelatine coated 10 cm^2 Nunc dishes at a 1:200 split ratio, and incubated at 37°C/7% CO_2 for 5-9 days, until ESC colonies had formed that could be observed by eye. Media was changed every two days. The dishes were then washed with PBS before the addition of 0.01% trypsin (0.05% trypsin diluted 1:5 in PBS). Single colonies were aspirated using a pipette set at 20 µL, with a 200 µL tip, and transferred to individual wells of a 96-well plate (VWR). These individually picked colonies were incubated with 20 µL 0.05% trypsin for three minutes at 37°C before resuspending with 100 µL ES media. ESCs were then plated on inactivated-MEFs on a 24-well plate (for J1 ESCs), or a 0.2% gelatine-coated 24 well plate (for E14 ESCs). ESCs were then incubated at 37°C/7% CO_2, and media changed every two days until the cells reached 70% confluency. ESCs were subsequently passaged and expanded as outlined in section 2.1.5.3.

2.2   Generating mouse ESCs that overexpress TrkA or TrkB

2.2.1   Rationale

To generate an inducible expression system of TrkA or TrkB in ESCs (Figure 2.1), E14 and J1 *Rosa26-CreER^{T2};Mapt-loxP-STOP-loxP-HA-rTrkA,* or *-rTrkB* mouse ESC lines were generated.

In these ESCs the Trk receptors were expressed under the neuron-specific microtubule associated protein (*Mapt)* promoter (Binder et al., 1985; Jaisser, 2000). In this model, TrkA and TrkB were tagged with hemagglutinin (HA), a small sequence consisting of nine amino acids that is widely used and has not been reported to interrupt the activity of the protein it is tagged to (Nikoletopoulou et al., 2010). By having a HA tag, it is possible to discriminate between endogenous Trk expression and the exogenous tagged construct.

However due to the presence of a loxP-STOP-loxP sequence preceding the Trk receptor sequences in this construct, they would not be expressed under physiological conditions. In order to express TrkA or TrkB, the loxP-flanked STOP needs to be excised, which can be achieved using a Cre recombinase enzyme. In the current model, the Cre recombinase was fused to a triple mutated human oestrogen receptor (Cre-ER^{T2}) (Jaisser, 2000), and expressed under the ubiquitous *Rosa26* promoter (Soriano, 1999). Through interactions with heat-shock protein 90 (Hsp90), Cre-ER^{T2} is normally sequestered in the cytoplasm (Hayashi and McMahon, 2002; Mattioni et al., 1994; Nagy, 1999; Picard, 1994). However, upon Cre-ER^{T2} binding the synthetic ligand 4-hydroxytamoxifen (tamoxifen), Hsp90 is disrupted, and Cre-ER^{T2} translocated into the nucleus (Feil et al., 1997; Tian et al., 2006) (Figure 2.1). When in the nucleus, the Cre enzyme can recombine the loxP-flanked STOP cassette (Jones-Villeneuve et al., 1982). In this way, the expression of TrkA or TrkB in neurons could be temporally controlled by the addition of tamoxifen to cultures of these genetically modified ESCs (Hayashi and McMahon, 2002; Mattioni et al., 1994; Picard, 1994).
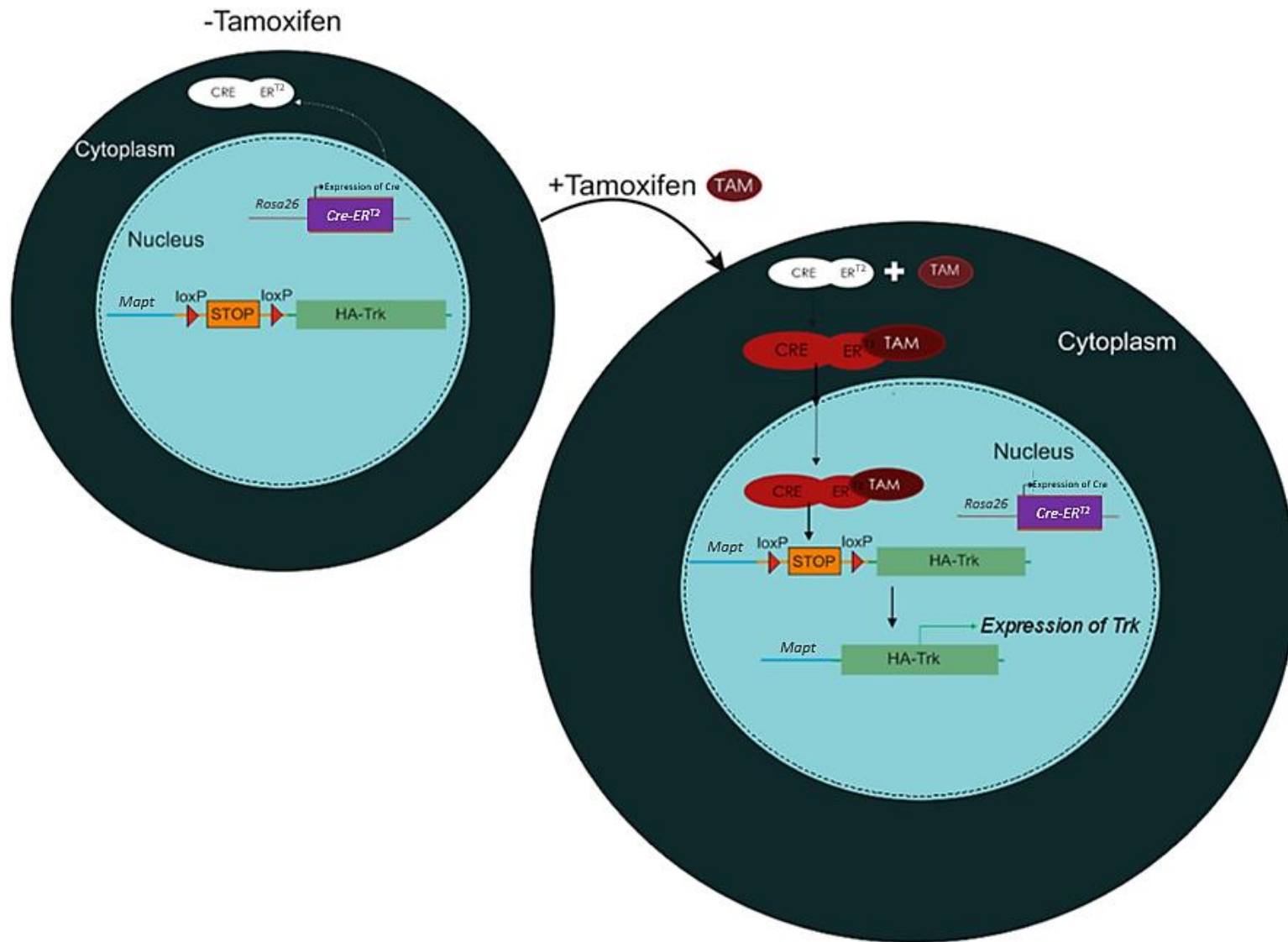
Figure 2.1 Tamoxifen-induced expression of TrkA or TrkB in ESCs. A Cre recombinase-oestrogen receptor fusion protein (CreER[T2]; purple) is expressed under the ubiquitous *Rosa26* promoter and remains in the cytoplasm (navy), thus preventing its binding to nuclear DNA. With the addition of tamoxifen to ESC cultures, the activated CreER[T2] (red) protein translocates into the nucleus where it excises the loxP-flanked STOP cassette (orange) that immediately precedes the *Trk* receptor sequences (green), allowing temporal control of *Trk* receptor expression in ESCs.

2.2.2 Generating pMapt-loxp-STOP-loxP-HA-rTrkA and -rTrkB plasmids

2.2.2.1 Preparation of Agar plates

3.5% agar (Sigma-Aldrich) was dissolved in ddH$_2$O and autoclaved. After cooling to 50°C, agar was supplemented with either 50 µg/mL kanamycin (Sigma-Aldrich), or 50 µg/mL ampicillin (Sigma-Aldrich). For details of when each antibiotic was used, see section 2.2.5. The agar was then poured into 10 cm^2 petri dishes and left until the agar had set. Dishes were stored at 4°C for up to one month. One hour before use, agar plates were opened and placed face down in a 37°C incubator to remove any excess moisture.

2.2.2.2 Preparation of L-broth

2.5% L-broth (Sigma) was dissolved in ddH$_2$O and autoclaved. Antibiotics were added (as outlined in section 2.2.2.1) once L-broth had cooled to room temperature. L-broth was stored at 4°C for up to two weeks.

2.2.2.3 Digestion and purification

2 µg of an existing plasmid (pSIEG) that contains a 1.5 kilobase (kb) loxP-STOP-loxP sequence was digested with *EcoRI* (NEB) and *XbaI* (NEB) (Figure 2.2) at 37°C for three hours. Subsequently the mixture was incubated with large Klenow DNA polymerase (NEB) and deoxynucleotide triphosphates (dNTPs, NEB) for one hour at 37°C to blunt the ends. This was then incubated at 70°C to inactivate the enzymes. The digested, blunted 1.5 kb STOP fragment was purified following the microcentrifuge protocol of the QIAquick gel extraction kit (Qiagen) from step 2 of the protocol (the addition of QG buffer). This mixture was then electrophoresed on a 1% agarose (Thermo Fisher Scientific) gel supplemented with 0.2 µg/mL ethidium bromide (Sigma-Aldrich) for two hours. The corresponding 1.5 kb band was manually excised from the gel and transferred to a fresh 1.5 mL tube. The DNA was then extracted

following the microcentrifuge protocol of the QIAquick gel extraction kit from step 1 of the protocol.

Meanwhile, 2 µg of pMapt-HA-rTrkA or -rTrkB plasmids were linearised by digestion with *PmeI* (NEB) (Figure 2.2) at 37°C for three hours. The mixture was subsequently incubated with antarctic phosphatase (NEB) at 37°C for one hour to dephosphorylate vector ends, preventing self-ligation of the plasmid. After this, the enzymes were inactivated by incubation of this mixture at 70°C for fifteen minutes. The linearised plasmids were then electrophoresed on a 1% agarose gel supplemented with 0.2 µg/mL ethidium bromide for one hour. The corresponding band ~10 kb was manually excised from the gel, and placed into dialysing tubes (Sigma-Aldrich) filled with 300 µL TAE buffer (40 mM tris base (Thermo Fisher Scientific), 20 mM acetic acid (Sigma-Aldrich), 1 mM ethylenediaminetetraacetic acid (EDTA; Sigma-Aldrich), in distilled water) and electrophoresed for three to four hours, until the DNA could no longer be visualised in the gel. The resulting DNA solution was transferred to a 1.5 mL tube (Eppendorf) and precipitated with 50 µL 3 M sodium acetate (NaOAc, Sigma-Aldrich), and 500 µL 100% isopropanol (Sigma-Aldrich) overnight at 4°C. The next day the mixture was centrifuged for fifteen minutes at 20000 rcf, and the supernatant removed. The DNA pellet was washed with 70% ethanol (VWR) and centrifuged for a further five minutes at 20000 rcf, and the supernatant was aspirated. The DNA pellet was then eluted in 30 µL buffer EB (Qiagen).

2.2.2.4   Ligation

3 µL of linearised, purified pMapt-HA-rTrkA or -rTrkB plasmid were each ligated to 6 µL of the purified loxP-STOP-loxP fragment using quick T4 DNA ligase (NEB) for ten minutes at room temperature (Figure 2.2). 4 µL of the ligation mixture was then transformed into one shot TOP10 *Escherichia coli (E.coli)* (Thermo Fisher Scientific) by heat shock through immersion in a 42°C water bath for thirty seconds. After recovery in 300 µL super optimal broth with catabolite repression (S.O.C.) media (Thermo Fisher Scientific) for up to one hour at 37°C, bacteria were spread onto agar plates supplemented with ampicillin. Dishes were incubated overnight at 37°C to allow colony formation.
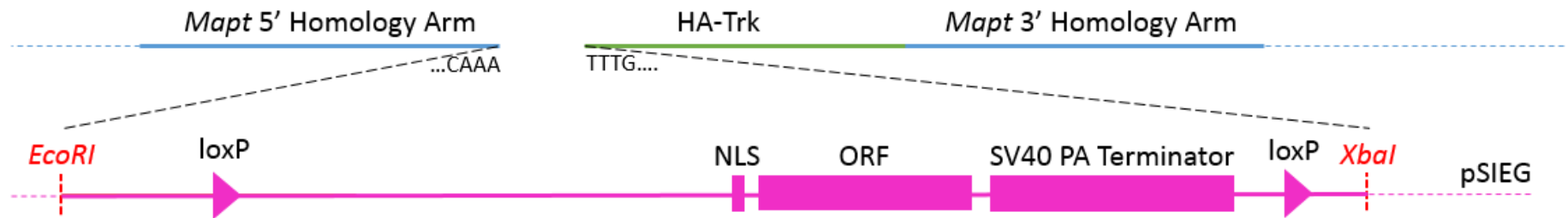
Figure 2.2 Generation of pMapt-loxP-STOP-loxP-HA-rTrkA and -rTrkB vectors. A) Existing pMapt-HA-rTrkA and -rTrkB constructs were linearised by restriction digestion with *PmeI* enzyme. B) The loxP-STOP-loxP cassette was isolated from the pSIEG plasmid by digestion with *EcoRI* and *XbaI*, and then ligated into the linearised pMapt-HA-rTrkA and -rTrkB vectors. NLS – nuclear localisation signal, ORF – open reading frame, SV40 PA terminator – poly A terminator sequence.

2.2.2.5   Extracting DNA from bacterial colonies

Bacterial colonies were picked the next morning using a 10 µL pipette, and individually added to 4 mL L-broth (Sigma-Aldrich) with 50 µg/mL ampicillin into 12 mL plastic culture tubes (Fisher Scientific). Bacteria were incubated overnight at 37°C on a shaker. DNA was then extracted from 1.8 mL samples of each bacterial culture using a miniprep kit (Qiagen) following the manufacturer protocol. The remaining bacteria were stored at 4°C until required.

2.2.2.6   Identifying cultures with the desired plasmid

To identify which bacterial clones contained the correct plasmid (insertion of the loxP-STOP-loxP cassette in the correct orientation), 2 µL of DNA, extracted via miniprep, was digested with *HindIII* (NEB) for one hour at 37°C. Digested DNA was then electrophoresed on a 1% agarose gel with 0.2 µg/mL ethidium bromide for one hour. Gels were imaged in a UV docking station (Biorad). Based on analysis of the digested band sizes (Chapter 3), the clones thought to have the required plasmid were amplified by incubating 100 µL of the remaining bacterial stock in 100 mL L-broth supplemented with 50 µg/mL ampicillin overnight in a 37°C shaker. DNA was then extracted from these bacteria using a maxiprep kit (Qiagen), following the manufacturer protocol. DNA was sequenced using Sanger sequencing (Eurofins) to confirm the sequence.

2.2.3 Targeting the *Mapt* locus

2.2.3.1 Theory

Clustered regularly interspaced short palindromic repeats (CRISPR) is a technique for genome-editing where a single-guide RNA (sgRNA) forms Watson-Crick base-pairs with target genomic DNA(Ran et al., 2013). This guides a Cas9 endonuclease to the site of the sgRNA, where Cas9 cleaves the double-stranded DNA, three base pairs up from a 5' NGG protospacer adjacent motif (Figure 2.3). To repair these breaks in the DNA, cells undergo a homology-directed repair pathway when a template donor (construct) with sequences homologous to the damaged DNA is present, resulting in insertion of the construct (Ran et al., 2013).
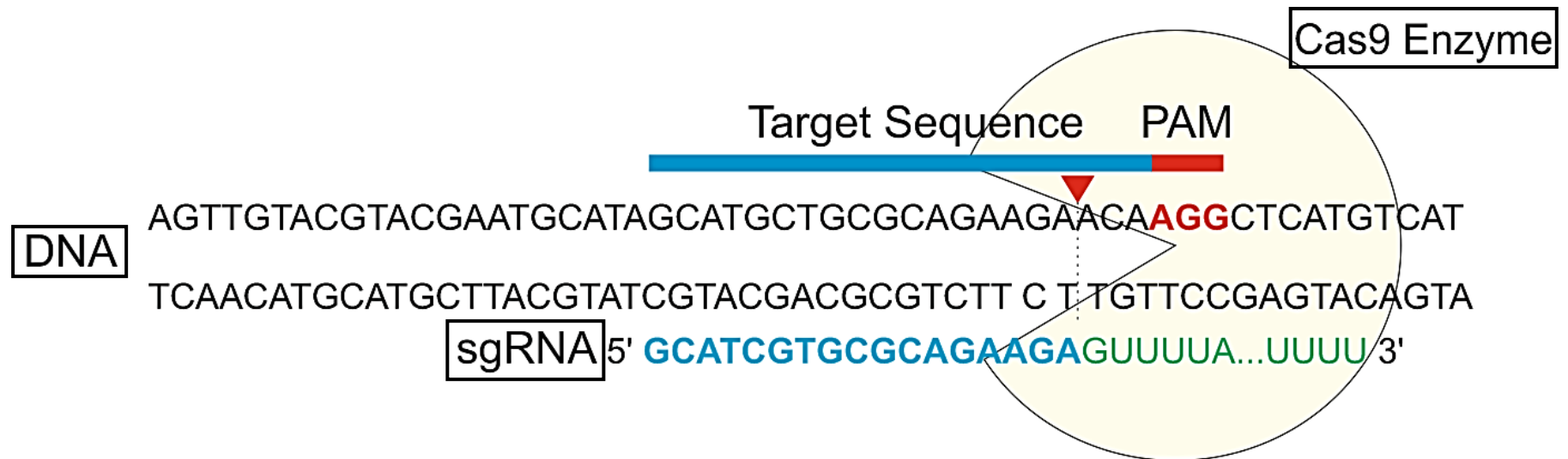
Figure 2.3 CRISPR genome editing. A single guide RNA (sgRNA) forms Watson-Crick base pairs with the target DNA. The sgRNA guides the Cas9 endonuclease to cleave both DNA strands (site indicated by red arrow and dashed line), three base pairs up from a NGG protospacer adjacent motif (PAM). This break in the DNA stimulates endogenous DNA repair mechanisms, which allows insertion of a construct with homologous sequences to the break site.

2.2.3.2 Generating sgRNA

sgRNA for the *Rosa26* and *Mapt* target sites were designed using an online tool (http://crispr.mit.edu/). The resulting sequences (*Mapt*: CTCCAGGCTTTGAACCAGTA and *Rosa26*: CTAGCAGTTTAAACAAAT) were incorporated into a 455 nucleotide sequence template (Figure 2.4), and ordered from IDT. The sgRNA fragment was then amplified through PCR using the reagents and cycle conditions outlined in Table 2.1.

TGTACAAAAAAGCAGGCTTTAAAGGAACCAATTCAGTCGACTGGATC
CGGTACCAAGGTCGGGCAGGAAGAGGGCCTATTTCCCATGATTCCTT
CATATTTGCATATACGATACAAGGCTGTTAGAGAGATAATTAGAATT
AATTTGACTGTAAACACAAAGATATTAGTACAAAATACGTGACGTAG
AAAGTAATAATTTCTTGGGTAGTTTGCAGTTTTAAAATTATGTTTTAA
AATGGACTATCATATGCTTACCGTAACTTGAAAGTATTTCGATTTCTT
GGCTTTATATATCTTGTGGAAAGGACGAAACACC**GNNNNNNNNNNN**
NNNNNNNNNGTTTTAGAGCTAGAAATAGCAAGTTAAAATAAGGCTA
GTCCGTTATCAACTTGAAAAAGTGGCACCGAGTCGGTGCTTTTTTTCT
AGACCCAGCTTTCTTGTACAAAGTTGGCATTA

Figure 2.4 Single-guide RNA template sequence. . The sequence of the entire sgRNA is indicated above. **Black** nucleotides indicate a U6 promoter. **Green**, bold nucleotides indicate the guide sequence which is determined by the target DNA. **Blue** nucleotides are the guide RNA scaffold. **Red** nucleotides indicate the termination signal.

Table 2.1 Amplifying *Rosa26* and *Mapt* sgRNA fragments

Reagents	Final Concentration	PCR Conditions
Nuclease-free water (Qiagen)	Up to 50 µL	
5x Phusion high fidelity buffer (NEB)	1 x	
10 mM dNTPs (NEB)	0.2 mM	98°C - 30 seconds
Forward primer (Thermo Fisher Scientific) (TGTACAAAAAAGCAGGCTTTAAAG)	0.5 µM	98°C - 10 seconds 58°C - 30 seconds x35 cycles 72°C - 30 seconds
10 µM reverse primer (Thermo Fisher Scientific) (TAATGCCAACTTTGTACAAGAAAG)	0.5 µM	72°C - 5 minutes
gBlocks gene fragment (IDT)	1 ng	
Phusion DNA polymerase (NEB)	1 unit	

The resulting PCR products were then blunted with large Klenow polymerase for one hour at 37°C, and gel purified following the microcentrifuge protocol of the QIAquick gel extraction kit. To allow further amplification, sgRNA were ligated into a generic cloning vector (TopoII-isomerase, Thermo Fisher Scientific) with salt solution (Thermo Fisher Scientific) at a 4:1:1 ratio respectively at room temperature for five minutes. 2 µL of the ligation mixture was then transformed into one shot TOP10 *E. coli* through 30 second heat shock by immersion in a 42°C water bath, and left to recover in 300 µL S.O.C. media for one hour shaking at 37°C. The transformed *E. coli* were spread on agar dishes supplemented with 50 µg/mL kanamycin (Sigma-Aldrich) and left overnight at 37°C to allow the bacteria to form colonies. Colonies were picked using a 10 µL pipette tip, and individually added to 4 mL L-broth supplemented with 50 µg/mL kanamycin in 12 mL plastic culture tubes. These were incubated at 37°C overnight, on a shaker. DNA was then extracted from 1.8 mL bacteria samples the next day using a miniprep kit (Qiagen), following the manufacturer protocol. Remaining bacteria were frozen at -80°C in 40% glycerol. To diagnose whether insertion of the sgRNA into the bacteria was successful, the DNA extracted via miniprep was digested using restriction enzymes *BamHI* (NEB) and *XbaI* (NEB) for three hours at 37°C, and electrophoresed on a 1% agarose gel supplemented with 0.2 µg/mL ethidium bromide for one hour. After selecting clones with bands corresponding to successful insertion (~5 kb, ~400 bp, and ~100 bp) the sequence was confirmed via Sanger sequencing. To amplify the plasmid, frozen bacterial stocks were added to 100 mL L-broth supplemented with 50 µg/mL kanamycin and incubated in a 37°C shaker overnight. The next day an endonuclease free, plasmid maxiprep (Qiagen) was performed, following manufacturer guidelines.

2.2.4 Targeting *Rosa26*

2.2.4.1 Strategy

Zinc finger nucleases (ZFNs) are composed of a nonspecific DNA cleavage domain of the *FokI* restriction endonuclease and a combination of zinc finger proteins that constitute the DNA binding domains. Each zinc finger can recognise three nucleotides, so that multiple zinc fingers can be assembled to recognise specific DNA sequences in target genes. ZFNs are used in heterodimer pairs to cleave the target site, as the *FokI* nuclease domain requires dimerization to create a double stranded break in the target DNA. As in CRISPR, this double stranded break induces the process of homology-directed recombination (Beerli and Barbas, 2002; Beerli et al., 2000; Liu, Segal, et al., 1997). The *Rosa26* locus was targeted to generate J1 *Rosa26-CreER^{T2}, Rosa26-loxP-STOP-loxP-HA-rTrkA* and *−rTrkB* E14 ESCs. pRosa26-CreER^{T2} was gifted by Professor Francis Stewart (Dresden University), and pRosa26- loxP-STOP-loxP-HA-rTrkA and −rTrkB plasmids generated by Dr. Xinsheng Nan (Cardiff University).

2.2.4.2 Targeting ESCs with Rosa26 ZFNs

In order to target the *Rosa26* locus, the mRosa26 CompoZr Targeted Integration Kit (Sigma-Aldrich) was utilised. The three targeting constructs (pRosa26-CreER^{T2}, pRosa26-loxP-STOP-loxP-HA-rTrkA, and -rTrkB) were cloned into the kit-provided donor plasmid, pZDonor-mRosa26, by Dr. Xinsheng Nan following the manufacturer protocol.

2.2.5 Transfection of E14 & J1 ESCs

J1 wild type cells underwent two rounds of transfection sequentially; the first round of transfections targeted the *Rosa26* locus to establish a J1 *Rosa26-CreER^{T2}* line, and the second to *Mapt* to generate J1 *Rosa26-CreER^{T2};Mapt-loxP-STOP-loxP-HA-rTrkA* or *-rTrkB* ESCs (Table 2.2). As E14 *Rosa26-CreER^{T2}* cells had been previously generated by Dr. Xinsheng Nan, these ESCs only underwent one round of transfections to target

Mapt in order to generate the corresponding E14 *Rosa26-CreER^{T2};Mapt-loxP-STOP-loxP-HA-rTrkA* or *-rTrkB* ESCs. J1 and E14 wild type ESCs were also transfected once to generate *Mapt-loxP-STOP-loxP-HA-rTrkA* or *–rTrkB* ESC lines without Cre.

As E14 *Rosa26-loxP-STOP-loxP-HA-rTrkA* ESCs had been previously generated by Dr. Xinsheng Nan, the corresponding E14 *Rosa26-loxP-STOP-loxP-HA-rTrkB* ESCs were produced here.

Before targeting, wild type ESCs were cultured and expanded as outlined in section 2.1. The day prior to transfection, ESCs were passaged at a 1:5 split ratio onto a minimum of two T75 flasks. On the day of transfection, ESCs were washed once with PBS before the addition of 0.05% trypsin. Cells were incubated for three minutes at 37°C before trypsin was inactivated by the addition of ES media. The cell suspension was then centrifuged at 180 rcf for three minutes before resuspension of the cell pellet in ES media, and counted using a nucleocounter (Chemometec) following the manufacturer protocol. 5×10^6 dissociated ESCs were transferred to a 50 mL falcon tube per transfection, and centrifuged again at 180 rcf for three minutes. The pellet was then resuspended in 100 μL P3 transfection solution (82 μL Amaxa Buffer and 18 μL P3 supplement; Lonza) and 10 µL of respective DNA mixture. Where CRISPR targeting was required, the DNA mixture contained the corresponding sgRNA, targeting construct and Cas9 enzyme at a 1 µg: 10 µg: 1 µg ratio, respectively, and made up to a total volume of 10 μL. Where zinc finger targeting of the Rosa26 locus was used, 10 µg of the ZFN-plasmid (generated in section 2.2.4.2) was used.

The entire suspension was then transferred to a cuvette (Lonza) and placed into a 4D-Amaxa Nucleofector X-unit (Lonza) where the cells were transfected using the manufacturer program CG-104. After transfection, a drop of media was added to the cuvette using a Pasteur pipette (Lonza) and cells transferred to a new 50 mL falcon tube containing 10 mL ES media. Transfected cells were then seeded onto either 0.2% Gelatine-coated 10 cm^2 Nunc dishes if transfecting E14 ESCs, or on pre-prepared inactivated puromycin/geneticin-resistant (depending on the targeting construct; Table 2.2) MEFs on 10 cm^2 Nunc dishes if transfecting J1 ESCs. Varying volumes of transfected ESCs were plated, from 0.625-2.5 mL per dish. This was to ensure the optimal density for picking colonies. Dishes were then incubated at 37°C/7% CO$_2$. 24-48 hours later, the respective selection antibiotic was applied:

Geneticin (250 µg/mL) or puromycin (1.5 µg/mL). Media supplemented with the selection antibiotic was subsequently changed every two days.

When individual ESC colonies were visible by eye, the dishes were washed with PBS before the addition of 0.01% trypsin (0.05% trypsin diluted 1:5 in PBS). Single colonies were aspirated using a pipette set at 20 µL, with a 200 µL tip, and transferred to individual wells of a 96-well plate that contained 20 µL 0.05% trypsin. ESCs were incubated in trypsin for three minutes before resuspending in 100 µL of ES media. Resuspended cells were then transferred to a 24-well plate (0.2% gelatine-coated for E14 ESCs, inactivated puromycin-/geneticin-resistant MEFs for J1s) and cultured in ES media with the respective selection antibiotic. Between 50-100 colonies were picked per transfection. ESCs were incubated at 37°C/7% CO_2 on these 24-well plates, and media changed every two days (supplemented with antibiotic) until the cells in individual wells reached 70-80% confluency.

Individual wells were then washed once with PBS before incubation with 100 µL 0.05% trypsin for three minutes at 37°C. After the addition of 1 mL ES media. 1/10th of the cell suspension was transferred to a new 24-well plate (0.2% gelatine-coated for E14 ESCs, or with pre-prepared inactivated MEFs for J1 ESCs) for passaging as outlined in section 2.1, and the remaining cell suspension transferred to an Eppendorf tube for genomic DNA extraction (section 2.2.6).

Table 2.2 List of generated ESC lines

Line	Starting Mutation	Targeting Method	Targeting Construct	Resistance	MEFs	Resulting ESC Line	Reference
E14	Wild Type	Zinc Finger	*Rosa26-CreER^{T2}*	Puromycin	NA	E14 *Rosa26-CreER^{T2}*	Chapter 3 E14 Control *
E14	Wild Type	CRISPR	*Mapt-loxP-STOP-loxP-HA-rTrkA*	Geneticin	NA	E14 *Mapt-loxP-STOP-loxP-HA-rTrkA*	Chapter 3 E14 No CreER^{T2} Control
E14	Wild Type	CRISPR	*Mapt-loxP-STOP-loxP-HA-rTrkB*	Geneticin	NA	E14 *Mapt-loxP-STOP-loxP-HA-rTrkB*	Chapter 3 E14 No CreER^{T2} Control
E14	*Rosa26-CreER^{T2}*	CRISPR	*Mapt-loxP-STOP-loxP-HA-rTrkA*	Geneticin	NA	E14 *Rosa26-CreER^{T2};Mapt-loxP-STOP-loxP-HA-rTrkA*	Chapter 3 E14 Experimental TrkA
E14	*Rosa26-CreER^{T2}*	CRISPR	*Mapt-loxP-STOP-loxP-HA-rTrkB*	Geneticin	NA	E14 *Rosa26-CreER^{T2};Mapt-loxP-STOP-loxP-HA-rTrkB*	Chapter 3 E14 Experimental TrkB
J1	Wild Type	Zinc Finger	*Rosa26-CreER^{T2}*	Puromycin	Puromycin-resistant	J1 *Rosa26-CreER^{T2}*	Chapter 3 J1 Control
J1	*Rosa26-CreER^{T2}*	CRISPR	*Mapt-loxP-STOP-loxP-HA-rTrkA*	Geneticin	Geneticin-resistant	J1 *Rosa26-CreER^{T2};Mapt-loxP-STOP-loxP-HA-rTrkA*	Chapter 3 J1 Experimental TrkA
J1	*Rosa26-CreER^{T2}*	CRISPR	*Mapt-loxP-STOP-loxP-HA-rTrkB*	Geneticin	Geneticin-resistant	J1 *Rosa26-CreER^{T2};Mapt-loxP-STOP-loxP-HA-rTrkB*	Chapter 3 J1 Experimental TrkB
E14	Wild Type	Zinc Finger	*Rosa26-loxP-STOP-loxP-HA-rTrkA-IRES-EGFP*	Puromycin	NA	E14 *Rosa26-loxP-STOP-loxP-HA-rTrkA-IRES-EGFP*	Chapter 4 Blastocyst Injections *
E14	Wild Type	Zinc Finger	*Rosa26-loxP-STOP-loxP-HA-rTrkB-IRES-EGFP*	Puromycin	NA	E14 *Rosa26-loxP-STOP-loxP-HA-rTrkB-IRES-EGFP*	Chapter 4 Blastocyst Injections

ESCs indicated with an asterisk were generated by Dr. Xinsheng Nan.

2.2.6   Genotyping ESCs and neurons

2.2.6.1   Extracting DNA

Cell suspensions in 1.5 mL tubes were centrifuged at 180 rcf for one minute, and the pellet resuspended in 500 µL DNA lysis buffer (10 mM Tris (Thermo Fisher Scientific) pH 8.0, 1 mM calcium chloride ($CaCl_2$; Sigma-Aldrich), 100 mM sodium chloride (NaCl; Sigma-Aldrich), 0.5% sodium dodecyl sulfate (SDS; Sigma-Aldrich), 5 mg/mL proteinase K (Promega)). Samples were then incubated at 50°C overnight. DNA was precipitated the next morning by the addition of 500 µL 100% isopropanol, and 50 µL 3 M NaOAc, inverted, and centrifuged at top speed at 20000 rcf for fifteen minutes at room temperature. Supernatant was carefully removed, and 500 µL 70% ethanol added. Samples were centrifuged for a further five minutes at 20000 rcf before resuspending the DNA pellet in 30 µL Tris-EDTA buffer (TE buffer; Qiagen).

2.2.6.2   Genotyping PCR

To test that the respective constructs were inserted into the correct region in ESCs, primer pairs were generated with a forward primer upstream of the construct's *Rosa26* or *Mapt* 5' homology arm, and a reverse primer in the construct itself. Therefore a polymerase chain reaction (PCR) would only amplify a product if the construct was inserted into the correct region. This was achieved using the Long-range Sequal Prep PCR kit (Thermo Fisher Scientific) following manufacturer guidelines with two points of note; 1) Enhancer A (provided in the kit) was used instead of enhancer B, and 2) 1 µL of DNA mixture was used as a template. The PCR primers are outlined in Table 2.3, and cycling (Table 2.3) carried out in a BIORAD T100 Thermal cycler. After amplification the mixture was supplemented with 4 µL DNA loading buffer (10 mM Tris-HCl (pH 7.5), 50 mM EDTA, 50% glycerol, 1 mg/mL bromophenol blue (Sigma)) and loaded onto a 1% agarose gel supplemented with 0.2 µg/mL ethidium bromide, and electrophoresed for one hour. Bands were detected using a UV docking station.

Table 2.3 Genotyping primers and PCR conditions for transfected ESCs

Genotyping for insertion of:	Forward Primer	Reverse Primer	PCR Conditions		
Rosa26-CreER^{T2}	TACGCCACAGGGAGTCCAAGAATG	GACCGACGATGAAGCATGTTTAGC	95°C 3 minutes 95°C 30 seconds 57°C 30 seconds 68°C 4.5 minutes 72°C 5 minutes	x 35 cycles	
Mapt-loxP-STOP-loxP-HA-rTrkA	CCCATGGCAGCTCACAAGTATC	ATCCCGCTGGTTTTCCACAT	95°C 3 minutes 95°C 30 seconds 60.3°C 30 seconds 68°C 4.5 minutes	x 10 cycles	
			95°C 30 seconds 60.3°C 30 seconds 68°C 4.5 minutes (+ 10 sec/cycle)	x25 cycles	
			72°C 5 minutes		
Mapt-loxP-STOP-loxP-HA-rTrkB	CCCATGGCAGCTCACAAGTATC	CCAAATTCCCAACGTCCCAGTACAAG	95°C 3 minutes 95°C 30 seconds 60.3°C 30 seconds 68°C 7 minutes	x 10 cycles	
			95°C 30 seconds 60.3°C 30 seconds 68°C 7 minutes (+ 10sec/cycle)	x25 cycles	
			72°C 5 minutes		
Rosa26-loxP-STOP-loxP-HA-rTrkB	CAAGCGGGTGGTGGGCAGGAATGCG	TCGGCAGGAGCAAGGTGAGATGAC	95°C 3 minutes 95°C 30 seconds 60°C 30 seconds 68°C 2.5 minutes	x 35 cycles	
			72°C 5 minutes		

2.2.7 Karyotyping

2.2.7.1 General considerations

All cell lines detailed in this thesis were selected based on having the correct number of chromosomes. This was especially important where cells were being used to create transgenic mice. The karyotype of each ESC line was calculated as the percentage of cells with the correct number of chromosomes (forty in mice (Schnedl, 1971)).

2.2.7.2 Karyotyping

The day before karyotyping individual ESC clones were passaged at a 1:5 split ratio onto 0.2% gelatine-coated T25 flasks as outlined in section 2.1.5.3. Plates were incubated at 37°C/7% CO_2 overnight. The next day demecolcine solution (0.1 µg/mL; Sigma-Aldrich) was added to the cells for two hours and cells placed back at 37°C/7% CO_2. Cells were then washed with PBS and incubated with 0.05% trypsin for three minutes at 37°C. Cells were resuspended in 5 mL ES media and transferred to a 15 mL falcon tube (Corning) for centrifugation at 340 rcf for three minutes. Supernatant was removed, and the cell pellet washed with PBS before centrifugation again at 340 rcf for three minutes. Cells were washed one further time with PBS, and the supernatant removed. Cells were then resuspended in 2 mL PBS and 6 mL hypotonic 0.0375 M potassium chloride (KCl; Sigma-Aldrich) solution, and incubated at 37°C for twelve minutes to allow the cells to swell. Samples were then centrifuged for five minutes at 244 rcf, and the supernatant aspirated. 3.5 mL methanol/acetic acid mixture (3:1 volume:volume ratio, -20°C; Sigma-Aldrich) was then added dropwise to the cells and left for twenty minutes at room temperature. Samples were centrifuged for five minutes at 244 rpm, and supernatant removed before a further 3.5 mL methanol/acetic acid mixture was added to the cells. Cells were centrifuged at 244 rcf for five minutes, and supernatant aspirated until around 0.1 mL was left. Cells were resuspended in this volume, and dropped from a height of around thirty centimetres onto polylysine adhesion slides (VWR). Two drops of cell suspension were added per slide. Slides were left to air dry, before adding 150 µL 4',6-diamidino-2-phenylindole (DAPI, 1:4000 in ddH_2O, Sigma-Aldrich). Coverslips (24 mm x 50 mm; VWR) were placed on top of the cells and slides imaged immediately.

2.2.7.3 *Imaging and analysis*

Slides were imaged using a fluorescence microscope at x40 magnification. Images were taken for a minimum of ten cells per clone (Figure 2.5). Chromosomes were counted using the cell counter plugin on ImageJ software. The chromosomes were counted for each cell, taking note of any abnormalities such as translocations. The percentage of cells with the correct number of chromosomes were then calculated. Clones with over 70% of cells with forty chromosomes were expanded and used for cell culture or generating transgenic mice.
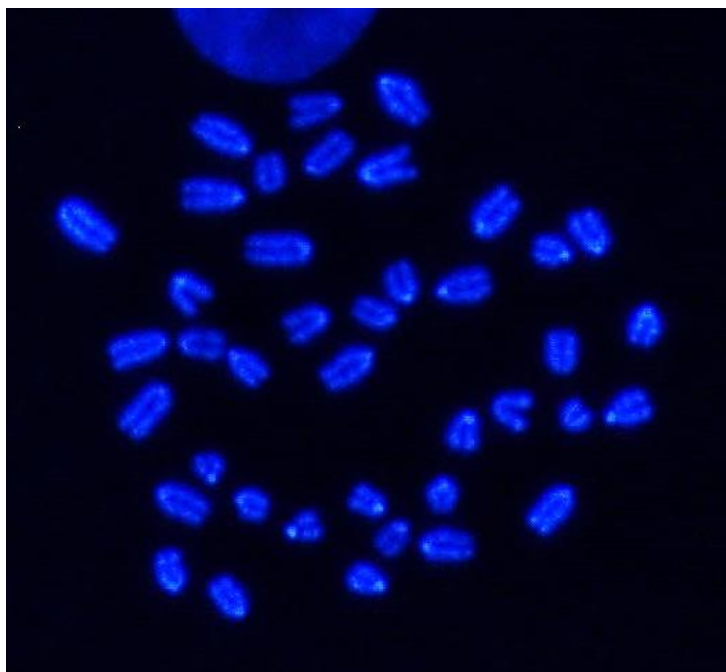
Figure 2.5 Visualisation of chromosomes. Representative image of forty, individual chromosomes (blue). Note that chromosomes are distinguishable from one another, and are not fused.

2.3 Differentiating ESCs into cortical-like neurons

2.3.1 Preparing ESCs

Targeted or wild type ESCs were differentiated following a well-established protocol (Bibel et al., 2004, 2007) (Figure 2.6). In brief, ESCs were passaged 4-6 times after thawing, as outlined in section 2.1.5.2. In the case of cells with a J1 background, ESCs were passaged a further two times on 0.2% gelatine-coated T75 flasks before differentiation. This was done to reduce the ratio of feeders to ESCs, as the presence of feeders can result in aggregates sticking to the dish and subsequently affect the quality of the differentiation.

2.3.2 Generating cellular aggregates

When ESCs were of a good quality (see publication for details (Bibel et al., 2004, 2007)), they were passaged as outlined in section 2.1.5.3, but after centrifugation the cell pellet was resuspended in CA media. Cells were counted using the nucleocounter, and 4×10^6 cells plated per 10 cm^2 uncoated petri dish in 15 mL CA media. Dishes were incubated at 37°C/7% CO_2 for eight days to allow formation of cellular aggregates (CAs). CA media was gently changed every two days using a 25 mL stripette to transfer CAs to a 50 mL falcon tube. CAs were left to settle, before the supernatant was carefully removed and 15 mL fresh CA media added. Cells were then gently transferred to a new 10 cm^2 petri dish (Figure 2.6). Retinoic acid (5 µM; Sigma-Aldrich) was added on media changes at day 4 and day 6 to trigger neuronal differentiation(Bain et al., 1996; Jones-Villeneuve et al., 1982). On the sixth day of aggregation, poly-DL-ornithine hydrobromide (PORN; Sigma-Aldrich) was diluted in Borate buffer (150 mM boric acid (Sigma-Aldrich), pH 8.3) and filtered to create a stock which could be kept up to one week at 4°C. This was then freshly diluted 1:5 in ddH$_2$O (Thermo Fisher Scientific), and 0.5 mL plated per well in 12-well plates. Plates were incubated at 37°C/7% CO_2 for twenty-four hours, and washed the next day three times with ddH$_2$O. Wells were then coated in 8.3 µg/mL laminin (Thermo Fisher Scientific) for twenty-four hours at 37°C/7% CO_2 until use.

2.3.3 Plating of neural progenitors

On the eighth day of aggregation, CAs were dissociated by incubation with freshly prepared 0.05% trypsin (Sigma-Aldrich; diluted in PBS-0.05% EDTA) for three minutes at 37°C. Dissociated CAs were gently re-suspended in CA media before centrifuging at 180 rcf for three minutes. The cell pellet was resuspended and gently triturated in N2 media (DMEM-F12 (Thermo Fisher Scientific), 1 mM Glutamax, 25 µg/mL Insulin (Roche), 1% N2 supplement, 1% NEAA, 50 µM 2-mercaptoethanol and 1X penicillin-streptomycin) before being passed through a cell strainer to remove any intact aggregates. Cells were counted using a nucleocounter, and plated in N2 media onto the pre-prepared poly-DL-ornithine/laminin coated plates (section 2.3.2) at a density of 0.75-2 x10^6 cells depending on the density required for each experiment. N2 media was changed at two hours, and again one day after dissociation.

Media was changed to complete media 2, 4, 8 and 12 days after dissociation (Bibel et al., 2007). To make complete media, 100X stock of the supplement was first prepared (Table 2.4). This stock was aliquoted and stored at -80°C for up to one year. Next, a BSA solution was prepared consisting of 1 g BSA (Sigma-Aldrich), 2 mg transferrin (Sigma-Aldrich) and 1.6 mg insulin (Roche) in 30 mL DMEM. Complete media was prepared on the day of use as outlined in Table 2.5.

A

ES Media
ESCs
T25 flask

**ESCs on 0.2 %
Gelatine**

B

Cellular Aggregates
CA Media
10 cm Uncoated Dish
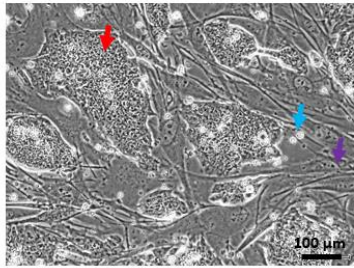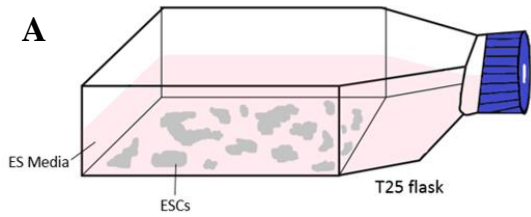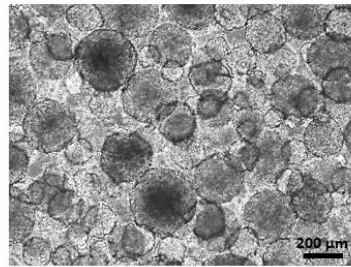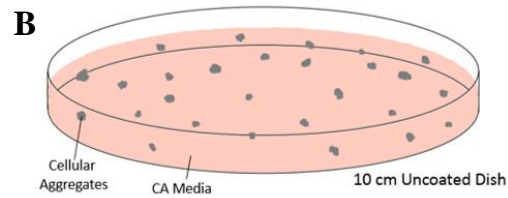
**Cellular Aggregates
(Day 0-4)**

C

Cellular Aggregates
CA Media + Retinoic Acid
10 cm Uncoated Dish
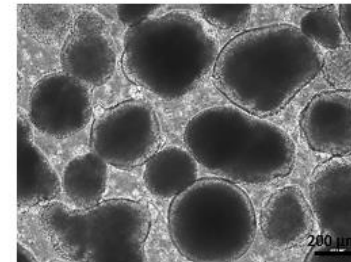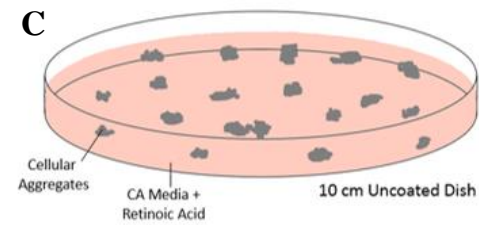
**Cellular Aggregates +
R.A. (Day 4-8)**

D

Neuronal Progenitors
N2 Media
12-Well Nunc Plate
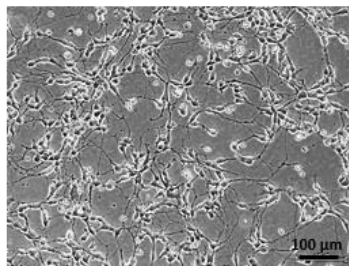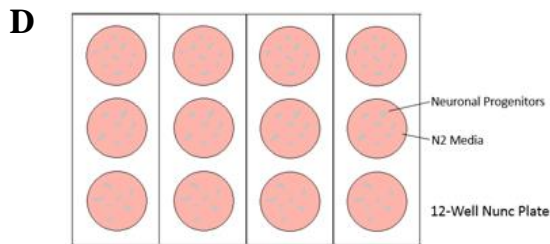
**Dissociated Neuronal Progenitors
(DIV0-DIV2)**

E

Neurons
Complete Media
12-Well Nunc Plate
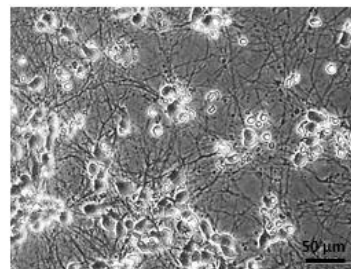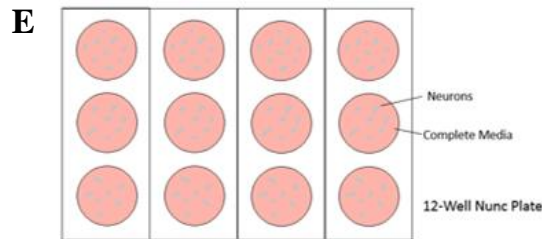
**Neurons
(DIV2 onwards)**

Figure 2.6 Neuronal differentiation of mouse ESCs. E14 ESCs were cultured on 0.2 % gelatine for 4-6 passages. J1 mouse ESCs were cultured on MEFs for 4-6 passages before culturing on A) 0.2 % gelatine for 2-3 passages to remove MEFs (red arrow: ESCs, blue arrow: dying cells, purple arrow: remaining MEFs). B) ESCs were passaged and 4×10^6 cells added to a non-adherent petri dish in CA media to allow the cells to aggregate for eight days, C) retinoic acid (R.A.) was applied to the cellular aggregates (CAs) for the final four days. D) On the eighth day the CAs were dissociated, and plated onto poly-DL-ornithine/laminin coated dishes in N2 media. E) After two days in N2 media (DIV2), the cells were cultured in complete media which was changed at DIV4, DIV8 and DIV12.

Table 2.4 Preparation of 100X complete media supplement

Reagents	Final Concentration (µg/mL)	For 200 mL of 100X stock (mg)
L-alanine	2.00	40.0
Biotin	0.10	2.0
L-carnitine	2.00	40.0
Ethanolamine	1.00	20.0
D-galactose	15.00	300.0
L-proline	7.76	155.2
Putrescine	16.10	322.0
Sodium pyruvate	25.00	500.0
Sodium selenite	0.016	0.32
Vitamin B12	0.34	6.8
Zinc sulphate	0.19	3.9
Catalase	2.56	51.2
Glutathione	1.00	20.0
Linoleic acid	1.00	20.0
Linolenic acid	1.00	20.0
Progesterone	0.006	0.12
All-trans retinol	0.10	2.0
Retinylacetate	0.10	2.0
Tocopherol	1.00	20.0
Tocopherolacetate	1.00	20.0

Blue group (L-alanine through Glutathione): Dissolved in 26.6 mL ddH$_2$O

Red group (Linoleic acid through Tocopherolacetate): Dissolved in 26.6 mL Ethanol

Diluted in 172 mL DMEM

All reagents sourced from Sigma-Aldrich.

Table 2.5 Complete media reagents

Reagents	Volume (mL)
DMEM	358
Penicillin-Streptomycin (100x)	4
100x Stock Supplement	4
Superoxide dismutase (2.5 mg/mL)	0.4
BSA Solution	30
Glutamax (100x)	4

2.4 Animal husbandry

Procedures, breeding and maintenance were carried out in accordance with Home Office Animals (Scientific Procedures) Act, ASPA, 1986 under PPL 30/3137. All animals were housed in a 10/14 hour light cycle with food (Global Rodent) and water available *ad libitum*. The temperature was maintained at 19-23°C and humidity between 45-65%. Animals were weaned around three to six weeks of age, depending on the line, and a maximum of five adult mice kept per cage. Embryonic ages were established by timed mating, and animals plug-checked the following morning to confirm breeding had occurred. Embryonic ages were confirmed according to Theiler staging criteria (Theiler, 2014). All mice were culled by cervical dislocation.

2.5 Generation of TrkA- and TrkB-overexpressing mice

2.5.1 Preparation of cells

E14 *Rosa26-loxP-STOP-loxP-HA-rTrkA* ESCs were generated by Dr. Xinsheng Nan in our laboratory and the recombined and verified (see section 2.2.5) ESCs injected into blastocysts at the University of Cambridge. The resulting mice were subsequently transferred to Cardiff University (December 2016).

E14 *Rosa26-loxP-STOP-loxP-HA-rTrkB* ESCs were generated as outlined in sections 2.2.4. ESCs with the correct karyotype (section 2.2.7) were thawed and passaged according to the protocol described in section 2.1.5.3. The night before blastocyst injections occurred, the ESCs were passaged at a 1:3-1:5 split ratio. The next day ESCs were passaged and resuspended in 10 mL of CA media before being placed on ice for transfer to the site of blastocyst injection.

2.5.2 Blastocyst injection

Blastocyst injections to generate *Rosa26-loxP-STOP-loxP-HA-rTrkB* mice were carried out by Asif Jeelani as part of the JBIOS (Cardiff University) blastocyst

injection service. In brief, prior to injection, CD1 females were crossed with vasectomised CD1 males to induce pseudopregnancy. On the day of injection, the injection chamber and microscope stage were pre-cooled to 10°C, and the injection needle aligned. A single expanded blastocyst was then immobilised with a holding pipette using slight suction and individual ESCs aspirated into the injection needle. The needle was introduced into the blastocoel cavity and ESCs slowly expelled into the blastocyst before withdrawing the injection needle. Injected blastocysts were then implanted in to the uterus of anaesthetised pseudopregnant female mice. After transfer, the mouse was sutured and placed in a heat recovery unit for post-operative care according to ASPA guidelines. Females gave birth to litters and offspring were observed for any chimerism in coat colour. Any chimeric pups were crossed with wild type C57BL6/J mice, and their offspring genotyped. Pups were then continuously outbred to C57BL6/J mice for a minimum of three generations to reduce the potential for any off target mutations during transfection of ESCs affecting the mice.

2.6   Genotyping mice

2.6.1   Ear-notching

Ear notches were taken for identification of transgenic mice in accordance with Home Office Animals (Scientific Procedures) Act, ASPA, 1986 and establishment regulations. Spare tissue from this procedure was then processed for genotyping.

2.6.2   DNA extraction

DNA was extracted from ear notches by incubation with 500 µL DNA lysis buffer overnight at 50°C. 500 µL 100% isopropanol and 50 µL 3 M sodium acetate was added to each sample and inverted before centrifugation at 20000 rcf for fifteen minutes at room temperature. Supernatant was aspirated, and the cell pellet washed with 70% ethanol. The samples were centrifuged for a further five minutes at 20000 rcf before resuspending the DNA pellet in 30 µL TE buffer. The DNA concentration (ng/µL) was estimated using a BioSpectrometer® (Eppendorf).

2.6.3   Genotyping

The DNA samples were used for genotyping using long-range sequal-prep PCR kit following the manufacturer protocol with enhancer A. The primers are outlined in Table 2.6, and thermal cycling (Table 2.6) carried out in a BIORAD T100 Thermal cycler. After amplification the mixture was supplemented with 4 μL DNA loading buffer and loaded onto a 1% agarose gel supplemented with 0.2 μg/mL ethidium bromide for gender, cre, MECP2 (as an internal control) and Rosa26 genotyping, or a 3% agarose gel for *Rosa26-loxP-STOP-loxP-HA-rTrkA* and *−rTrkB* genotyping. Loaded gels were then electrophoresed for one hour and bands detected using a UV docking station.

Table 2.6 Primers and PCR conditions for genotyping mice

Genotyping For:	Forward Primer	Reverse Primer	Band Size (bp)	PCR Conditions		
Gender	CTGAAGCTTTTGGCTTTGAG	GGTTTCTTAAACCGTCACC	X: 331 Y: 302	95°C 3 minutes 95°C 30 seconds 58.5°C 30 seconds ⎤ x 35 cycles 68°C 4.5 minutes 72°C 5 minutes		
Cre	GGTTATGCGGCGGATCCGAAAAGAAA	ACCCGGCAAAACAGGTAGTTATTCGGATCA	381	Same as above		
Rosa26	AAGGGAGCTGCAGTGGAGTA	GTCCCTCCAATTTTACACC	275	Same as above		
MECP2 Internal Control	AAATTGGGTTACACCGCTGA	CTGTATCCTTGGGTCAAGCTG	465	Same as above		
Rosa26-loxP-STOP-loxP-HA-rTrkA	CGCAGGGACTTCCTTTGTCCCAAATC	GCTGGGAAGGAGACGCTGACTTG	2823 (mutant) 1506 (excised)	95°C 3 minutes 95°C 30 seconds 60°C 30 seconds ⎤ x 35 cycles 68°C 3 minutes 72°C 5 minutes		
Rosa26-loxP-STOP-loxP-HA-rTrkB	CGCAGGGACTTCCTTTGTCCCAAATC	CCAAATTCCCAACGTCCCAGTACAAG	2721 (mutant) 1404 (excised)	Same as above		

2.7   Basic morphological measurements

After culling, all experimental embryos were weighed, and then imaged using a digipad (Medline) and dissecting light microscope (VWR). The body area was measured for each pup using ImageJ software.

2.8   Histology

2.8.1   Fixation

Homozygous *Rosa26-loxP-STOP-loxP-HA-rTrkA* and –*rTrkB* males were time mated with heterozygous *CMV-Cre* females, and females plug checked the next morning. Between 11.5-18.5 days *pc*, mothers were culled by cervical dislocation, and embryos dissected out from the yolk sac in ice-cold PBS. Developmental stage was confirmed according to Theiler's criteria (Graham et al., 2015). In the case of P0 pups, animals were culled by cervical dislocation on the morning of birth. Tail samples were taken for genotyping following the procedure outlined in section 2.6. At this stage, embryos $\geq$ E13.5 had the skin removed to enable better fixation and processing. Embryos were incubated in 4% paraformaldehyde (PFA; Sigma-Aldrich) at 4°C. If embryos were $\leq$ E13.5 they were incubated in PFA overnight, or for two days if $\geq$ E15.5. Following this, the PFA was replaced with 70% ethanol, and embryos stored at 4°C for a minimum of one day.

2.8.2   Paraffin embedding

Paraffin wax (Sigma-Aldrich) was heated to 60°C, and embryos were simultaneously processed on a roller as outlined in Table 2.7.

Table 2.7 Paraffin processing of embryos

Step	Reagent	Time (hour)	Temperature
1	95% Ethanol	1	Room Temperature
2	95% Ethanol	1	Room Temperature
3	100% Ethanol	1	Room Temperature
4	100% Ethanol	1	Room Temperature
5	100% Ethanol	1	Room Temperature
6	Xylene[1]	1	Room Temperature
7	Xylene	1	Room Temperature
8	Paraffin Wax	1	60°C
9	Paraffin Wax	1	60°C

[1] – purchased from Sigma-Aldrich

22 x 22 mm plastic moulds (VWR) were filled with pre-warmed paraffin wax and left at 60°C for ten minutes to allow bubbles to settle. Embryos were then placed in these moulds in the required orientation, and transferred to a -20°C cold plate. Once the paraffin started to solidify, a cassette (Sigma-Aldrich) was placed on top of the mould and more paraffin wax poured on top. Once the paraffin had solidified, the blocks were transferred to 4°C until use.

2.8.3 Microtome and staining

Blocks were mounted on the microtome (Leica RM2245) and 10 µm transverse sections were sliced. Sections were floated in a 42°C water bath and transferred onto superfrost plus slides (VWR). Slides were left to dry at 50°C overnight and stored at room temperature. Slides were then transferred to the Bioimaging Hub and haematoxylin and eosin stainings were performed by Derek Scarborough (Cardiff University, Bioimaging Hub) before being collected.

2.8.4 Imaging and quantification

Structures of interest were identified via light microscopy. Images were taken of structures using a digipad.

Ganglia volumes were estimated following the Cavalieri method (Coggeshall, 1992). In brief, images of stained sections were taken at pre-determined intervals across the entire ganglia. The area of each ganglia section was measured in ImageJ, and averaged to give ā. This value was then used to calculate the volume using equation 1, where t is the section thickness, and s is the total number of sections the ganglia can be observed on.

$$\textbf{Equation 1. } \textit{Ganglia Volume } (\textbf{\textit{V}}_{\textbf{\textit{ref}}}) = \text{ā} \times \text{t} \times \text{s}$$

To calculate the number of neurons per ganglia, cell bodies were counted in ganglia sections at pre-determined intervals, and averaged to give a value for Q-. This value was then used to calculate the total number of neurons in each ganglia using equation 2. $a_{Ref.}$ was the average section area per ganglia, h was the section thickness.

$$\textbf{Equation 2. } \textit{Neuronal Count } (\textbf{\textit{N}}_{\textbf{\textit{v}}}) = \frac{Q-}{(\textbf{\textit{a}}_{\textbf{\textit{Ref.}}} \times \textbf{\textit{h}})} \; .$$

Estimates of volume and counts per ganglia were then averaged across the left and right ganglia for each embryo. Statistics were calculated in IBM SPSS statistics software (version 25) for Windows. Data were tested for normality, and the relevant test applied (stated in each figure).

2.9 iDISCO

2.9.1   Fixation

To complete iDISCO (Immunolabelling-enabled three-dimensional imaging of solvent-cleared organs) analysis, homozygous *Rosa26-loxP-STOP-loxP-HA-rTrkA* males were time-mated with heterozygous *CMV-Cre* females, and females plug checked the next morning. 15.5 days *pc*, mothers were culled by cervical dislocation, and embryos dissected out from the yolk sac in ice-cold PBS. Developmental stage was confirmed according to Theiler's criteria (Graham et al., 2015). Embryos were then left for five minutes in ice-cold PBS to drain blood from the umbilical cord to reduce background flourescence. Tail samples were taken for genotyping, and embryos fixed in 4% PFA for two days at 4°C.

2.9.2   iDISCO: immunolabelling and clearing

Embryos were immunolabelled and cleared according to the January 2015 version of the protocol by Renier et al. (2017) (see Table 2.8 for outline of procedure). In brief, fixed embryos were transferred to 20 mL glass vials (Thermo Fisher Scientific) and washed with PBS three times to remove excess PFA before dehydration at room temperature (RT) in methanol/PBS in 20% increments, from 0% up to 100% methanol. Embryos were then incubated overnight at 4°C in a solution of 5% hydrogen peroxide (H_2O_2; Sigma-Aldrich). Samples were then washed with 80% methanol before gradually washing in decreasing methanol/PBS solutions in 20% increments, supplemented with 0.2% Triton X-100 (TX; Sigma-Aldrich). Embryos were incubated overnight at 37°C in 0.2% Triton X-100, 20% DMSO and 0.3 M glycine diluted in PBS.

For blocking, the embryos were incubated for two days at 37°C in a solution of 0.2% Triton X-100, 20% DMSO and 6% donkey serum (Sigma-Aldrich) in PBS. Embryos were then washed in PtWH (0.2% Tween, 10 µg/mL Heparin in PBS) twice for one hour before incubation for two days at 37°C with primary antibody (α-TrkA (1:300) R&D) in 5% DMSO, 3% donkey serum in PtWH. To remove excess antibody,

embryos were washed for one day in PtWH, before incubation with secondary antibody (Donkey anti-goat Alexa Fluor 546 (Thermo Fisher Scientific)). Samples were kept in the dark after the addition of secondary antibody. Embryos were then washed for two days at room temperature in PtWH before clearing with 50% tetrahydrofuran (THF; Sigma-Aldrich) in water overnight at room temperature. It is important that after this stage the steps are carried out in glass vials as THF can react with plastic. The next morning, embryos were incubated in 80% THF for one hour, before two washes with 100% THF for one hour each. This was removed and the embryos kept in dichloromethane (DCM; Sigma-Aldrich) until the embryos sank to the bottom. Embryos were incubated in DiBenzyl Ether (DBE; Sigma-Aldrich) for two hours. At this stage the vials need to be filled completely to prevent oxidation. After replacing with fresh DBE, embryos were stored in the dark at room temperature for up to a few months for imaging.

Table 2.8 iDISCO protocol

Day 1			Day 2			Day 3			Day 4		
Temp.	Time	Solution	Temp.	Time	Solution	Temp.	Time	Solution	Temp.	Time	Solution
RT	30 min.	PBS	RT	30 min.	80% MeOH/PBS	37°C	2 Days	0.2% TX/20% DMSO/6% Donkey Serum/PBS	"	"	"
RT	30 min.	PBS	RT	30 min.	80% MeOH/ 0.2% TX/PBS						
RT	30 min.	PBS	RT	30 min.	60% MeOH/ 0.2% TX/PBS						
RT	30 min.	20% MeOH/ PBS	RT	30 min.	40% MeOH/ 0.2% TX/PBS						
RT	30 min.	40% MeOH/ PBS	RT	30 min.	20% MeOH/ 0.2% TX/PBS						
RT	30 min.	60% MeOH/ PBS	RT	30 min.	0.2% TX/PBS						
RT	30 min.	80% MeOH/ PBS	RT	1 hour	0.2% TX/PBS						
RT	30 min.	100% MeOH	RT	1 hour	0.2% TX/PBS						
RT	1 hour	100% MeOH	37°C	Overnight	0.2% TX/20% DMSO/0.3 M Glycine/PBS						
RT	3-6 hours	100% MeOH									
4°C	Overnight	5% H_2O_2/ MeOH									

Day 5			Day 6			Day 7			Day 8			Day 9		
Temp.	Time	Solution	Temp.	Time	Solution	Temp.	Time	Solution	Temp.	Time	Solution	Temp.	Time	Solution
RT	1 hour	0.2% Tween/10 µg/mL Heparin/PBS (PtWH)	"	"	"	RT	10 min.	PtWH	37°C	2 Days	Secondary Antibody/3% Donkey Serum/PtWH	"	"	"
RT	1 hour	PtWH				RT	15 min.	PtWH						
37°C	2 Days	Primary Antibody/5% DMSO/3% Donkey Serum/PtWH				RT	30 min.	PtWH						
						RT	1 hour	PtWH						
						RT	2 hours	PtWH						
						RT	Overnight	PtWH						

Keep in the dark from now on

Day 10			Day 11			Day 12		
Temp.	Time	Solution	Temp.	Time	Solution	Temp.	Time	Solution
RT	10 min.	PtWH	RT	2 hours	PtWH	RT	1 hour	80% THF/ H2O
RT	15 min.	PtWH	RT	2 hours	PtWH	RT	1 hour	100% THF
RT	30 min.	PtWH	RT	2 hours	PtWH	RT	1 hour	100% THF
RT	1 hour	PtWH	-every 2 hours until end of the day-			RT	<1 hour (until embryo sinks)	DCM
RT	2 hours	PtWH	RT	Overnight	50% THF/ H_2O	RT	<2 hours (until embryos clear)	DBE
RT	2 hours	PtWH				RT	Store	DBE
-every 2 hours until end of the day-								
RT	Overnight	PtWH						

2.9.3 Creating the imaging chamber

Imaging chambers were 3D printed using the 5mm, or 8mm .sti files (Renier et al., 2017). These chambers were printed with Visijet M3 Crystal by Printit-3D (http://www.printit-3d.com/). The chamber was secured to a microscope slide (VWR) with Kwik-sil epoxy (WPI) which is compatible with DBE.

2.9.4 Imaging

Embryos were transferred to the chamber, and the chamber filled with DBE and covered with a glass coverslip. Embryos were imaged with confocal microscopy (LSM 780, Zeiss) using Zen black software (Zeiss). Z stack imaging allowed optical sections of the embryos, and the tiles stitched together. A 3D composite image was generated by using 'max intensity projection' in the Zen Black software.

2.10 Immunohistochemistry

2.10.1   Fixation and embedding

Homozygous *Rosa26-loxP-STOP-loxP-HA-rTrkA* males were time mated with heterozygous *CMV-Cre* females, and females plug checked the next morning. 13.5 days *pc*, mothers were culled by cervical dislocation, and embryos dissected out from the yolk sac in ice-cold PBS. Developmental stage was confirmed according to Theiler's criteria (Graham et al., 2015). Tail samples were taken for genotyping following the procedure outlined in section 2.6. Heads were separated from the body, and skin removed. Embryos were incubated in 4% PFA at 4°C overnight. The next day embryos were transferred to 30% sucrose (Fisher Scientific) solution in 15 mL falcon tubes, and incubated at 4°C until embryos sank to the bottom. At this point, embryos were transferred to moulds filled with optimum cutting temperature (O.C.T.) compound (VWR) and placed on dry ice to set. Embedded embryos were then transferred to -80°C.

2.10.2   Sectioning and staining

Embedded embryos were sectioned at 20 μm thickness on a cryostat (LM3050S) and placed on polysine slides. Slides were stored at -80°C.

Slides were washed with PBS once before incubation with PBST-S (0.1% TX, 10% donkey serum (Sigma-Aldrich) in PBS) for one hour at room temperature. Slides were then incubated overnight at 4°C with anti-cleaved caspase-3 (CST) antibody diluted 1:400 in PBST-S. The next day, slides were washed three times with PBS before incubation with a secondary antibody (donkey anti-rabbit Alexa Fluor 647; Fisher Scientific) diluted 1:1000 in PBST-S, for one hour at room temperature. Slides were washed again three times with PBS before incubation with DAPI (1:4000 diluted in ddH$_2$O) for five minutes. Slides were washed one further time with PBS, followed by ddH$_2$O before being left to dry at room temperature. Coverslips were then mounted onto the slides using DAKO mounting medium (Agilent Technologies).

2.10.3   Imaging and analysis

Slides were imaged using confocal microscopy. Images were taken at pre-determined intervals across the entire ganglia. Where regions of interest were larger than the field of view, tile scans were obtained and stitched together. To count the number of cleaved caspase-3 positive cells, images were thresholded in ImageJ, and the number of positive cells counted using the cell counter plugin. Counts were averaged across the individual ganglia, and this was again averaged across the left and right ganglia for each embryo. This was then calculated as a fold increase compared to controls.

2.11 Western blotting

2.11.1   Protein extraction

Limbs were washed with PBS before the addition of ice-cold protein lysis buffer (50 mM Tris-HCl (Sigma-Aldrich), 150 mM sodium chloride, 1 mM EDTA, 1% Triton X-100, 0.2% Sodium deoxycholate (Sigma-Aldrich)) supplemented with the following enzymes: 1.5 mM aprotinin (Sigma-Aldrich), 100 mM 1-10 phenantroline (Sigma-Aldrich), 100 mM 6-aminohexanoic acid (Sigma-Aldrich), 1% protease inhibitor cocktail (Sigma-Aldrich), 1% phosphatase inhibitor cocktail (Sigma-Aldrich) and sodium orthovanadate (Sigma-Aldrich). The limbs were then crushed using pestles (VWR) and incubated for thirty minutes on ice. Samples were vortexed every five minutes during this time. Samples were then centrifuged at 20000 rcf for ten minutes at 4°C, and the supernatant stored at -80°C until use.

2.11.2   Quantifying protein

The concentration of protein in each sample was determined by the use of a Pierce^{TM} BCA assay kit (Thermo Fisher Scientific) following the manufacturer protocol. Protein samples were diluted between 1:10-1:200 depending on the expected concentration. Triplicates were performed to ensure the calculated concentrations were accurate. Plates were incubated at 37°C for thirty minutes before absorbance analysis using a microplate reader (FLUOstar® Omega microplate reader) at 562 nm excitation wavelength. The concentration of the protein in each sample was quantified using a standard curve.

2.11.3   Sample preparation

Samples were diluted to 1 μg/μL in lysis buffer supplemented with 4x lithium dodecyl sulfate buffer (LDS; 106 mM Tris HCl, 106 mM Tris Base, 0.74 mM LDS (Sigma-Aldrich), 0.5 mM EDTA, 1 M glycerol, 0.2 mM Brilliant Blue (Sigma-Aldrich), 0.175 mM Phenol Red (Sigma-Aldrich)) and 50 mM dithiothreitol (DTT; Invitrogen) to a total volume of 31 μL per well/sample, and incubated for ten minutes at 70°C.

2.11.4   Western blot and membrane transfer

30 μL of sample was electrophoresed on NuPAGE^{TM} Novex^{TM} 4-12% Bis-Tris gels (Thermo Fisher Scientific) at 120 V for 1.5 hours in running buffer (50 mM 2-(N-morpholino)ethanesulfonic acid (MES; Sigma-Aldrich), 50 mM Tris base, 0.1% SDS, 1 mM EDTA, pH 7.3). After electrophoresis the gel was removed and protein transferred to a nitrocellulose membrane (GE Healthcare) using semi-dry transfer machines (GE Healthcare). Here the membrane and blotting papers were soaked in transfer buffer (25 mM Bicine (Sigma-Aldrich), 25 mM Bis-Tris (Sigma-Aldrich), 1 mM EDTA, 20% methanol). Transfer was then carried out at 17 V for one hour. After transfer the membranes were washed once with TBS-T (24.7 mM Tris base, 137 mM NaCl, 2.6 mM KCl, 0.1% Tween-20 (Sigma-Aldrich), pH 7.5).

2.11.5   Primary and secondary antibodies

Membranes were then incubated with blocking buffer (1% BSA, 5% blocking reagent (Biorad) in TBS-T) for one hour at room temperature, before incubation with primary antibody (Table 2.9) diluted in blocking solution overnight at 4°C. The membranes were washed three times with TBS-T for twenty minutes before incubation with secondary antibodies (Table 2.9) diluted in blocking solution for one hour at room temperature. Membranes were washed again with TBS-T three times for twenty minutes.

Table 2.9 Antibodies used for western blot

Antibody	Type	Dilution	Species	Company	Catalogue Number
αHA	mAb	1:2000	Rat	Roche (via Sigma-Aldrich)	ROAHAHA
αpan-Trk	pAb	1:2000	Rabbit	Santa Cruz	sc-11
αGAPDH	pAb	1:5000	Chicken	Abcam	ab83956
αrat-HRP	pAb	1:4000	Goat	R&D	HAF005
αrabbit-HRP	pAb	1:4000	Goat	Promega	W4011
αchicken-HRP	IgY	1:15000	Goat	Abcam	ab6877

2.11.6 Detection and stripping

Membranes were incubated with 1 mL LumiGLO® Reserve Chemiluminescent Substrate kit (KPL) at room temperature for two minutes. The LumiGLO® was removed and signal detected using a ChemiDoc™ MP system together with Imagelab software (Biorad).

After developing the membranes were washed for ten minutes in TBS-T before incubation with stripping buffer (Sigma-Aldrich) for fifteen minutes at room temperature. Membranes were washed three further times for ten minutes in TBS-T and then the process continued from section 2.11.5 for the internal control (GAPDH).

3. Generating an in *vitro* model of TrkA- and TrkB-overexpressing neurons

3.1. Introduction

The observation by Nikoletopoulou et al. (2010) that TrkA acts as a dependence receptor provided a plausible explanation as to why NGF-dependent neurons die during development. However the mechanisms of TrkA-induced cell death remain undefined. In order to further elucidate the mechanisms of TrkA-induced cell death, mouse ESCs were generated as in the Nikoletopoulou et al. (2010) paper, but with two key differences; 1) the presence of a loxP-flanked STOP cassette preceding the Trk receptors, preventing expression without Cre-dependent recombination, and 2) a CreER^{T2} sequence under the ubiquitous *Rosa26* promoter, where the Cre recombinase activity is induced by addition of Tamoxifen (Figure 3.1).
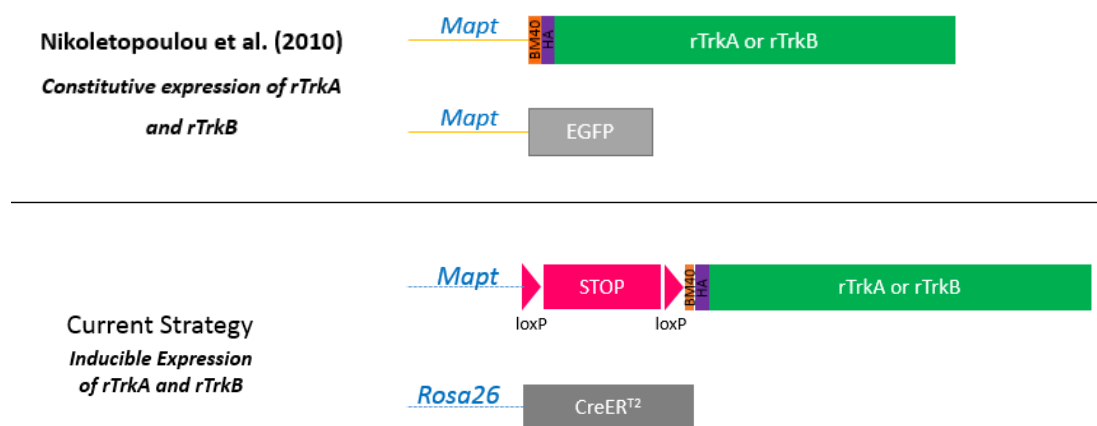
Figure 3.1 Comparison of Nikoletopoulou et al. (2010) and current strategies. A) In the previous publication, HA-tagged (purple) TrkA and TrkB (green) are expressed under the *Mapt* locus constitutively. The BM40 signal sequence is indicated in (orange) before HA. B) The current strategy has a loxP-flanked STOP cassette preceding the *Trk* receptor sequences, so that it cannot be expressed under physiological conditions. In this case, expression of TrkA and TrkB is induced by the addition of Tamoxifen to the ESC culture, which activates the CreER^{T2} protein (expressed under the ubiquitous *Rosa26* locus) to excise the STOP cassette.

These ESCs were differentiated into homogenous populations of glutamatergic, cortical-like neurons (Bibel et al., 2004, 2007), as used in the Nikoletopoulou et al. (2010) paper. In this way, the expression of TrkA and TrkB could be temporally controlled during differentiation of ESCs into mature neurons. The benefit of neuronal models derived from mouse embryonic stem cells (ESCs), compared to primary cultures, is that due to the pluripotency and proliferation potential of ESCs, an unlimited number of any cell type can be produced, provided there is an established differentiation protocol. This is advantageous in that there is an unlimited supply of material for analysis without the need for sacrificing animals.

This *in vitro* model was generated with the aim of testing:

1) The effects of delayed TrkA expression in post-mitotic neurons,
2) The biochemical mechanisms of TrkA-induced cell death,
3) Whether, and at what point, TrkA-induced cell death in neurons could be rescued by NGF addition.

This chapter firstly outlines the production of the pMapt-loxP-STOP-loxP-HA-rTrkA and -TrkB targeting plasmids, and the generation and validation of the required ESC lines.

3.2. Generation of pMapt-loxP-STOP-loxP-HA-rTrkA and -rTrkB vectors

The targeting constructs were first generated (outlined in section 2.2.2). The pMapt-loxP-STOP-loxP-HA-rTrkA and -rTrkB plasmids were produced by linearising the pMapt-HA-rTrkA and -rTrkB plasmids (as used in Nikoletopoulou et al.'s 2010 paper with *PmeI,* and a 1.5 kb loxP-STOP-loxP sequence ligated into this location (Figure 3.2). The plasmid ligation mixture was then transformed into *E. coli,* and DNA extracted from individual colonies for restriction analysis using *HindIII. HindIII* restriction sites in the pMapt-loxP-STOP-loxP-HA-rTrkA (Figure 3.3) and rTrkB (Figure 3.4) plasmids were different, and so are depicted in separate figures.

In the original pMapt-HA-TrkA plasmid, *HindIII* restriction gives rise to three DNA fragments; >10 kb, 2.2 kb, and 600 bp (Figure 3.3, A). However after ligation of the loxP-STOP-loxP cassette into the linearised pMapt-HA-rTrkA plasmid in the correct orientation, *HindIII* digestion resulted in five separate DNA fragments; >10 kb, 3.7 kb, 60 bp, 40 bp, and 600 bp (Figure 3.3, B). Alternatively in the pMapt-HA-rTrkB plasmid, *HindIII* restriction results in two DNA fragments; >10 kb, and 2.2 kb (Figure 3.4A). When there was ligation of the loxP-STOP-loxP cassette in the correct orientation, *HindIII* digestion resulted in four DNA fragments; >10 kb, 3.7 kb, 60 bp, and 40 bp (Figure 3.4B). The bands >100 bp band could be visualised after separation by electrophoresis on an agarose gel, in order to identify the bacterial samples that contained the correct plasmid (Figure 3.3, D, and Figure 3.4, D). The plasmid DNA sequence was then confirmed by Sanger sequencing, and the bacteria amplified. DNA was extracted from these bacteria by maxiprep to obtain a high concentration of the required plasmid.
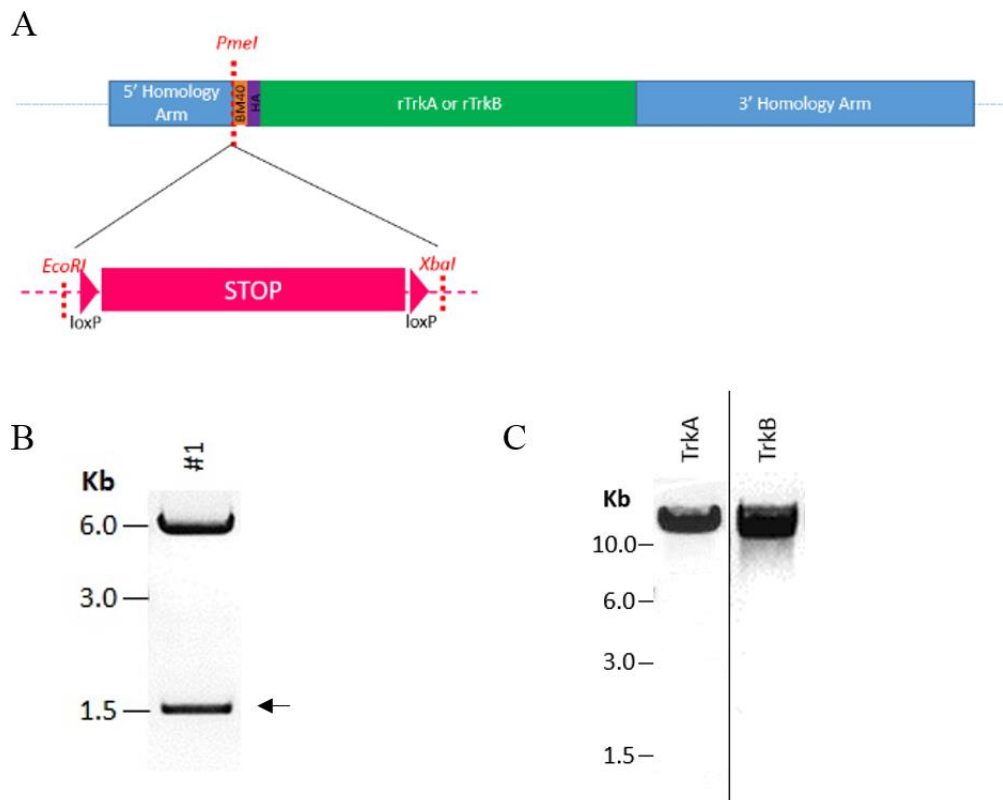
Figure 3.2 Generation of pMapt-loxP-STOP-loxP-HA-rTrkA and -rTrkB plasmids. A) The existing plasmid contained a BM40 sequence (orange) preceding a HA-tagged (purple) rat *TrkA* or *TrkB* (green) sequence, flanked by two homology arms for the mouse *Mapt* gene (blue). The plasmid was linearised using the restriction enzyme *PmeI* (red). In this break, the loxP-flanked STOP cassette (pink), excised from another construct using *EcoRI* and *XbaI* (red) was ligated to form the new plasmid. B) Agarose gel (1%) electrophoresis of the digested loxP-STOP-loxP sequence. The desired STOP cassette sat at 1.5kb (indicated by an arrow), and was purified from the gel to separate it from the plasmid backbone (~6kb band). C) The pMapt-HA-rTrkA or -rTrkB plasmids (indicated by TrkA or TrkB here) when digested with *PmeI* only gave rise to one ~12kb fragment after electrophoresis on an 1% agarose gel as there is only one *PmeI* restriction site.
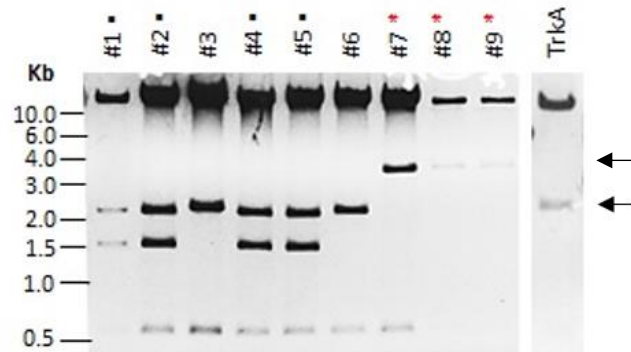
Figure 3.3 Restriction analysis of pMapt-loxP-STOP-loxP-HA-rTrkA plasmid. A) The *HindIII* restriction sites in pMapt-HA-rTrkA plasmid gave rise to three DNA fragments; >10 kb, 2.2 kb, and 600 bp. B) When there was ligation of the loxP-STOP-loxP cassette into the linearised pMapt-HA-rTrkA plasmid in the correct orientation, *HindIII* digestion would result in five DNA fragments; >10 kb, 3.7 kb, 60 bp, 40 bp, and 600 bp. C) When the STOP cassette had been inserted in the wrong orientation, *HindIII* restriction would result in five DNA fragments; >10 kb, 2.2 kb, 40 bp, 1.5 kb, and 600 bp. D) Example 1% agarose gel of *HindIII* digested plasmids. Numbers indicate different *E. coli* clones. TrkA indicates an example of *HindII* digestion of the existing pMapt-HA-rTrkA plasmid. Black squares by the clone number indicates samples with incorrect orientation of the STOP cassette, and red asterisks mark clones with correct orientation of the STOP cassette. The band sizes of interest are indicated by a black arrow.
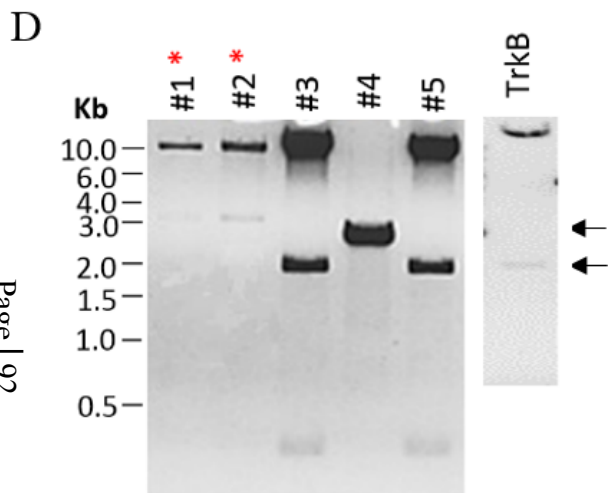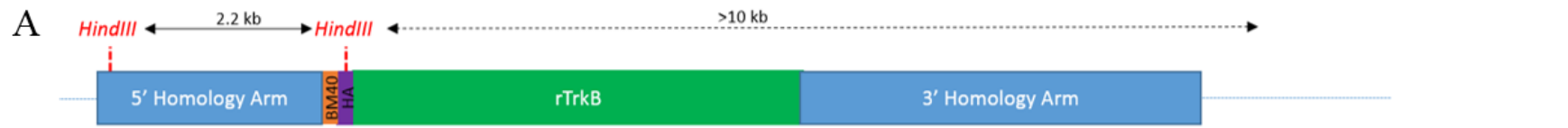
Figure 3.4 Restriction analysis of pMapt-loxP-STOP-loxP-HA-rTrkB plasmid. A) The *HindIII* restriction sites in pMapt-HA-rTrkB plasmid gave rise to two DNA fragments; >10 kb, and 2.2 kb. B) When there was ligation of the loxP-STOP-loxP cassette in the correct orientation, *HindIII* digestion resulted in four DNA fragments; >10 kb, 3.7 kb, 60 bp, and 40 bp. C) When the STOP cassette had been ligated in the wrong orientation, *HindIII* restriction would result in four DNA fragments; >10 kb, 2.2 kb, 40 bp, 1.5 kb and 600 bp. D&E) Example 1% agarose gel of *HindIII* digested plasmids. Numbers indicate plasmids from *E.coli* clones when trying to generate the D) pMapt-loxP-STOP-loxP-HA-rTrkB plasmids. Black squares by the clone number indicates samples with incorrect orientation of the STOP cassette, and red asterisks mark clones with correct orientation of the STOP cassette. The lane labelled TrkB indicates an example of *HindII* digestion of the existing pMapt -HA-rTrkB.

3.3. Generating *R26-CreER^{T2};Mapt-LSL-TrkA* and *-TrkB* ESCs

Wild type mouse ESCs can be of different genetic backgrounds, and are initially derived from different mice. As it has been noted that there can be an effect of genetic background on results, two lines of both *Rosa26-CreER^{T2};Mapt-loxP-STOP-loxP-HA-rTrkA* and *-rTrkB* (hereby referred to as *R26-CreER^{T2};Mapt-LSL-TrkA* or *–TrkB)* ESCs were generated; one on an E14 background, and the other on a J1 background. J1s are derived from male 129/terSv mice and require culture on mouse embryonic fibroblasts to maintain pluripotency (Li et al., 1992), whilst E14s are derived from male 129/Ola mice and can be cultured without fibroblasts (Hooper et al., 1987). This was to ensure that the results obtained with one cell line could be replicated, therefore validating the findings. Mouse ESCs of different genetic backgrounds can behave differently, for example as indicated by the results of histone H3 lysine 9 acetylation (Hezroni et al., 2011).

3.3.1. E14 background

In order to excise the loxP-flanked STOP cassette, we required an ESC line that expressed CreER^{T2}. As E14 *Rosa26-CreER^{T2}* ESCs were readily available, where CreER^{T2} is expressed ubiquitously, these ESCs were targeted with the pMapt-loxP-STOP-loxP-HA-rTrkA and pMapt-loxP-STOP-loxP-HA-rTrkB constructs (section 3.2), aided by CRISPR-guided targeting (section 2.2.3). Genotyping PCR confirmed a targeting success rate of between 25-35% (Figure 3.5), and clones were karyotyped to ensure they had the correct number of chromosomes (>70% of cells with forty chromosomes). The results indicated that the ESC lines outlined in Table 3.1 were suitable to continue with for experiments.

Table 3.1 E14 *R26-CreER^{T2};Mapt-LSL-TrkA* and *-TrkB* ESC lines

ESCs	Line	Clone	Karyotype (%)
E14	*Rosa26-CreER^{T2};Mapt-loxP-STOP-loxP-HA-rTrkA*	#36	70
E14	*Rosa26-CreER^{T2};Mapt-loxP-STOP-loxP-HA-rTrkA*	#208	70
E14	*Rosa26-CreER^{T2};Mapt-loxP-STOP-loxP-HA-rTrkB*	#13	75
E14	*Rosa26-CreER^{T2};Mapt-loxP-STOP-loxP-HA-rTrkB*	#16	75
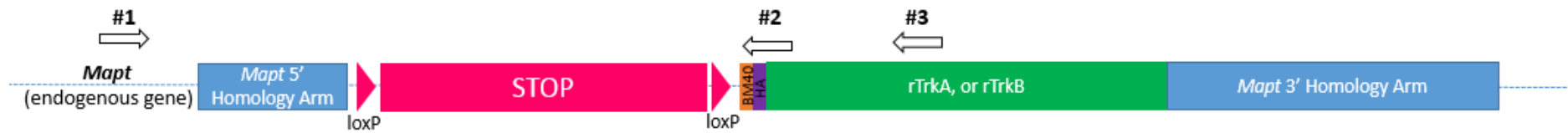
Figure 3.5 Genotyping PCR determining insertion of the pMapt-loxP-STOP-loxP-HA-rTrkA and -rTrkB constructs into the endogenous *Mapt* gene of ESCs. Expected location of the pMapt-loxP-STOP-loxP-HA-rTrkA and -rTrkB constructs in the endogenous *Mapt* gene in ESCs. Arrows marked #1-3 indicate genotyping primer pair locations (details in methods section 2.2.6), with the arrow direction indicating whether it is forward or reverse primer. Pair #1 and #2 are used to genotype *Mapt-lox-STOP-loxP-HA-rTrkA* ESCs, whilst pair #1 and #3 are used to genotype *Mapt-loxP-STOP-loxP-HA-rTrkB* ESCs.

3.3.2. J1 Background

As J1 *Rosa26-CreER^{T2}* ESCs were unavailable, wild type J1s were targeted in two stages; first with a pRosa26-CreER^{T2} zinc finger nuclease targeting kit (section 2.2.4), and once a J1 *Rosa26-CreER^{T2}* line had been established they were targeted with the pMapt-loxP-STOP-loxP-HA-rTrkA and -rTrkB plasmids.

3.3.2.1. Testing the effects of antibiotic-resistant MEFs on antibiotic selection

During targeting, antibiotics were applied to select for cells that had integrated the construct, and therefore expressed the antibiotic resistance gene contained within the plasmid. Whereas the pRosa26-CreER^{T2} construct contained a selection cassette to puromycin, the pMapt-loxP-STOP-loxP-HA-rTrkA and -rTrkB constructs contained a selection cassette to neomycin. However, any ESCs that did not contain the construct would die upon exposure to antibiotics.

Though the concentrations of both puromycin and neomycin for effective selection had been tested on both E14 and J1 ESCs grown on gelatine, it was observed that from 150 picked J1 clones, none had the correct construct. This was due to the concentration of antibiotic being too low, resulting in a higher proportion of surviving non-targeted clones. The sensitivity of J1 ESCs to different concentrations of puromycin or neomycin when grown on antibiotic-resistant MEFs of different densities was tested (Figure 3.6, neomycin results not shown). The results indicated that when grown on antibiotic-resistant MEFs, J1s were less susceptible to antibiotic-induced death. A new concentration of 1.5 μg/mL puromycin and 250 μg/mL for MEFs was selected for targeting of J1 ESCs.
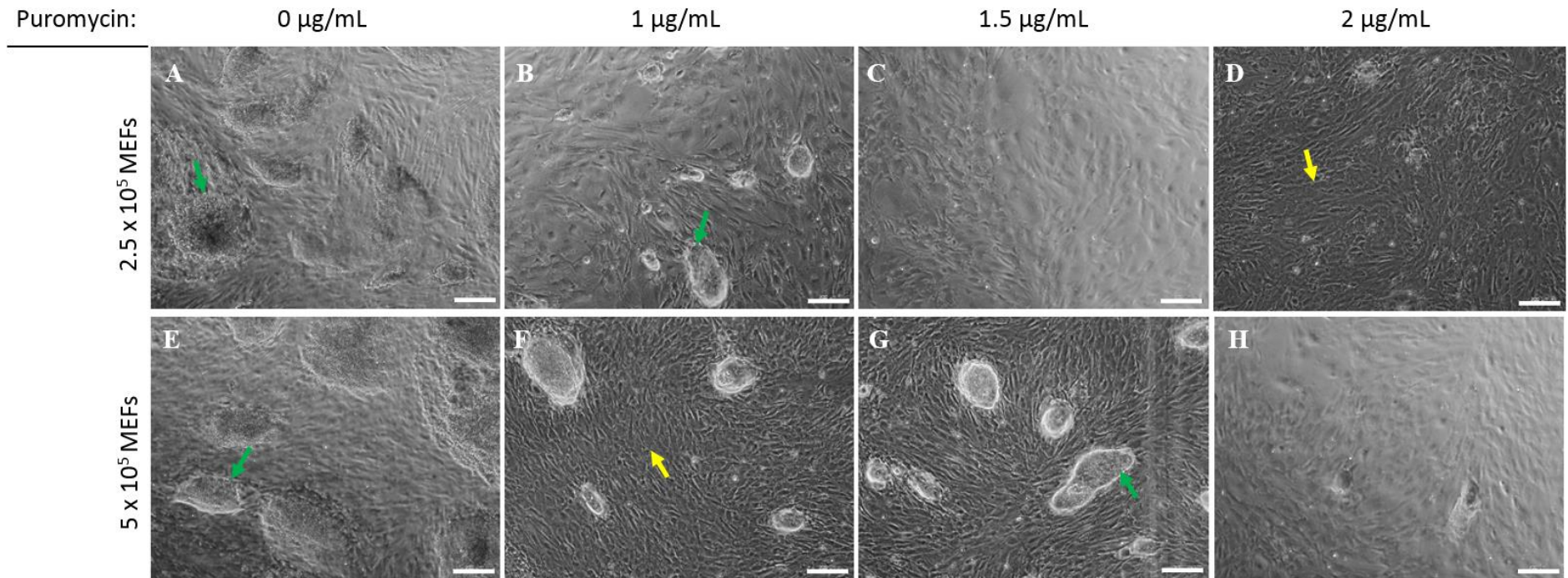
Figure 3.6 J1 ESCs were more resistant to puromycin selection when cultured on puromycin-resistant MEFs. One thousand J1 ESCs were plated on either 2.5 x10^5 (A-D), or 5 x10^5 (E-H) puromycin-resistant MEFs/well. ESCs were either grown (A, E) without any antibiotics, or with (B, F) 1 μg/mL, (C, G) 1.5 μg/mL, or (D, H) 2 μg/mL puromycin. ESC colonies (noted by shiny borders and clusters of cells) are indicated by green arrows, and MEFs by yellow arrows. Scale Bars: 200 μm.

3.3.2.2.   Production of J1 Rosa26-CreER^{T2} ESCs

Wild type J1 ESCs were targeted with the pRosa26-CreER^{T2} construct as outlined in section 2.2. Genotyping confirmed a targeting success rate of 49%, and clones were karyotyped to ensure they had the correct chromosomal number. The lines detailed in Table 3.2 were determined to be suitable to continue with for the second round of targeting.

Table 3.2 J1 *Rosa26-CreER^{T2}* ESC Lines

ESCs	Line	Clone	Karyotyping (%)
J1	*Rosa26-CreER^{T2}*	CL1	77
J1	*Rosa26-CreER^{T2}*	CL24	77
J1	*Rosa26-CreER^{T2}*	CL20	73
J1	*Rosa26-CreER^{T2}*	CL12	92
J1	*Rosa26-CreER^{T2}*	CL27	77

3.3.2.3.   Generation of J1 R26-CreER^{T2};Mapt-LSL-TrkA and -TrkB ESCs

J1 *Rosa26-CreER^{T2}* ESCs were then targeted with the pMapt-loxP-STOP-loxP-HA-rTrkA and -rTrkB constructs as outlined in section 2.2.5. Genotyping confirmed a targeting success rate of 10% for both the TrkA and TrkB constructs. Positive clones were karyotyped to ensure they had the correct chromosomal number. The clones outlined in Table 3.3 were deemed suitable for experiments.

Table 3.3 J1 *Rosa26-CreER^{T2};Mapt-LSL-TrkA* and *-TrkB* ESC lines

ESCs	Line	Clone	Karyotyping (%)
J1	*Rosa26-CreER^{T2};Mapt-loxP-STOP-loxP-HA-rTrkA*	A12	75
J1	*Rosa26-CreER^{T2};Mapt-loxP-STOP-loxP-HA-rTrkA*	A8	75
J1	*Rosa26-CreER^{T2};Mapt-loxP-STOP-loxP-HA-rTrkB*	B15	70
J1	*Rosa26-CreER^{T2};Mapt-loxP-STOP-loxP-HA-rTrkB*	B18	70

3.4. Tamoxifen-induced recombination in ESCs and ESC-derived neurons

To ensure that TrkA and TrkB receptor expression was dependent on tamoxifen treatment, 0.8 μg/mL of tamoxifen was applied to E14 *R26-CreER^{T2};Mapt-LSL-TrkA* and *-TrkB* ESCs (Figure 3.7, A and B). E14 genetically modified ESCs were the first available lines, and so are focused on for the preliminary tests outlined in this chapter.

Genotyping PCR of treated ESCs demonstrated that there was complete excision of the STOP cassette in the DNA of selected ESC clones. Furthermore there was no expression of the exogenous Trk receptors without tamoxifen treatment. As tamoxifen can be cytotoxic (Majumdar et al., 2001), one question was what stage of the *in vitro* differentiation procedure, application time, and concentration of tamoxifen would allow efficient recombination of the STOP cassette in neurons without affecting the quality of the neuronal culture. To do this, the E14 *R26-CreER^{T2};Mapt-LSL-TrkA* clone #36 was differentiated into neurons (section 2.3 (Bibel et al., 2007)), and 0.1 μg/mL tamoxifen added at either day 6 (48 hours), or day 8 of the cellular aggregation procedure (2 hours, or 48 hours). These timings were selected to fit with media changes within the differentiation procedure. It was observed that there were many non-neuronal cells in this differentiation (Figure 3.7, D and E), although there were enough neurons to extract DNA (See section 3.6 for further details). There was

full deletion of the STOP cassette in the DNA of cells in all test conditions (Figure 3.7, C). Additionally, incubation with tamoxifen at the ESC, cellular aggregate, neural progenitor, nor mature neuronal stages resulted in toxicity to the neurons (Figure 3.7, D and E), and deletion of the STOP cassette was complete in all cases.

A *R26-CreER^(T2);Mapt-LSL-TrkA*

B *R26-CreER^(T2);Mapt-LSL-TrkB*

C *R26-CreER^(T2);Mapt-LSL-TrkA*

R26-CreER^(T2);Mapt-LSL-TrkA

R26-CreER^(T2);Mapt-LSL-TrkA +TAM
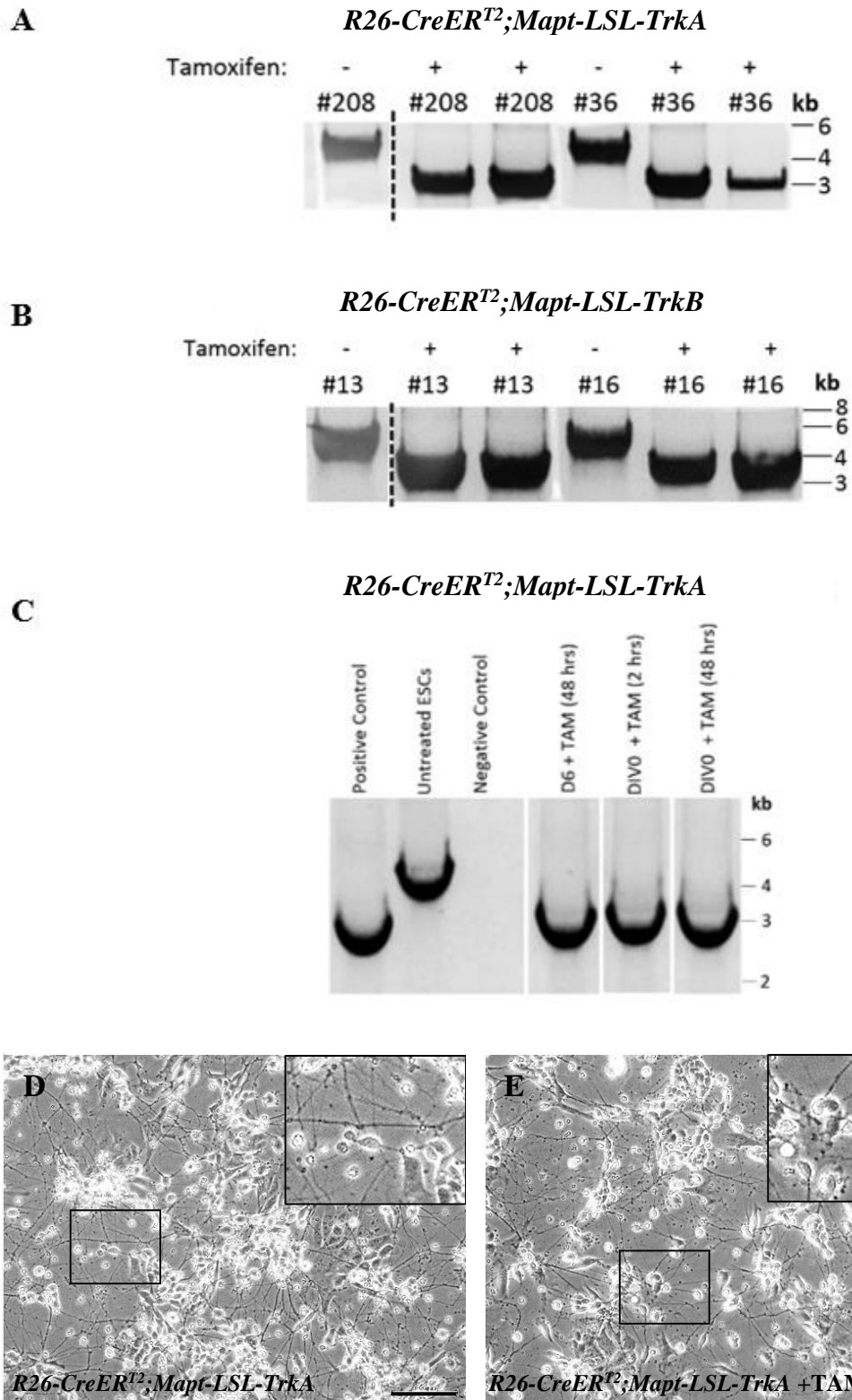
Figure 3.7 Tamoxifen treatment resulted in Cre-mediated recombination of the loxP-flanked STOP cassette in the DNA of ESCs and ESC-derived neurons. A) E14 *R26-CreER^{T2};Mapt-LSL-HA-rTrkA,* or B) *-rTrkB* ESCs were treated with 0.8 µg/mL tamoxifen for 48 hours. DNA was then extracted at DIV2 and a genotyping PCR reaction, run on a gel, tested for deletion of the 1.5 kb loxP-flanked STOP cassette. Numbers above each lane refer to ESC lines derived from different clones. Replicates are from different dishes of Tamoxifen-treated ESCs. The negative control was an E14 *Rosa26-CreER^{T2}* line. C) The STOP cassette was removed in neurons when 0.1 µg/mL tamoxifen was added, at either D6 CAs for 48 hours, or to neural progenitors immediately after dissociation of D8 CAs for either 2 or 48 hours. DNA was extracted from the neurons two days after treatment, and a genotyping PCR reaction run on the gel demonstrated here. The negative control was a E14 *R26-CreER^{T2}* line and the positive control was DNA from tamoxifen treated E14 *R26-CreER^{T2};Mapt-LSL-HA-rTrkA* clone #36 in figure A. D) Example of tamoxifen untreated neuronal culture derived from E14 *R26-CreER^{T2};Mapt-LSL-HA-rTrkA* clone #208, and example image of E) neurons derived from tamoxifen-treated ESCs. Insets are 200% magnification. Scale bars: 100 µm.

3.5. Expression of TrkA and TrkB protein

Next it was confirmed whether excision of the STOP cassette in the DNA of tamoxifen-treated ESCs or neurons related to expression of the respective Trk receptor at the protein level. To do this, ESCS were treated with tamoxifen (0.8 µg/mL; 48 hours as ESCs), and differentiated. Protein samples were then extracted from E14 *Rosa26-CreER^{T2};Mapt-LSL-TrkA* and *-TrkB* neurons from D8 of cellular aggregation to DIV8 (8 days after plating neuronal progenitors) (section 2.11). Western blot analysis indicates that HA-tagged TrkA and TrkB protein is present after tamoxifen treatment, but without tamoxifen no HA-tagged TrkA and TrkB protein could be detected (Figure 3.8). This confirms that the system is reliable.
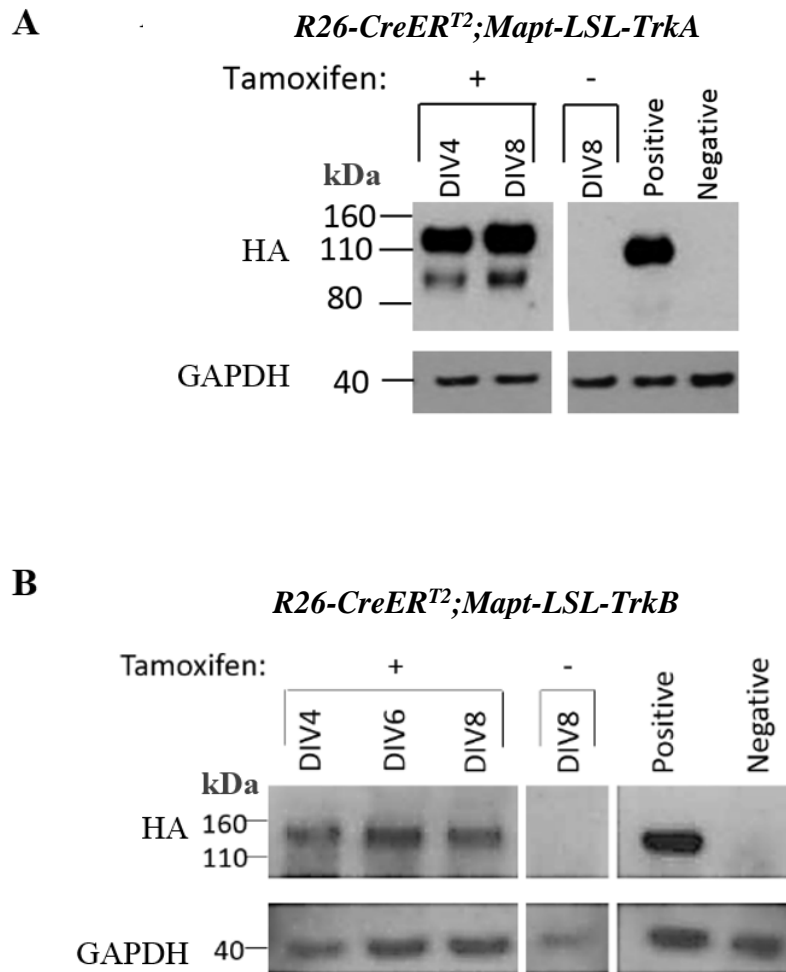
Figure 3.8 Tamoxifen treatment resulted in expression of HA-tagged TrkA and TrkB protein in ESC-derived neurons. A) *R26-CreER^{T2};Mapt-LSL-TrkA,* and B) *R26-CreER^{T2};Mapt-LSL-TrkB* ESCs were treated with 0.8 μg/mL tamoxifen for two days before neuronal differentiation. The resulting neurons were checked for expression of the HA-tagged TrkA and TrkB proteins (~140 kDa) by western blot using αHA antibody. DIV refers to days *in vitro*; the age of neurons after dissociation of the cellular aggregates. Loading control bands are GAPDH (~38 kDa).

3.6. Differentiation of *R26-CreER^{T2};Mapt-LSL-TrkA* and *-TrkB* ESCs into neurons

3.6.1. Differentiation into cortical-like neurons

To differentiate targeted ESCs into homogeneous, glutamatergic, cortical-like populations of neurons a well-established protocol was utilised (Bibel et al., 2004, 2007) that is routinely used for mouse ESCs of different genetic backgrounds such as J1 and E14 (Figure 3.9, A, B), even with genetic modifications such as E14 *Rosa26-CreER^{T2}* (Figure 3.9, C). However as mentioned above, the *R26-CreER^{T2};Mapt-LSL-TrkA* and *-TrkB* ESCS did not consistently produce homogenous neuronal cultures with either a E14, or J1 background (Figure 3.9, D and E), even when tamoxifen was not added for the respective Trk receptor to be expressed. As it had been confirmed that Trk expression is not leaky, this indicated that it was an issue with the cell lines themselves, and not an unknown effect of the Trk receptors. The resulting "neuronal" cultures included a comparatively high number of non-neuronal cells, and the few neurons that were generated clumped together in clusters. These neurons could not be cultured for more than a few days without dying due to rapid expansion of the dividing, non-neuronal cells. The neuronal cultures were not improved even after tailoring aspects of the ESC culture protocol such as time between passages and seeding density (not shown) to improve the quality of ESCs before differentiation which has been found to correlate with neuronal quality (Bibel et al., 2004) .

Careful observation of cellular aggregates (CAs) demonstrated that there were differences in their formation (Figure 3.10). While wild type E14 and J1 ESCs formed large, light, aggregates with clearly defined boundaries (Figure 3.10A, Figure 3.10B) at D8, *R26-CreER^{T2};Mapt-LSL-TrkA* and *-TrkB* aggregates had a bubbly border, and were smaller, and denser (Figure 3.10D, Figure 3.10E). E14 *R26-CreER^{T2}* (Figure 3.10C) and E14 *Mapt-LSL-TrkA* (Figure 3.10F) ESCs on the other hand formed CAs that were in between those of wild types and *R26-CreER^{T2};Mapt-LSL-TrkA* and *−TrkB* ESCs.

Furthermore, the yield of neural progenitors (the number of cells obtained after dissociating D8 cellular aggregates) has been found to be linked to neuronal culture quality (Bibel et al., 2007). Whereas wild type J1 or E14 ESCs resulted in 20-35 x10^6 neural progenitors per dish of aggregates, both E14 and J1 *R26-CreER^{T2};Mapt-LSL-TrkA* and *-TrkB* ESCs consistently produced yields of <15 x10^6 neural progenitors per dish of aggregates.
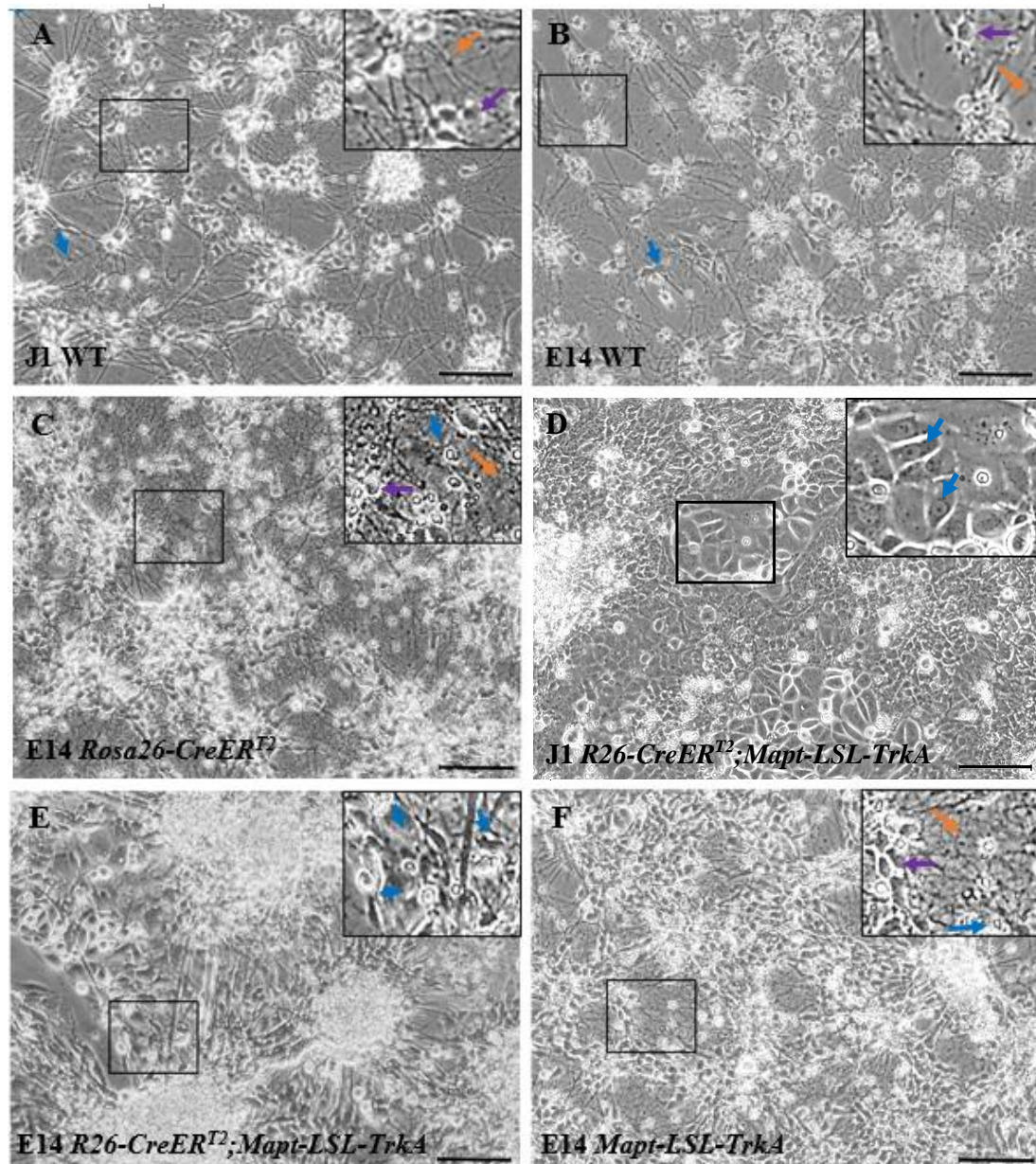
Figure 3.9 Differentiation of ESCs into neurons. Cortical-like neurons can be derived from both A) J1 and B) E14 wild type ESCs. Images shown are 8 days after dissociation of aggregates (DIV8). Neuronal cultures derived from C) E14 *Rosa26-CreER^{T2}* are also able to differentiate into homogenous populations of neurons (DIV8). However *R26-CreER^{T2};Mapt-LSL-TrkA* ESCs on either a D) J1 or E) E14 background (DIV8) show many non-neuronal cells, clusters of neuronal somas and thick, cable like axons by DIV8. F) E14 *Mapt-LSL-TrkA* ESCs were able to differentiate into homogenous populations of neurons. All neurons were plated at 0.75 x10^6 density. Axons are indicated by orange arrows, soma by purple arrows, and non-neuronal cells by blue arrows. Scale bars: 100 μm.
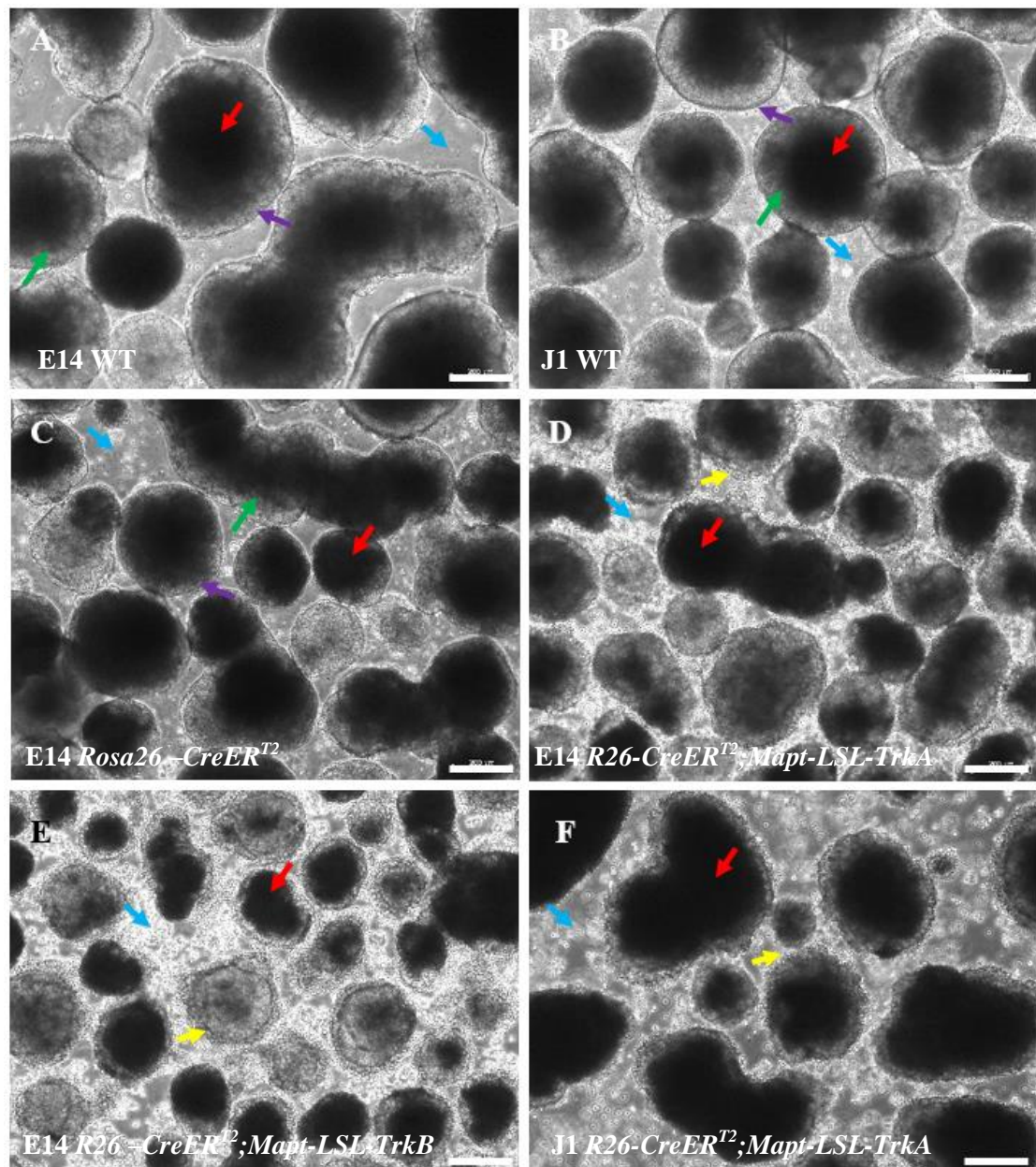
Figure 3.10 D8 cellular aggregates of different ESC lines. D8 Cellular aggregates from wild type A) E14 or B) J1 ESCs form large, round aggregates with a dense dark centre (red arrow) with a lighter gradient (green arrow) towards clearly defined borders (purple arrow). There are few free-floating, dying (white) cells (blue arrow). C) E14 *Rosa26-CreER^{T2}* ESCs also seem to form nice aggregates by D8, although they are smaller in size, and denser in the centre. However the borders are still clear. D) E14 *R26-CreER^{T2};Mapt-LSL-Trk*A (clone #36), or E) *-TrkB* (clone #13), and F) J1 *R26-CreER^{T2};Mapt-LSL-TrkA* (clone A12) form dense aggregates with undefined edges (yellow arrow), with lots of dying cells. Scale bars: 200 μm.

3.6.2. Differences between ESC clones

The inability to produce homogenous neuronal cultures with *R26-CreER^{T2};Mapt-LSL-TrkA* and *-TrkB* ESCs also did not vary with the clone (Figure 3.11), nor was it improved by sub-cloning. Again, yields of neural progenitors from different clones and subclones were consistently $< 15 \text{ x}10^6$ per dish of aggregates. As there was no observable difference between the J1 or E14 lines, the efforts detailed in this chapter to improve neuronal cultures show example differentiations from E14 *R26-CreER^{T2};Mapt-LSL-TrkA* clones #36 and #208.
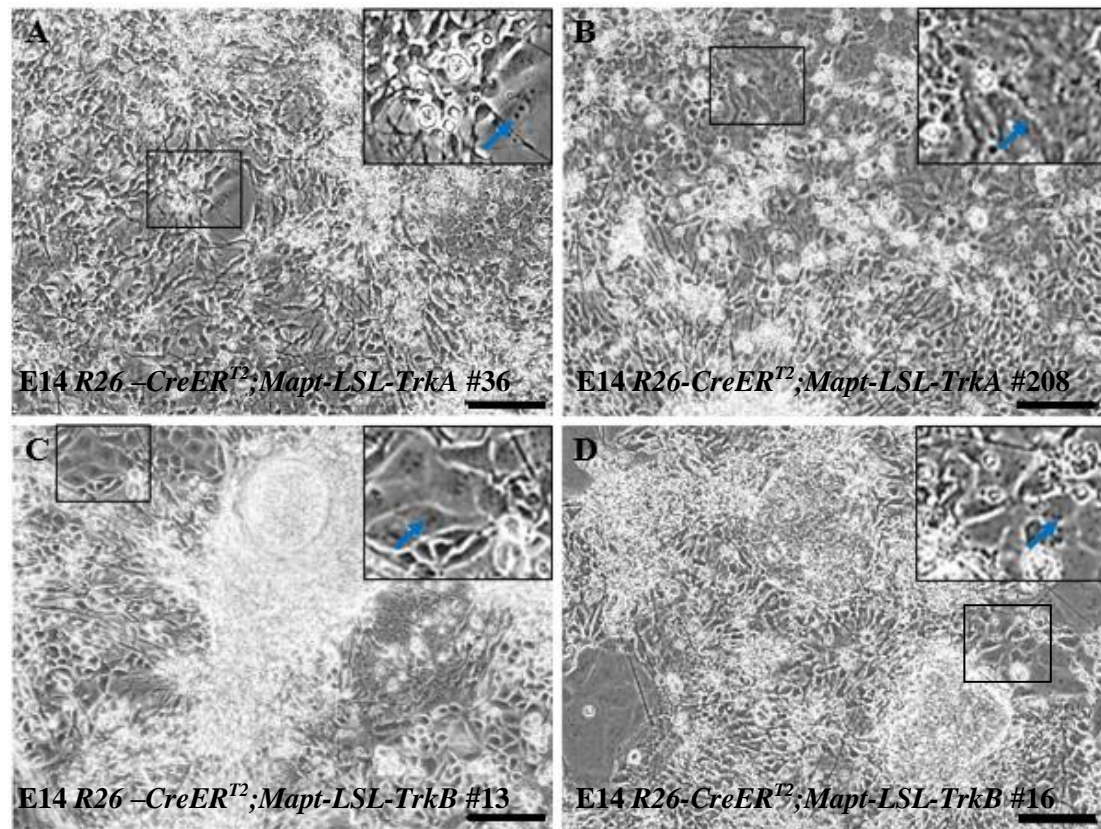
Figure 3.11 Comparison of neuronal culture quality using different ESC clones.
Neurons at DIV8 from A) *R26-CreER^T2;Mapt-LSL-TrkA* clone #36 and B) clone #208,
C) *R26-CreER^T2;Mapt-LSL-TrkB* clone #13 and D) clone #16. Non-neuronal cells are
indicated by blue arrows. Scale bars: 100 μm. Insets are 200% magnification.

3.6.3. Adapting ESC culture media

As mentioned previously, neuronal differentiation is strongly dependent upon the quality of the ESC culture upon starting the differentiation process, particularly as spontaneously differentiating ESCs will not give rise to neuronal cells and contaminate the culture with non-neuronal cells (Bibel et al., 2007; Wu et al., 2012). This is similar to well documented findings that a high number of ESC passages, which affects chromosomal stability (Rebuzzini et al., 2015), and karyotype may affect differentiation potential (Zhang et al., 2016). As the quality of ESC culture has been linked to neuronal differentiation homogeneity (Bibel et al., 2007), it was tested whether different ESC culture conditions could improve the differentiation of the targeted ESCs. Whilst the ability to generate cultures of wild type neurons of different backgrounds indicated that this was not an issue with tissue culture reagents or application of the protocol, fresh stocks of reagents were prepared, and the targeted cell lines differentiated by another person within the lab who routinely used this protocol. However this yielded the same results. Another possibility was that the LIF generated in house was not effective at preventing cells from differentiating. Whilst the ESCs looked morphologically like they were undifferentiated, it is possible that the molecular machinery with in house LIF may have pushed the ESCs towards differentiating into a non-neuronal cell type. However, using commercial recombinant LIF also did not improve neuronal differentiation quality (image not shown).

Next, the effects of ES Media as described by Bibel et al. (2007) was compared to another established ES culture media; serum-free 2I +LIF media (Silva et al., 2008) (section 2.1.5.5). 2I+LIF media is serum-free, and whilst it may lack the unidentified nutrients and growth factors thought to be provided by serum, it also bypasses the variability between batch numbers. However in this thesis, different batches of bovine calf serum used in ES media was tested for their effect on ESC culture quality, and the same, single batch then used throughout. The second major difference between ESC and 2I+LIF media is that 2I+LIF includes inhibitors of glycogen synthase kinase-3 (GSK-3) and mitogen-activated protein kinase (MAPK)/extracellular signal related kinases (Erk) 1 and 2 pathway. Inhibiting the MAPK/Erk pathway prevents the growth of primed epiblast stem cells (EpiScs) (Silva et al., 2008), a specified lineage that ESCs can differentiate into but maintain a similar morphology to ESCs to the untrained eye,

while inhibiting GSK-3 stimulates ESC self-renewal (Ying and Smith, 2017). 2I+LIF media supplemented with 15% FBS, referred to as 2I +LIF +15% FBS, was also tested.

ESCs cultured in 2I +LIF +15% FBS appeared to be the best quality in comparison to ES or 2I +LIF media in terms of morphology (shiny borders, small, uniform ESCs, few differentiating ESCs) and proliferated quickly (1-2 days). However these ESCs still gave rise to poor quality neuronal cultures (Figure 3.12). The yield of neural progenitors was again an indicator of poor differentiation, with each media type ultimately producing <15 x10^6 progenitors per dish of CAs.
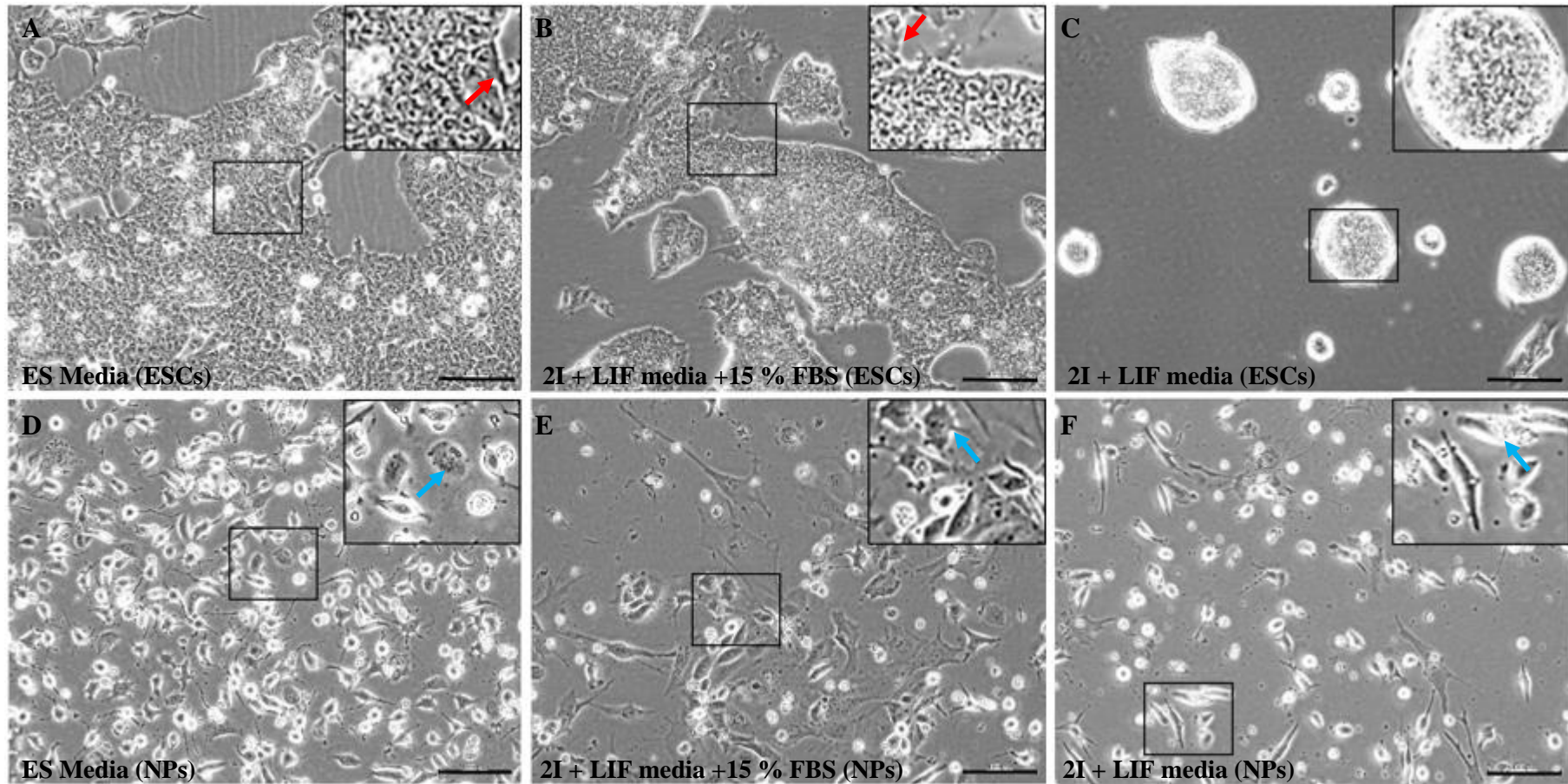
Figure 3.12 Adapting ESC media improved ESC, but not neuronal quality. Clone #208 ESCs and the resulting neuronal cultures at DIV4 (NPs) when cultured in (A, D) ES media, (B, E) 2I + LIF media, or (C, F) 2I + LIF + 15% FBS. Spontaneously differentiating cells are indicated by red arrows, and non-neuronal cells indicated by blue arrows. Scale bars: 100 μm. Insets are 200% magnification.

3.6.4. Culturing targeted E14 ESCs on MEFs

Although ESCs with E14 background are classically cultured on gelatine-coated dishes (Hooper et al., 1987), it is possible that culturing targeted ESCs on mouse embryonic fibroblasts (MEFs) could improve the quality of the ESCs, and subsequently their ability to differentiate. Although the exact mechanism by which MEFs improve ESC pluripotency is undefined, it is thought that the secretion of growth factors and small molecules that are known to be important in proliferation, such as activin-A and transforming growth factor beta (TGFβ), may play a role (Eiselleova et al., 2008; Ogawa et al., 2006; Tamm et al., 2013). Whilst culturing targeted ESC clones #36 and #208 on MEFs improved the morphological quality of the ESC culture (section 3.6.4) (Figure 3.13), these cells were still unable to generate cultures with a higher proportion of neurons than non-neuronal cells (Figure 3.13). Furthermore, combining both 2I+LIF+15% FBS media and culture on MEFs did not improve neuronal culture (Figure 3.14). Similarly, the neuronal progenitor yield in all treatment conditions was $<10 \times 10^6$ per dish of CAs.
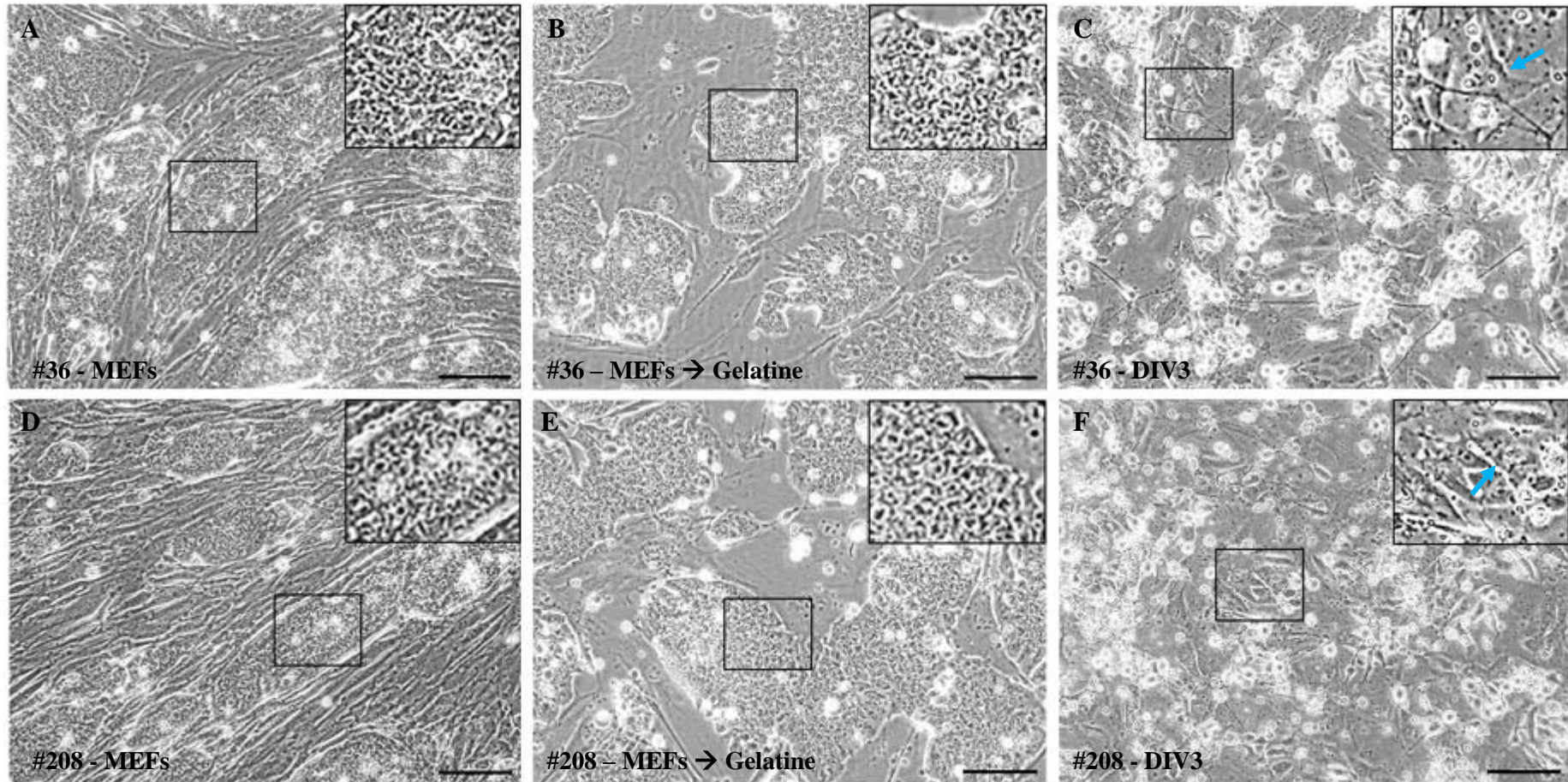
Figure 3.13 Targeted E14 ESC quality is improved by grown on MEFs but does not affect resulting neuronal culture. *R26-CreER^{T2};Mapt-LSL-TrkA* clone #36 (A-C) or clone #208 (D-F) ESCs on (A, D) feeders, (B, E) after two passages on gelatine, and (C, F) DIV3 neurons. Scale bars: 100 μm. Insets are 200 % magnification.
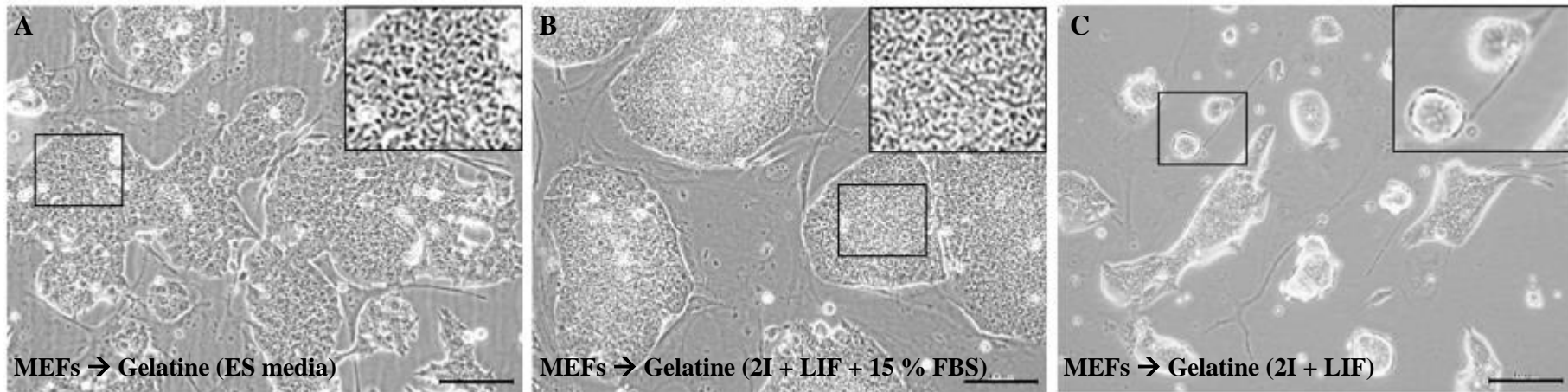
Figure 3.14 Targeted E14 ESC quality is improved by growth on MEFs in combination with 2I+LIF+15% FBS media. *R26-CreER^{T2};Mapt-LSL-TrkA* clone #36 (A-C) ESCs grown on feeders before passaging twice on gelatine with A) ES media, B) 2I + LIF + 15% FBS media, or C) 2I + LIF media. Scale bars: 100 μm. Insets are 200% magnification.

3.7. Summary

This chapter outlined the adaptation of the pMapt-HA-rTrkA and –rTrkB plasmids, used by Nikoletopoulou et al. (2010), by the addition of a loxP-flanked STOP cassette preceding the HA sequence (Figure 3.1). Analysis by restriction digestion with *HindIII* indicated bacterial clones that had the expected band sizes for insertion of the loxP-STOP-loxP cassette (Figure 3.3, and Figure 3.4). The plasmid was then completely sequenced by Sanger sequencing, and sections of sequence were compared to all known sequences by use of the basic local alignment search tool (BLAST, National Institute of Health).

The generated plasmids were then transfected into *Rosa26-CreER^{T2}* mouse ESCs of two genetic backgrounds; J1 and E14 (Section 3.3), to generate novel mouse ESC lines (Table 3.1 and Table 3.3). Application of tamoxifen to the E14 *R26-CreER^{T2};Mapt-LSL-TrkA* and *–TrkB* ESCs resulted in complete excision of the loxP-flanked STOP cassette (Figure 3.7), which corresponded with expression of HA-tagged TrkA and TrkB protein (Figure 3.8). Furthermore, HA-tagged protein could not be detected in untreated cells, indicating that there was no leaky expression of the Trk receptors. This supports that cells not treated with tamoxifen could act as a valid control line. While these cultures had numerous non-neuronal cells (Figure 3.8), these would not contribute to the detection of HA-tagged protein due to HA-TrkA and HA-TrkB being expressed under the neuronal-specific *Mapt* promoter. It subsequently became evident that *R26-CreER^{T2};Mapt-LSL-TrkA* and *-TrkB* ESCs could not be differentiated into homogenous neuronal cultures using the well-established differentiation protocol described by Bibel et al. (2004) (Figure 3.9). A few days after dissociation of CAs there were many non-neuronal cells which continued to proliferate (Figure 3.9). As neurons are post-mitotic, non-neuronal cells quickly overtake the cultures and outcompete neurons for nutrients and space. As a result, in these cultures neurons could only be cultured for a maximum of eight days before dying. As the endogenous levels of Trk receptors increase slowly during the course of this neuronal differentiation protocol, it therefore turned out not to be possible to rigorously compare the levels of endogenous *versus* exogenous Trk in these ESC-derived neurons (see Bibel et al., 2004 & 2007, and Nikoletopoulou et al., 2010).

It was observed that the difficulty in generating homogenous neuronal cultures was not a shortcoming of the differentiation procedure itself, as pure cultures could be derived from both wild type, and alternative genetically-modified ESC lines of both J1 and E14 genetic backgrounds (Figure 3.9). Furthermore, the dissimilarities in differentiation potential between wild type, and *R26-CreER^{T2};Mapt-LSL-TrkA* and -*TrkB* ESCs were distinctly visible by D4 of the cellular aggregation process. Instead of forming large, light, aggregates with clearly defined boundaries like their wild type counterparts, the *R26-CreER^{T2};Mapt-LSL-TrkA* and -*TrkB* aggregates had a bubbly border, and were smaller, and more dense (Figure 3.10). Additionally, there were more dying cells observed during the aggregation process, and a lower yield of neural progenitor cells at D8. These observations indicate that the difficulty in differentiation started during aggregation, as there were no obvious issues with proliferation. Efforts to improve the quality of ESC cultures using alternative media (Figure 3.12) or culturing ESCs on MEFs (Figure 3.13Figure 3.14) also did not improve the differentiation capacity. Therefore these genetically-modified cells were not further used in this thesis. Possible reasons for the difficulty in differentiating these ESCs are discussed further in section 7.2.

4. Generation of *in vivo* TrkA- and TrkB-overexpression models

4.1. Introduction

To elucidate the role of TrkA overexpression *in vivo*, it was of interest to determine whether the ubiquitous expression of TrkA would affect mouse development. As TrkA overexpression under the control of the *Mapt* promoter has been previously reported to induce widespread apoptosis across the nervous system and the premature death of embryos (Nikoletopoulou et al., 2010), a different strategy was used. This chapter describes the generation of a mouse model where HA-tagged TrkA is expressed under the ubiquitous *Rosa26* promoter (Soriano, 1999), allowing the effects of TrkA expression to be determined in all cell types throughout development. The construct contains an IRES-EGFP sequence to allow visualisation of TrkA expression. Constitutive expression of TrkA was prevented by the inclusion of a loxP-flanked STOP cassette in these mice, and thus allowing the maintenance of a stable colony. Given the reported differences between the phenotype of mice overexpressing TrkA and TrkB, a similar mouse line was generated allowing the conditional expression of TrkB.
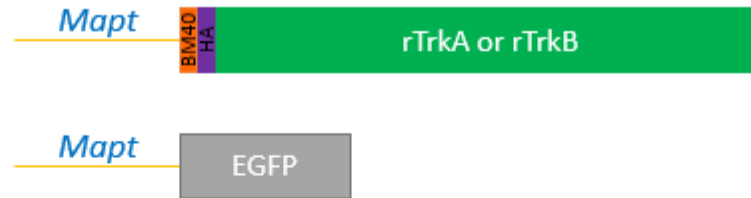
Figure 4.1 Comparison of the current in vivo strategy with previous work. A) In Nikoletopoulou et al. (2010) HA-tagged (purple) *TrkA* and *TrkB* (green) are expressed under the *Mapt* locus constitutively. The BM40 signal sequence is indicated in orange. The constructs also contain an IRES-EGFP sequence (black) to allow visualisation of Trk-expressing cells. B) The current strategy has a loxP-flanked STOP cassette preceding the *Trk* receptor sequences, so that they cannot be expressed under physiological conditions, thus allowing the stable breeding and maintenance of these mouse lines. In order to drive expression of HA-TrkA and HA-TrkB, these mice can be crossed with various Cre driver lines to allow excision of the STOP cassette. The Cre driver lines can be selected according to experimental requirements in terms of location and timing of desired TrkA, or TrkB expression.

4.2. Generation of TrkA and TrkB ESCs

Rosa26-loxP-STOP-loxP-HA-rTrkA-IRES-EGFP (herein referred to as *R26-LSL-TrkA*) ESCs were generated previously by Dr. Xinsheng Nan. To generate the corresponding *TrkB* ESCs, wild type E14 ESCs were first targeted with pRosa26-loxP-STOP-loxP-HA-rTrkB-IRES-EGFP constructs (as outlined in section 2.2.5) to generate the corresponding *R26-LSL-TrkB* ESCs. Genotyping confirmed correct targeting (outlined in section 2.2.6), and clones were karyotyped to ensure they had the correct number of chromosomes (Table 4.1). Clones with >70% karyotype were selected (section 2.2.7) and tested for mycoplasma (section 2.1.1).

Table 4.1 *Rosa26-loxP-STOP-loxP-TrkB-IRES-GFP* Clones

ESCs	Line	Clone	Karyotype (%)
E14	*Rosa26-loxP-STOP-loxP-TrkB-IRES-EGFP*	B50	79
E14	*Rosa26-loxP-STOP-loxP-TrkB-IRES-EGFP*	B13	80
E14	*Rosa26-loxP-STOP-loxP-TrkB-IRES-EGFP*	B44	73
E14	*Rosa26-loxP-STOP-loxP-TrkB-IRES-EGFP*	B46	83

4.3. Generation of TrkA- and TrkB-overexpressing mice

Both *R26-LSL-TrkA* and *–TrkB* mice were generated by injections of genetically modified mouse ESCs into blastocysts (as outlined in section 2.5). *R26-LSL-TrkA* mice were generated through a collaboration with Cambridge University, and the corresponding *–TrkB* mice were generated by the JBIOS unit at Cardiff University. Born pups were observed for chimerism (Figure 4.2). Chimeric coats were generated by the fact that E14 ESCs were derived from the mouse strain 129/Ola, which have an agouti or chinchilla coat colour (Hooper et al., 1987), while the injected blastocysts were derived from C57BL/6J mice. Therefore chimeric offspring from these injections indicate that the injected, mutant ESCs are contributing to some of the cells that make up the mouse. These chimeras were bred with C57BL/6J mice, and had germline

transmission of the *R26-LSL-TrkA* and *-TrkB* gene, which was confirmed by genotyping PCR. These mice were backcrossed with C57BL/6J for a minimum of four generations. Backcrossing reduces the chances of pups inheriting off-target genetic mutations that may have occurred during targeting of the original ESCs.
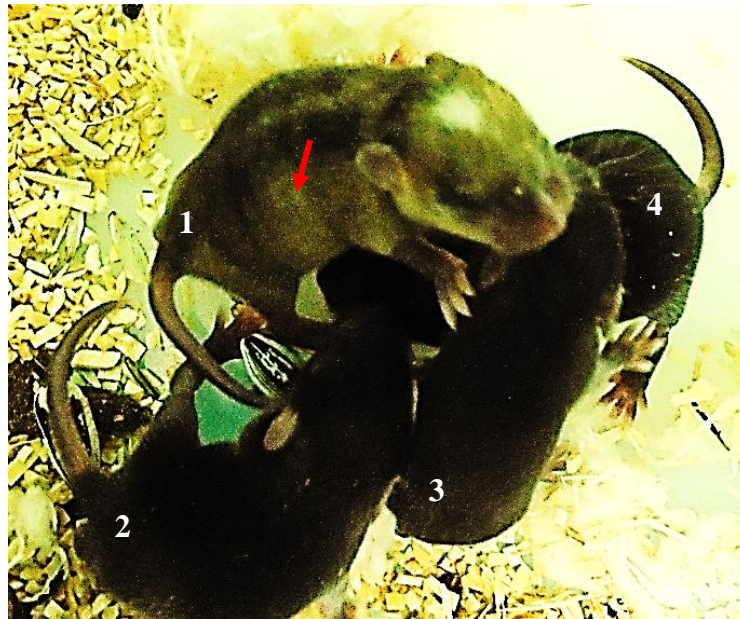
Figure 4.2 Chimeric pups. Representative image of chimeric offspring from *R26-LSL-TrkB* blastocyst injections. A) Numbers 1-4 indicate the different mouse pups. The coat colour of mice 2-4 is solid black, indicating that they are not chimeras. The patchy coat colour (indicated by red arrow) of mouse 1 indicates that it is a chimera; made up of both *R26-LSL-TrkB* ESCs (Agouti), and wild type cells from the injected blastocyst (Black).

4.4.Breeding and maintenance of *R26-LSL-TrkA* and –*TrkB* mice

R26-LSL-TrkA and –*TrkB* mice did not demonstrate any obvious phenotype, were fertile, and gave birth to litters of a reasonable size (Table 4.2). Furthermore these mice seemed to have normal mothering ability, and the offspring were viable based on the observation that there was no abnormal loss of pups prior to weaning (Table 4.2). *R26-LSL-TrkA* had a normal lifespan of >1 year in animal housing. Due to the late generation of *R26-LSL-TrkB* mice, it has only been possible to observe homozygotes up to 8 months of age. However at the time of writing there were no observable phenotypes or effect on survival. It is important to note that the litter size reported in Table 4.2 for C57BL/J wild types is lower than normally expected (around eight pups per litter). This may be a reflection of a heavy breeding regimen.

Table 4.2 Breeding of wild type, and *R26-LSL-TrkA* and –*TrkB* mice

	C57BL/6J	*R26-LSL-TrkA* (het x het)	*R26-LSL-TrkB* (het x het)
Average Litter Size at P0 (N)	5.4 (5)	7.4 (9)	6.1 (7)
Average Litter Size at Weaning (N)	5.2 (5)	6.9 (9)	5.6 (7)
Weaning Age	P21-P28	P21-P28	P21-P28

N = number of litters.

4.5.Cre-mediated recombination using a ubiquitous Cre driver

CMV-Cre (C57BL/6J background) (Schwenk et al., 1995) animals were bred with *R26-LSL-TrkA* and -*TrkB* to allow excision of the STOP cassette. In *CMV-Cre* mice, Cre expression, driven by the human cytomegalovirus (CMV) promoter, is randomly inserted into the X chromosome (Schwenk et al., 1995). As males (XY) only inherit their single X chromosome from their mother, crosses were used where *R26-LSL-TrkA* or -*TrkB* homozygous males were crossed with *CMV*-Cre heterozygous females. Using this breeding scheme both male and female offspring could inherit *CMV-Cre*

(Figure 4.3), allowing analysis of any gender based discrepancies in the results. Using this breeding scheme it is also important to note that all animals would inherit the *R26-LSL-TrkA* or *-TrkB* gene from the homozygous father, allowing relevant littermate controls to be analysed where *CMV-Cre* was not inherited (Figure 4.3).

Breeding

Heterozygous Female

CMV-Cre

✖

Homozygous Male

R26-LSL-TrkA
or
R26-LSL-TrkB

Offspring

25 % Female

R26-LSL-TrkA
or
R26-LSL-TrkB

(control)

25 % Female

CMV-Cre;R26-LSL-TrkA
or
CMV-Cre;R26-LSL-TrkB

(experimental)

25 % Male

R26-LSL-TrkA
or
R26-LSL-TrkB

(control)

25 % Male

CMV-Cre;R26-LSL-TrkA
or
CMV-Cre;R26-LSL-TrkB

(experimental)
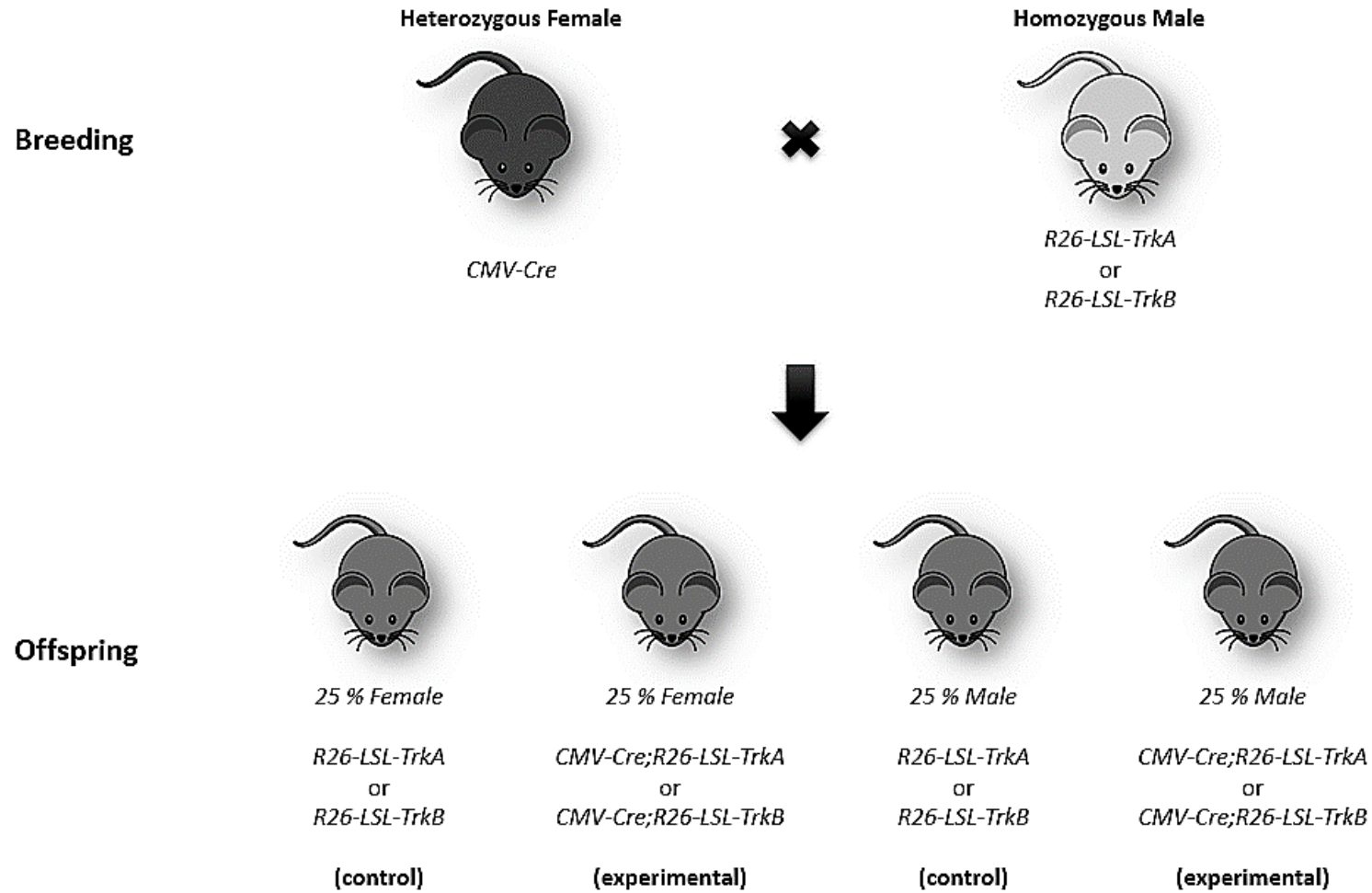
Figure 4.3 Breeding scheme and expected offspring

4.6. Efficiency of Cre-mediated recombination

Deletion of the STOP cassette in offspring from *R26-LSL-TrkA* and *-TrkB* homozygous male and *CMV-Cre* heterozygous female crosses was determined by genotyping PCR of tails from culled litters (or ear notches in >P14 pups) (Figure 4.4A and B). The PCR for the *R26-LSL-TrkA* and *-TrkB* genes produced a 2.8 and 2.7 kb product (denoted floxed-STOP band), whilst deletion of the 1.5 kb STOP cassette produced a 1.4 and 1.3 kb product (denoted Δ band). However in some cases, where offspring inherited both the *CMV-Cre* and *R26-LSL-TrkA* or *-TrkB* genes, no deletion could be observed as revealed by the lack of a detectable Δ band (Figure 4.4A and B). Additionally, some mice exhibited partial recombination indicating that not all cells had excision of the STOP cassette characterised as indicated by the presence of both the floxed-STOP, and Δ bands. This inefficiency in deletion was observed in both male and female offspring (Figure 4.4A, and B). Offspring were categorised into three groups (Table 4.3); <95% deletion (determined by the presence of the floxed-STOP, Δ bands, and Cre), >95% deletion (determined by the complete absence of a floxed-STOP band, and only visualisation of the Δ band, along with Cre), or age, sex-matched littermate controls (only visualisation of the floxed-STOP band, no Cre). To reduce variability in the data, only offspring with complete (>95%) excision of the STOP cassette (herein referred to as TrkA- or TrkB-overexpressing) were used for analysis, and those with <95% deletion were not included.

Table 4.3 Grouping of experimental/control offspring based on PCR

| | | Presence(+)/Absence(-) of PCR Band | | |
		Floxed-STOP	Δ	Cre
Name	**TrkA- or TrkB- overexpressors**	-	+	+
	Controls (age, and sex-matched)	+	-	-
	<95% Deletion (not analysed)	+	+	+
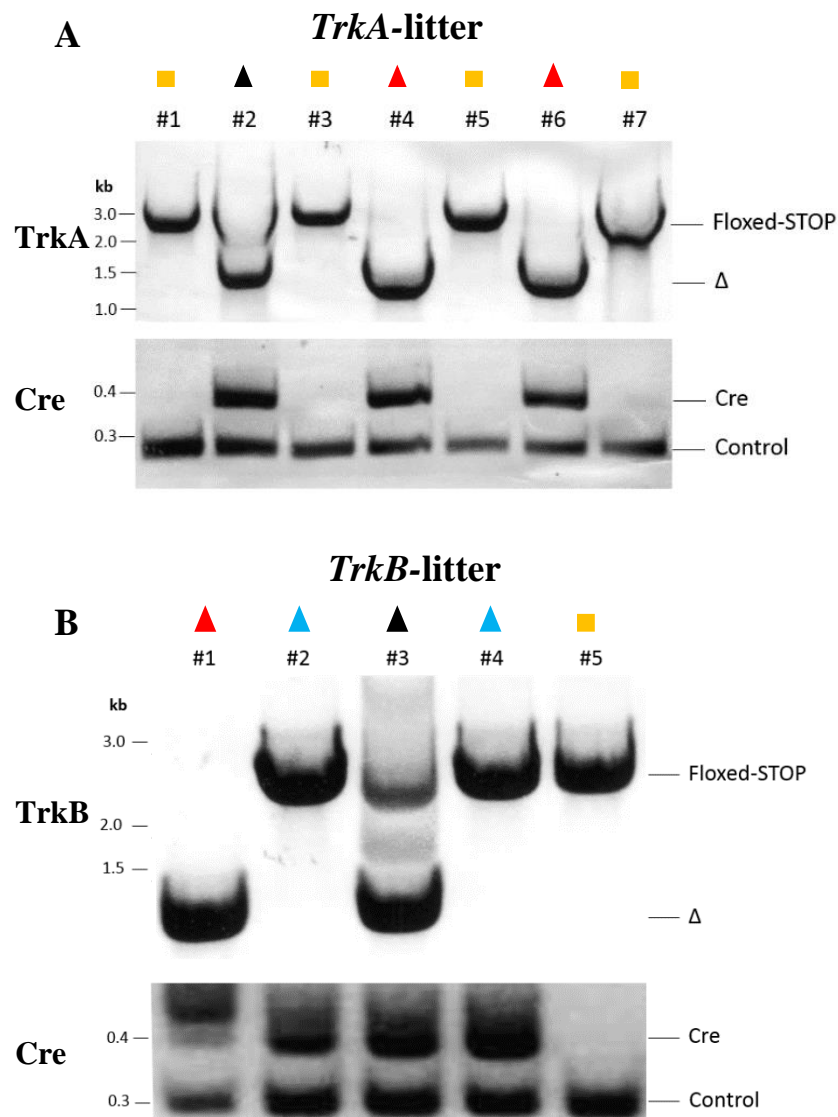
Figure 4.4 Examples of genotyping PCR bands. Examples of genotyping PCR for offspring of A) *R26-LSL-TrkA* and B) *R26-LSL-TrkB* homozygous males crossed with *CMV-Cre* heterozygous females. The floxed-STOP band around 2.8 and 2.7 kb, represents the intact *R26-LSL-TrkA* or *–TrkB* gene. Δ indicates the resulting 1.4 and 1.3 kb band that appears when the 1.5 kb floxed-STOP sequence has been excised in *–TrkA* and *–TrkB* embryos. The expected 381 bp band indicates whether *CMV-Cre* has been inherited. The control band around 275 bp indicates an internal control for *Rosa26* to indicate that the PCR reaction had worked. #1-7 indicates different samples. Red triangles indicate mice that inherited Cre and *R26-LSL-TrkA* or *TrkB* with >95% excision. Black triangles indicate animals that inherited Cre and *R26-LSL-TrkA* or *TrkB* and only a percentage of cells had complete excision. Blue triangles indicate embryos that inherited both genes and had no excision of the loxP-flanked STOP cassette. Orange squares indicate *R26-LSL-TrkA* and *–TrkB* mice that did not inherit Cre (referred to as controls). Controls were sex-matched to experimental animals.

4.7. Detection of TrkA and TrkB protein

The result of the excision of the STOP cassette observed via genotyping PCR was also examined at the protein level. To this end hind limb protein extracts were separated by SDS gel electrophoresis and examined after membrane transfer using antibodies to the HA tag. Tagged TrkA or TrkB could only be detected in the limbs of TrkA- (Figure 4.5B) or TrkB-overexpressors (Figure 4.6B), and not in controls animals not expressing Cre (Figure 4.5B, and Figure 4.6B). Using the pan-Trk antibody that recognises a conserved sequence in the carboxyterminal of TrkA, TrkB and TrkC, there was a massive increase in the levels of Trk-immunoreactive material in Trk-overexpressing embryos compared with lysates of control animals (Figure 4.5A, Figure 4.6A). This is not surprising given the very low levels of Trk expression in the developing limbs (Hallbook et al., 1995; Klein, Martin-Zanca, et al., 1990), possibly reflecting the developing limb innervation.
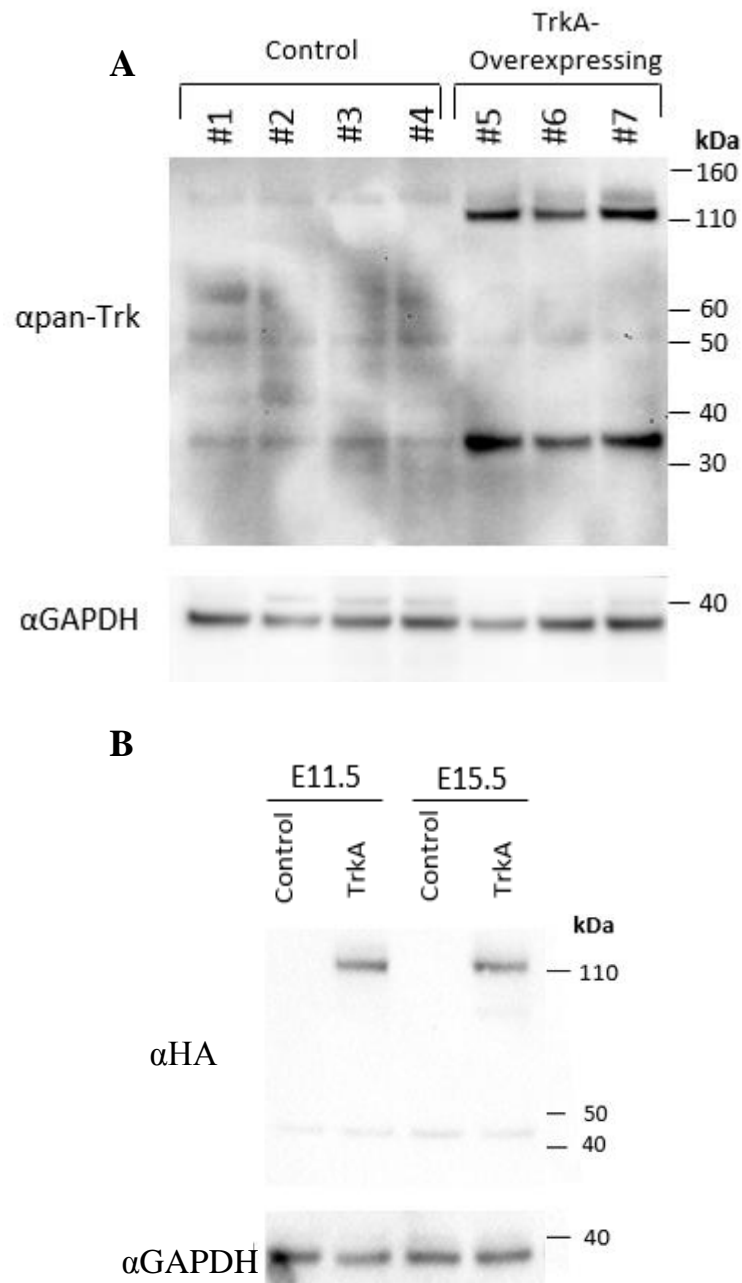
Figure 4.5 Western blot analysis of E18.5 TrkA- litters. Representative western blots of E18.5 limbs from TrkA-overexpressing embryos (#5-#7) compared to controls (#1-#4) using an A) αpan-Trk antibody that detects TrkA-C. Expected band size for pan-Trk – 110-140 kDa. Numbers #1-7 indicates different embryos from different litters. B) HA-tagged exogenous TrkA in limbs of E11.5 and E15.5 litters. Expected HA band size – 110-140 kDa. αGAPDH is used as a loading control ~38 kDa. Size of bands is indicated by the kDa ladder on the right hand side.
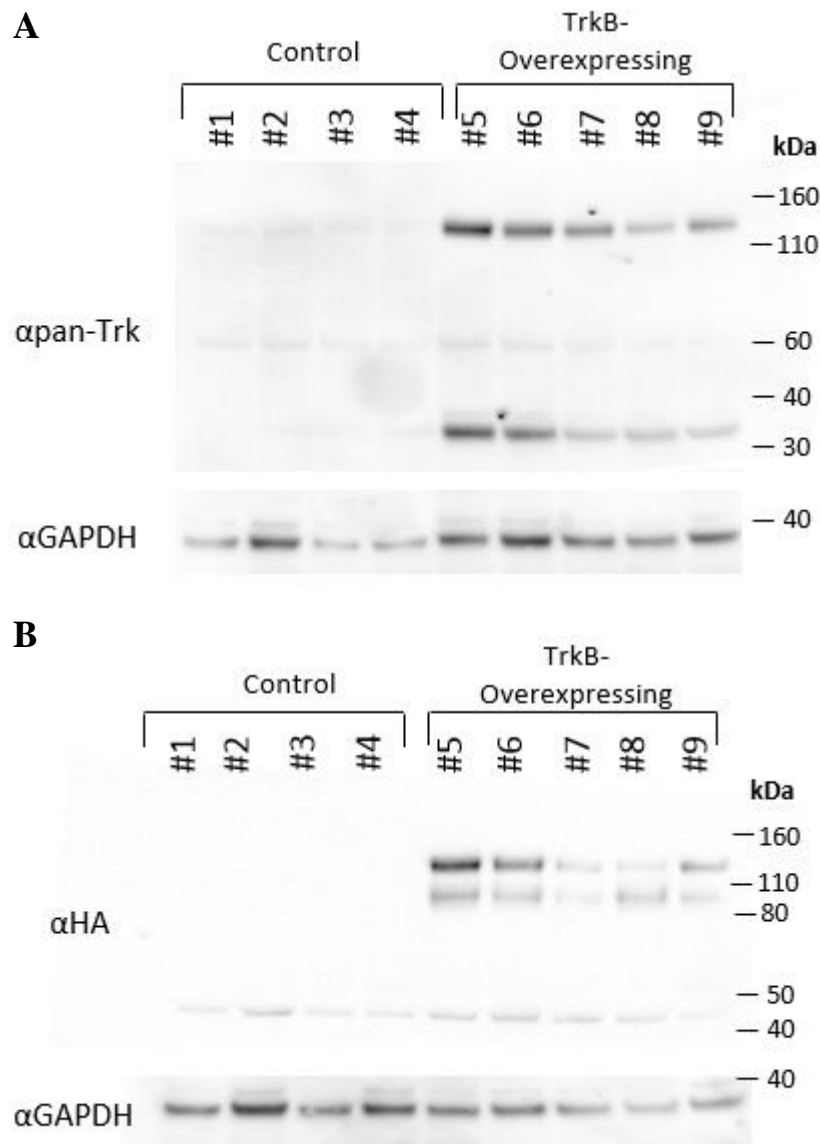
Figure 4.6 Western blot analysis of E18.5 TrkB- litters. Western blot analysis of E18.5 limbs from TrkB-overexpressing embryos (#5-#9) compared to controls (#1-#4) using an A) α pan-Trk antibody that detects TrkA-C (expected band size – 110-140 kDa), and B) αHA antibody that detects only the HA-tagged exogenous TrkB (expected band size – 110-140kDa). αGAPDH is used as a loading control (~38 kDa). Numbers #1-9 indicates different embryos from different litters. Size of bands is indicated by the kDa ladder on the right hand side.

4.8. Detection of GFP early in embryonic development

It is well-established that *Rosa26* is expressed in all cell types (Friedrich and Soriano, 1991; Zambrowicz et al., 1997), and that *CMV-Cre* is active from the earliest stages of development and in embryonic stem cells (Schwenk et al., 1995). To confirm that TrkA/TrkB were expressed at early developmental stages, expression of IRES-EGFP at E6.5 was analysed (Figure 4.7B and Figure 4.7C) in embryos with >95% deletion of the STOP cassette, as determined by genotyping PCR (Figure 4.7A).
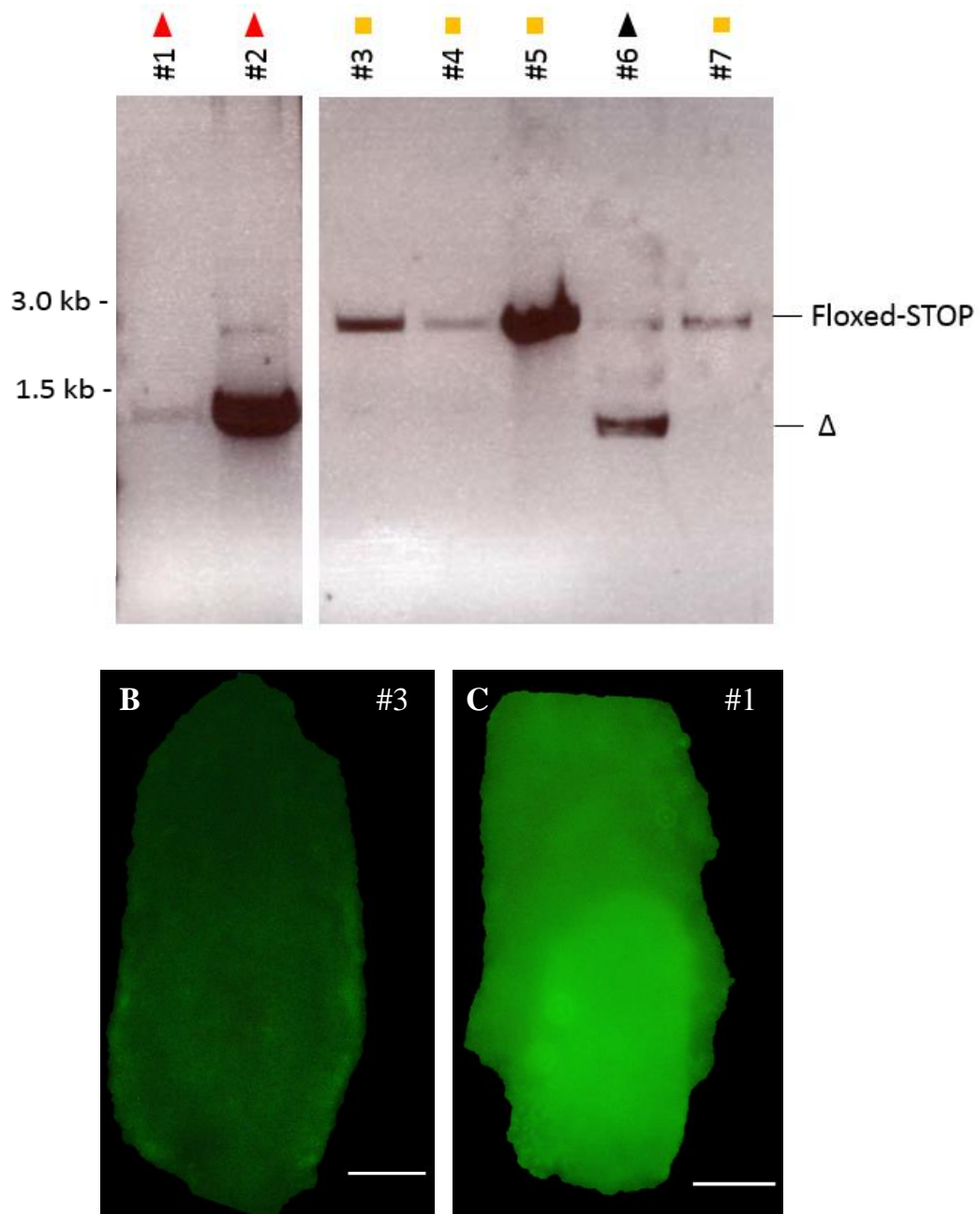
Figure 4.7 STOP cassette excision in E6.5 Embryos. A) Genotyping PCR for E6.5 TrkA (#1-2), and TrkB (#3-7) litters. The floxed-STOP band around 2.7-2.8 kb represents the intact R26-LSL-TrkA or –TrkB sequence. Δ indicates the the resulting 1.3-1.4 kb band that appears when the 1.5 kb loxP-STOP-loxP sequence has been excised. #1-7 indicates different samples. Red triangles indicate embryos with >95% excision. Black triangles indicate offspring where only a percentage of cells had complete excision. Orange squares indicate *R26-LSL-TrkA* and *–TrkB* controls. B,C) Representative images of GFP flourescence across E6.5 embryos; B) embryo #3, and C) embryo #1. Scale bars: 50 μm.

4.9. Summary

This chapter outlined the generation and characterisation of novel *in vivo* mouse lines conditionally expressing TrkA and TrkB under the control of the ubiquitous *Rosa26* promoter (Mao et al., 2001; Soriano, 1999; Zambrowicz et al., 1997) (Figure 4.1). STOP cassette excision in TrkA- and TrkB-overexpressing embryos was evident as early as E6.5 (Figure 4.7). Exploitation of the IRES-GFP sequence in the transgene, demonstrated that STOP cassette excision at E6.5 could be associated with increased EGFP levels across the entire embryo compared to controls (Figure 4.7). The widespread, regular pattern of EGFP fluorescence across the entire E6.5 TrkA- and TrkB-overexpressing embryos supports the idea that expression of TrkA and TrkB under the *Rosa26* promoter is ubiquitous, and occurs during early developmental stages i.e. shortly after blastocyst implantation. As constitutive TrkA expression in neurons has been reported to result in widespread loss of the nervous system, the ability to generate a line constitutively expressing TrkA may not be feasible. Preceding the *TrkA* or *TrkB* sequences with a STOP cassette prevented constitutive expression of TrkA or TrkB, allowing maintenance and breeding of a stable transgenic mouse line. No indications were found for expression of the Trk constructs in the absence of Cre-mediated recombination (Figure 4.5 and Figure 4.6). The control lines designated *R26-LSL-TrkA* and *–TrkB* could be maintained as homozygotes without any detectable viability of fertility problems.

Although any Cre-driver line can be used in combination with the lines generated here, a *CMV-Cre* driver line where a *CMV*-Cre construct was randomly inserted into the X chromosome, was utilised. As males (XY) inherit their only X chromosome from their mother, the breeding schemes used involved *CMV*-Cre heterozygous females to ensure that both male and female offspring inherited *CMV-Cre.* In this way, TrkA- or TrkB-overexpressing offspring of both genders could be studied, to control for any potential gender differences (Figure 4.3). However, for reasons that are unclear, complete excision of the STOP cassette was not evident in some embryos that inherited both the *CMV-Cre* and *R26-LSL-TrkA* or *-TrkB* genes (Figure 4.4). Therefore, only animals with >95% excision of the STOP cassette, as determined by genotyping PCR, were included for analysis for the remainder of this thesis. These mice were designated TrkA- or TrkB-overexpressing, and age, sex-matched, littermate

R26-LSL-TrkA or *–TrkB* mice were designated as controls. Partial excision of stop cassette has observed before by others using the *CMV-Cre* line (Fan et al., 2015; Schwenk et al., 1995).

The experimental strategy described in the above appeared to work as anticipated as the HA tag could only be detected in TrkA- or TrkB-overexpressing embryos (Figure 4.5B and Figure 4.6B). Furthermore TrkA- or TrkB- protein, as detected by a pan-Trk antibody, was also elevated in comparison to controls (Figure 4.5A, and Figure 4.6A), supporting the idea that there is overexpression of TrkA and TrkB. Although the GAPDH loading controls do indicate a slight variation in the amount of protein loaded on the gel, the binary pattern of presence or absence of the protein is striking. The 35 and 45 kDa fragments detected by western blotting are most likely proteolytic products of the Trk receptors (Chao and Bothwell, 2002).

5. Analysis of TrkA-overexpressing embryos

5.1. Introduction

As outlined in chapter 4, a mouse model was generated that conditionally expressed TrkA. This *in vivo* model was generated with the aims of exploring the consequences of ubiquitous TrkA expression from the earliest stages of development with a focus on embryonic lethality, gross morphology and cell death. This was achieved by crossing with a *CMV-Cre* line. As outlined in chapter 4, only mice with >95% deletion, referred to as TrkA-overexpressing, were analysed. Controls were designated as sex-matched, littermate *R26-LSL-TrkA* mice that did not inherit the *CMV-Cre* gene.

5.2. Survival of TrkA-overexpressing mice

Given that TrkA has been previously reported to act as a "dependence receptor", we first explored if its ubiquitous expression would result in widespread death of embryos during development. Survival of TrkA-overexpressing embryos was recorded at various embryonic and postnatal ages through genotyping PCR (Figure 5.1). Amongst ten litters analysed postnatally, only one TrkA-overexpressing pup survived until P14. Litters were observed from birth twice daily, and no remains of pups were found that could be genotyped, indicating that TrkA-overexpressing pups must have been cannibalised within a few hours or days of birth. A Kruskal-Wallis test indicated there was a statistically significant difference in the percentage of surviving TrkA-overexpressing embryos across age ($\chi^2(5) = 12.677$, $p = 0.027$). Dunn's pairwise tests were carried out for the groups (adjusted using Bonferroni correction), and found a significant difference between the percentage of TrkA-overexpressing pups at P14 compared to all other ages (Figure 5.1). The one TrkA-overexpressing pup that did survive postnatally was much smaller than their littermates, and had to be culled at P15 due to being small and sick.
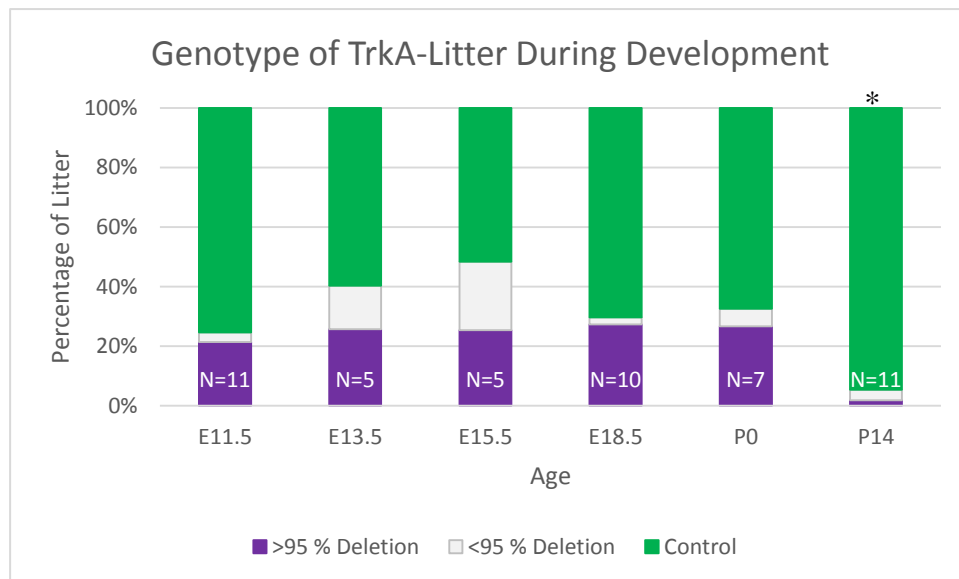
Figure 5.1 Genotype of TrkA-litters during development. The percentage of surviving *CMV-Cre;R26-LSL-TrkA* offspring with >95% deletion (purple, termed TrkA-overexpressors), *CMV-Cre;R26-LSL-TrkA* mice with <95% deletion (grey, termed partial TrkA-expressors), and *R26-LSL-TrkA* (green, termed controls) animals per litter during different developmental stages. The percentage of TrkA-overexpressing mice per litter is stable during embryonic development, but dropped dramatically between P0-P14 (* - *p* <0.05, Kruskal-Wallis test with Dunn's pairwise comparisons). N = number of litters at each age.

5.3. Morphological analysis

TrkA-overexpressors were examined for the presence of morphological deficits with the expectation that TrkA-overexpressing animals may show increased cell death across all cell types, and may therefore be demonstrably smaller than littermate controls. However no gross morphological differences between TrkA-overexpressors and controls were observed across development (Figure 5.2). Measurements of body size and weight were recorded across E11.5-P0, and a two-way ANOVA conducted examining the effect of age and genotype on body size of the TrkA-litters (Figure 5.3A). A statistically significant interaction between the effects of genotype and age ($F(1,40) = 4.904$, $p = 0.033$) was detected. Examining this interaction using Bonferroni pairwise comparisons revealed a slight, but significant reduction in the body area of TrkA-overexpressors ($M = 174.73$ mm^2, SD $\pm$ 11.74) and their sex-matched littermates ($M = 188.54$ mm^2, SD $\pm$ 11.40) at E18.5 ($p = 0.007$, Figure 5.3A). However there was no significant difference between TrkA-overexpressing embryos ($M = 49.23$ mm^2, SD $\pm$ 5.98) and their littermates ($M = 49.88$ mm^2, SD $\pm$ 6.54) at E13.5 ($p = 0.885$, Figure 5.3A). As expected during development, there was a significant increase in body area between E13.5 and E18.5 embryos regardless of genotype ($p < 0.001$, Figure 5.3A). However the reduction in body area at E18.5 was not matched by any significant difference in the weight of P0 TrkA-overexpressors ($M = 1.55$ g, SD $\pm$ 0.11), and their sex-matched, littermate controls ($M = 1.63$ g, SD $\pm$ 0.12) (t(18) = 1.446, $p = 0.165$; Figure 5.3B). The weight of P0 offspring was obtained from six litters, with an average litter size of 4.7 (SD $\pm$ 1.2) pups.

	Control	**TrkA-overexpressing**
E13.5		
E18.5		
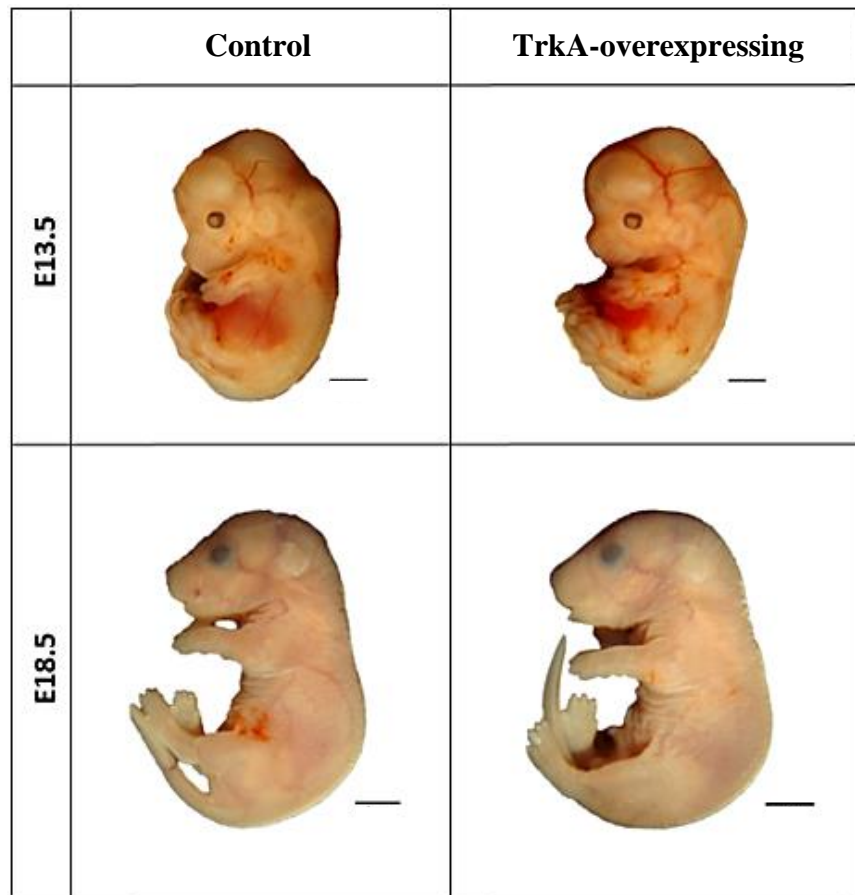
Figure 5.2 Morphology of TrkA-overexpressing embryos at E13.5 and E18.5. Representative images of TrkA-overexpressing male embryos at E13.5 and E18.5, compared to littermate controls. Scale bars are 1.5 mm for E13.5 embryos, and 3 mm for E18.5 embryos.
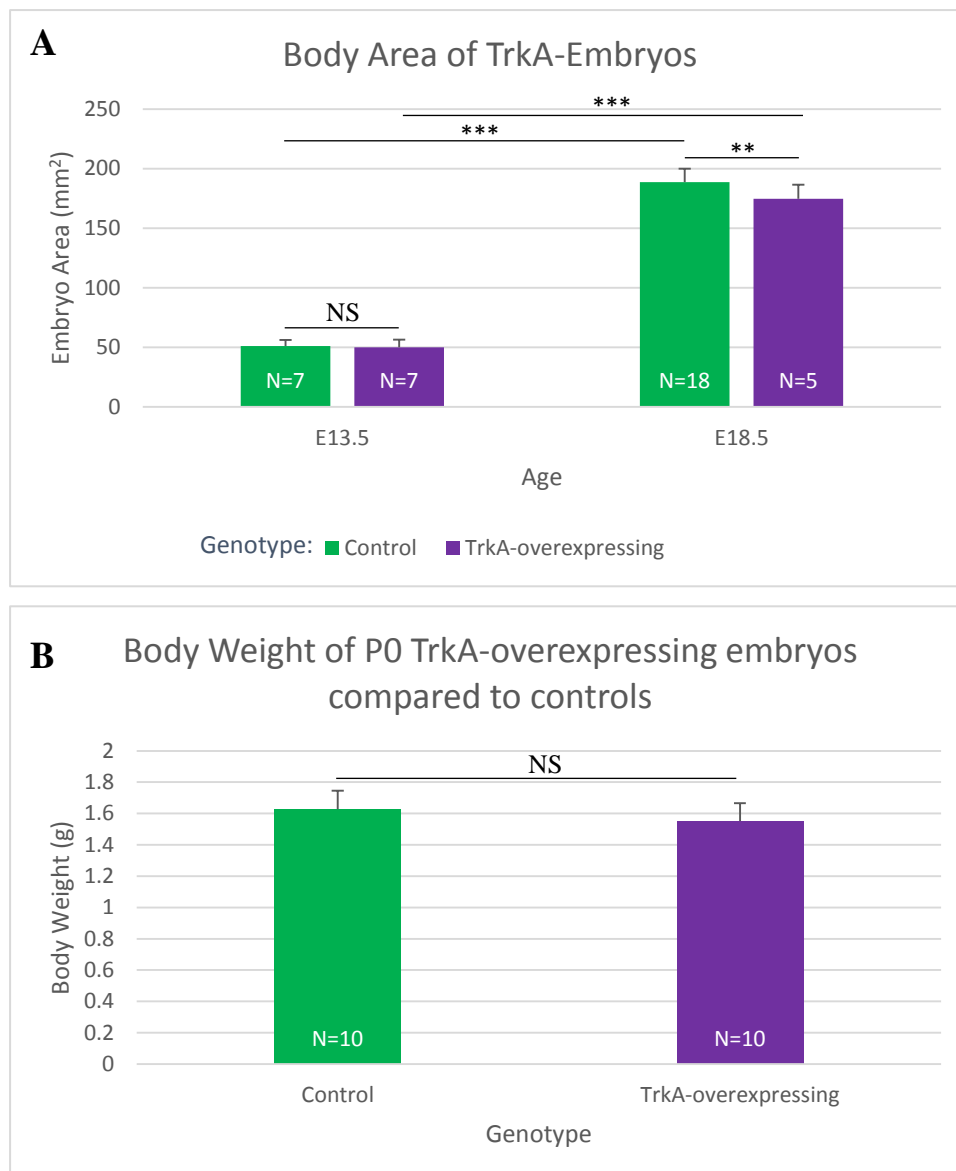
Figure 5.3 Size and weight of TrkA-overexpressing embryos. A) The area of embryos at E13.5 and E18.5 is similar between TrkA-overexpressing embryos (purple) and their littermates (green). NS – not significant, ** - p <0.01, *** - p < 0.001 (two-way ANOVA with post-hoc Bonferroni pairwise comparisons). B) The weight of pups at P0 is similar between TrkA-overexpressing embryos and their littermates. Data from six litters, average litter size = 4.7 (SD ± 1.2). NS – not significant (independent t-test). Error Bars - standard deviation. N = number of embryos analysed per group.

To further analyse the morphology of TrkA-overexpressing litters, haematoxylin and eosin staining was performed on transverse sections of offspring from E11.5-P0. It was observed that the general morphology of the eye, spinal cord, cerebellum and nose appeared to be normal in terms of size, and structure at E18.5 between genotypes (Figure 5.4). To quantify if there were any changes to the number of CNS neurons, cortices were dissected from litters at E18.5, and dissociated. The total number of neurons was counted, and there appeared to be no significant difference in the number of cortical neurons between TrkA-overexpressors (M = 2.34 x10^6 neurons, SD $\pm$ 0.83) and the sex-matched littermate controls (M = 2.25 x10^6 neurons, SD $\pm$ 0.81) (t(5) = -0.154, p = 0.884; Figure 5.5). This altogether indicates that whilst TrkA-overexpressing pups die soon after birth, the overexpression of TrkA across all cell types throughout development did not result in generalised cell death.

Control   TrkA-overexpressing
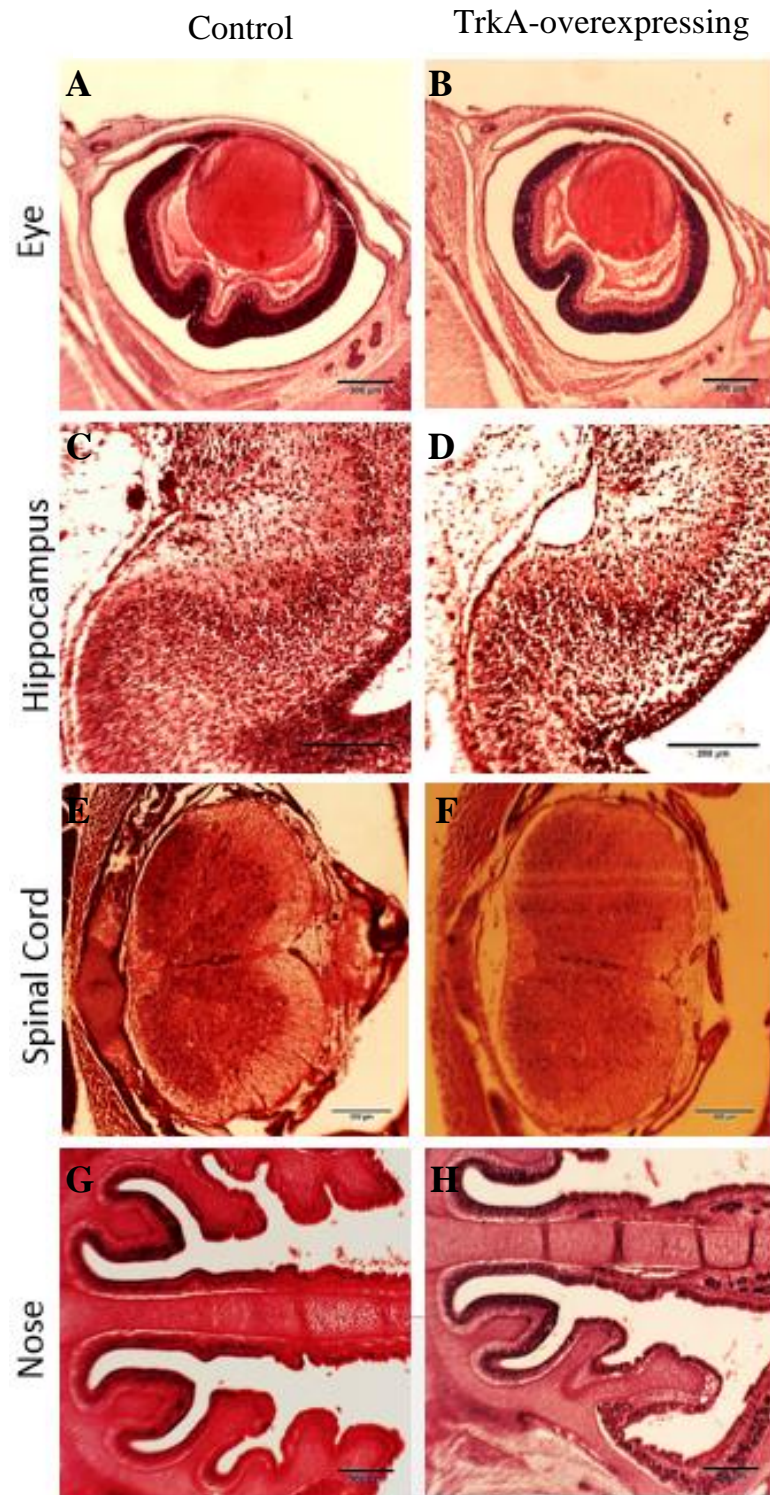
Figure 5.4 The eye, hippocampus, spinal cord and nose in E18.5 of control *versus*
TrkA-overexpressing embryos. Representative images of the eye (A,B),
hippocampus (C,D), spinal cord (E,F), and nose (G,H) in E18.5 TrkA-overexpressing
embryos (B,D,F,H) compared to littermate controls (A,C,E,F). Scale bars: 300 μm,
except B,C where scale bars are 200 μm.
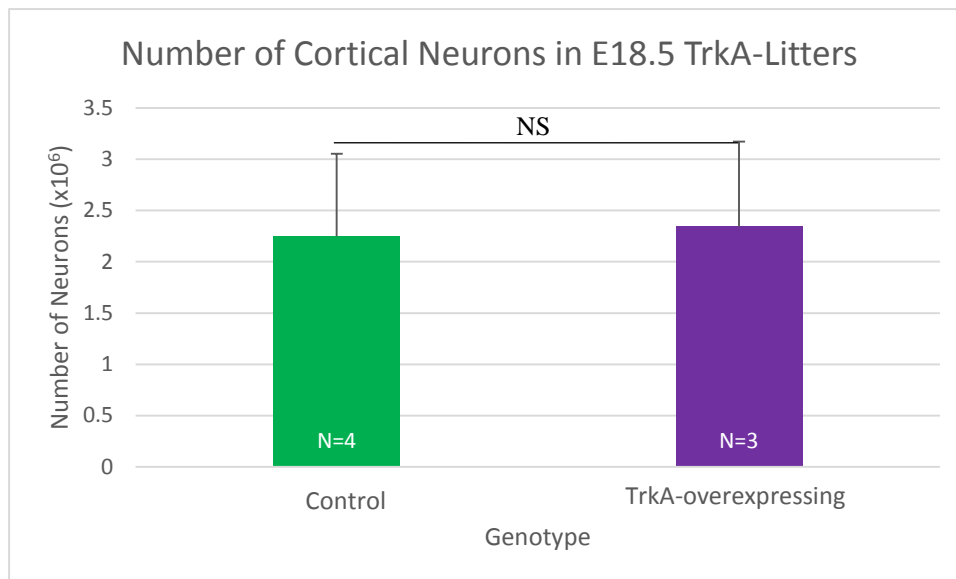
Figure 5.5 Number of cortical neurons in E18.5 TrkA-litters. Number of neurons in dissociated cortices of TrkA-overexpressing mice (purple) compared to controls (green). N = number of embryos analysed from two litters. Error bars - standard deviation. NS – not significant (independent t-test).

5.4. iDISCO analysis

The observation that TrkA-overexpressors died in the first few days postnatally, but did not have any obvious morphological phenotype, indicated that TrkA over-expression may cause the loss of specific populations of cells that are critical for postnatal survival. As this phenotype (as outlined in the introduction) has been previously reported in mice lacking both *Ngf* alleles, sympathetic and sensory ganglia were examined in detail. The plausibility of this hypothesis was first examined in whole mounts of TrkA-litter heads using 3D imaging of immunolabelled solvent-cleared whole embryos (short iDISCO(Renier et al., 2017)) using antibodies to TrkA. This antibody was first validated with E12 wild-type embryos (Figure 5.6). As expected, this antibody specifically marked known TrkA-expressing structures such as the trigeminal, dorsal root, and superior cervical ganglia (Figure 5.6A). Using this method, the differences between the earlier, and later formed dorsal root ganglia (DRG) could also be observed (Figure 5.6B). iDISCO was therefore next used to explore a possible loss of ganglia and/or nerves using E15.5 TrkA-overexpressing embryos compared to controls.

iDISCO using a TrkA antibody in E15.5 TrkA-overexpressing embryo heads demonstrated that there was a consistent loss of the trigeminal, superior cervical and dorsal root ganglia in TrkA-overexpressing embryos compared to their littermates (Figure 5.7). As expected, there was also widespread TrkA staining across the head of TrkA-overexpressing mice not limited to neuronal structures. This staining pattern was not observed in littermate controls, where TrkA staining was restricted to specific neuronal structures.
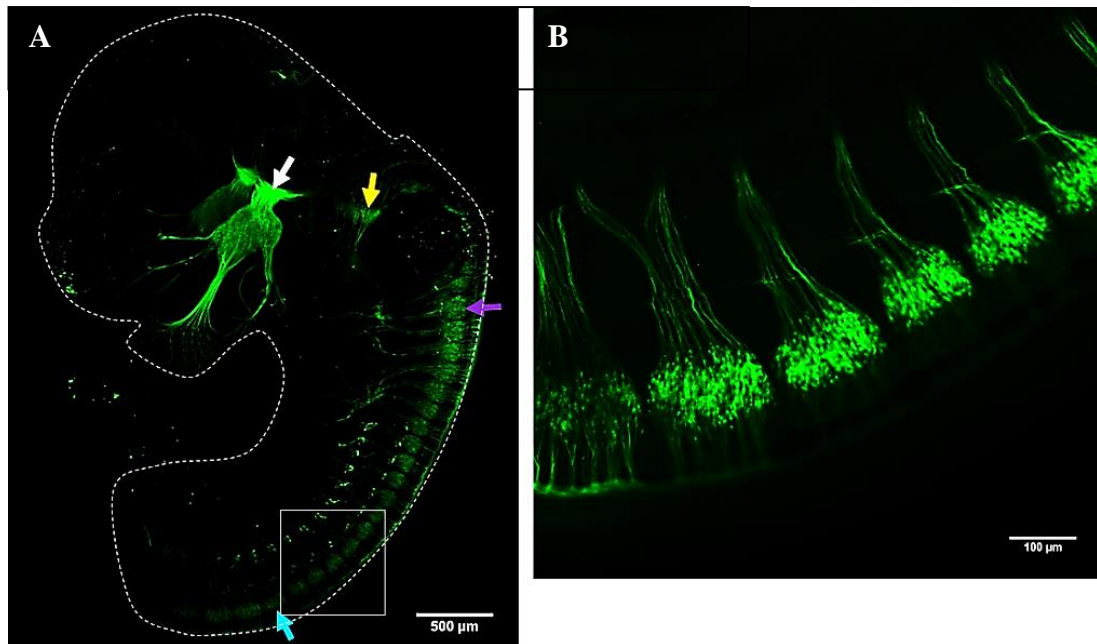
Figure 5.6 Validation of TrkA iDISCO staining. Representative images of iDISCO staining using a TrkA antibody in E12 wild type embryos. A) The whole embryo (indicated by dotted white boundary) can be visualised using iDISCO, without the need for sectioning. TrkA antibody seems to be specific, and compatible with this method, as only known TrkA-expressing cells can be visualised. These include the trigeminal ganglia (white arrow), the superior cervical ganglia (yellow arrow), and the dorsal root ganglia. The expected developmental gradient can be observed (more mature ganglia: purple arrow, younger ganglia blue arrow). Scale bar: 500 μm. The grey box indicates the area taken for higher magnification images in B) magnified images of the dorsal root ganglia demonstrate characteristic TrkA staining patterns. Scale bar: 100 μm.
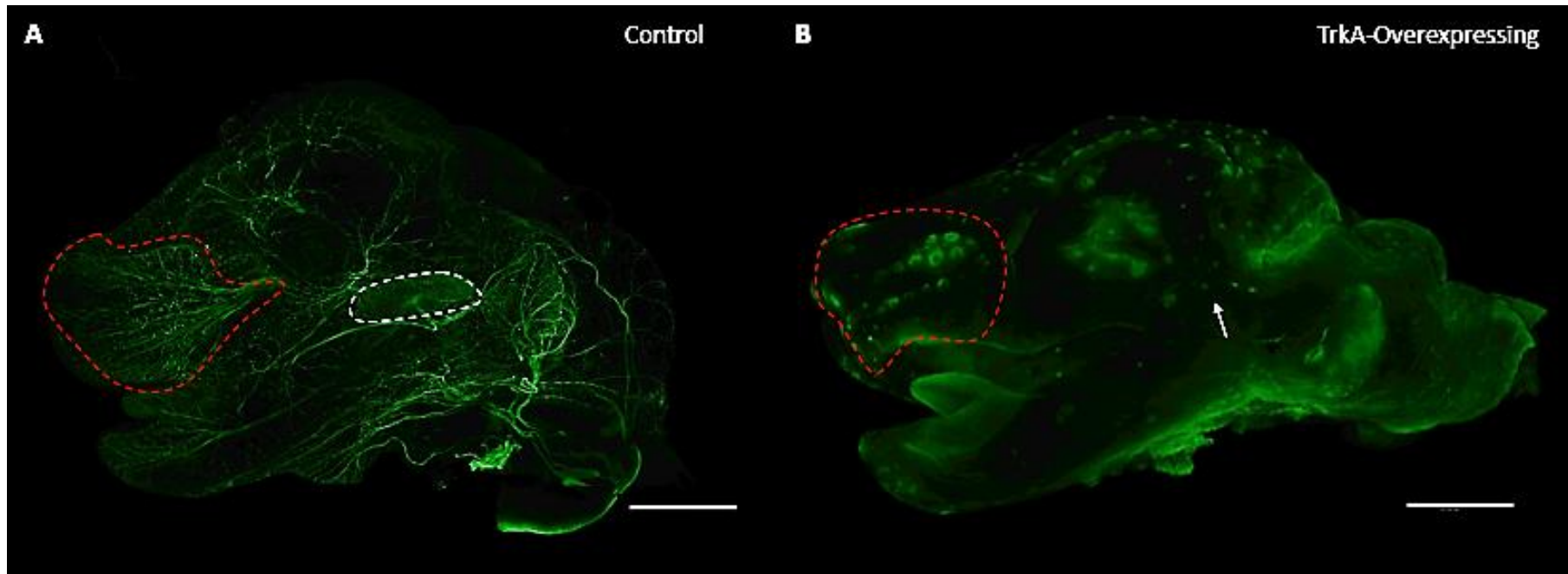
Figure 5.7 TrkA iDISCO staining of TrkA-overexpressor *versus* littermate control. Representative images of iDISCO staining using a TrkA antibody in E15.5 A) control *versus* B) TrkA-overexpressing mice. Note the general TrkA staining outside the nervous system of TrkA-overexpressing embryos, while in the littermate control there is specific neuronal staining, including the indication of ganglia e.g. the trigeminal ganglia (dotted white line in A, missing ganglia indicated by white arrow in B). Ectopic TrkA staining can also be identified in areas such as the whisker pad (red dotted line). Scale bars: 500 μm.

5.5. Volume of sensory and sympathetic ganglia

Given the iDISCO observations that sensory and sympathetic ganglia in the head may be affected in TrkA-overexpressing embryos at E15.5, haematoxylin and eosin stainings were performed on transverse sections of TrkA-litters at E11.5, E15.5, E18.5 and P0. Ganglia that appeared to be lost via iDISCO were selected for analysis, including the superior cervical (sympathetic; SCG), dorsal root (sensory; DRG, C1) and trigeminal ganglia (sensory; TG). As these ganglia endogenously express TrkA, the analysis also included ganglia expressing little (sensory; nodose-petrosal ganglia, NPG, (Wetmore and Olson, 1995)) or no (sensory, vestibular ganglia, VG, (Schecterson and Bothwell, 1994)) endogenous TrkA. E11.5-P0 time points were chosen as they correspond with the periods of formation, and naturally occurring cell death across these ganglia ((Coughlin et al., 1977; White et al., 1998); for more detail see section 7.4).

Two-way ANOVA revealed that there was a significant interaction of age and genotype in ganglia that endogenously express TrkA, such as the SCG ($F_{(2,27)}$ = 13.817, p <0.001), DRG ($F_{(2,23)}$ = 4.669, p = 0.02) and TG ($F_{(2,24)}$ = 34.761, p <0.001, Table 5.1). Bonferroni pairwise comparisons revealed that the volume of the SCG in TrkA-overexpressing mice was not significantly different at E15.5 compared to littermate controls (p = 0.546), but at E18.5 and P0 the volume of the SCG was significantly reduced compared to littermates (p<0.001, Table 5.1, Figure 5.8A, and Figure 5.8B). Comparisons also indicated that the DRG volume was not significantly different between TrkA-overexpressors and sex-matched littermates at early stages such as E11.5 (p = 0.972) and E15.5 (p = 0.930, Table 5.1), but were significantly reduced compared to littermates by E18.5 (p = 0.001, Figure 5.8C, and Figure 5.8D). Similarly, there was no significant difference between genotypes in the trigeminal ganglia at E11.5 (p = .618, Table 5.1), while there was a significant reduction in the trigeminal ganglia volume in TrkA-overexpressing embryos compared to littermates at E15.5 and E18.5 (p<0.001, Table 5.1, Figure 5.8E, Figure 5.8F).

In the NPG, where a fraction of sensory neurons have been reported to endogenously express TrkA (Wetmore and Olson, 1995), there was no significant interaction of age

and genotype ($F(2,30) = 2.323$, $p = 0.115$), however there was a main effect of genotype ($F(1,30) = 5.517$, $p = 0.026$), and pairwise comparisons revealed that at E18.5 there was a slight, but significant reduction in the NPG volume ($p = 0.021$, Table 5.1) in TrkA-overexpressors (Figure 5.9A) compared to the sex-matched littermates (Figure 5.9B). However at E15.5 ($p = 0.712$), and P0 ($p = 0.058$) there was no significant difference between the genotypes. Meanwhile in the vestibular ganglia which has no endogenous TrkA expression (Schecterson and Bothwell, 1994), one way ANOVA analysis of the volume of the vestibular ganglia at E18.5 indicated that there was no significant difference between TrkA-overexpressing embryos (Figure 5.9C) and littermate controls ($F(1,8) = 1.758$, $p = 0.222$, Figure 5.9D, Table 5.1).
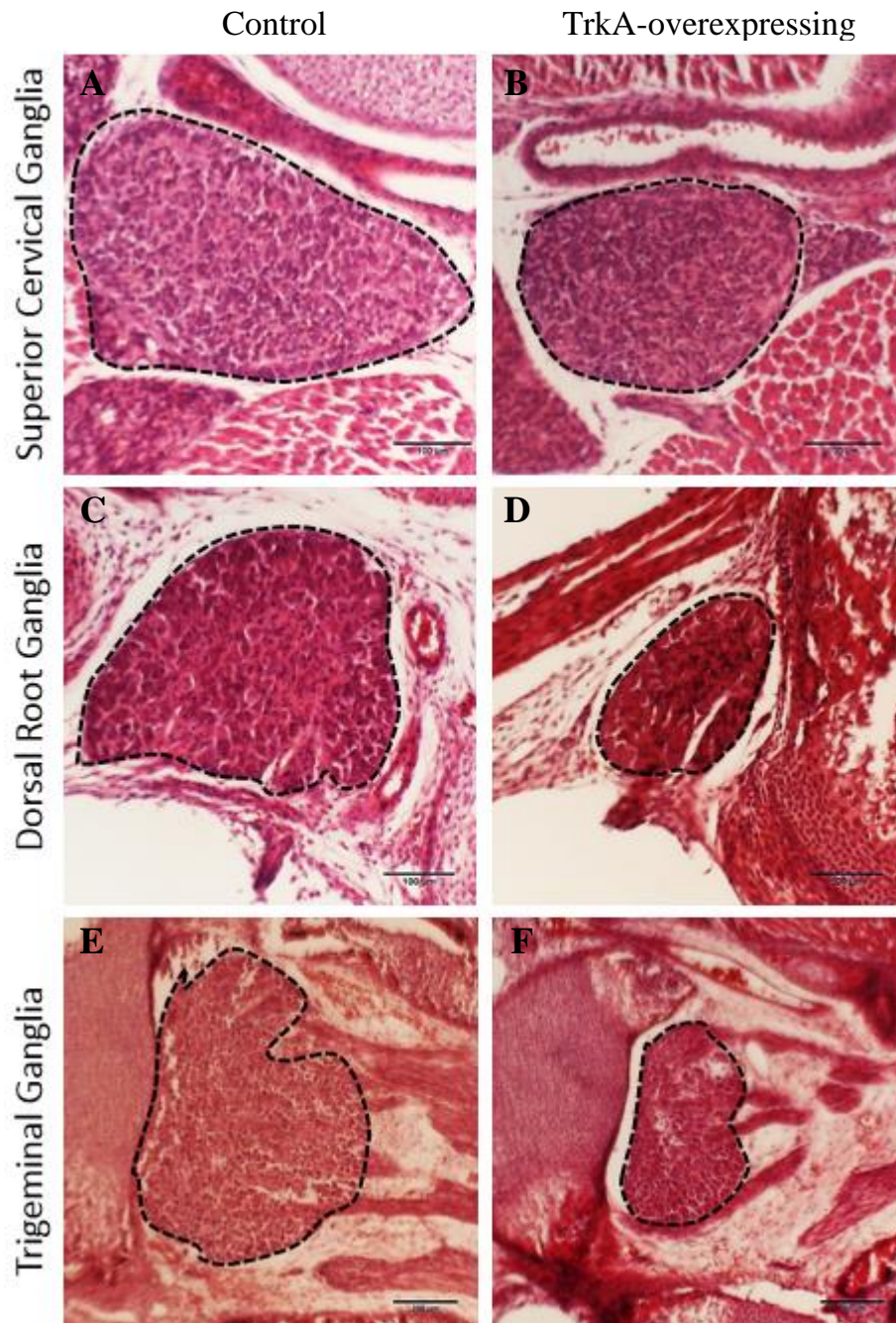
Figure 5.8 The superior cervical, dorsal root, and trigeminal ganglia in E18.5 TrkA litters. Representative images of the superior cervical (A,B), C1 dorsal root (C,D), and trigeminal (E,F) ganglia in E18.5 TrkA-overexpressing embryos (B,D,F) which appear to be reduced in size compared to their sex-macthed, littermate controls (A,C,E). Ganglia are indicated by black, dotted lines. Scale bars A-D: 100 μm, scale bars E-F: 200 μm.
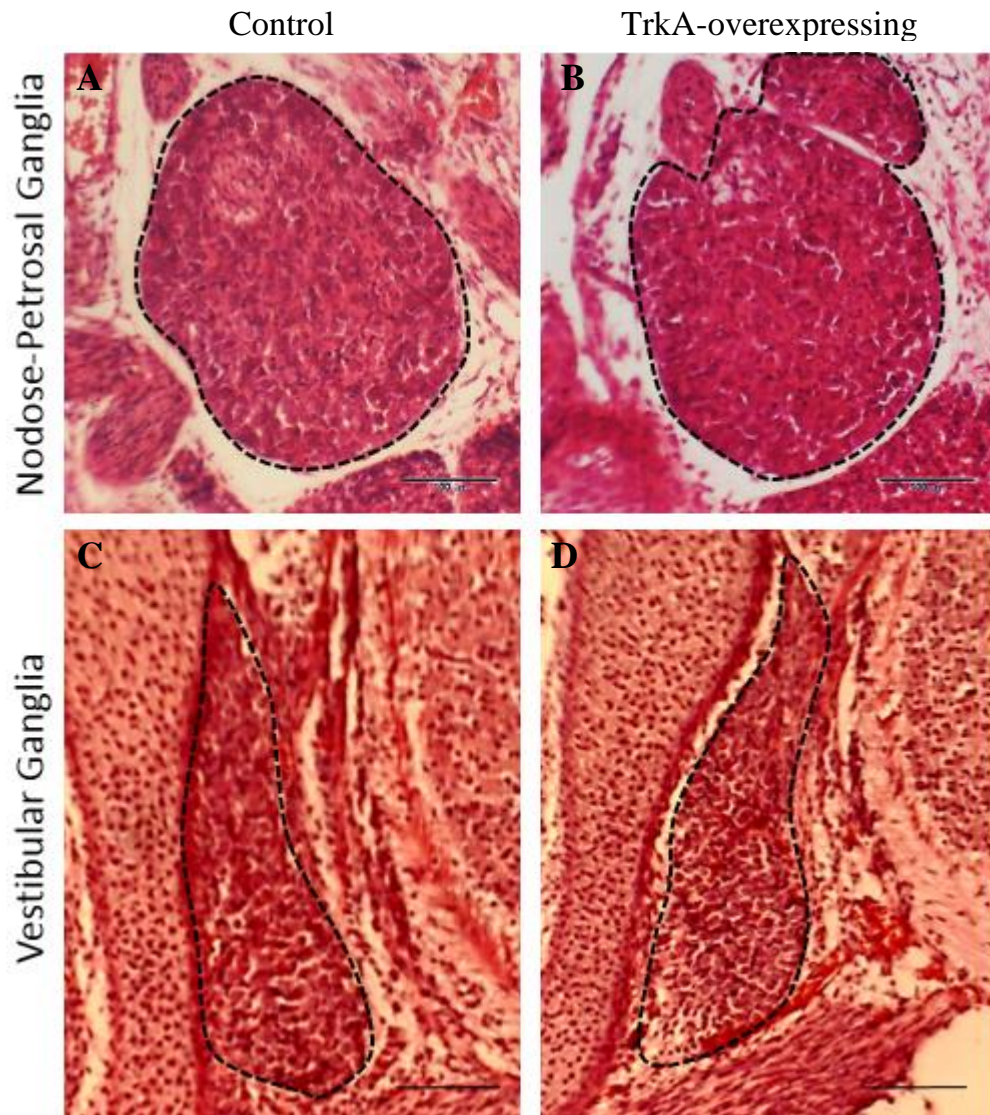
Figure 5.9 The nodose-petrosal and vestibular ganglia in E18.5 TrkA-litters. Representative images of the nodose-petrosal (A,B), and vestibular (C,D) ganglia in E18.5 TrkA-overexpressing embryos (B,D) appear to be similar in size compared to their sex-matched, littermate controls (A,C). Ganglia are indicated by black, dotted lines. Scale bars: 100 μm.

Table 5.1 Volume of sensory and sympathetic ganglia in TrkA-litters

	E11.5			E15.5			E18.5			P0		
	Control x10^4 μm^3 (±SD) $^{(N)}$	TrkA-over expressing x10^4 μm^3 (±SD) $^{(N)}$	Remaining % vs. Control (p)	Control x10^4 μm^3 (±SD) $^{(N)}$	TrkA-over expressing x10^4 μm^3 (±SD) $^{(N)}$	Remaining % vs. Control (p)	Control x10^4 μm^3 (±SD) $^{(N)}$	TrkA-over expressing x10^4 μm^3 (±SD) $^{(N)}$	Remaining % vs. Control (p)	Control x10^4 μm^3 (±SD) $^{(N)}$	TrkA-over expressing x10^4 μm^3 (±SD) $^{(N)}$	Remaining % vs. Control (p)
Sensory Ganglia												
Dorsal Root (C1)	386 (±107) (5)	340 (±54) (4)	88% NS	1061 (±350) (4)	504 (±114) (7)	47% NS	5890 (±5373) (4)	940 (±414) (5)	16% **	*NA*		
Trigeminal	4581 (±697) (5)	3820 (±2400) (3)	85% NS	11229 (±2785)(5)	3781 (±1587) (8)	34% ***	24562 (±937) (4)	7059 (±3046)(5)	29% ***	*NA*		
Vestibular	*NA*			*NA*			2145 (±205) (4)	1981 (±184)(6)	92% NS	*NA*		
Nodose-petrosal	*NA*			1080 (±116)(5)	1178 (±287) (8)	109% NS	2314 (±397) (6)	1691 (±363)(7)	73% *	2578 (±793) (5)	2004 (634) (5)	77% NS
Sympathetic Ganglia												
Superior Cervical	*NA*			2225 (±338)(5)	2027 (±804) (9)	91% NS	5108 (±180) (4)	2811 (±415)(5)	55% ***	5023 (±751) (5)	2536 (±324) (5)	50% ***

Volume counts were determined from haematoxylin and eosin stainings as detailed in section 2.8. N= number of embryos analysed, indicated in superscript brackets, from a minimum of three litters per time point. Two of each ganglia were counted per embryo and averaged. NS - not significant, * - p < 0.05, ** - p < 0.01, *** - p < 0.001 compared to littermate controls (two-way ANOVA with Bonferroni pairwise comparisons, except the vestibular ganglia where one-way ANOVA was performed).

5.6. Neuronal counts in sensory and sympathetic ganglia

To determine whether the reduction in ganglia volume was due to a loss of neurons, or if the reduction could be explained by events preceding the time of naturally occurring cell death, counts were performed on these ganglia across E11.5-P0 as outlined in section 2.8.4.

A two-way ANOVA was performed for the number of neurons in the SCG, which revealed a significant interaction between genotype and age ($F(2,26)= 7.762$, $p = 0.002$), of which there was a significant main effect of age ($F(2,26) = 5.789$, $p = 0.008$) and genotype ($F(1,26) = 10.960$, $p = 0.003$). Probing of this interaction with Bonferroni pairwise comparisons revealed that at E15.5 there was no significant difference in the number of SCG neurons between genotypes ($p = 0.218$), although there was a significant reduction in the number of SCG neurons in E18.5 ($p = 0.005$) and P0 ($p = 0.001$) TrkA-overexpressors compared to sex-matched littermate controls. Pairwise comparisons also indicated that while the number of neurons in the SCG of control animals significantly increased between E15.5-E18.5 ($p = 0.002$), as is expected of normal development, there was no further increase in the number of neurons in the SCG across age in the TrkA-overexpressing embryos ($p = 1.000$, Figure 5.10A).

In the dorsal root ($F(2,23) = 15.081$, $p < 0.001$), and trigeminal ($F(2,24) = 27.028$, $p < 0.001$) ganglia there was a significant interaction of age and genotype. Bonferroni pairwise comparisons indicated that there was no difference in the number of neurons between genotypes in the E11.5 dorsal root ($p = 0.243$) or trigeminal ($p = 0.350$), ganglia, but in both ganglia by E15.5 and E18.5 this was statistically significant ($p < 0.001$) (Figure 5.10C).

Two-way ANOVA showed there was also a significant interaction between age and genotype for the nodose-petrosal ganglia ($F(2,30) = 3.983$, $p = 0.029$). Bonferroni pairwise comparisons revealed that while the number of neurons in the NPG was not significantly different between genotypes at E15.5 ($p = 0.195$, Figure 5.11B) and E18.5 ($p = 0.114$, Figure 5.11B), there was a significant decrease in the number of NPG neurons between TrkA-overexpressing neurons and littermate controls at P0 ($p = 0.023$, Figure 5.11B). By contrast, in the vestibular ganglia at E18.5 one-way

ANOVA showed there was no significant difference in the number of neurons between TrkA-overexpressors and littermates ($F(1,8) = 0.557$, $p = 0.477$, Figure 5.11A).

A Number of Neurons in the Superior Cervical Ganglia of TrkA-Litters Over Development

B Number of Neurons in the Trigeminal Ganglia of TrkA-Litters Over Development

C Number of Neurons in the Dorsal Root Ganglia of TrkA-Litters Over Development
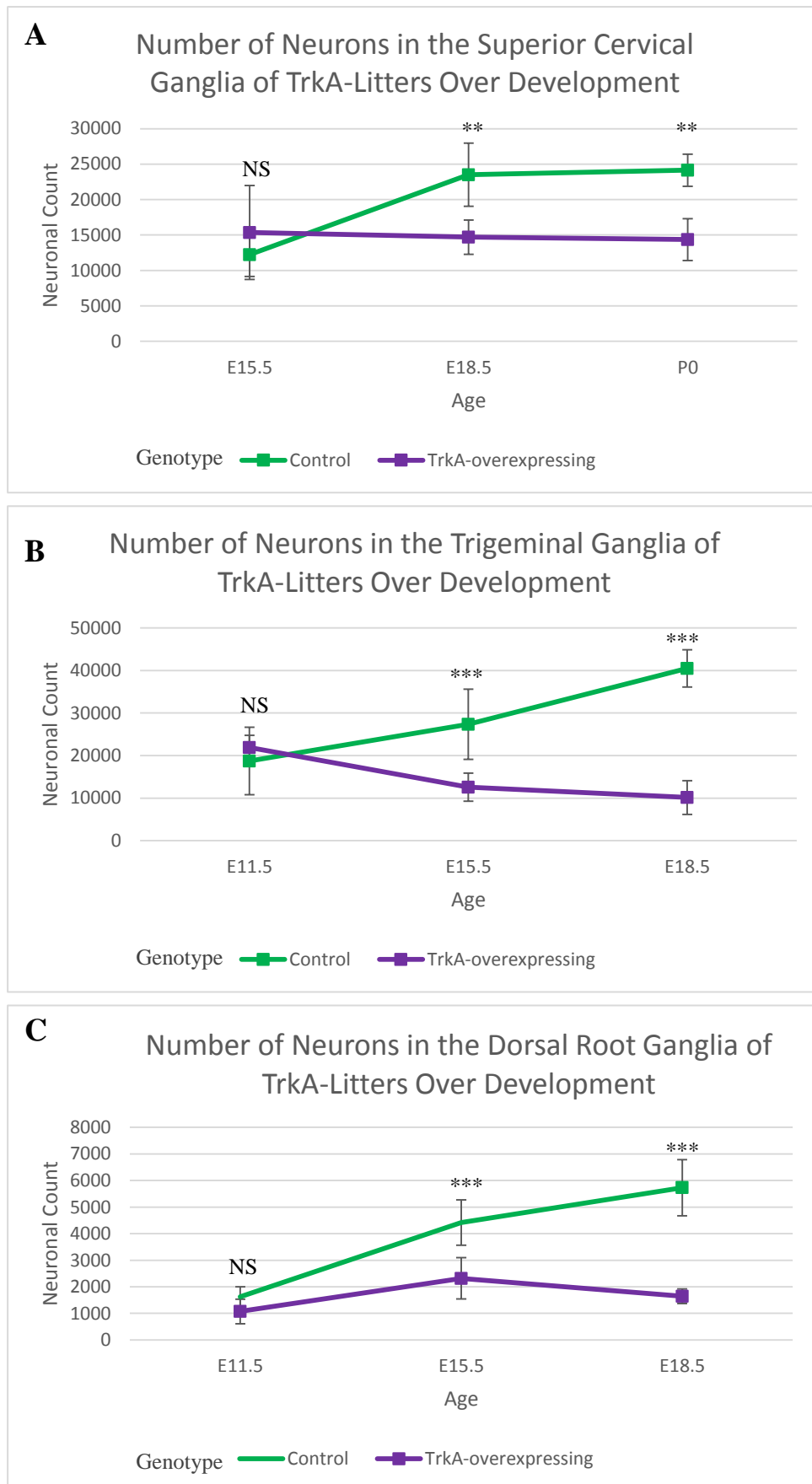
Figure 5.10 Number of neurons in the superior cervical, trigeminal and dorsal root ganglia in TrkA-overexpressing embryos. A) The number of neurons in the A) superior cervical, B) trigeminal and C) dorsal root ganglia of TrkA-overexpressing embryos (purple) compared to littermate controls (green) over development. Neuronal counts were determined on sections stained with haematoxylin and eosin. Number of embryos analysed in each group are the same as outlined in Table 5.1, from a minimum of three litters per age. Two of each ganglia were counted per embryo and averaged. NS - not significant, * - $p < 0.05$, ** - $p < 0.01$, *** - $p < 0.001$ compared to littermate controls (Two-way ANOVA with Bonferroni pairwise comparisons).
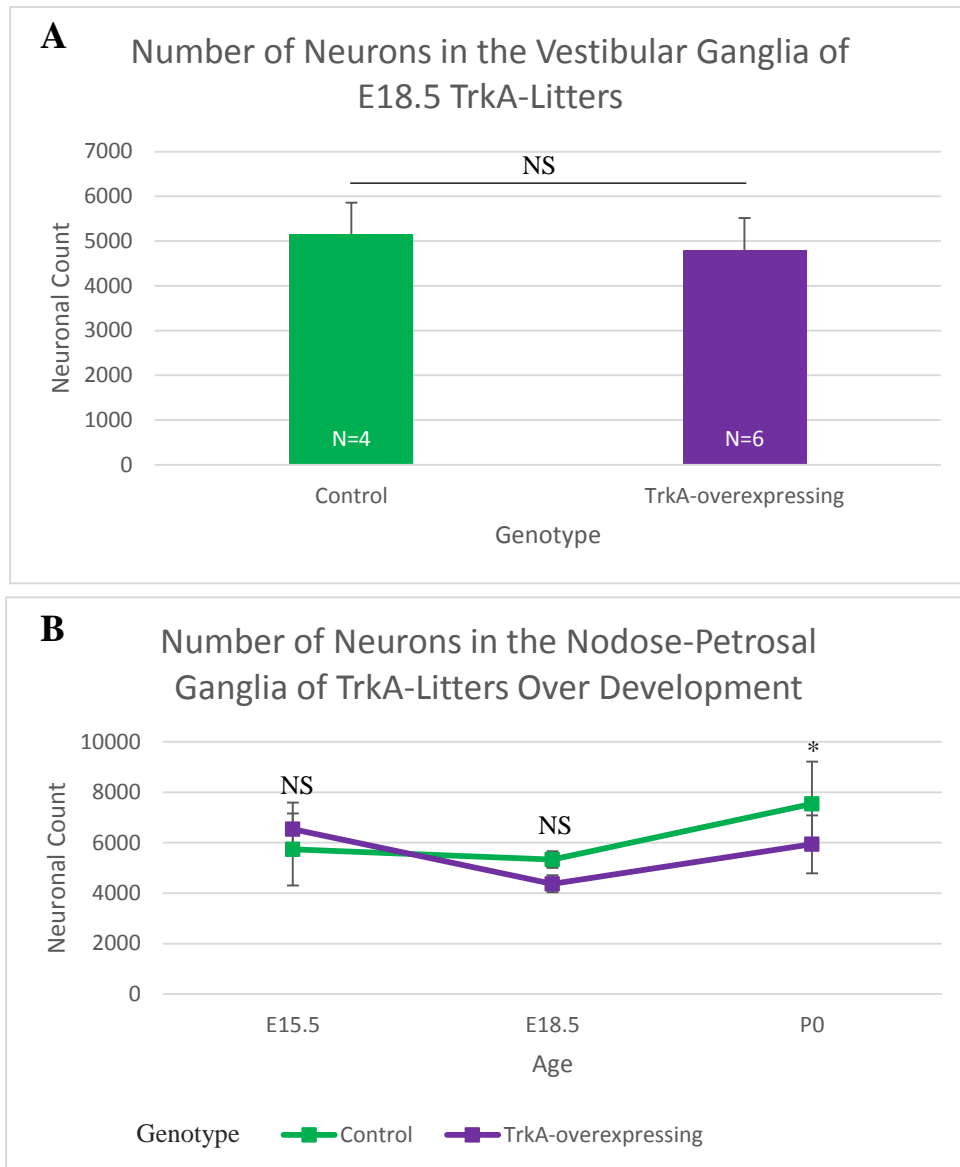
Figure 5.11 Number of neurons in the nodose-petrosal and vestibular ganglia of TrkA-overexpressing embryos over development. A) Number of neurons in the vestibular ganglia of TrkA-overexpressing embryos (purple) compared to littermate controls (green) at E18.5. NS – not significant (one-way ANOVA). B) Number of neurons in the nodose-petrosal ganglia of TrkA-overexpressing embryos compared to littermate controls over development. NS - not significant, * - $p < 0.05$, ** - $p < 0.01$, *** - $p < 0.001$ compared to littermate controls (Two way ANOVA with Bonferroni pairwise comparisons). Neuronal counts were determined on sections stained with haematoxylin and eosin. Number of embryos analysed are the same as outlined in Table 5.1, from a minimum of three litters per age. Two of each ganglia were counted per embryo and averaged.

5.7. Apoptosis in sensory and sympathetic ganglia

To confirm that the reduction in the number of neurons in these ganglia was due to apoptosis, immunohistochemistry was performed on E13.5 TrkA-overexpressing embryos using antibodies to cleaved (active) caspase-3. Both the trigeminal (Figure 5.12; $F(1,6) = 58.043$, $p<0.001$) and dorsal root ganglia (C1) (Figure 5.13; $F(1,6) = 25.740$, $p = 0.002$) of TrkA-overexpressing embryos demonstrated a significantly increased number of cleaved caspase-3 positive cells, indicating that there were higher levels of apoptosis in the sensory and sympathetic ganglia of TrkA-overexpressing mice compared to their littermates.
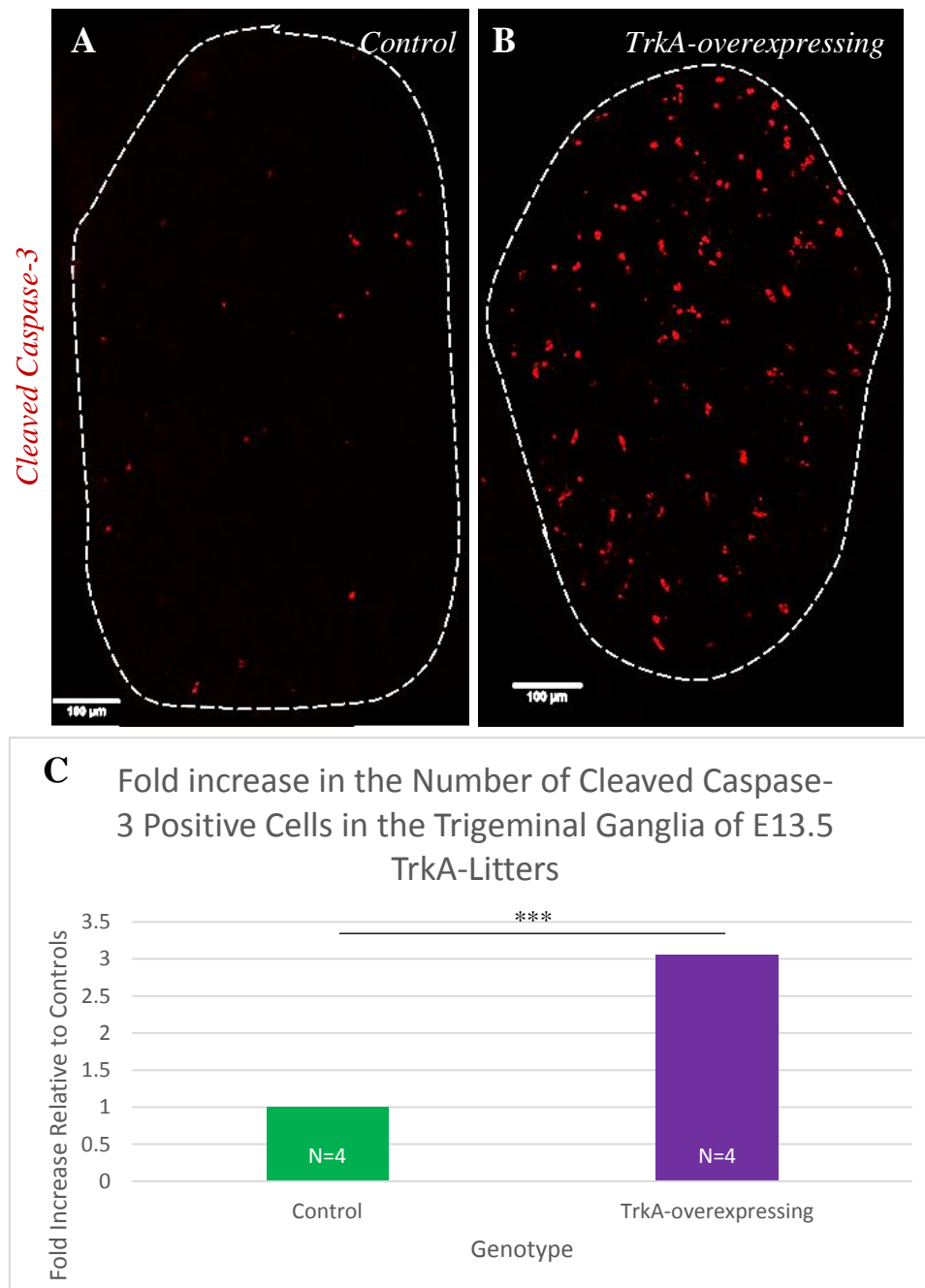
Figure 5.12 Caspase-3 activation in the trigeminal ganglia of TrkA-litters at E13.5. Representative images of cleaved caspase-3 staining (red) in the trigeminal ganglia of A) control littermates and B) TrkA-overexpressing embryos. The ganglia are indicated by white dotted lines. Scale bars: 100 μm. C) Quantification of cleaved caspase-3 staining. Values were normalised to controls. N = number of embryos analysed, from two litters. *** - $p < 0.001$ (one-way ANOVA).
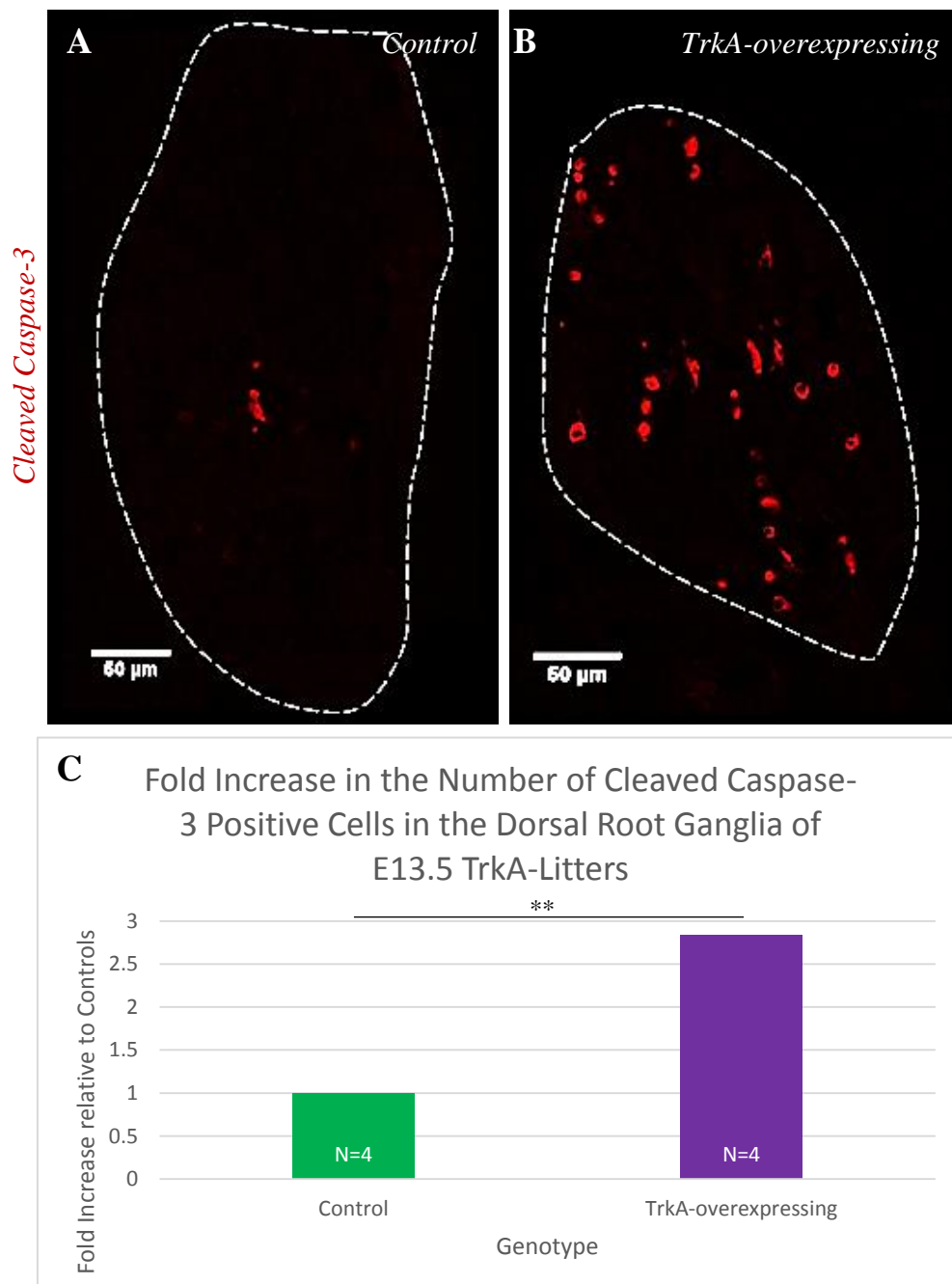
Figure 5.13 Caspase-3 activation in the dorsal root ganglia of TrkA-litters at E13.5. Representative images of cleaved caspase-3 staining in C1 dorsal root ganglia in A) littermate controls, and B) TrkA-overexpressing mice at E13.5. The ganglia are indicated by the white dotted lines. Scale bars: 50 μm. C) Quantification of cleaved-caspase 3 counts. Values were normalised to control. N = number of embryos analysed from two litters. ** - $p < 0.01$ (one-way ANOVA).

5.8. Summary

This chapter outlined the consequences of ubiquitously overexpressing TrkA from the earliest stages of mouse development. The most obvious results of this genetic manipulation was the early postnatal death of nearly all pups soon after birth (Figure 5.1). The results also indicated that in spite of the early and ubiquitous expression of this receptor, development proceeded normally as TrkA-overexpressing embryos appeared to have no gross morphological defects (Figure 5.2), except for a slight, but significant reduction in overall body area (Figure 5.3A). This reduction in body area came late in development at E18.5, and was not present at E13.5 (Figure 5.3A), indicating that the effects of TrkA-overexpression occur late in development. Furthermore, the gross morphology across various CNS tissues such as the hippocampus, eye, nose and spinal cord in TrkA-overexpressing embryos remained remarkably normal during development (Figure 5.4). More specific analyses using the iDISCO staining technique revealed a clear and complete loss of structures that endogenously express TrkA in the head of E15.5 TrkA-overexpressing embryos, such as the trigeminal and superior cervical ganglia (Figure 5.7).

This analysis also revealed areas of intense TrkA staining in structures that do not normally express TrkA, such as the whiskers (Martin-Zanca et al., 1990), yet the morphology of these structures appeared normal (Figure 5.7). The notion that TrkA-overexpression may lead to selective death of neurons endogenously expressing TrkA was confirmed by detailed histological examination of the specific ganglia. Quantification of the volume and the number of neurons indicated a loss of cranial sensory and sympathetic ganglia that endogenously express TrkA. Histological analysis of the SCG, of which >95% of neurons are reported to endogenously express TrkA (Schecterson and Bothwell, 1994), showed that there was a significant reduction in the volume of the SCG by E18.5 (Figure 5.8A, Figure 5.8B, Table 5.1), as a result of a reduction in the number of neurons (Figure 5.10A). The notion that TrkA overexpression closely follows the pattern of naturally occurring cell death is further supported by the observation that gangliogenesis did not seem to be affected. Indeed during the period of SCG formation (between E13-E18) (Coughlin and Collins, 1985), there was no significant difference between TrkA-overexpressing and control embryos in the volume of the SCG at E15.5 (Table 5.1), nor the number of neurons (Figure

5.10A), indicating that TrkA-induced cell death may only occur in post mitotic neurons. Given the early postnatal death of the most pups, older SCG could not be analysed.

Analysis of the volume and neuronal numbers of other sensory ganglia confirmed that ganglia that endogenously express TrkA are affected in TrkA-overexpressing mice (Table 5.1). This included the C1 dorsal root (DRG; Figure 5.8B and Figure 5.8C), and trigeminal (TG; Figure 5.8D and Figure 5.8E) ganglia, which are a collection of mixed TrkA-C-expressing sensory ganglia. While 45% of DRG neurons endogenously express TrkA (Wetmore and Olson, 1995), around 75% of neurons express TrkA in the TG (Huang et al., 1999). Correspondingly, the DRG and TG had a reduction of 62% DRG neurons (Figure 5.10C) and 75% TG neurons (Figure 5.10B) at E18.5 in TrkA-overexpressing embryos compared to sex-matched littermate controls. These figures are similar to those previously reported in $Ngf^{-/-}$ mice, of 70-90% loss of TG and DRG neurons (Chen et al., 1997; Crowley et al., 1994; Fagan et al., 1996; Smeyne et al., 1994). As in the SCG, the DRG and TG were not significantly different at E11.5 or E15.5 (Table 5.1, Figure 5.10B, Figure 5.10C) during the period of ganglia formation (E12- E14.5 for DRG (White et al., 1998), E9.5-E13.5 for TG (Huang et al., 1999)) in TrkA-overexpressing embryos compared to their littermates, further supporting the idea that apoptosis caused by TrkA overexpression follows the pattern of normally occurring neuronal death. This was reflected by a three-fold increase in cleaved caspase-3 staining in both the trigeminal (Figure 5.12) and dorsal root (Figure 5.13) ganglia over and above on-going cell death observed in control embryos.

Given the lack of phenotype outside of ganglia endogenously expressing TrkA, it was of interest to determine whether TrkA overexpression had any effect on ganglia not endogenously expressing TrkA in most neurons. A small, but statistically significant decrease in the number of NPG neurons could be observed in TrkA-overexpressing embryos (Figure 5.11A), possibly corresponding to the small number of TrkA-expressing, NGF-dependent in these ganglia (Wetmore and Olson, 1995). No such decrease could be observed in the vestibular ganglia (Figure 5.11B), which do not usually express TrkA (Schecterson and Bothwell, 1994).

In summary, ubiquitous TrkA overexpression during mouse development does cause cell death, and the early postnatal death of the pups, but the death is limited to cell

types endogenously expressing TrkA during normal development. This restricted phenotype is reminiscent of embryos lacking *Ngf* (see section 7.4.3).

6. Characterisation of TrkB-overexpressing mice

6.1. Introduction

Chapter 5 detailed how ubiquitous expression of TrkA during development resulted in perinatal lethality, and the loss of NGF-dependent neurons. As TrkA and TrkB are related receptors, but previous reports have indicated that TrkB may not act as a dependence receptor (Nikoletopoulou et al., 2010; Tauszig-Delamasure et al., 2007), it was of interest to explore the consequences of also overexpressing TrkB using a similar approach (Chapter 4). As with TrkA-overexpressors, only mice with >95% deletion of the STOP cassette were selected for analysis. Likewise the embryos designated controls were sex-matched, littermates without excision of the stop cassette preceding TrkB.

6.2. Survival of TrkB-overexpressing mice

Unlike was the case with TrkA, there was no significant decrease in the percentage of TrkB-overexpressing embryos over development as determined by a one-way ANOVA ($F(4,10) = 0.546$, p = 0.706) (Figure 6.1). As only mice with >95% deletion were included for analysis the high values for the standard deviation is to be expected due to the variability in Cre-excision efficiency. Postnatal TrkB-overexpressing animals did not show any obvious phenotypes. Furthermore TrkB-overexpressing pups not only survived normally, but were fertile and able to give birth to litters (N = 2 litters, $M = 6.5$ pups per litter).
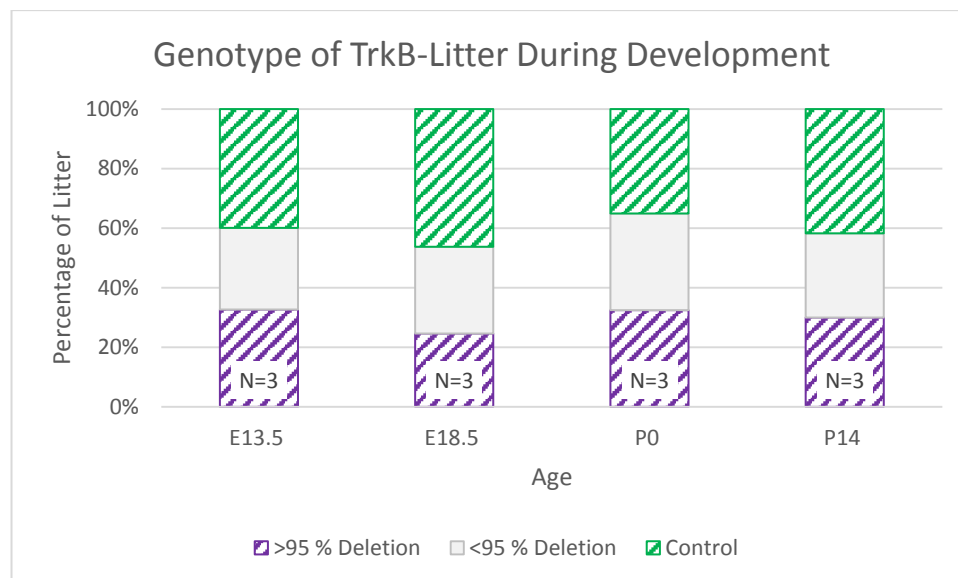
Figure 6.1 Genotype of TrkB-litters during development. The percentage of surviving *CMV-Cre;R26-LSL-TrkB* animals with >95% deletion (purple stripes, termed TrkB-overexpressors), *CMV-Cre;R26-LSL-TrkB* mice with <95% deletion (grey block, termed partial TrkB-expressors), and *R26-LSL-TrkB* offspring (green stripes, termed controls) per litter at different developmental ages is shown. The percentage of TrkB-overexpressing offspring per litter is stable over embryonic and postnatal development. N = number of litters analysed. No significant difference between percentage of TrkB-overexpressing animals over time (one-way ANOVA).

6.3. Morphological analyses

TrkB-overexpressing embryos were indistinguishable from controls (Figure 6.2), and a two-way ANOVA performed on body size at both E13.5 and E18.5 (Figure 6.3A) did not reveal any significant interaction between age and genotype ($F_{(1, 25)} = 1.925$, $p = 0.178$). Similarly, there was no significant main effect of genotype ($F_{(1,25)} = 0.448$, $p = 0.509$), a result confirmed by Bonferroni pairwise comparisons. As expected, there was a significant main effect of age ($F_{(1,25)} = 2634.785$, $p < 0.001$) regardless of genotype as embryos obviously grew in size between E13.5 to E18.5.

An independent t-test also revealed that there was no significant difference in the weight of TrkB-overexpressors ($M = 1.26$ g, SD $\pm$ 0.17) and controls ($M = 1.28$ g, SD $\pm$ 0.10) at E18.5 ($t_{(11)} = 0.373$, $p = 0.717$; Figure 6.3B). The weight of E18.5 pups was obtained from two litters, with an average litter size of 7.5 (SD $\pm$ 4.9) pups. In support of the lack of any clear morphological differences, TrkB-overexpressing mice did not display any obvious phenotype, including in particular balance or breathing or feeding deficits (for discussion see section 7.5.4).
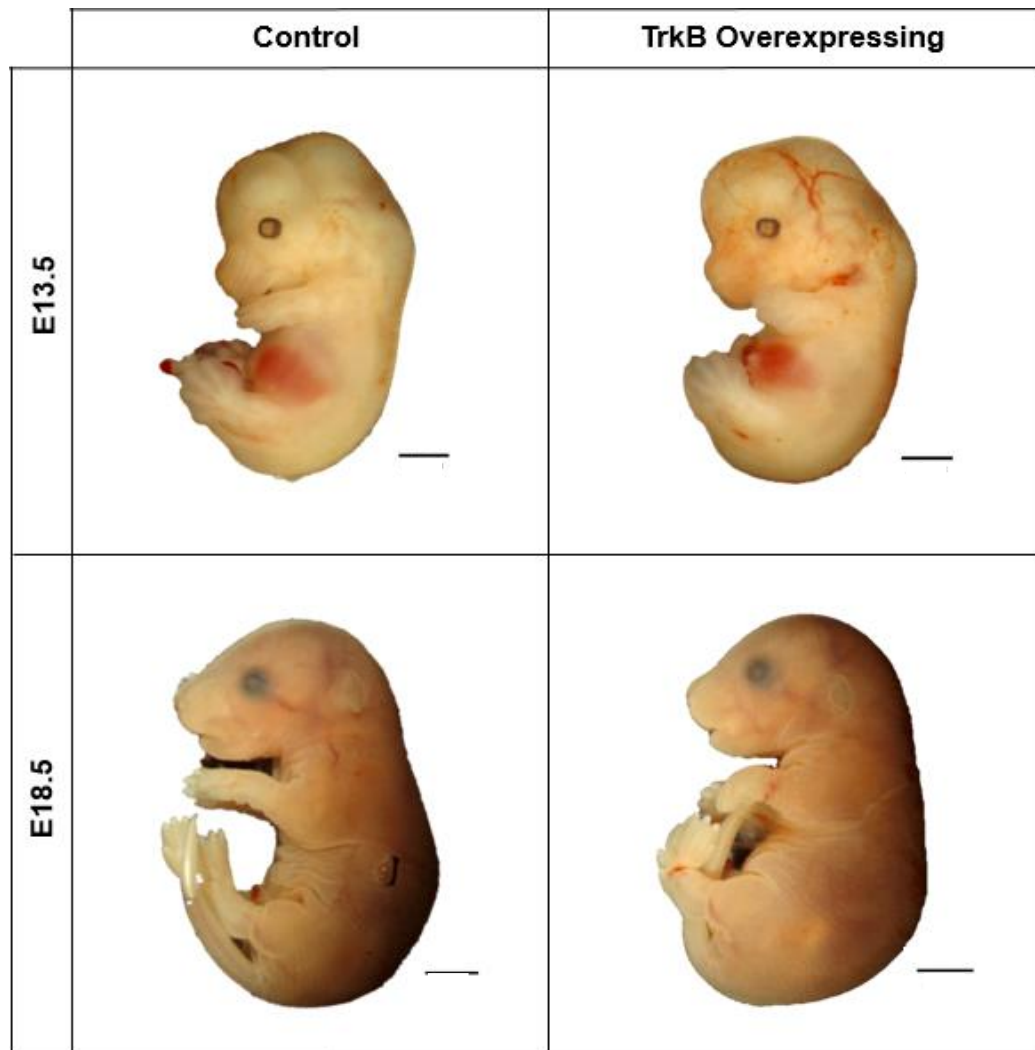
Figure 6.2 Morphology of TrkB-overexpressing embryos at E13.5 and E18.5. Representative images of male TrkB-overexpressing embryos at E13.5 and E18.5, compared to controls. Scale bars are 1.5 mm for E13.5 embryos, and 3 mm for E18.5 embryos.
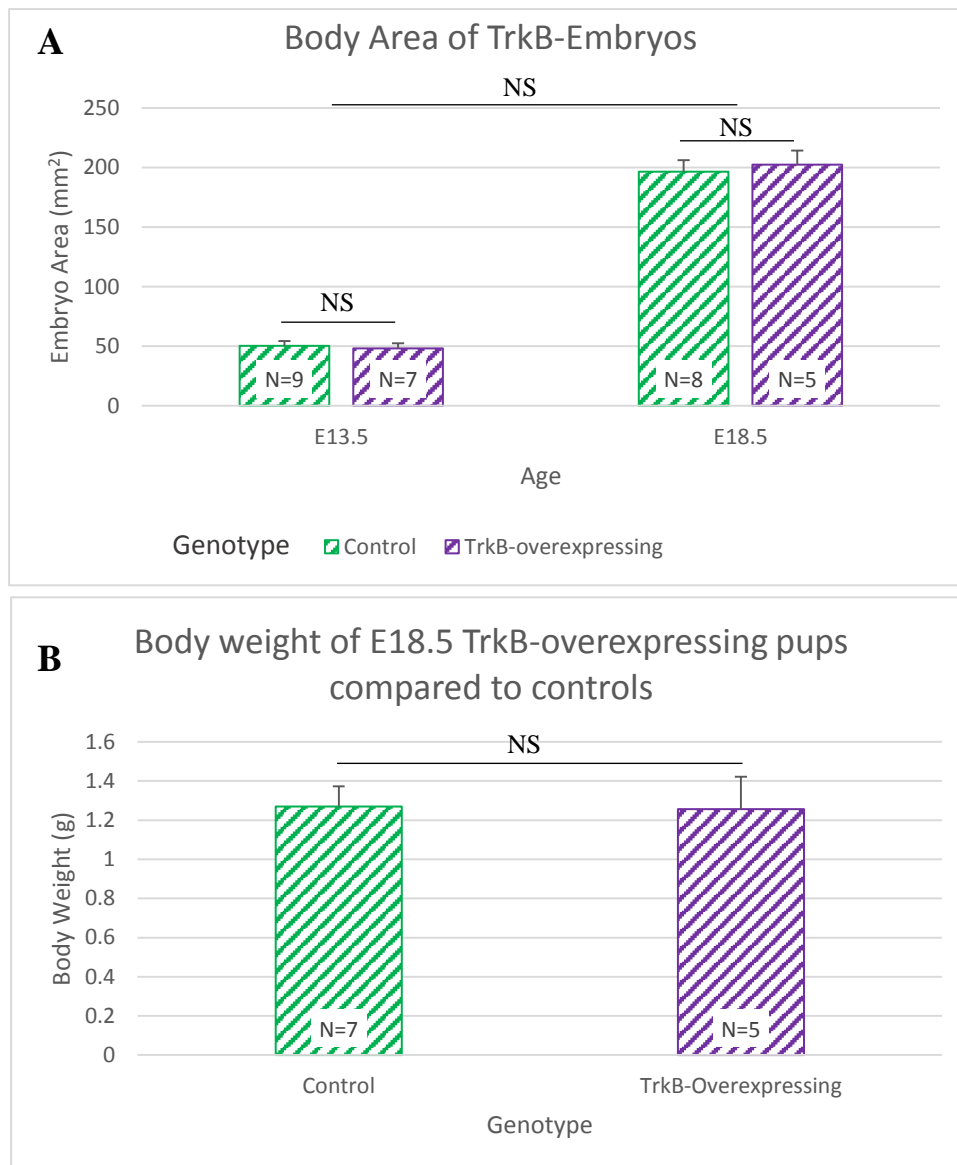
Figure 6.3 Size and weight of TrkB-overexpressing embryos. A) The area of embryos at E13.5 and E18.5 is similar between TrkB-overexpressing embryos (purple) compared to their littermates (green). NS - not significant, *** - p <0.001 (two-way ANOVA with Bonferroni pairwise comparisons). B) The weight of embryos at E18.5 is similar between TrkB-overexpressing animals and sex-matched, littermate controls. Data from two litters, average litter size = 7.5 (SD ± 4.9). NS – not significant (independent t-test). Error bars - standard deviation. N = number of embryos analysed per group.

The TrkB-overexpressing embryos were further analysed by performing haematoxylin and eosin stainings on transverse sections of TrkB-overexpressing embryos and sex-matched, littermate controls between E13.5 and E18.5. The general morphology of a number of structures including the nose, eye, spinal cord, and hippocampus appeared to be normal in terms of general appearance and size in TrkB-overexpressing embryos. Side-by-side comparisons with controls at E18.5 failed to reveal any differences in the morphology of most structures (Figure 6.4). To quantify if there were any changes to the number of CNS neurons, cortices were dissected from E18.5 litters, dissociated and the total number of cells counted. No statistically significant difference was observed in the number of cells dissociated from the cerebral cortex between TrkB-overexpressing pups ($M = 3.96 \times 10^6$, SD $\pm$ 0.80) and controls ($M = 4.33 \times 10^6$, SD $\pm$ 0.41) (t(5) = 0.720, $p = 0.504$; Figure 6.5). Taken together, these results indicate that the overexpression of TrkB across all cell types throughout development did not result in any gross morphological phenotypes.
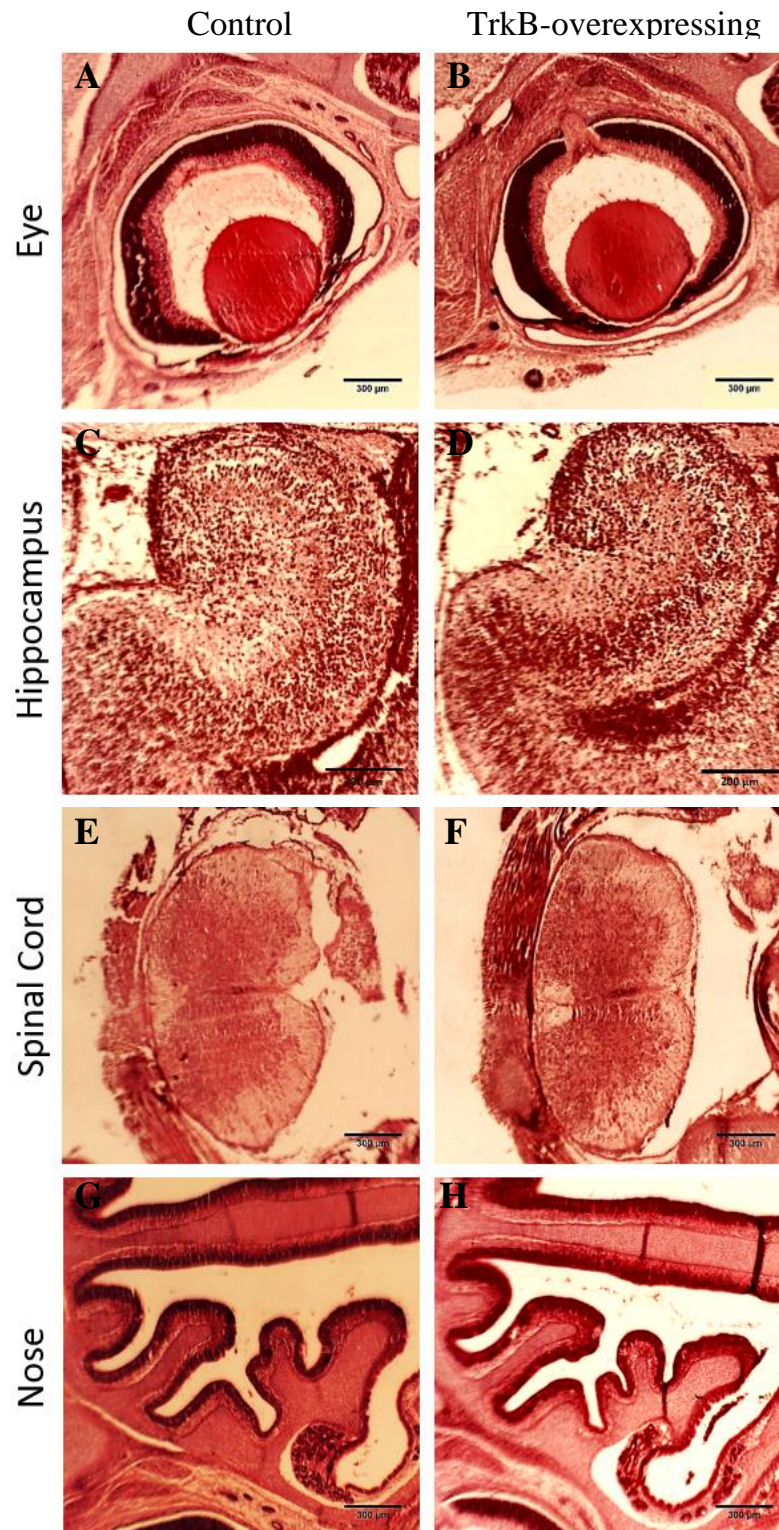
Figure 6.4 The eye, hippocampus, spinal cord, and nose structures in E18.5 TrkB-overexpressing embryos. Representative images of the eye (A,B), hippocampus (C,D), spinal cord (E,F), and nose (G,H) in E18.5 TrkB-overexpressors (B,D,F,H) compared to sex-matched, littermate controls (A,C,E,F). Scale bars: 300 μm, except B,C where scale bars are 200 μm.
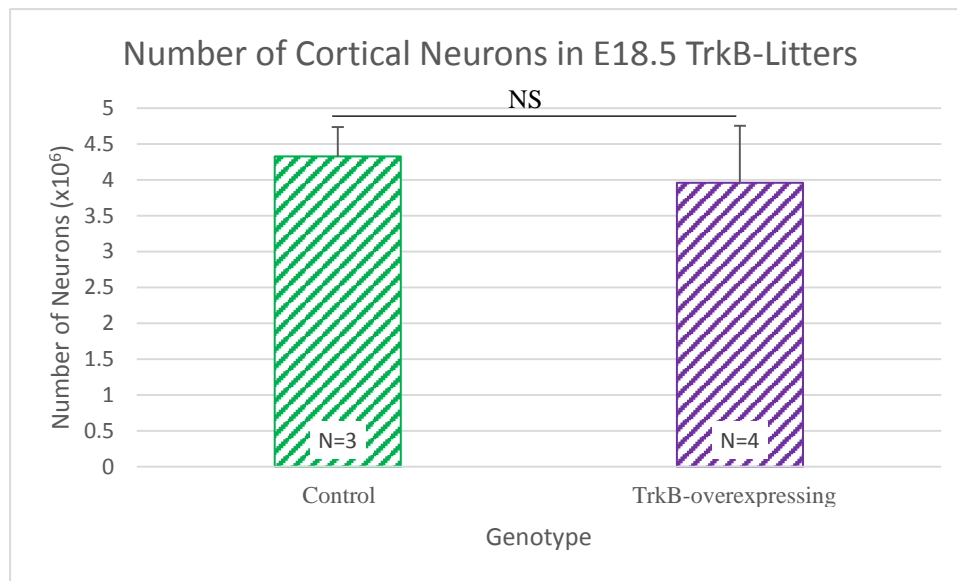
Figure 6.5 Number of cortical neurons in E18.5 TrkB-litters. Number of neurons in dissociated cortices of TrkB-overexpressing mice (purple) compared to controls (green). N = number of embryos analysed from one litter. Error bars - standard deviation. NS – not significant (independent t-test).

6.4. Volume of sensory and sympathetic ganglia

The superior cervical (SCG), dorsal root (DRG), nodose-petrosal (NPG), trigeminal (TG), and vestibular (VG) ganglia of TrkB-overexpressing embryos and control littermates were analysed at E13.5 and E18.5, the same developmental period as with TrkA-overexpressing embryos.

Quantification of ganglia volume revealed that in the SCG there was no significant difference in ganglia volume between the two genotypes at E18.5 ($F(1,7) = 1.849$, $p = 0.216$; Figure 6.6A and Figure 6.6B, Table 6.1). Two way ANOVA analysis indicated that there was a significant interaction of genotype and age in the volume of the NPG ($F(1,11) = 57.272$, $p < 0.001$) Bonferroni pairwise comparisons indicated that there was a significant reduction in the volume of the NPG between TrkB-overexpressing (Figure 6.7A) and controls (Figure 6.7B) both at E13.5 ($p = 0.031$), and E18.5 ($p < 0.001$) (Table 6.1). Furthermore, while there was no significant interaction between genotype and age in volume of the vestibular ganglia ($F(1,11) = 1.393$, $p = 0.263$), there was a main effect of genotype ($F(1,11) = 24.44$, $p < 0.001$). Bonferroni pairwise comparisons revealed that there was a significant decrease in the volume of vestibular ganglia at both E13.5 ($p = 0.033$), and at E18.5 ($p = 0.001$) (Table 6.1) in TrkB-overexpressors (Figure 6.7D) compared to the sex-matched, littermate controls (Figure 6.7C).

In the dorsal root ganglia volume there was no significant interaction between genotype and age ($F(1,11) = 3.472$, $p = 0.089$). However there was a significant main effect of genotype ($F(1,11) = 7.59$, $p = 0.019$), and Bonferroni pairwise comparisons revealed that while the DRG volume was not different between genotypes at E13.5 ($p = 0.576$), by E18.5 there was a significant reduction in the DRG volume in TrkB-overexpressing embryos (Figure 6.6D) compared to controls ($p = 0.004$, Figure 6.6C, Table 6.1). Similarly, there was a significant main effect of both genotype ($F(1,11) = 31.567$, $p < 0.001$) and age ($F(1,11) = 262.746$, $p < 0.001$) in the trigeminal ganglia with a significant interaction between the two factors ($F(1,11) = 5.449$, $p = 0.04$). Bonferroni pairwise comparisons demonstrated no significant difference between TrkB-overexpressing embryos and controls in trigeminal ganglia volume at E13.5 ($p = 0.057$), while there was a significant reduction the trigeminal ganglia

volume at E18.5 in TrkB-overexpressors (Figure 6.6F) compared to sex-matched, littermate controls ($p<0.001$, Figure 6.6E, Table 6.1).
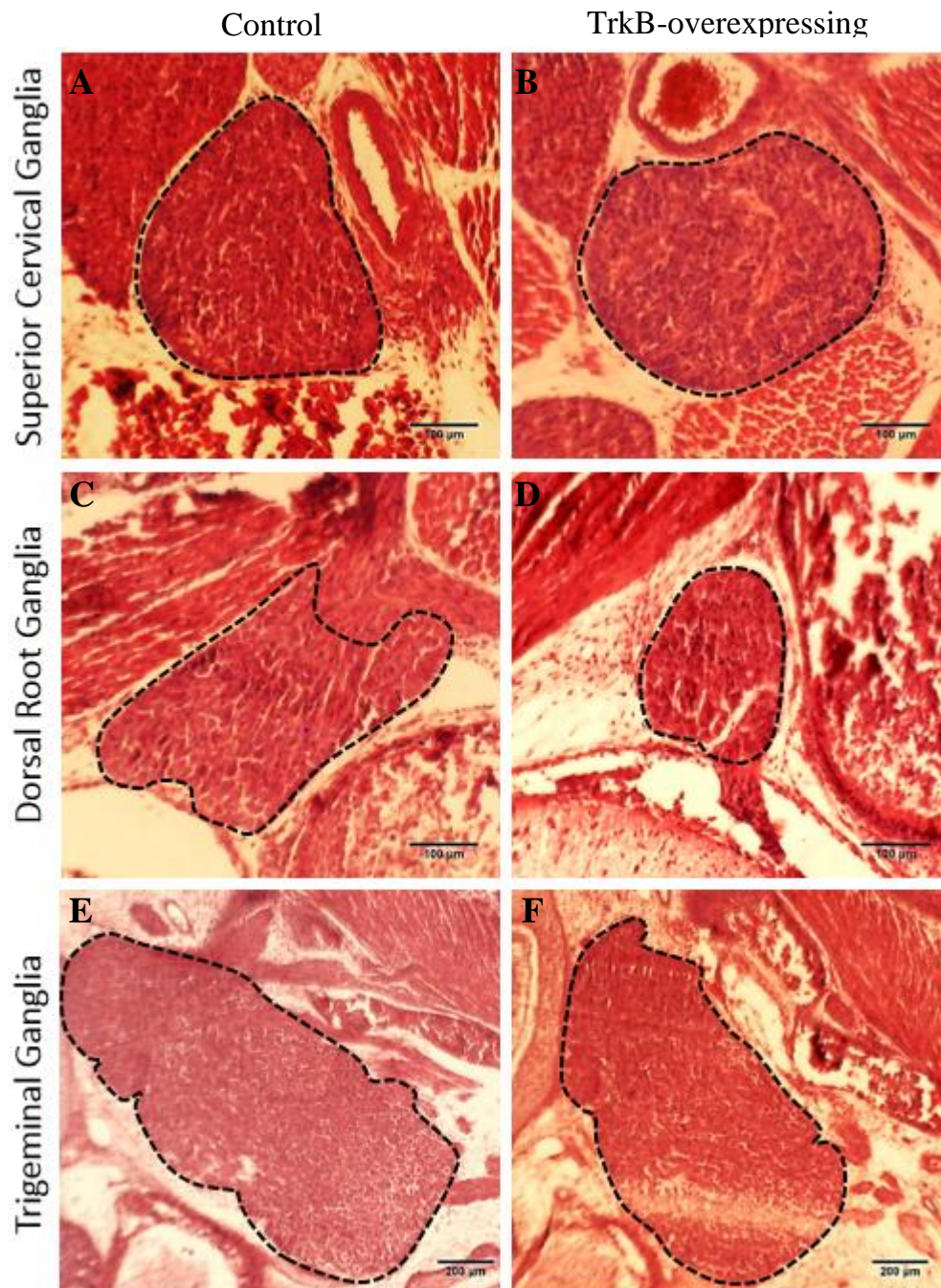
Figure 6.6 The superior cervical, dorsal root, and trigeminal ganglia in E18.5 TrkB-overexpressing-embryos. Representative images of the superior cervical (A,B), C1 dorsal root (C,D), and trigeminal (E,F) ganglia in E18.5 TrkB-overexpressing embryos (B, D, F) compared to littermates (A, C, E). Ganglia are indicated by black, dotted lines. Scale bars A-D: 100 µm, scale bars E-F: 200 µm.
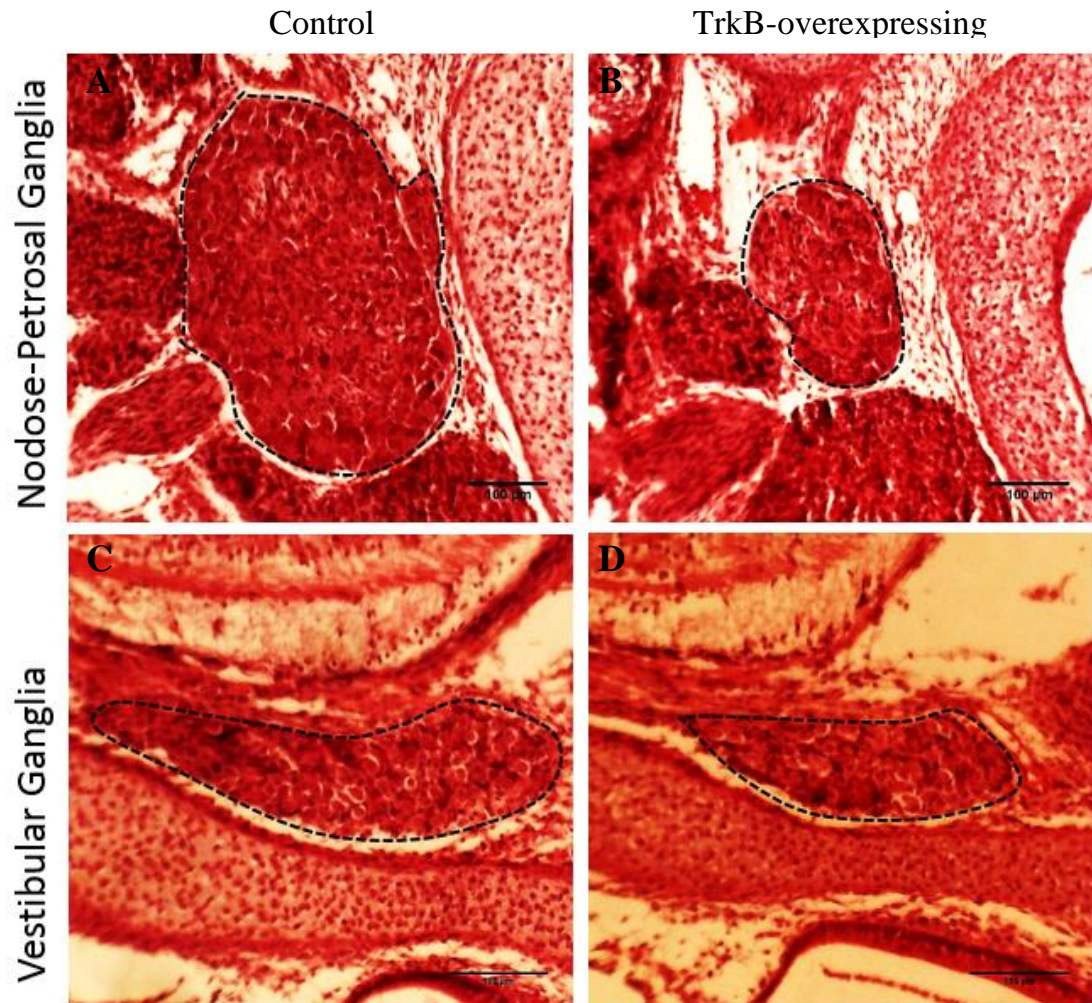
Figure 6.7 The nodose-petrosal and vestibular ganglia in E18.5 TrkB-overexpressing embryos. Representative images of the nodose-petrosal (A,B), and vestibular (C,D) ganglia in E18.5 TrkB-overexpressing embryos (B, D) compared to littermates (A, C). Ganglia are indicated by black, dotted lines. Scale bars: 100 μm.

Table 6.1 Volume of sensory and sympathetic ganglia in TrkB-litters

	E13.5			E18.5		
	Control x10^4 μm^3 (±SD) [N]	TrkB-overexpressing x10^4 μm^3 (±SD) [N]	Remaining % vs. Control (p)	Control x10^4 μm^3 (±SD) [N]	TrkB-overexpressing x10^4 μm^3 (±SD) [N]	Remaining % vs. Control (p)
Sensory Ganglia						
Dorsal Root (C1)	832 (±36) [3]	610 (±141) [3]	73% NS	2458 (±415) [4]	1311 (±682) [5]	53% **
Trigeminal	8693 (±989) [3]	6447 (±396) [3]	74% NS	21370 (±2074) [4]	15933 (±901) [5]	75% **
Vestibular	1187 (±158) [3]	826 (±172) [3]	70% NS	1570 (±146) [4]	982 (±219) [5]	63% ***
Nodose	943 (±140) [3]	666 (±213) [3]	71% *	1626 (±159) [4]	251 (±25) [5]	15% ***
Sympathetic Ganglia						
Superior Cervical	*NA*			4707 (±123) [4]	4480 (±311) [5]	95% NS

Volume counts were determined from haematoxylin and eosin stainings as detailed in section 2.8.4. N - numbers of embryos analysed per group from a minimum of two litters per age, indicated in superscript brackets. Two of each ganglia were counted per embryo and averaged. NS - not significant, * - p < 0.05, ** -p < 0.01, *** - p < 0.001 compared to littermate controls (two-way ANOVA with Bonferroni pairwise comparisons, except superior cervical ganglia where a one-way ANOVA was performed).

6.5. Neuronal counts in sensory and sympathetic ganglia

To determine whether the reduction in ganglia volume was due to a reduction of neuronal number, neurons were counted in these ganglia at E13.5 and E18.5 as outlined in section 2.8.4.

Two-way ANOVAs revealed a significant interaction of age and genotype in the NPG ($F(1,11) = 24.565$, $p <0.001$), VG ($F(1,11) = 5.264$, $p = 0.042$), and DRG ($F(1,11) = 4.967$, $p =0.048$). Bonferroni pairwise comparisons indicated that there was no significant difference in the number of neurons between TrkB-overexpressors and controls at E13.5 in the NPG ($p = 0.115$), VG ($p = 0.172$), and DRG ($p = 0.728$) indicating that ganglia initially formed normally. However by E18.5 TrkB-overexpressing embryos showed a significant decrease in the number of neurons in the NPG ($p <0.001$, Figure 6.9A), VG ($p <0.001$, Figure 6.9B), and DRG ($p = 0.002$, Figure 6.8A). While there was no interaction between genotype and age in the trigeminal ganglia ($F(1,11) = 2.287$, $p = 0.159$), there was also a main effect of genotype, regardless of age ($F(1,11) = 5.495$, $p = 0.039$). Similar to the NPG, VG and DRG, the number of neurons in the TG was not significantly different between TrkB-overexpressing embryos and controls at E13.5 ($p = 0.601$), but by E18.5 this difference was significant ($p = 0.011$, Figure 6.8A). Conversely, the number of neurons in the SCG at E18.5 was not significantly different between genotypes ($F(1,7) = 4.733$, $p = 0.066$, Figure 6.8C).

A Number of Neurons in the Dorsal Root Ganglia of TrkB-Litters

B Number of Neurons in the Trigeminal Ganglia of TrkB-Litters

C Number of Neurons in the Superior Cervical Ganglia of TrkB Animals at E18.5
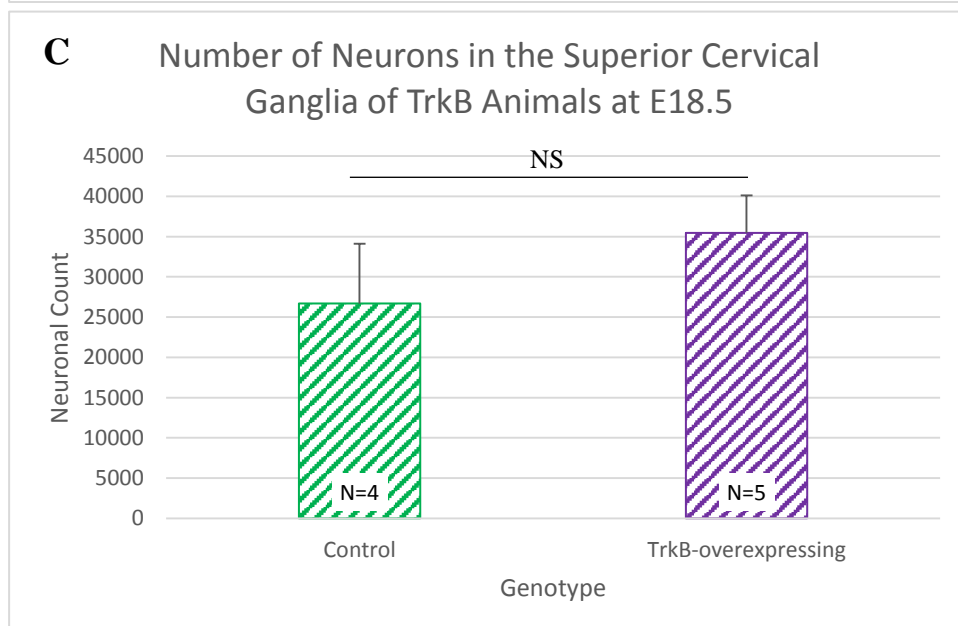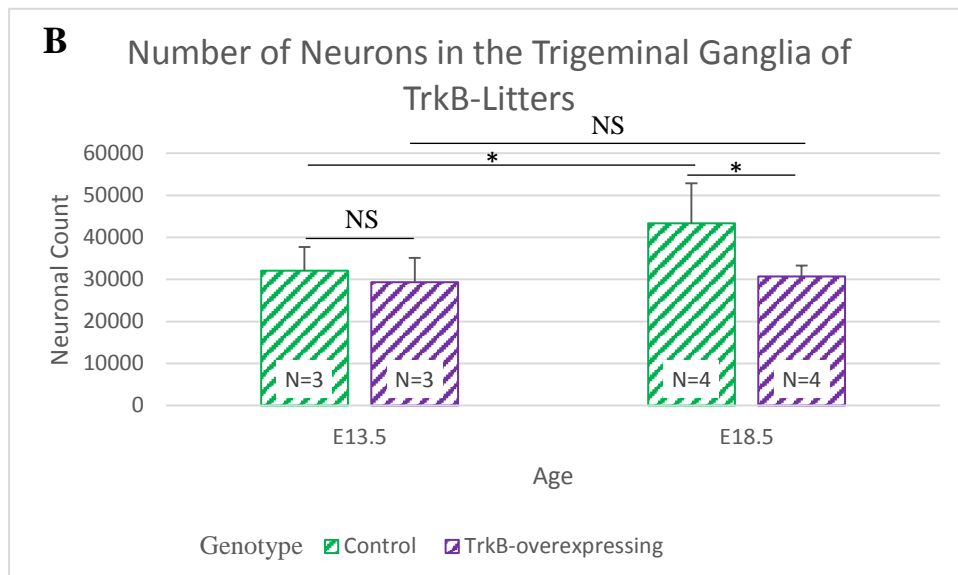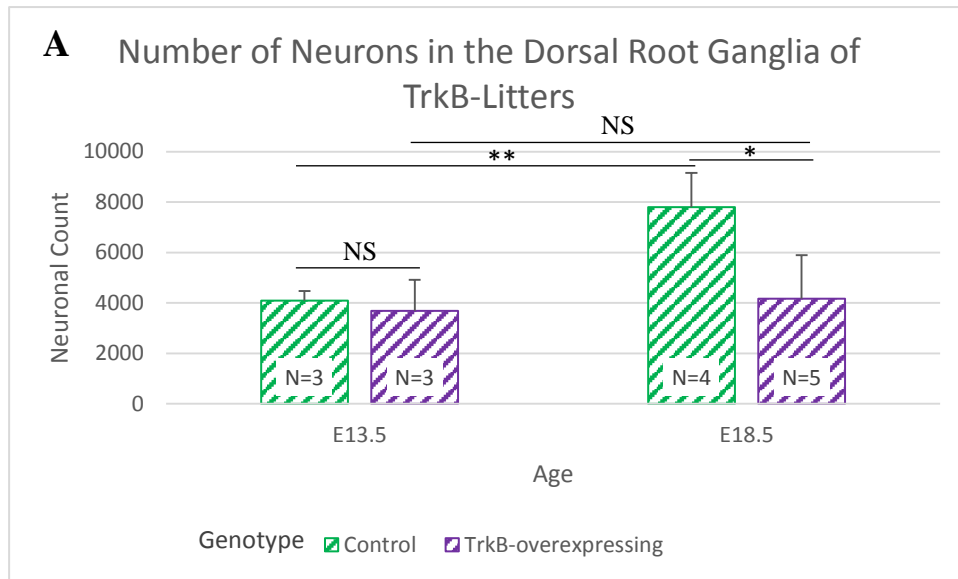
Figure 6.8 Number of neurons in the dorsal root, trigeminal and superior cervical ganglia in TrkB-overexpressing embryos. Number of neurons in E13.5 and E18.5 A) dorsal root ganglia, and B) trigeminal ganglia. Number of neurons in the C) superior cervical ganglia at E18.5. Error bars – standard deviation. N = number of embryos from a minimum of two litters per age. NS – not significant, * - $p <0.05$, ** - $p <0.01$ (two-way ANOVA with Bonferroni pairwise comparisons, other than the SCG where a one-way ANOVA was performed).
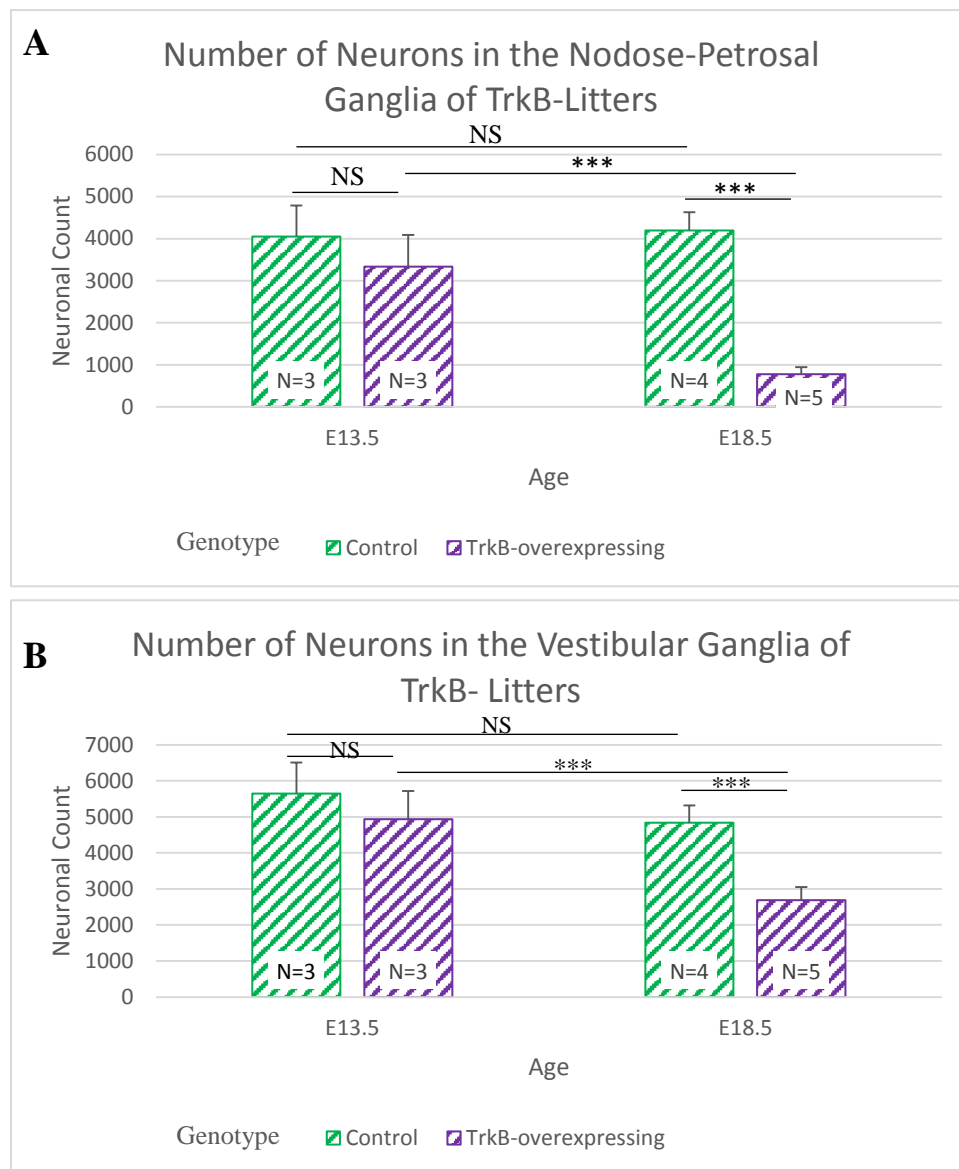
Figure 6.9 Number of neurons in the nodose-petrosal and vestibular ganglia of TrkB-litters. Number of neurons in the A) nodose-petrosal and B) vestibular ganglia at E13.5 and E18.5. Error bars – standard deviation. N = number of embryos analysed per group, from a minimum of two litters per age. NS – not significant, *** - p <0.001 (two-way ANOVA with Bonferroni pairwise comparisons).

6.6. Summary

This chapter described the consequence of ubiquitous TrkB-overexpression throughout mouse development. Unlike with TrkA overexpression (Chapter 5), TrkB overexpression did not result in any clear, gross morphological phenotypes (Figure 6.2). Indeed, embryos were normal in terms of body size (Figure 6.3A) and weight (Figure 6.3B), and CNS tissues such as the hippocampus, eye and nose appeared remarkably normal (Figure 6.4). Furthermore there was no effect of TrkB-overexpression on pup survival (Figure 6.1); TrkB-overexpressing mice survived into adulthood (Figure 6.1), and were also fertile giving birth to viable litters when crossed together.

Gangliogenesis of nodose-petrosal (NPG) and vestibular (VG) ganglia did not seem to be affected in TrkB-overexpressors, as there was no significant difference between genotypes VG or NPG neuronal counts at E13.5 (Figure 6.9). This time point is during the period of ganglia formation of the VG (E13 to E16 (Ernfors et al., 1995)) and the NPG (E13.5 to E18 (Forgie et al., 2000; Katz et al., 1990; Piñón et al., 1997)). By E18.5, there was a significant reduction in the volume of these ganglia in TrkB-overexpressing mice compared to controls (Table 6.1). The reduction in ganglia volume appears to be due to the significant loss of 92% of NPG and 45% of VG neurons at E18.5 (Figure 6.9). In other sensory ganglia expressing all three Trk receptors such as the dorsal root and trigeminal ganglia, there was a significant reduction in the number of neurons at E18.5 in TrkB-overexpressing mice compared to controls. As in the NPG and VG, the volume (Table 6.1) and number of neurons (Figure 6.9), were not different between TrkB-overexpressing mice and the controls at E13.5, which is during the period of ganglia formation (E12 to E14.5 for DRG, E9.5-E13.5 for TG (Huang et al., 1999; White et al., 1998)). This data supports the notion that loss of neurons in TrkB-overexpressing mice follows the pattern of naturally occurring cell death. In the superior cervical ganglia (SCG) that do not endogenously express TrkB there was no significant reduction in the ganglia volume (Table 6.1) or in the number of neurons (Figure 6.8) across any age. In summary, ubiquitous TrkB-overexpression during mouse development resulted in significant reductions in the number of neurons in sensory ganglia. This decrease was particularly marked in the NPG, whilst the number of neurons in the SCG remained unchanged.

These results indicate that the overexpression of TrkA and TrkB using the same strategy leads to very different results not only with regard to the peripheral ganglia affected by this genetic manipulation but also in terms of the overall postnatal survival.

7. Discussion

7.1. Summary of the main findings

The main objective of this study was to explore the roles of the TrkA receptor from the earliest stages of development. Still very little is known about the functions of this receptor in the absence of activation by their ligands, beyond a single report that TrkA induces cell death in the absence of activation by NGF (Nikoletopoulou et al., 2010). A conditional expression strategy was chosen given the previous knowledge that TrkA expression may lead to the death of the embryos (Nikoletopoulou et al., 2010). TrkB was used as a control given that it is a closely related receptor, and has not been reported to cause cell death (Nikoletopoulou et al., 2010; Tauszig-Delamasure et al., 2007). To undertake this study, a two-pronged approach was developed utilising an *in vitro* neuronal assay to further examine the mechanisms of TrkA dependence receptor activity, whilst concurrently generating, and analysing ubiquitous TrkA- and TrkB-overexpression in animal models. Unexpectedly, the *in vitro* models turned out not to be practicable within the context of this thesis (Chapter 3). However examination of the *in vivo* models demonstrated that the overexpression of TrkA and TrkB under the control of the *Rosa26* promoter led to contrasting outcomes: while overexpression of TrkA led to early postnatal death, the overexpression of TrkB led to viable and fertile animals with no overt phenotypes. This chapter discusses the generation and technical aspects of the *in vitro* and *in vivo* models, and analyses possible reasons for the differences between TrkA- and TrkB- overexpressing mice.

7.2. Overexpression of TrkA- and TrkB- *in vitro*

Chapter 3 outlined the generation of targeting constructs and various mouse ESCs with the aim of generating a model of conditional TrkA and TrkB overexpression in neurons under the same *Mapt* promoter used in the previous study by Nikoletopoulou et al. (2010). The Trk sequences were preceded by a loxP-flanked STOP cassette which prevented constitutive expression of the receptors until the STOP cassette had been excised by Cre-recombinase. Utilising the CreER^T2 system, where Cre remains inactive until the addition of Tamoxifen, *R26-CreER^T2;Mapt-LSL-TrkA* and *−TrkB*

ESCs were successfully generated. In order to further elucidate the effects of TrkA and TrkB, these ESCs were differentiated following a well-established protocol to generate cortical-like, glutamatergic neurons (Bibel et al., 2004, 2007). However, while wild type mouse ESCs were able to differentiate into homogenous populations of neurons, *R26-CreER^{T2};Mapt-LSL-TrkA* and *TrkB* ESCs, even those not treated with tamoxifen, were unable to generate sufficiently pure neuronal populations, thus preventing meaningful further analyses. Possible reasons for these ESCs not to differentiate, and the various parameters tested, are discussed in the following sections.

7.2.1. Differentiation protocol

The inability of untreated *R26-CreER^{T2};Mapt-LSL-TrkA* and *TrkB* ESCs to differentiate did not appear to be a shortcoming of the differentiation procedure itself, as homogenous cultures of neurons could be derived from both wild type, and alternative genetically-modified ESC lines of both J1 and E14 genetic backgrounds. This also indicates that the issue was not due to manual handling of the ESCs, a notion supported by the observation that other lab members attempting the differentiation of *R26-CreER^{T2};Mapt-LSL-TrkA* and *–TrkB* ESCs encountered similar problems. The ability to generate wild type ESC-derived neurons also indicated that there was no issue of culture media components. These were thoroughly checked, by batch number, to ensure they were not faulty. Although other differentiation protocols to generate glutamatergic, cortical-like neurons from mouse ESCs do exist (Alsanie et al., 2017; Gaspard et al., 2009), these do not result in the same level of neuronal culture homogeneity as the Bibel et al. (2004) protocol and would not have been suitable as alternative differentiation protocols.

7.2.2. ESC quality

The quality of the initial ESC culture is known to affect the quality of neuronal differentiation (Kolodziejczyk et al., 2015). Indicators of quality include: the proliferation rate of ESCs, their morphology, and the number of spontaneously

differentiating cells (Bibel et al., 2007). However the inability to generate homogenous neuronal populations with *R26-CreER^T2;Mapt LSL-TrkA* and *-TrkB* ESCs does not seem to be an issue of the ESC quality. Indeed, efforts to maximise the quality of ESC cultures, such as adapting the culture media, passaging frequency, split ratios, and substrate, did improve the appearance of the ESCs, but it did not result in any improved neuronal culture outcome with the *R26-CreER^T2;Mapt-LSL-TrkA* and *TrkB* ESCs. Furthermore, the ESCs routinely tested negative for mycoplasma, and were selected on the basis of having the correct karyotype. However it is possible that events such as chromosome duplications, deletions or recombination may have occurred in the genetically-modified loci that affected the differentiation capacity of the ESCs. This seems unlikely as multiple clones of different genetic backgrounds had the same differentiation issues, although if these cells are to be used in the future, it may be important to test chromosome stability via fluorescence *in situ* hybridisation (Gaztelumendi and Nogués, 2014).

7.2.3. Genetic modification

Individually targeted *R26-CreER^T2* or *Mapt-LSL-TrkA* and *-TrkB* ESCs were able to differentiate into neurons. However *Mapt-LSL-TrkA* and *−TrkB* ESCs did show a reduction in the homogeneity of the resulting neuronal culture, suggesting that the effects could have been due to off-targeting effects. In the future this could be tested through southern blotting, and perhaps could be resolved by testing different sgRNAs when targeting the *Mapt* locus with CRISPR.

The observation that neuronal differentiation was mostly affected in ESCs with both the *R26-CreER^T2* and *Mapt-LSL-TrkA* and *-TrkB* constructs raised the question as to whether the CreER^T2 system was leaky, resulting in TrkA and TrkB expression that may affect differentiation. However it was demonstrated that expression of TrkA and TrkB only occurred when tamoxifen was applied, and expression of either receptor could not be detected in untreated cultures. Furthermore, as *R26-CreER^T2* ESCs were able to be differentiate into homogenous populations of neurons, it does not seem that there is an interaction of the inactive CreER^T2 protein in this differentiation procedure.

It is important to note that *Mapt* or *Rosa26* are widely targeted both *in vitro* and *in vivo,* and in the majority of cases has not been reported to impair neuronal development *in vivo* or *in vitro* (Friedrich and Soriano, 1991; Garcia et al., 2012; Harada et al., 1994; Nikoletopoulou et al., 2010; Tucker et al., 2001; Zambrowicz et al., 1997). *Mapt* encodes a major microtubule-associated protein (tau), and it has been shown that the nervous system of tau-deficient mice (*Mapt$^{-/-}$*) is essentially normal (Harada et al., 1994). This is thought to be due to several other microtubule-associated proteins compensating for the absence of tau (Harada et al., 1994). However more recent studies have indicated that in the case of haploinsufficiency of tau (as observed in *Mapt$^{+/-}$* mice) there is no compensatory increase in microtubules such as MAP-1A, and that compensation only occurs when tau is completely knocked out (Zheng et al., 2017). This could potentially explain why the targeting of both *Mapt* alleles in the study by Nikoletopoulou et al. (2010) did not affect neuronal differentiation. Conceivably, targeting a single *Mapt* allele in this thesis may have interfered with the differentiation process. Whether the ESCs target one, or both *Mapt* allels could be analysed in the future by southern blotting, or by quantitative PCR for *Mapt* mRNA levels. Additionally, the function of *Rosa26* has not yet been identified, but mice with a disrupted *Rosa26* locus are viable, fertile and do not exhibit any noticeable abnormalities (Friedrich and Soriano, 1991; Zambrowicz et al., 1997). Yet, there have not been detailed studies specifically investigating the effect of disrupted *Rosa26* function on *in vitro* neuronal differentiation. It is therefore also possible that targeting of *Rosa26* could have contributed to the inability for cells to differentiate into homogenous neuronal populations.

7.2.4. Use of antimitotic agents

Even if neurons could be generated using *R26-CreER^{T2};Mapt-LSL-TrkA* and *TrkB* ESCs, the presence of large numbers of non-neuronal cells affected the survival of neurons by DIV8. Non-neuronal cells proliferate, whilst post-mitotic neurons cannot, resulting in non-neuronal cells outcompeting neurons for space, and nutrients from the media (Burry, 1983). Whilst this is a common problem in primary cultures, where neurons are isolated from tissues that contain multiple cell types, the benefits of using this particular neuronal differentiation protocol is that it normally generates a very

high proportion, up to 95% of glutamatergic neurons, and another 4% are other neuronal types. A small (<1%) proportion of the resulting culture are non-neuronal cells, but after even three weeks in culture, they do not proliferate enough to overtake the dish (Bibel et al., 2004, 2007). Some ESC differentiation protocols allow for the use of antimitotic drugs to prevent over-proliferation of non-neuronal cells, and antimitotics have been found to improve the survival of neurons in cultures (Burry, 1983; Oorschot, 1989). One of the most commonly used antimitotics is 5-flourdeoxyuridine (5FdU). 5FdU is an inhibitor of thymidine synthase, and thereby prevents nucleotide synthesis in proliferating cells (Mori et al., 2017). However the use of this drug leads to cytotoxic effects that affect the conclusions drawn from cell culture experiments, especially when neuronal death may have been one of the possible outcomes of the proposed genetic manipulation (Oorschot, 1989). Furthermore, studies have reported that even at concentrations where 5FdU does not result in cell death, neurons do not appear as healthy (Burry, 1983; Oorschot, 1989), while lower concentrations are no longer effective at inhibiting non-neuronal proliferation. Whilst cytosine arabinoside (Ara-C), a deoxycytidine analogue which inhibits DNA polymerase, is reported to be the least harmful of the antimitotics to neuronal culture, it still affects neuronal health and survival (Burry, 1983). As one of the main aims of generating this *in vitro* model was to dissect the mechanisms of TrkA-induced cell death, applying mitotic inhibitors that are cytotoxic would invalidate any results obtained from this *in vitro* model. It is of note that the first report on the death-inducing activity of TrkA was based on the use of the same *in vitro* differentiation protocol using a similar HA-tagged TrkA construct inserted in the *Mapt* locus (Nikoletopoulou et al., 2010).

7.2.5. Alternative routes to express Cre

The generation of *Mapt-LSL-TrkA* and *-TrkB* ESCs that could differentiate into neurons, albeit of questionable purity compared with wild type ESCs, suggested a need to test alternative methods of excising the STOP cassette in neurons. However transfection of neural progenitors/neurons with a Cre plasmid, either by electroporation, viruses, biolistics or biochemical methods such as Lipofectamine 2000, are not typically not very efficient (Karra and Dahm, 2010; Ohki et al., 2001).

An alternative to this could be a cell-permeable Cre; a purified Cre protein from *E.coli*. Here the Cre-recombinase enzyme is modified so that the protein also contains an N-terminal histidine tag (H6), a translocation peptide from HIV-TAT (TAT), and a nuclear localisation sequence (NLS). This fusion protein is referred to as HTN-Cre (or HTNC), and due to the presence of TAT and NLS is able to enter the nucleus and excise the STOP cassette preceding the Trk receptor sequences. However, this approach also failed to reach the desired efficiency and in addition, it turned out to be incompatible with prolonged neuronal survival (Haupt et al., 2007; Nolden et al., 2006; Peitz et al., 2002). As the ability to generate a healthy, homogenous population of TrkA-overexpressing neurons was a prerequisite to performing meaningful biochemical analyses on *in vitro* cultures, these methods were not explored further.

7.2.6. Summary of *in vitro* experiments

In summary, the expression of TrkA and TrkB in genetically-modified mouse ESCs could be temporally controlled by tamoxifen, but the ESCs could not be differentiated into neurons of sufficient purity, despite extensive optimisation as detailed above. Although this prevented testing of our hypotheses, these ESC lines may still be compatible with differentiation protocols that produce alternative neuronal populations.

7.3. *In vivo* TrkA- and TrkB-overexpression models

7.3.1. Generation of TrkA- and TrkB- mice

As constitutive expression of TrkA under the control of the *Mapt* promoter has been previously reported to be lethal embryonically (Nikoletopoulou et al., 2010), the *TrkA*, as well as the *TrkB* sequences here were preceded by a loxP-STOP-loxP sequence. In this way, expression of the receptors could only occur after a Cre-mediated recombination event, thus allowing the establishment of a stable transgenic line. By crossing these mouse lines, designated *R26-LSL-TrkA* and *R26-LSL-TrkB,* with different Cre driver lines, the expression of TrkA or TrkB can be controlled in terms of the timing of expression, and the cell types or tissues that express TrkA or TrkB. To ensure ubiquitous and early expression of the Trk constructs in the embryos, a *Cre*

line was used where Cre was under the control of the human cytomegalovirus (*CMV*) promoter that had been randomly inserted into the X chromosome (Schwenk et al., 1995).

7.3.2. Excision of the STOP cassette

As described in Chapter 4, complete excision of the STOP cassette was not evident in both male and female embryos that inherited both the *CMV-Cre* and *R26-LSL-TrkA* or *-TrkB* genes. To control for this only offspring with >95% deletion of the STOP cassette, as demonstrated by genotyping PCR, were included for analysis (hereby referred to as TrkA- or TrkB-overexpressing). Genotyping of tail (E11.5-E18.5 embryos), ear notches (pups) and whole embryos (E6.5 embryos) indicated that the variability in excision efficiency was present regardless of the age of the offspring. While it could be argued that genotyping tail or ear tissue may not guarantee that recombination has occurred in a similar extent across all cells in the entire embryo, observation of IRES-EGFP at E6.5 (Chapter 4) is consistent with the notion that at E6.5 Cre is active across the embryo. Importantly, genotyping PCR also predicted the levels of overexpressed Trk protein as determined by western blot (Chapter 4). It is of note that a previous study utilised a very similar *in vivo* strategy to the one outlined in this thesis with a different RTK family member, namely Met, the receptor for hepatocyte growth factor (Fan et al., 2015). In their experiments, Met was conditionally expressed under the control of the *Rosa26* promoter, with a STOP cassette preceding the Met construct, which was excised by crossing with the same *CMV-Cre* driver line used here. In line with the findings reported here, the authors reported that the efficiency of recombination varied among offspring, with the degree of STOP cassette excision observed by genotyping PCR being reflected by the extent of β-galactosidase staining across entire E10.5 embryos. The authors also observed that the degree of β-galactosidase staining seemed to be equivalent between tissues. As a result, the authors restricted their analysis to embryos where genotyping indicated almost complete excision of the stop cassette, the same approach as used in this thesis. In line with the observations outlined in chapter 4, Fan et al. (2015) also did not observe any effects of gender on the efficiency of recombination.

For this reason, while it may seem an obvious query that incomplete excision could be due to X inactivation affecting the expression of *CMV-Cre*, this does not seem to be the case. X inactivation occurs in females, and is a process of dosage compensation; ensuring comparable expression levels of genes that are found on the X chromosome between males (that only inherit one X chromosome, XY) and females (that inherit two, XX). While females inherit one from their mother (designated Xm) and one from their father (designated Xp), while males inherit their only X chromosome from their mother (Augui et al., 2011; Krietsch et al., 1982; Takagi and Sasaki, 1975). There are two types of X chromosome inactivation. In imprinted X chromosome inactivation Xp is preferentially inactivated during the preimplantation stages of embryogenesis, while Xm is constitutively active after fertilisation (Augui et al., 2011; Krietsch et al., 1982; Takagi and Sasaki, 1975). Random X inactivation however occurs around the time of blastocyst implantation, and silences either Xm or Xp in each cell of the female embryo, resulting in mosaic expression of X-linked genes that continue throughout life (Lyon, 1961). Therefore females that inherit *CMV-Cre* from their mother have a uniform, early expression of Cre prior to blastocyst implantation/X-inactivation, ultimately resulting in uniform expression of TrkA/TrkB across the embryo. However female pups that inherit *CMV-Cre* from their father will have Cre activated later, around the time of X-inactivation, and ultimately result in mosaic expression (Mak et al., 2004; Okamoto et al., 2004; Patrat et al., 2009; Tan et al., 1993) of TrkA/TrkB. The finding of incomplete excision in male offspring observed here (also previously reported by Fan et al., 2015), seems to exclude the possibility that X inactivation is the cause of the partial Cre recombination, as X inactivation occurs only in females. Furthermore, incomplete recombination was consistently observed in our breeding scheme where *CMV-Cre* was inherited from the mother, which in theory should bypass the issues associated with paternal X-inactivation.

7.3.3. Functionality of the model

Littermate controls were established as *R26-LSL-TrkA* or *-TrkB* mice (hereby referred to as "controls") that did not inherit the *CMV-Cre* gene. Indeed, HA-tagged TrkA or TrkB could only be detected in TrkA- and TrkB-overexpressors, while HA could not be detected in controls. This is expected, as the HA epitope is not endogenously found

in mice (Wilson et al., 1984). Thus, lack of detection indicated that there was no leaky expression of TrkA or TrkB protein in the controls. Further confirmation that the model design worked came with the observation that excision of the loxP-flanked STOP cassette could be detected in offspring by genotyping PCR as early as E6.5 (Chapter 4). Furthermore STOP cassette excision correlated with increased levels of green fluorescence due to the IRES-EGFP sequence in the TrkA- and TrkB-overexpressing embryos. By contrast, very little fluorescence could be detected in the littermate controls, presumably a result of autofluorescence (Chapter 4). Additionally, Trk receptor levels, as assessed using pan-Trk antibodies in western blot analysis of limb extracts (that contain very low levels of endogenous Trk), as well as the use of a TrkA-specific antibody in iDISCO, were clearly increased in Trk overexpressing mice compared to controls. These results therefore suggested that TrkA and TrkB were widely expressed early during embryogenesis.

7.4. TrkA-overexpression

7.4.1. Effects in early development

TrkA-overexpressing mice did not reveal any obvious early developmental deficits in comparison to the sex-matched, littermate controls and up until E18.5, TrkA-overexpressing embryos were still normal in terms of weight. However, a comparative analysis of late embryos did reveal a slight, but significant reduction in body size, for reasons that are unclear. This was followed by the early postnatal death of all TrkA-overexpressing pups.

7.4.2. Cell counts

A detailed analysis of the embryos at E18.5 revealed differences in the size of specific sensory and sympathetic ganglia in TrkA-overexpressing embryos compared to the sex-matched, littermate controls. To quantify these observations, a well-established method of calculating unbiased ganglia volumes and neuronal counts, was used (Sterio, 1984). This technique combines the Cavalieri method which calculates total ganglia volume, and the physical dissector method to calculate neuronal number (Coggeshall, 1992) (see section 2.8.4) for details). To ensure that values reported here were accurate, control counts for both TrkA and TrkB controls for each ganglia were compared to those previously reported in the literature. These counts vary somewhat depending on the background strain, and counting method, so averages were taken where data was not available for C57BL/6J mice. Overall, counts appeared to be consistent with what has been reported in the literature (Table 7.1).

Table 7.1 Comparison of neuronal counts

		Reported Neuronal Count (x10³)	Observed Neuronal Count (x10³)
Ganglia	Superior Cervical Ganglia	17 [1]	25
	C1 Dorsal Root Ganglia	5 [2]	6.7
	Nodose-Petrosal Ganglia	4.5 [3]	4.7
	Vestibular Ganglia	5.0 [4]	5.0
	Trigeminal ganglia	30 [5]	40

[1] – Bamji et al. 1998; Kameda et al. 2012; Kameda et al. 2008; Patrik Ernfors et al. 1994; Farinas et al. 1994; Liu et al. 1995, [2] - Farinas et al. 1994, [3] - P Ernfors et al. 1994; Farinas et al. 1994; Fox et al. 2001; ElShamy & Ernfors 1997), [4] - Katayama et al., 2009; Liu et al., 2000; Schimmang et al., 1997, [5] - Ernfors, Lee and Jaenisch, 1994; De Felipe et al., 1999; Liu et al., 1995; Smeyne et al., 1994.

In contrast, the number of neurons recorded for TrkA-overexpressing mice at E18.5 were significantly lower than their littermate controls in specific ganglia. Remarkably, neuronal loss seemed to only be observed in NGF-dependent ganglia known to express TrkA in large number of neurons such as the TG (Huang et al., 1999), DRG (Mu et al., 1993; Wetmore and Olson, 1995), and SCG (Wetmore and Olson, 1995). Meanwhile in the NPG where 13% of NPG neurons express TrkA (Wetmore and Olson, 1995), there was a modest, but significant reduction of neuronal numbers in TrkA-overexpressing embryos. In the VG, a group of placode-derived sensory neurons that do not endogenously express TrkA (Schecterson and Bothwell, 1994), there was no significant loss of neurons in the TrkA-overexpressing mice compared to controls. In sensory ganglia displaying reduced cell numbers, immunohistochemical staining for cleaved caspase-3 indicated that the neuronal losses were likely to be explained by increased cell death via apoptosis, as indicated by a three-fold increase in caspase-3 activity. This result therefore supports the notion that TrkA overexpression induces cell death once NGF-dependent neurons have left the cell cycle. Indeed, there was no evidence for neurogenesis being affected as there were no significant differences

between genotypes at early developmental stages, such as E11.5 for the DRG and TG, and E15.5 for the SCG. This indicates that the overexpression of TrkA did not affect gangliogenesis, adding weight to the notion that TrkA may not act as a dependence receptor during early development. Furthermore, this observation, combined with the low-level of caspase-3 staining in control DRG and TG (Chapter 5), indicates that the timing of neuronal loss in TrkA-overexpressing mice seems to occur within the window of naturally occurring cell death; E12-E14.5 in DRG, and E11.5-P4 in the TG (White et al., 1998).

7.4.3. Comparison with *Ngf⁻ᐟ⁻* models

The phenotype of TrkA-overexpressing animals outlined in this thesis are reminiscent of what has been reported in *Ngf⁻ᐟ⁻* pups (Table 7.2). This appears to include the early postnatal death of most TrkA-overexpressors, and them being slightly smaller in size than their sex-matched, littermate controls by E18.5. These similarities extend to the proportion of neurons lost in sensory ganglia (Table 7.2). At first glance it appears that the SCG may not quite follow the expected pattern, as it almost entirely ablated   in *Ngf⁻ᐟ⁻* mice by P10 (Chen et al., 1997; Crowley et al., 1994; Fagan et al., 1996; Smeyne et al., 1994). However, due to the early postnatal lethality in TrkA-overexpressing mice, the latest analysable time point here was P0, where the number of SCG neurons was reduced by ~40% in TrkA-overexpressors. As naturally occurring cell death in the SCG continues during the first postnatal weeks (Coughlin et al., 1977), it could be anticipated that loss of SCG neurons would be more severe at later time points. In line with this notion, the one TrkA-overexpressing pup that survived until P14 demonstrated marked ptosis; the drooping of eyelids which indicates a loss of SCG neuron functionality.

Table 7.2 Proportion of neurons lost: comparison with *Ngf⁻/⁻* mice

Ganglia/Genotype	Reduction in Neuronal Number (%)	
	Ngf⁻/⁻ [1]	*TrkA-overexpressing* [2]
DRG	70-90	72
TG	70-90	75
SCG	95-100	37
VG	0	7
NPG	15	18

Values calculated from: [1] (Chen et al., 1997; Crowley et al., 1994; Smeyne et al., 1994), between E18.5-P5. [2] TrkA-overexpressing reduction calculated at E18.5.

7.4.4. Interpretation of results

Superficially, the results of TrkA overexpression reported here resemble those obtained previously in a paradigm of TrkA-overexpression using the *Mapt* locus that led to an early lethal phenotype (Nikoletopoulou et al., 2010). However, the cell death phenotype observed here is much more specific than previously observed by Nikoletopoulou and colleagues, as only TrkA-expressing, NGF-dependent neurons were eliminated in the TrkA-overexpressing mice, whilst in the previous study, the entire nervous system had been eliminated by E13.5. It appears likely that the use of a different promoter, *Rosa26* versus *Mapt*, may explain this apparent discrepancy. A possible explanation for the more selective phenotype described in the above is that increasing TrkA levels over and above the endogenous levels of TrkA may be sufficient to tilt the balance towards cell death. Moderate levels of TrkA-overexpression driven by the *Rosa26* promoter, as opposed to higher levels of TrkA generated by the use of the *Mapt* promoter, could readily explain the selectivity for neurons endogenously expressing TrkA in the current TrkA-overexpression model. Indeed, the *Mapt* promoter is strong enough to drive visible levels of GFP expression during neurogenesis (Tucker et al., 2001), whilst the Rosa26 locus is known to be expressed at low levels in post-mitotic neurons (Allen Institute for Brain Science, 2004a, 2004b).

However there is another explanation for the findings reported here that appears more plausible as it would also explain the observations made with mice overexpressing TrkB (see below). NGF has long been known to be secreted in limited amounts during development by the target tissues innervated by neurons requiring NGF for their survival (Bibel and Barde, 2000). This widely accepted model accounts for the phenomenon of naturally occurring cell death by the failure of the dying neurons to access sufficient quantities of the survival factor NGF. It has been directly demonstrated that the provision of additional quantities of NGF during normal development almost completely suppresses cell death in dorsal root ganglia (Hamburger et al., 1981). Given this well-documented phenomena, it is conceivable that the ubiquitous expression of TrkA as achieved here acts to scavenge secreted NGF (Figure 7.1). In this way, the overexpression of TrkA may prevent sufficient access of TrkA-expressing nerve terminals to NGF secreted by peripheral sources, such as the developing whisker pad. Indeed, the results of the iDISCO experiment using TrkA antibodies (Chapter 5) demonstrated increased immunoreactivity in the whisker follicles where selective *Ngf* gene expression has been documented (Bandtlow et al., 1987; Davies et al., 1987).
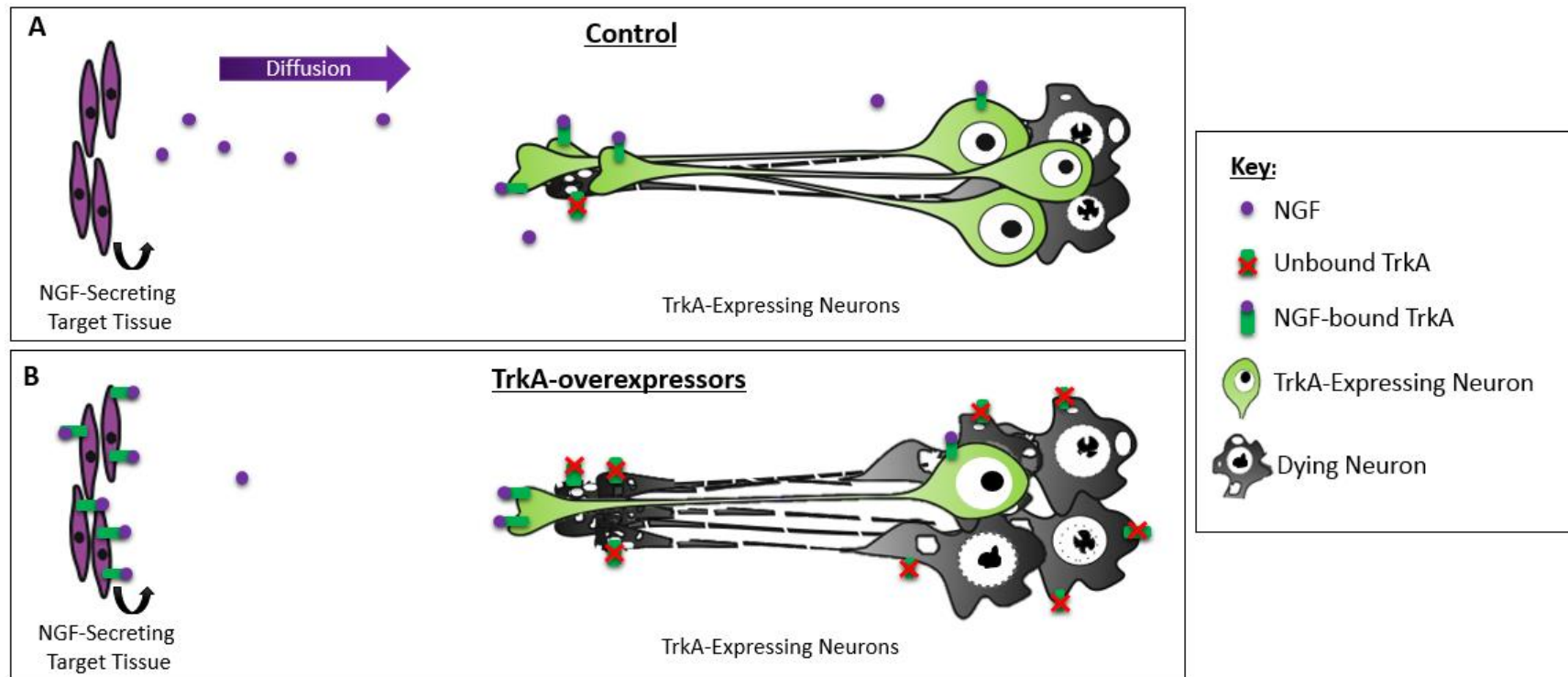
Figure 7.1 Proposed mechanism of cell death in TrkA-overexpressors. A) Schematic of the well-established paradigm of naturally occurring cell death in wild types (controls). NGF, secreted by target tissues, diffuses and binds to TrkA receptors on innervating neurons. Where TrkA does not bind NGF, the neurons undergo apoptosis and die. B) In TrkA-overexpressing mice, NGF may be sequestered by the overexpressed TrkA receptors in the target tissue. In this way, less NGF is available to the axon terminals of innervating neurons, resulting in increased neuronal death compared to that of controls.

7.5. TrkB-overexpression

7.5.1. General effects of TrkB-overexpression

Using the same overexpression strategy as in the TrkA mice, very different results were obtained in TrkB-overexpressing mice. While TrkA pups died perinatally, TrkB pups survive postnatally, did not exhibit any clear phenotype in comparison to littermates, became sexually mature, and were even able to give birth to viable litters. Additionally, TrkB-overexpressing animals were normal in terms of weight and body size across age. Due to logistical constraints TrkB-overexpressors were not generated until June 2018, and as a result the phenotypes in adults could not yet be examined in aging adults. However at the time of writing, TrkB-overexpressing mice do not show any overt phenotypes by six months of age.

7.5.2. Loss of sensory neurons

Detailed histological analyses revealed a significant loss of neurons in specific sensory ganglia, most notably in ganglia endogenously expressing TrkB that are reported to depend on BDNF and NT4 for survival, such as the NPG (Ernfors et al., 1992; Ernfors, Lee and Jaenisch, 1994; Huang et al., 1999; Jones et al., 1994), VG (Ernfors et al., 1992; Ernfors, Lee and Jaenisch, 1994; Jones et al., 1994; Schecterson and Bothwell, 1994; Ylikoski et al., 1993), TG (Ernfors, Lee and Jaenisch, 1994; Huang et al., 1999; Jones et al., 1994; Liebl et al., 1997; Wetmore and Olson, 1995), and C1 DRG (Kashiba et al., 1995; Liebl et al., 1997, 2000; Wetmore and Olson, 1995). In contrast, in the SCG where there have been no reports of neurons expressing TrkB, nor of BDNF/NT4-dependency for survival (Ernfors, Lee and Jaenisch, 1994; Jones et al., 1994; Wetmore and Olson, 1995), there was no significant loss of neurons in TrkB-overexpressing mice. Whilst stainings for cleaved caspase-3 have not yet been completed for the ganglia of TrkB-overexpressing embryos to confirm that the loss of neurons in these ganglia is attributable to increased cell death (as discussed for the TrkA-overexpressing embryos, section 7.4.2), this appears to be the most likely explanation given the observation that gangliogenesis was not affected in the VG, NPG, DRG and TG of TrkB-overexpressing mice. This is supported by observations

that there were no significant differences between genotypes in the number of neurons in these ganglia at E13.5.

7.5.3. Comparison with *Bdnf*^{-/-} and *Ntf4*^{-/-} models

As with TrkA-overexpressors, TrkB-overexpressing mice were compared to knockout models of the respective ligands; *Bdnf* and *Ntf4*. While *Bdnf*^{-/-} mice die within the first postnatal week, and demonstrate severe movement and breathing deficits (Conover et al., 1995; Erickson et al., 1996; Ernfors, Lee and Jaenisch, 1994; Hellard et al., 2004; Jones et al., 1994; Liu et al., 1995), *Ntf4*^{-/-} mice are long-lived and have no obvious phenotype (Conover et al., 1995). TrkB-overexpressing pups therefore appear to phenocopy *Ntf4*^{-/-} mice as TrkB-overexpressors survived postnatally and were fertile. However upon closer comparison of the neuronal losses in sensory and sympathetic ganglia, it became obvious that the losses in the VG, NPG and TG of TrkB-overexpressing mice compared to *Ntf4*^{-/-} were much larger (Table 7.3).). In fact, TrkB-overexpressing mice showed a pattern and proportion of loss more reminiscent of *Bdnf*^{-/-},*Ntf4*^{-/-} double knockout pups (Table 7.3). However double knockouts die within 48 hours of birth (Liu et al., 1995), which is in sharp contrast with the results obtained with TrkB-overexpressing pups. Furthermore, the proportion of neurons lost in TrkB-overexpressing mice still appears to be slightly less in VG compared to *Bdnf*^{-/-},*Ntf4*^{-/-} pups. The reduced losses in the VG may therefore explain the lack of severe balance deficits in TrkB-overexpressing animals that are characteristic of *Bdnf* knockouts.

Table 7.3 Proportion of neurons lost: comparison with *Bdnf^{-/-};Ntf4^{-/-}* mice

Ganglia/Genotype	Reduction in Neuronal Number (%)			
	Bdnf^{-/-} [1]	*Ntf4^{-/-}* [2]	*Bdnf^{-/-};Ntf4^{-/-}* [3]	*TrkB-overexpressing* [4]
DRG	30	15	None	47
TG	30-40	None	10-30	29
SCG	None	None	None	None
VG	75-90	21	82	45
NPG	40-60	40-60	80-90	82

Values calculated from: [1] *- Conover et al., 1995; Erickson et al., 1996; Ernfors, Lee and Jaenisch, 1994; Hellard et al., 2004; Jones et al., 1994; Liu et al., 1995 ,* [2] *- Conover et al., 1995; Erickson et al., 1996; Ernfors, Lee and Jaenisch, 1994; Liu et al., 1995,* [3] *- Conover et al., 1995; Liebl et al., 2000; Liu et al., 1995, between E18.5-P5.* [4] *- TrkB-overexpressing values reported for E18.5.*

7.5.4. Interpretation of results

As discussed for TrkA (section 7.4.4), the results obtained with TrkB-overexpressing mice may be due to the receptor acting as a BDNF/NT4 scavenger. Whilst TrkB overexpression would then be expected to phenocopy mice carrying germ line deletions of *Bdnf* and *Ntf4*, this is clearly not the case (see above) as TrkB-overexpressing pups survived postnatally and were fertile, whilst *Bdnf^{-/-}* and *Ntf4^{-/-}* die shortly after birth (Liu et al., 1995). One possible explanation for this apparent discrepancy could be that a proportion of the neurons comprising peripheral sensory ganglia express *Bdnf*, including the TG, NPG and DRG (Wetmore and Olson, 1995; Zhou et al., 1998). BDNF secretion by BDNF-responsive neurons has been proposed to be part of an autocrine signalling mechanism thought to play a role in axonal elongation after lesions (Acheson et al., 1995), and neuronal survival during development (Brady et al., 1999). These BDNF-secreting neurons would be expected not to depend on an exogeneous BDNF supply and thus to escape the scavenging effect of overexpressed TrkB. In this setting, neurons secreting BDNF may even have a

survival advantage by activating additional TrkB in the overexpressing embryos. This notion fits well with the results obtained with the TrkA-overexpressing embryos as, by contrast with the situation with BDNF, NGF-dependent neurons have *not* been reported to express the *Ngf* gene (Wetmore and Olson, 1995).
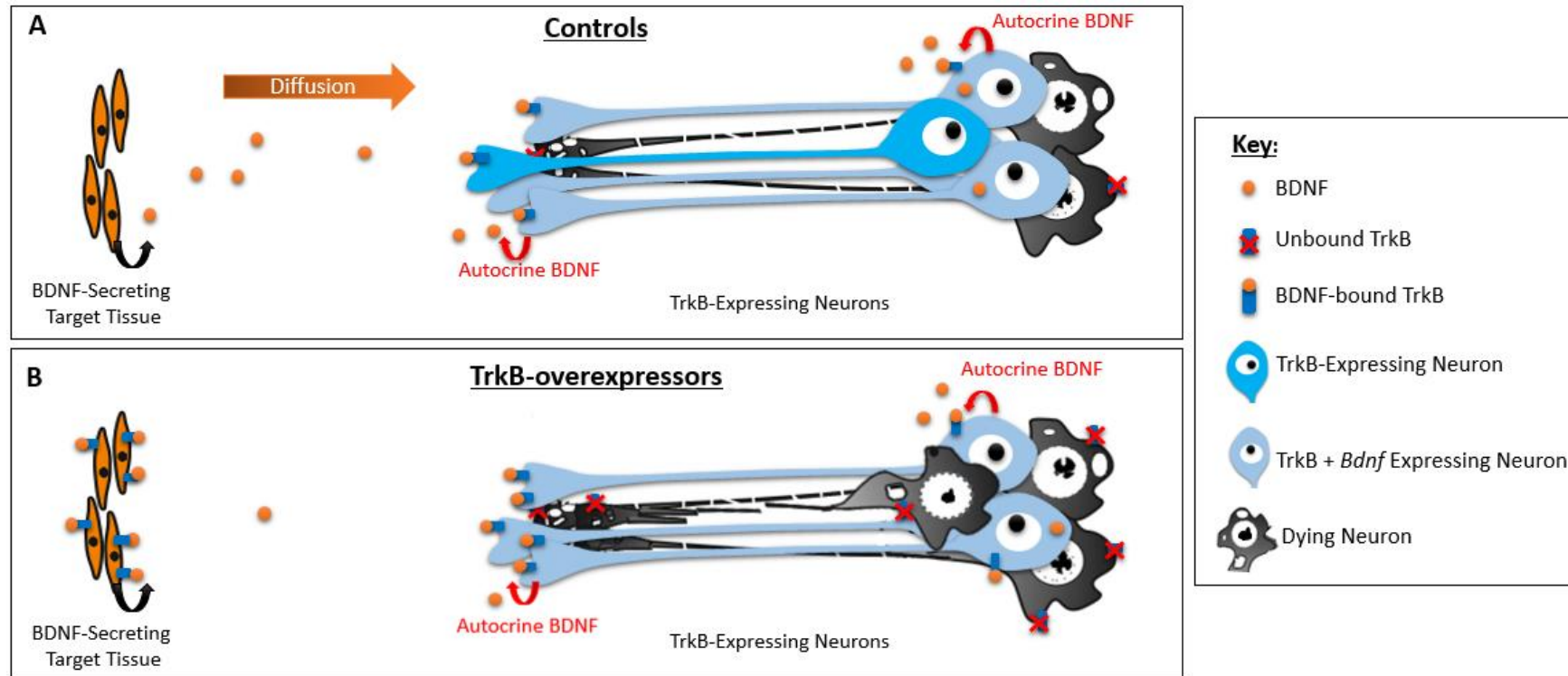
Figure 7.2 Proposed mechanism of cell death in TrkB-overexpressors. A) Schematic demonstrating the well-established paradigm of naturally occurring cell death in wild types (controls). BDNF, secreted both by target tissues and a proportion of the innervating neurons, binds to TrkB receptors on sensory neurons. Where TrkB does not bind BDNF, the neurons undergo apoptosis and die. B) In TrkB-overexpressing mice, BDNF may be sequestered by the overexpressed TrkB receptors in the target tissue, so less BDNF is available for innervating neurons. However as BDNF is synthesised by a proportion of the sensory neurons, these neurons survive TrkB-overexpression.

7.6. Conclusions and perspectives

The results detailed in this thesis demonstrate remarkable differences in the phenotype of transgenic animals expressing two closely related tyrosine kinase receptors. While a similar, general conclusion was previously reported (Nikoletopoulou et al., 2010), the mechanisms best explaining the corresponding phenotypes are significantly different. Firstly, the experimental design by Nikoletopoulou and colleagues involved the constitutive expression of TrkA and TrkB under the *Mapt* promoter. Due to the use of this neuron-specific promoter, conclusions could only be drawn about Trk receptor function in neurons. Due to early lethality of TrkA-overexpressing embryos, it was not possible to establish a transgenic mouse line constitutively expressing TrkA. Embryos were therefore generated using a tetraploid complementation method. As this technique leads to significant late embryonic lethality (H. Lickert, personal communication), it was not possible to achieve analysis of postnatal embryos. Indeed, in the previous study, no embryos were observed past E16.5 irrespective of which Trk receptor was expressed. By contrast, this thesis detailed the generation of mouse lines conditionally expressing TrkA and TrkB under the control of the Rosa26 promoter. This opens the possibility to, in future studies, use selective Cre drivers to assess and compare the expression of these receptors in specific tissues of interest.

As discussed, ubiquitous TrkA and TrkB overexpression led to a much more specific phenotype than anticipated from the work by Nikoletopoulou et al.. In particular, the overexpression of the Trk receptors did not appear to affect early embryogenesis or gangliogenesis. These mice instead exhibited a specific loss of neurons in sympathetic and sensory ganglia. Given the wealth of data accumulated in the neurotrophin field, this specificity may be plausibly explained by a scavenging function of the overexpressed receptors: the ubiquitous expression of TrkA and TrkB would deprive neurotrophin-dependent neurons from neurotrophins secreted by the corresponding target tissues as they would be retained at the sites of secretion. This scavenging function in the future could be directly demonstrated by overexpressing Trk mutant receptors that lack the corresponding neurotrophin-binding domain, to separate the dependence-receptor role from sequestering.

The most novel and unexpected finding was that TrkB-overexpressing mice, whilst losing significant numbers of BDNF- and NT4-dependent neurons, show prolonged

postnatal survival, unlike previous reports for mice lacking the corresponding ligands (Conover et al., 1995; Erickson et al., 1996; Ernfors, Lee and Jaenisch, 1994; Hellard et al., 2004; Jones et al., 1994; Liebl et al., 2000; Liu et al., 1995). The proposed mechanism of sensory neuron survival as a result of autocrine BDNF signalling could be further explored by examining the phenotype of surviving neurons in TrkB-overexpressors. Detailed studies with *Bdnf* and *Ntf4* knockouts led to the conclusion that BDNF is essential for the survival of a small population of chemoreceptor afferents critically involved in the control of respiration, and in line with the proposed autocrine hypothesis, these neurons also express the *Bdnf* gene (Brady et al., 1999; Erickson et al., 1996; Wetmore and Olson, 1995). Interestingly, many neurons have been shown to co-express BDNF and tyrosine hydroxylase, the rate limiting enzyme in the biosynthesis of catecholamines (Nagatsu et al., 1964). Experiments are underway to determine the phenotypic identity, as well as the connectivity, of the surviving NPG neurons in TrkB overexpressing mice. Using X-clarity and whole-mounts, the projections of the NPG including the carotid body and the baroreceptor fields will be investigated using antibodies to both neurofilaments and tyrosine hydroxylase. The results will be compared with those obtained using pups lacking *Bdnf*. In sum, these results suggest that autocrine signalling *in vivo* may represent a hitherto underappreciated aspect of the mechanism of BDNF action in the developing nervous system.

Bibliography

Acheson, A., Conover, J.C., Fandl, J.P., Dechiara, T.M., Russell, M., Thadani, A., Squinto, S.P., et al. (1995), "A BDNF autocrine loop in adult sensory neurons prevents cell death", *Nature*, Vol. 374 No. 6521, pp. 450–453.

Adams, J. and Cory, S. (2001), "Life-or-death decisions by the Bcl-2 protein family", *Trends in Biochemical Sciences*, Vol. 26 No. 1, pp. 61–66.

Alcantara, S., Frisen, J., del Rio, J., Soriano, E., Barbacid, M. and Silos-Santiago, I. (1997), "TrkB signaling is required for postnatal survival of CNS neurons and protects hippocampal and motor neurons from axotomy-induced cell death.", *Journal of Neuroscience*, Vol. 17, pp. 3623–3633.

Alderson, R.F., Alterman, A.L., Barde, Y.A. and Lindsay, R.M. (1990), "Brain-derived neurotrophic factor increases survival and differentiated functions of rat septal cholinergic neurons in culture", *Neuron*, Vol. 5 No. 3, pp. 297–306.

Allen Institute for Brain Science. (2004a), "Allen Mouse Brain Atlas - Mapt".

Allen Institute for Brain Science. (2004b), "Allen Mouse Brain Atlas - Rosa26".

Allsopp, T.E., Wyatt, S., Paterson, H.F. and Davies, A.M. (1993), "The proto-oncogene bcl-2 can selectively rescue neurotrophic factor-dependent neurons from apoptosis", *Cell*, Vol. 73 No. 2, pp. 295–307.

Alsanie, W.F., Niclis, J.C., Hunt, C.P., De Luzy, I.R., Penna, V., Bye, C.R., Pouton, C.W., et al. (2017), "Specification of murine ground state pluripotent stem cells to regional neuronal populations", *Scientific Reports*, Vol. 7 No. 1, p. 16001.

Aravind, L., Dixit, V.M. and Koonin, E. V. (2001), "Apoptotic molecular machinery: Vastly increased complexity in vertebrates revealed by genome comparisons", *Science*, Vol. 291 No. 5507, pp. 1279–1284.

Augui, S., Nora, E.P. and Heard, E. (2011), "Regulation of X-chromosome inactivation by the X-inactivation centre", *Nature Reviews Genetics*, Vol. 12 No. 6, pp. 429–442.

Bain, G., Ray, W.J., Yao, M. and Gottlieb, D.I. (1996), "Retinoic acid promotes

neural and represses mesodermal gene expression in mouse embryonic stem cells in culture", *Biochemical and Biophysical Research Communications*, Vol. 223 No. 3, pp. 691–694.

Bakhshi, A., Jensen, J.P., Goldman, P., Wright, J.J., McBride, O.W., Epstein, A.L. and Korsmeyer, S.J. (1985), "Cloning the chromosomal breakpoint of t(14;18) human lymphomas: clustering around Jhon chromosome 14 and near a transcriptional unit on 18", *Cell*, Vol. 41 No. 3, pp. 899–906.

Baldwin, A.N., Bitler, C.M., Welcher, A.A. and Shooter, E.M. (1992), "Studies on the structure and binding properties of the cysteine-rich domain of rat low affinity nerve growth factor receptor (p75NGFR)", *Journal of Biological Chemistry*, Vol. 267 No. 12, pp. 8352–8359.

Bamji, S.X., Majdan, M., Pozniak, C.D., Belliveau, D.J., Aloyz, R., Kohn, J., Causing, C.G., et al. (1998), "The p75 neurotrophin receptor mediates neuronal apoptosis and is essential for naturally occurring sympathetic neuron death", *The Journal of Cell Biology*, Vol. 140 No. 4, pp. 911–923.

Bandtlow, C.E., Heumann, R., Schwab, M.E. and Thoenen, H. (1987), "Cellular localization of nerve growth factor synthesis by in situ hybridization.", *The EMBO Journal*, Vol. 6 No. 4, pp. 891–899.

Barde, Y.A., Edgar, D. and Thoenen, H. (1982), "Purification of a new neurotrophic factor from mammalian brain.", *The EMBO Journal*, Vol. 1 No. 5, pp. 549–553.

Barker, P.A., Barbee, G., Misko, T.P. and Shooter, E.M. (1994), "The low affinity neurotrophin receptor, p75LNTR, is palmitoylated by thioester formation through cysteine 279", *Journal of Biological Chemistry*, Vol. 269 No. 48, pp. 30645–30650.

Batistatou, A., Merry, D.E., Korsmeyer, S.J. and Greene, L.A. (1993), "Bcl-2 affects survival but not neuronal differentiation of PC12 cells", *The Journal of Neuroscience*, Vol. 13 No. 10, pp. 4422–44228.

Beerli, R. and Barbas, C. (2002), "Engineering polydactyl zinc-finger transcription factors", *Nature Biotechnology*, Vol. 20 No. 2, pp. 135–141.

Beerli, R.R., Dreier, B. and Barbas, C.F. (2000), "Positive and negative regulation of

endogenous genes by designed transcription factors", *Proceedings of the National Academy of Sciences*, Vol. 97 No. 4, pp. 1495–1500.

Bender, C.E., Fitzgerald, P., Tait, S.W., Llambi, F., McStay, G.P., Tupper, D.O., Pellettieri, J., et al. (2012), "Mitochondrial pathway of apoptosis is ancestral in metazoans", *Proceedings of the National Academy of Sciences*, Vol. 109 No. 13, pp. 4904–4909.

Berkemeier, L.R., Winslow, J.W., Kaplan, D.R., Nikolics, K., Goeddel, D. V and Rosenthal, A. (1991), "Neurotrophin-5: a novel neurotrophic factor that activates trk and trkB.", *Neuron*, United States, Vol. 7 No. 5, pp. 857–866.

Bernabeu, R.O. and Longo, F.M. (2010), "The p75 neurotrophin receptor is expressed by adult mouse dentate progenitor cells and regulates neuronal and non-neuronal cell genesis.", *BMC Neuroscience*, Vol. 11, p. 136.

Bibel, M. and Barde, Y.A. (2000), "Neurotrophins: Key regulators of cell fate and cell shape in the vertebrate nervous system", *Genes and Development*, Vol. 14 No. 23, pp. 2919–2937.

Bibel, M., Richter, J., Lacroix, E. and Barde, Y. (2007), "Generation of a defined and uniform population of CNS progenitors and neurons from mouse embryonic stem cells", *Nature Protocols*, Vol. 2 No. 5, pp. 1034–1043.

Bibel, M., Richter, J., Schrenk, K., Tucker, K.L., Staiger, V., Korte, M., Goetz, M., et al. (2004), "Differentiation of mouse embryonic stem cells into a defined neuronal lineage", *Nature Neuroscience*, Vol. 7 No. 9, pp. 1003–1009.

Binder, L.I., Frankfurter, A. and Rebhun, L.I. (1985), "The distribution of tau in the mammalian central nervous central nervous", *The Journal of Cell Biology*, Vol. 101 No. 4, pp. 1371–1378.

Boeshore, K.L., Luckey, C.N., Zigmond, R.E. and Large, T.H. (1999), "TrkB isoforms with distinct neurotrophin specificities are expressed in predominantly nonoverlapping populations of avian dorsal root ganglion neurons.", *The Journal of Neuroscience*, Vol. 19 No. 12, pp. 4739–47.

Borasio, G.D., Markus, A., Wittinghofer, A., Barde, Y.A. and Heumann, R. (1993), "Involvement of ras p21 in neurotrophin-induced response of sensory, but not

sympathetic neurons", *The Journal of Cell Biology*, Vol. 121 No. 3, pp. 665–672.

Bradshaw, R.A., Blundell, T.L., Lapatto, R., McDonald, N.Q. and Murray-Rust, J. (1993), "Nerve growth factor revisited", *Trends in Biochemical Sciences*, Vol. 18 No. 2, pp. 48–52.

Brady, R.R., Zaidi, S.I.S.I., Mayer, C.C. and Katz, D.M.D.M. (1999), "BDNF is a target-derived survival factor for arterial baroreceptor and chemoafferent primary sensory neurons.", *The Journal of Neuroscience*, Vol. 19 No. 6, pp. 2131–2142.

Bredesen, D.E., Ye, X., Tasinato, A., Sperandio, S., Wang, J.J.L., Assa-Munt, N. and Rabizadeh, S. (1998), "p75(NTR) and the concept of cellular dependence: seeing how the other half die", *Cell Death and Differentiation*, Vol. 5 No. 5, pp. 365–371.

Brenner, S. (1974), "The Genetics of Caenorhabditis elegans", *Genetics*, Vol. 77 No. 1, pp. 71–94.

Bruno, M.A. and Cuello, A.C. (2006), "Activity-dependent release of precursor nerve growth factor, conversion to mature nerve growth factor, and its degradation by a protease cascade", *Proceedings of the National Academy of Sciences*, Vol. 103 No. 17, pp. 6735–6740.

Bueker, E.D. (1948), "Implantation of tumors in the hind limb field of the embryonic chick and the developmental response of the lumbosacral nervous system.", *The Anatomical Record*, United States, Vol. 102 No. 3, pp. 369–389.

Burry, R.W. (1983), "Antimitotic drugs that enhance neuronal survival in olfactory bulb cell cultures", *Brain Research*, Vol. 261 No. 2, pp. 261–275.

Chao, M. V. and Bothwell, M. (2002), "Neurotrophins: To Cleave or Not to Cleave", *Neuron*, Vol. 33 No. 1, pp. 9–12.

Chao, M. V, Bothwell, M.A., Ross, A.H., Koprowski, H., Lanahan, A.A., Buck, C.R. and Sehgal, A. (1986), "Gene transfer and molecular cloning of the human NGF receptor.", *Science*, United States, Vol. 232 No. 4749, pp. 518–521.

Chen, K.S., Nishimura, M.C., Armanini, M.P., Crowley, C., Spencer, S.D. and

Phillips, H.S. (1997), "Disruption of a single allele of the nerve growth factor gene results in atrophy of basal forebrain cholinergic neurons and memory deficits.", *The Journal of Neuroscience*, Vol. 17 No. 19, pp. 7288–7296.

Chen, Z.-Y. (2005), "Sortilin Controls Intracellular Sorting of Brain-Derived Neurotrophic Factor to the Regulated Secretory Pathway", *The Journal of Neuroscience*, Vol. 25 No. 26, pp. 6156–6166.

Chittenden, T., Flemington, C., Houghton, A.B., Ebb, R.G., Gallo, G.J., Elangovan, B., Chinnadurai, G., et al. (1995), "A conserved domain in Bak, distinct from BH1 and BH2, mediates cell death and protein binding functions", *The EMBO Journal*, Vol. 14 No. 22, pp. 5589–5596.

Cikala, M., Wilm, B., Hobmayer, E., Bottger, A. and David, C.N. (1999), "Identification of caspases and apoptosis in the simple metazoan Hydra.", *Current Biology : CB*, England, Vol. 9 No. 17, pp. 959–962.

Clary, D.O. and Reichardt, L.F. (1994), "An alternatively spliced form of the nerve growth factor receptor TrkA confers an enhanced response to neurotrophin 3.", *Proceedings of the National Academy of Sciences*, Vol. 91 No. 23, pp. 11133–11137.

Coggeshall, R.E. (1992), "A consideration of neural counting methods.", *Trends in Neurosciences*, Vol. 15 No. 1, pp. 9–13.

Cohen, G.M. (1997), "Caspases: the executioners of apoptosis.", *Biochemical Journal*, Vol. 326 No. Pt 1, pp. 1–16.

Cohen, S. (1960), "Purification of a nerve-growth promoting protein from the mouse salivary gland and its neuro-cytotoxic antiserum", *Proceedings of the National Academy of Sciences*, Vol. 46 No. 3, pp. 302–311.

Cohen, S., Levi-Montalcini, R. and Hamburger, V. (1954), "A nerve growth-stimulating factor isolated from sarcomas 37 and 180", *Proceedings of the National Academy of Sciences*, Vol. 40 No. 10, pp. 1014–1018.

Conover, J.C., Erickson, J.T., Katz, D.M., Bianchi, L.M., Poueymirou, W.T., McClain, J., Pan, L., et al. (1995), "Neuronal deficits, not involving motor neurons, in mice lacking BDNF and/or NT4", *Nature*, Vol. 375 No. 6528, pp.

235–238.

Conradt, B. and Horvitz, H.R. (1998), "The C. elegans Protein EGL-1 is required for programmed cell death and interacts with the Bcl-2-like protein CED-9", *Cell*, Vol. 93 No. 4, pp. 519–529.

Cordon-Cardo, C., Tapley, P., Jing, S.Q., Nanduri, V., O'Rourke, E., Lamballe, F., Kovary, K., et al. (1991), "The trk tyrosine protein kinase mediates the mitogenic properties of nerve growth factor and neurotrophin-3.", *Cell*, Vol. 66 No. 1, pp. 173–183.

Coronato, S. and Coto, C.E. (1991), "[Prevalence of Mycoplasma orale as a contaminant of cell cultures in Argentina].", *Revista Argentina de microbiologia*, Argentina, Vol. 23 No. 3, pp. 166–171.

Coughlin, M.D., Boyer, D.M. and Black, I.R.A.B. (1977), "Embryologic Development of a Mouse Sympathetic Ganglion in vivo and in vitro", *Proceedings of the National Academy of Sciences*, Vol. 74 No. 8, pp. 3438–3442.

Coughlin, M.D. and Collins, M.B. (1985), "Nerve growth factor-independent development of embryonic mouse sympathetic neurons in dissociated cell culture", *Developmental Biology*, Vol. 110 No. 2, pp. 392–401.

Crowder, R.J. and Freeman, R.S. (1998), "Phosphatidylinositol 3-kinase and Akt protein kinase are necessary and sufficient for the survival of nerve growth factor-dependent sympathetic neurons.", *The Journal of Neuroscience*, Vol. 18 No. 8, pp. 2933–2943.

Crowley, C., Spencer, S.D., Nishimura, M.C., Chen, K.S., Pitts-Meek, S., Armanini, M.P., Ling, L.H., et al. (1994), "Mice lacking nerve growth factor display perinatal loss of sensory and sympathetic neurons yet develop basal forebrain cholinergic neurons", *Cell*, Vol. 76 No. 6, pp. 1001–1011.

Cunningham, M.E. and Greene, L.A. (1998), "A function-structure model for NGF-activated TRK", *The EMBO Journal*, Vol. 17 No. 24, pp. 7282–7293.

Cunningham, M.E., Stephens, R.M., Kaplan, D.R. and Greene, L.A. (1997), "Autophosphorylation of activation loop tyrosines regulates signaling by the

TRK nerve growth factor receptor", *Journal of Biological Chemistry*, Vol. 272 No. 16, pp. 10957–10967.

Davies, A.M., Bandtlow, C., Heumann, R., Korsching, S., Rohrer, H. and Thoenen, H. (1987), "Timing and site of nerve growth factor synthesis in developing skin in relation to innervation and expression of the receptor", *Nature*, Vol. 326 No. 6111, pp. 353–358.

Davies, A.M., Minichiello, L. and Klein, R. (1995), "Developmental changes in NT3 signalling via TrkA and TrkB in embryonic neurons.", *The EMBO Journal*, Vol. 14 No. 8, pp. 4482–4489.

Deckwerth, T.L. and Johnson, E.M. (1993), "Temporal analysis of events associated with programmed cell death (apoptosis) of sympathetic neurons deprived of nerve growth factor", *The Journal of Cell Biology*, Vol. 123 No. 5, pp. 1207–1222.

Dekkers, M.P.J., Nikoletopoulou, V. and Barde, Y.-A. (2013), "Death of developing neurons: New insights and implications for connectivity", *The Journal of Cell Biology*, Rockefeller University Press, Vol. 203 No. 3, pp. 385–393.

Della-Bianca, V., Rossi, F., Armato, U., Dal-Pra, I., Costantini, C., Perini, G., Politi, V., et al. (2001), "Neurotrophin p75 Receptor Is Involved in Neuronal Damage by Prion Peptide-(106-126)", *The Journal of Biological Chemistry*, Vol. 276 No. 42, pp. 38929–38933.

Deshmukh, M. and Johnson, E.M. (1997), "Programmed cell death in neurons: focus on the pathway of nerve growth factor deprivation-induced death of sympathetic neurons.", *Molecular Pharmacology*, Vol. 51 No. 6, pp. 897–906.

Deshmukh, M., Vasilakos, J., Deckwerth, T.L., Lampe, P.A., Shivers, B.D. and Johnson, E.M. (1996), "Genetic and metabolic status of NGF-deprived sympathetic neurons saved by an inhibitor of ICE family proteases", *The Journal of Cell Biology*, Vol. 135 No. 5, pp. 1341–1354.

Dicou, E. (2008), "High levels of the proNGF peptides LIP1 and LIP2 in the serum and synovial fluid of rheumatoid arthritis patients: Evidence for two new cytokines", *Journal of Neuroimmunology*, Vol. 194 No. 1, pp. 143–146.

Dixon, J.E. and McKinnon, D. (1994), "Expression of the trk gene family of neurotrophin receptors in prevertebral sympathetic ganglia", *Developmental Brain Research*, Vol. 77 No. 2, pp. 177–182.

Dobrovolny, P.L. and Bess, D. (2011), "Optimized PCR-based Detection of Mycoplasma", *Journal of Visualized Experiments*, Vol. 52, p. 3057.

Doherty, J. and Baehrecke, E. (2018), "Life, death and autophagy", *Nature Cell Biology*, Vol. 20 No. 10, pp. 1110–1117.

Donovan, M.J., Hahn, R., Tessarollo, L. and Hempstead, B.L. (1996), "Identification of an essential nonneuronal function of neurotrophin 3 in mammalian cardiac development", *Nature Genetics*, Vol. 14 No. 2, pp. 210–213.

Drexler, H.G. and Uphoff, C.C. (2002), "Mycoplasma contamination of cell cultures: Incidence, sources, effects, detection, elimination, prevention.", *Cytotechnology*, United States, Vol. 39 No. 2, pp. 75–90.

Dreyfus, C.F. (1989), "Effects of nerve growth factor on cholinergic brain neurons", *Trends in Pharmacological Sciences*, Vol. 10 No. 4, pp. 145–149.

Du, J., Feng, L., Zaitsev, E., Je, H.S., Liu, X.W. and Lu, B. (2003), "Regulation of TrkB receptor tyrosine kinase and its internalization by neuronal activity and Ca2+influx", *The Journal of Cell Biology*, Vol. 163 No. 2, pp. 385–395.

Duce, I.R. and Keen, P. (1977), "An ultrastructural classification of the neuronal cell bodies of the rat dorsal root ganglion using zinc iodide-osmium impregnation.", *Cell and Tissue Research*, Vol. 185 No. 2, pp. 263–77.

Edwards, S.N., Buckmaster, A.E. and Tolkovsky, A.M. (1991), "The Death Programme in Cultured Sympathetic Neurones Can Be Suppressed at the Posttranslational Level by Nerve Growth Factor, Cyclic AMP, and Depolarization", *Journal of Neurochemistry*, Vol. 57 No. 6, pp. 2140–2143.

Edwards, S.N. and Tolkovsky, A.M. (1994), "Characterization of apoptosis in cultured rat sympathetic neurons after nerve growth factor withdrawal", *The Journal of Cell Biology*, Vol. 124 No. 4, pp. 537–546.

Eide, F.F., Vining, E.R., Eide, B.L., Zang, K., Wang, X.Y. and Reichardt, L.F. (1996), "Naturally occurring truncated trkB receptors have dominant inhibitory

effects on brain-derived neurotrophic factor signaling", *The Journal of Neuroscience*, Vol. 16 No. 10, pp. 3123–3129.

Eiselleova, L., Peterkova, I., Neradil, J., Slaninova, I., Hampl, A. and Dvorak, P. (2008), "Comparative study of mouse and human feeder cells for human embryonic stem cells.", *The International Journal of Developmental Biology*, Spain, Vol. 52 No. 4, pp. 353–363.

Ellis, H. (1986), "Genetic control of programmed cell death in the nematode C. elegans", *Cell*, Vol. 44 No. 6, pp. 817–829.

ElShamy, W.M. and Ernfors, P. (1996), "A Local Action of Neurotrophin-3 Prevents the Death of Proliferating Sensory Neuron Precursor Cells", *Neuron*, Vol. 16 No. 5, pp. 963–972.

ElShamy, W.M. and Ernfors, P. (1997), "Brain-derived neurotrophic factor, neurotrophin-3, and neurotrophin-4 complement and cooperate with each other sequentially during visceral neuron development.", *The Journal of Neuroscience*, Vol. 17 No. 22, pp. 17–22.

Enari, M., Sakahira, H., Yokoyama, H., Okawa, K., Iwamatsu, A. and Nagata, S. (1998), "A caspase-activated DNase that degrades DNA during apoptosis, and its inhibitor ICAD", *Nature*, Vol. 391 No. 6662, pp. 43–50.

Erickson, J.T., Conover, J.C., Borday, V., Champagnat, J., Barbacid, M., Yancopoulos, G. and Katz, D.M. (1996), "Mice lacking brain-derived neurotrophic factor exhibit visceral sensory neuron losses distinct from mice lacking NT4 and display a severe developmental deficit in control of breathing", *The Journal of Neuroscience*, Vol. 16 No. 17, pp. 5361–5371.

Ernfors, P., Hallbook, F., Ebendal, T., Shooter, E.M., Radeke, M.J., Misko, T.P. and Persson, H. (1988), "Developmental and regional expression of β-nerve growth factor receptor mRNA in the chick and rat", *Neuron*, Vol. 1 No. 10, pp. 983–996.

Ernfors, P., Ibáñez, C.F., Ebendal, T., Olson, L. and Persson, H. (1990), "Molecular cloning and neurotrophic activities of a protein with structural similarities to nerve growth factor: developmental and topographical expression in the brain.",

Proceedings of the National Academy of Sciences, Vol. 87 No. 14, pp. 5454–5458.

Ernfors, P., Lee, K.F. and Jaenisch, R. (1994), "Mice lacking brain-derived neurotrophic factor develop with sensory deficits.", *Nature*, ENGLAND, Vol. 368 No. 6467, pp. 147–150.

Ernfors, P., Lee, K.F., Kucera, J. and Jaenisch, R. (1994), "Lack of neurotrophin-3 leads to deficiencies in the peripheral nervous system and loss of limb proprioceptive afferents", *Cell*, Vol. 77 No. 4, pp. 503–512.

Ernfors, P., Merlio, J. -P and Persson, H. (1992), "Cells Expressing mRNA for Neurotrophins and their Receptors During Embryonic Rat Development", *European Journal of Neuroscience*, Vol. 4 No. 11, pp. 1140–1158.

Ernfors, P., Van De Water, T., Loring, J. and Jaenisch, R. (1995), "Complementary roles of BDNF and NT-3 in vestibular and auditory development", *Neuron*, Vol. 14 No. 6, pp. 1153–1164.

Esposito, D., Patel, P., Stephens, R.M., Perez, P., Chao, M. V., Kaplan, D.R. and Hempstead, B.L. (2001), "The Cytoplasmic and Transmembrane Domains of the p75 and Trk A Receptors Regulate High Affinity Binding to Nerve Growth Factor", *The Journal of Biological Chemistry*, Vol. 276 No. 35, pp. 32687–32695.

Estus, S., Zaks, W.J., Freeman, R.S., Gruda, M., Bravo, R. and Johnson, E.M. (1994), "Altered gene expression in neurons during programmed cell death: Identification of c-jun as necessary for neuronal apoptosis", *The Journal of Cell Biology*, Vol. 127 No. 6 I, pp. 1717–1727.

Evans, S.F., Irmady, K., Ostrow, K., Kim, T., Nykjaer, A., Saftig, P., Blobel, C., et al. (2011), "Neuronal brain-derived neurotrophic factor is synthesized in excess, with levels regulated by sortilin-mediated trafficking and lysosomal degradation", *The Journal of Biological Chemistry*, Vol. 286 No. 34, pp. 29556–29567.

Fagan, A.M., Garber, M., Barbacid, M., Silos-Santiago, I., Holtzman, D.M. and SilosSantiago, I. (1997), "A role for TrkA during maturation of striatal and

basal forebrain cholinergic neurons in vivo", *The Journal of Neuroscience*, Vol. 17 No. 20, pp. 7644–7654.

Fagan, A.M., Zhang, H., Landis, S., Smeyne, R.J., Silos-Santiago, I. and Barbacid, M. (1996), "TrkA, but not TrkC, receptors are essential for survival of sympathetic neurons in vivo.", *The Journal of Neuroscience*, Vol. 16 No. 19, pp. 6208–6218.

Fan, Y., Richelme, S., Avazeri, E., Audebert, S., Helmbacher, F., Dono, R. and Maina, F. (2015), "Tissue-Specific Gain of RTK Signalling Uncovers Selective Cell Vulnerability during Embryogenesis", *PLOS Genetics*, Public Library of Science, Vol. 11 No. 9, p. e1005533.

Farinas, I., Jones, K.R., Backus, C., Wang, X.Y. and Reichardt, L.F. (1994), "Severe sensory and sympathetic deficits in mice lacking neurotrophin-3.", *Nature*, England, Vol. 369 No. 6482, pp. 658–661.

Fariñas, I., Wilkinson, G.A., Backus, C., Reichardt, L.F. and Patapoutian, A. (1998), "Characterization of Neurotrophin and Trk Receptor Functions in Developing Sensory Ganglia: Direct NT-3 Activation of TrkB Neurons In Vivo", *Neuron*, Vol. 21 No. 2, pp. 325–334.

Fei, D. and Krimm, R.F. (2013), "Taste neurons consist of both a large TrkB-receptor-dependent and a small TrkB-receptor-independent subpopulation", *PLoS ONE*, Vol. 8 No. 12, p. e83460.

Feil, R., Wagner, J., Metzger, D. and Chambon, P. (1997), "Regulation of Cre recombinase activity by mutated estrogen receptor ligand-binding domains", *Biochemical and Biophysical Research Communications*, Vol. 237 No. 3, pp. 752–757.

De Felipe, C., Gonzalez, G.G., Gallar, J. and Belmonte, C. (1999), "Quantification and immunocytochemical characteristics of trigeminal ganglion neurons projecting to the cornea: Effect of corneal wounding", *European Journal of Pain*, Vol. 3 No. 1, pp. 31–39.

Flusberg, D.A. and Sorger, P.K. (2015), "Surviving apoptosis: Life-death signaling in single cells", *Trends in Cell Biology*, Vol. 25 No. 8, pp. 446–458.

Forgie, A., Kuehnel, F., Wyatt, S. and Davies, A.M. (2000), "In vivo survival requirement of a subset of nodose ganglion neurons for nerve growth factor", *European Journal of Neuroscience*, Blackwell Science Ltd, Vol. 12 No. 2, pp. 670–676.

Fox, E.A., Phillips, R.J., Baronowsky, E.A., Byerly, M.S., Jones, S. and Powley, T.L. (2001), "Neurotrophin-4 deficient mice have a loss of vagal intraganglionic mechanoreceptors from the small intestine and a disruption of short-term satiety.", *The Journal of Neuroscience*, Vol. 21 No. 21, pp. 8602–8615.

Freeman, R.S., Estus, S. and Johnson, E.M. (1994), "Analysis of cell cycle-related gene expression in postmitotic neurons: Selective induction of cyclin D1 during programmed cell death", *Neuron*, Vol. 12 No. 2, pp. 343–355.

Friedrich, G. and Soriano, P. (1991), "Promoter traps in embryonic stem cells: a genetic screen to identify and mutate developmental genes in mice.", *Genes & Development*, Vol. 5 No. 9, pp. 1513–1523.

Fritzsch, B., Sarai, P.A., Barbacid, M. and Silos-Santiago, I. (1997), "Mice with a targeted disruption of the neurotrophin receptor trkB lose their gustatory ganglion cells early but do develop taste buds", *International Journal of Developmental Neuroscience*, Vol. 15 No. 4–5, pp. 563–576.

Garcia, I., Huang, L., Ung, K. and Arenkiel, B.R. (2012), "Tracing synaptic connectivity onto embryonic stem cell-derived neurons", *Stem Cells*, Vol. 30 No. 10, pp. 2140–2151.

Garcia, I., Martinou, I., Tsujimoto, Y. and Martinou, J.C. (1992), "Prevention of programmed cell death of sympathetic neurons by the bcl-2 proto-oncogene.", *Science*, Vol. 258 No. 5080, pp. 302–304.

Garner, A.S. and Larget, T.H. (1994), "Isoforms of the avian TrkC receptor: A novel kinase insertion dissociates transformation and process outgrowth from survival", *Neuron*, Vol. 13 No. 2, pp. 457–472.

Gaspard, N., Bouschet, T., Herpoel, A., Naeije, G., van den Ameele, J. and Vanderhaeghen, P. (2009), "Generation of cortical neurons from mouse

embryonic stem cells", *Nature Protocols*, Vol. 4 No. 10, pp. 1456–1463.

Gaztelumendi, N. and Nogués, C. (2014), "Chromosome Instability in mouse Embryonic Stem Cells", *Scientific Reports*, Vol. 4, p. 5324.

Ginty, D.D. and Segal, R.A. (2002), "Retrograde neurotrophin signaling: Trk-ing along the axon", *Current Opinion in Neurobiology*, Vol. 12 No. 3, pp. 268–274.

Graham, E., Moss, J., Burton, N., Roochun, Y., Armit, C., Richardson, L. and Baldock, R. (2015), "The atlas of mouse development eHistology resource.", *Development (Cambridge, England)*, England, Vol. 142 No. 11, pp. 1909–1911.

Greenlund, L.J.S., Korsmeyer, S.J. and Johnson, E.M. (1995), "Role of BCL-2 in the survival and function of developing and mature sympathetic neurons", *Neuron*, Vol. 15 No. 3, pp. 649–661.

Grimes, M.L., Beattie, E. and Mobley, W.C. (1997), "A signaling organelle containing the nerve growth factor-activated receptor tyrosine kinase, TrkA", *Proceedings of the National Academy of Sciences*, Vol. 94 No. 18, pp. 9909–9914.

Grimes, M.L., Zhou, J., Beattie, E.C., Yuen, E.C., Hall, D.E., Valletta, J.S., Topp, K.S., et al. (1996), "Endocytosis of activated TrkA: evidence that nerve growth factor induces formation of signaling endosomes", *The Journal of Neuroscience*, Vol. 16 No. 24, pp. 7950–7964.

Guiton, M., Gunn-Moore, F.J., Glass, D.J., Geis, D.R., Yancopoulos, G.D. and Tavare, J.M. (1995), "Naturally occurring tyrosine kinase inserts block high affinity binding of phospholipase Cγ and Shc to trkC and neurotrophin-3 signaling", *The Journal of Biological Chemistry*, Vol. 270 No. 35, pp. 20384–20390.

Hallbook, F., Bäckström, A., Kullander, K., Kylberg, A., Williams, R. and Ebendal, T. (1995), "Neurotrophins and their receptors in chicken neuronal development", *International Journal of Developmental Biology*, Vol. 39 No. 5, pp. 855–868.

Hallbook, F., Ibanez, C.F. and Persson, H. (1991), "Evolutionary studies of the nerve growth factor family reveal a novel member abundantly expressed in Xenopus

ovary.", *Neuron*, Vol. 6 No. 5, pp. 845–858.

Hamburger, V. (1934), "The effects of wing bud extirpation on the development of the central nervous system in chick embryos", *Journal of Experimental Zoology*, Vol. 68 No. 3, pp. 449–494.

Hamburger, V., Brunso-Bechtold, J.K. and Yip, J.W. (1981), "Neuronal death in the spinal ganglia of the chick embryo and its reduction by nerve growth factor.", *The Journal of Neuroscience*, Vol. 1 No. 1, pp. 60–71.

Hamburger, V. and Levi-Montalcini, R. (1949), "Proliferation, differentiation and degeneration in the spinal ganglia of the chick embryo under normal and experimental conditions", *The Journal of Experimental Zoology*, Vol. 111 No. 3, pp. 457–501.

Harada, A., Oguchi, K., Okabe, S., Kuno, J., Terada, S., Ohshima, T., Sato-Yoshitake, R., et al. (1994), "Altered microtubule organization in small-calibre axons of mice lacking tau protein.", *Nature*, Vol. 369 No. 6480, pp. 488–491.

Harper, A.A. and Lawson, S.N. (1985), "Conduction velocity is related to morphological cell type in rat dorsal root ganglion neurones.", *The Journal of Physiology*, Vol. 359, pp. 31–46.

Hasan, W., Pedchenko, T., Krizsan-Agbas, D., Baum, L. and Smith, P.G. (2003), "Sympathetic neurons synthesize and secrete pro-nerve growth factor protein", *Journal of Neurobiology*, Vol. 57 No. 1, pp. 38–53.

Haupt, S., Edenhofer, F., Peitz, M., Leinhaas, A. and Brüstle, O. (2007), "Stage-Specific Conditional Mutagenesis in Mouse Embryonic Stem Cell-Derived Neural Cells and Postmitotic Neurons by Direct Delivery of Biologically Active Cre Recombinase", *Stem Cells*, Vol. 25 No. 1, pp. 181–188.

Hayashi, S. and McMahon, A.P. (2002), "Efficient recombination in diverse tissues by a tamoxifen-inducible form of Cre: a tool for temporally regulated gene activation/inactivation in the mouse.", *Developmental Biology*, Vol. 244 No. 2, pp. 305–18.

He, X.L. and Garcia, K.C. (2004), "Structure of Nerve Growth Factor Complexed with the Shared Neurotrophin Receptor p75", *Science*, Vol. 304 No. 5672, pp.

870–875.

Hellard, D., Brosenitsch, T., Fritzsch, B. and Katz, D.M. (2004), "Cranial sensory neuron development in the absence of brain-derived neurotrophic factor in BDNF/Bax double null mice.", *Developmental Biology*, Vol. 275 No. 1, pp. 34–43.

Hempstead, B.L., Martin-Zanca, D., Kaplan, D.R., Parada, L.F. and Chao, M. V. (1991), "High-affinity NGF binding requires coexpression of the trk proto-oncogene and the low-affinity NGF receptor.", *Nature*, Vol. 350 No. 6320, pp. 678–683.

Hendry, I.A., Stach, R. and Herrup, K. (1974), "Characteristics of the retrograde axonal transport system for nerve growth factor in the sympathetic nervous system", *Brain Research*, Vol. 82 No. 1, pp. 117–128.

Hendry, I.A., Stockel, K., Thoenen, H. and Iversen, L.L. (1974), "The retrograde axonal transport of nerve growth factor", *Brain Research*, Vol. 68 No. 1, pp. 103–121.

Hengartner, M.O. (2000), "The biochemistry of apoptosis.", *Nature*, Vol. 407 No. 6805, pp. 770–776.

Hengartner, M.O., Ellis, R. and Horvitz, H.R. (1992), "Caenorhabditis elegans gene ced-9 protects cells from programmed cell death", *Nature*, Vol. 356 No. 6369, pp. 494–499.

Hengartner, M.O. and Horvitz, H.R. (1994), "C. elegans cell survival gene ced-9 encodes a functional homolog of the mammalian proto-oncogene bcl-2", *Cell*, Vol. 76 No. 4, pp. 665–676.

Hertzberg, T., Fan, G., Finley, J.C.W., Erickson, J.T. and Katz, D.M. (1994), "BDNF supports mammalian chemoafferent neurons in vitro and following peripheral target removal in vivo", *Developmental Biology*, Vol. 166 No. 2, pp. 801–811.

Hezroni, H., Tzchori, I., Davidi, A., Mattout, A., Biran, A., Nissim-Rafinia, M., Westphal, H., et al. (2011), "H3K9 histone acetylation predicts pluripotency and reprogramming capacity of ES cells", *Nucleus*, Vol. 2 No. 4, pp. 300–309.

Hofer, M., Pagliusi, S.R., Hohn, A., Leibrock, J. and Barde, Y.A. (1990), "Regional distribution of brain-derived neurotrophic factor mRNA in the adult mouse brain.", *The EMBO Journal*, Vol. 9 No. 8, pp. 2459–64.

Hohn, A., Leibrock, J., Bailey, K. and Barde, Y.A. (1990), "Identification and characterization of a novel member of the nerve growth factor/brain-derived neurotrophic factor family", *Nature*, Vol. 344 No. 6264, pp. 339–341.

Holden, P.H., Asopa, V., Robertson, A.G.S., Clarke, A.R., Tyler, S., Bennett, G.S., Brain, S.D., et al. (1997), "Immunoglobulin-like domains define the nerve growth factor binding site of the TrkA receptor", *Nature Biotechnology*, Vol. 15 No. 7, pp. 668–672.

Hooper, M., Hardy, K., Handyside, A., Hunter, S. and Monk, M. (1987), "HPRT-deficient (Lesch-Nyhan) mouse embryos derived from germline colonization by cultured cells", *Nature*, Vol. 326 No. 6110, pp. 292–295.

Howard, A.D., Kostura, M.J., Thornberry, N., Ding, G.J., Limjuco, G., Weidner, J., Salley, J.P., et al. (1991), "IL-1-converting enzyme requires aspartic acid residues for processing of the IL-1 beta precursor at two distinct sites and does not cleave 31-kDa IL-1 alpha", *Journal of Immunology*, Vol. 147 No. 9, pp. 2964–2969.

Howe, C.L., Valletta, J.S., Rusnak, A.S. and Mobley, W.C. (2001), "NGF signaling from clathrin-coated vesicles: Evidence that signaling endosomes serve as a platform for the Ras-MAPK pathway", *Neuron*, Vol. 32 No. 5, pp. 801–814.

Huang, E.J., Wilkinson, G.A., Fariñas, I., Backus, C., Zang, K., Wong, S.L. and Reichardt, L.F. (1999), "Expression of Trk receptors in the developing mouse trigeminal ganglion: in vivo evidence for NT-3 activation of TrkA and TrkB in addition to TrkC", *Development (*, Vol. 126 No. 10, pp. 2191–2203.

Hubbard, S.R. and Miller, W.T. (2007), "Receptor tyrosine kinases: mechanisms of activation and signaling.", *Current Opinion in Cell Biology*, Vol. 19 No. 2, pp. 117–123.

Huebner, K., Isobe, M., Chao, M., Bothwell, M., Ross, A.H., Finan, J., Hoxie, J.A., et al. (1986), "The nerve growth factor receptor gene is at human chromosome

region 17q12-17q22, distal to the chromosome 17 breakpoint in acute leukemias", *Proceedings of the National Academy of Sciences*, Vol. 83 No. 5, pp. 1403–1407.

Ibáñez, C.F., Ernfors, P., Timmusk, T., Ip, N.Y., Arenas, E., Yancopoulos, G.D. and Persson, H. (1993), "Neurotrophin-4 is a target-derived neurotrophic factor for neurons of the trigeminal ganglion", *Development*, Vol. 117 No. 4, pp. 1345–1353.

Ichim, G., Genevois, A.L., Ménard, M., Yu, L.Y., Coelho-Aguiar, J.M., Llambi, F., Jarrosson-Wuilleme, L., et al. (2013), "The Dependence Receptor TrkC Triggers Mitochondria-Dependent Apoptosis upon Cobra-1 Recruitment", *Molecular Cell*, Vol. 51 No. 5, pp. 632–646.

Ip, N.Y., Ibáñez, C.F., Nye, S.H., McClain, J., Jones, P.F., Gies, D.R., Belluscio, L., et al. (1992), "Mammalian neurotrophin-4: structure, chromosomal localization, tissue distribution, and receptor specificity.", *Proceedings of the National Academy of Sciences*, Vol. 89 No. 7, pp. 3060–3064.

Jacobson, M.D., Weil, M. and Raff, M.C. (1997), "Programmed cell death in animal development.", *Cell*, Vol. 88 No. 3, pp. 347–354.

Jaisser, F. (2000), "Inducible gene expression and gene modification in transgenic mice.", *Journal of the American Society of Nephrology*, Vol. 11 Suppl 1, pp. S95–S100.

Jiang, Y., Chen, C., Li, Z., Guo, W., Gegner, J.A., Lin, S. and Han, J. (1996), "Characterization of the structure and function of a new mitogen- activated protein kinase (p38β)", *The Journal of Biological Chemistry*, Vol. 271 No. 30, pp. 17920–17926.

Jing, S., Tapley, P. and Barbacid, M. (1992), "Nerve growth factor mediates signal transduction through trk homodimer receptors", *Neuron*, Vol. 9 No. 6, pp. 1067–1079.

Johnson, D., Lanahan, A., Buck, C.R., Sehgal, A., Morgan, C., Mercer, E., Bothwell, M., et al. (1986), "Expression and structure of the human NGF receptor", *Cell*, Vol. 47 No. 4, pp. 545–554.

Jones-Villeneuve, E.M., McBurney, M.W., Rogers, K. a and Kalnins, V.I. (1982), "Retinoic acid induces embryonal carcinoma cells to differentiate into neurons and glial cells.", *The Journal of Cell Biology*, Vol. 94 No. 2, pp. 253–262.

Jones, K.R., Farinas, I., Backus, C. and Reichardt, L.F. (1994), "Targeted disruption of the BDNF gene perturbs brain and sensory neuron development but not motor neuron development.", *Cell*, Vol. 76 No. 6, pp. 989–999.

Jones, K.R. and Reichardt, L.F. (1990), "Molecular cloning of a human gene that is a member of the nerve growth factor family", *Proceedings of the National Academy of Sciences*, Vol. 87 No. 20, pp. 8060–8064.

Jullien, J., Guili, V., Derrington, E.A., Darlix, J.L., Reichardt, L.F. and Rudkin, B.B. (2003), "Trafficking of TrkA-green fluorescent protein chimerae during nerve growth factor-induced differentiation", *The Journal of Biological Chemistry*, Vol. 278 No. 10, pp. 8706–8716.

Kameda, Y., Ito, M., Nishimaki, T. and Gotoh, N. (2008), "FRS2α2F/2Fmice lack carotid body and exhibit abnormalities of the superior cervical sympathetic ganglion and carotid sinus nerve", *Developmental Biology*, Vol. 314 No. 1, pp. 236–247.

Kameda, Y., Saitoh, T., Nemoto, N., Katoh, T. and Iseki, S. (2012), "Hes1 is required for the development of the superior cervical ganglion of sympathetic trunk and the carotid body", *Developmental Dynamics*, Vol. 241 No. 8, pp. 1289–1300.

Kaplan, D.R., Hempstead, B.L., Martin-Zanca, D., Chao, M. V and Parada, L.F. (1991), "The trk proto-oncogene product: a signal transducing receptor for nerve growth factor.", *Science*, Vol. 252 No. 5005, pp. 554–558.

Karra, D. and Dahm, R. (2010), "Transfection Techniques for Neuronal Cells", *The Journal of Neuroscience*, Vol. 30 No. 18, pp. 6171–6177.

Kashiba, H., Noguchi, K., Ueda, Y. and Senba, E. (1995), "Coexpression of trk family members and low-affinity neurotrophin receptors in rat dorsal root ganglion neurons", *Molecular Brain Research*, Vol. 30 No. 1, pp. 158–164.

Katayama, K.I., Zine, A., Ota, M., Matsumoto, Y., Inoue, T., Fritzsch, B. and Aruga,

J. (2009), "Disorganized innervation and neuronal loss in the inner ear of slitrk6-deficient mice", *PLoS ONE*, Vol. 4 No. 11, pp. 1–12.

Katz, D.M., Erb, M., Lillis, R. and Neet, K. (1990), "Trophic regulation of nodose ganglion cell development: Evidence for an expanded role of nerve growth factor during embryogenesis in the rat", *Experimental Neurology*, Vol. 110 No. 1, pp. 1–10.

Kerr, J.F.R., Wyllie, A.H. and Currie, A.R. (1972), "Apoptosis : a Basic Biological Phenomenon With Wide-Ranging Implications in tissue kinetics", *British Journal of Cancer*, Vol. 26 No. 4, pp. 239–257.

Klein, R., Conway, D., Parada, L.F. and Barbacid, M. (1990), "The trkB tyrosine protein kinase gene codes for a second neurogenic receptor that lacks the catalytic kinase domain", *Cell*, Vol. 61 No. 4, pp. 647–656.

Klein, R., Jing, S., Nanduri, V., O'Rourke, E. and Barbacid, M. (1991), "The trk proto-oncogene encodes a receptor for nerve growth factor", *Cell*, Vol. 65 No. 1, pp. 189–197.

Klein, R., Lamballe, F., Bryant, S. and Barbacid, M. (1992), "The trkB tyrosine protein kinase is a receptor for neurotrophin-4", *Neuron*, Vol. 8 No. 5, pp. 947–956.

Klein, R., Martin-Zanca, D., Barbacid, M. and Parada, L.F. (1990), "Expression of the tyrosine kinase receptor gene trkB is confined to the murine embryonic and adult nervous system", *Development*, Vol. 109 No. 4, pp. 845–850.

Klein, R., Nanduri, V., Jing, S., Lamballe, F., Tapley, P., Bryant, S., Cordon-Cardo, C., et al. (1991), "The trkB tyrosine protein kinase is a receptor for brain-derived neurotrophic factor and neurotrophin-3", *Cell*, Vol. 66 No. 2, pp. 395–403.

Klein, R., Silos-Santiago, I., Smeyne, R.J., Lira, S.A., Brambilla, R., Bryant, S., Zhang, L., et al. (1994), "Disruption of the neurotrophin-3 receptor gene trkC eliminates la muscle afferents and results in abnormal movements.", *Nature*, Vol. 368 No. 6468, pp. 249–251.

Klein, R., Smeyne, R.J., Wurst, W., Long, L.K., Auerbach, B.A., Joyner, A.L. and

Barbacid, M. (1993), "Targeted disruption of the trkB neurotrophin receptor gene results in nervous system lesions and neonatal death", *Cell*, Vol. 75 No. 1, pp. 113–122.

Kluck, R.M., Bossy-Wetzel, E., Green, D.R. and Newmeyer, D.D. (1997), "The release of cytochrome c from mitochondria: A primary site for Bcl- 2 regulation of apoptosis", *Science*, Vol. 275 No. 5303, pp. 1132–1136.

Kolodziejczyk, A.A., Kim, J.K., Tsang, J.C.H., Ilicic, T., Henriksson, J., Natarajan, K.N., Tuck, A.C., et al. (2015), "Single Cell RNA-Sequencing of Pluripotent States Unlocks Modular Transcriptional Variation.", *Cell Stem Cell*, Vol. 17 No. 4, pp. 471–485.

Korsmeyer, S.J. (1999), "BCL-2 gene family and the regulation of programmed cell death", *Cancer Research*, Vol. 59 No. 7, p. 1693s–1700s.

Kothakota, S., Azuma, T., Reinhard, C., Klippel, A., Tang, J., Chu, K., McGarry, T.J., et al. (1997), "Caspase-3-generated fragment of gelsolin: Effector of morphological change in apoptosis", *Science*, Vol. 278 No. 5336, pp. 294–298.

Krietsch, W.K., Fundele, R., Kuntz, G.W., Fehlau, M., Bürki, K. and Illmensee, K. (1982), "The expression of X-linked phosphoglycerate kinase in the early mouse embryo.", *Differentiation; Research in Biological Diversity*, Vol. 23 No. 2, pp. 141–4.

Kuida, K., Zheng, T.S., Na, S., Kuan, C., Yang, D., Karasuyama, H., Rakic, P., et al. (1996), "Decreased apoptosis in the brain and premature lethality in CPP32-deficient mice.", *Nature*, Vol. 384 No. 6607, pp. 368–372.

Kumanogoh, H., Asami, J., Nakamura, S. and Inoue, T. (2008), "Balanced expression of various TrkB receptor isoforms from the Ntrk2 gene locus in the mouse nervous system", *Molecular and Cellular Neuroscience*, Vol. 39 No. 3, pp. 465–477.

Lamballe, F., Klein, R. and Barbacid, M. (1991), "trkC, a new member of the trk family of tyrosine protein kinases, is a receptor for neurotrophin-3.", *Cell*, Vol. 66 No. 5, pp. 967–979.

Lawson, S., Caddy, K.W.T. and Biscoe, T.J. (1974), "Development of rat dorsal root

ganglion neurones", *Cell and Tissue Research*, Vol. 153 No. 3, pp. 399–413.

Lawson, S.N. (1979), "The postnatal development of large light and small dark neurons in mouse dorsal root ganglia: a statistical analysis of cell numbers and size.", *Journal of Neurocytology*, Vol. 8 No. 3, pp. 275–94.

Lee, R., Kermani, P., Teng, K.K. and Hempstead, B.L. (2001), "Regulation of cell survival by secreted proneurotrophins.", *Science*, Vol. 294 No. 5548, pp. 1945–1948.

Lei, K. and Davis, R.J. (2003), "JNK phosphorylation of Bim-related members of the Bcl2 family induces Bax-dependent apoptosis", *Proceedings of the National Academy of Sciences*, Vol. 100 No. 5, pp. 2432–2437.

Leibrock, J., Lottspeich, F., Hohn, A., Hofer, M., Hengerer, B., Masiakowski, P., Thoenen, H., et al. (1989), "Molecular cloning and expression of brain-derived neurotrophic factor", *Nature*, Vol. 341 No. 6238, pp. 149–152.

Leon, A., Buriani, A., Dal Toso, R., Fabris, M., Romanello, S., Aloe, L. and Levi-Montalcini, R. (1994), "Mast cells synthesize, store, and release nerve growth factor.", *Proceedings of the National Academy of Sciences*, Vol. 91 No. 9, pp. 3739–3743.

Levi-Montalcini, R., Caramia, F. and Angeletti, P.U. (1969), "Alterations in the fine structure of nucleoli in sympathetic neurons following NGF-antiserum treatment", *Brain Research*, Vol. 12 No. 1, pp. 54–73.

Levi-Montalcini, R. and Cohen, S. (1956), "In vitro and in vivo effects of a nerve growth-stimulating agent isolated from snake venom", *Proceedings of the National Academy of Sciences*, Vol. 42 No. 9, pp. 695–699.

Levi-Montalcini, R., Meyer, H. and Hamburger, V. (1954), "In Vitro Experiments on the Effects of Mouse Sarcomas 180 and 37 on the Spinal and Sympathetic Ganglia of the Chick Embryo", *Cancer Research*, Vol. 14 No. 1, pp. 49–57.

Levi-Montalcini, R. and Cohen, S. (1960), "Effects of the extract of the mouse submaxillary salivary glands on the sympathetic system of mammals", *Annals of the New York Academy of Sciences*, Vol. 85 No. 1, pp. 324–341.

Levi-Montalcini, R. and Hamburger, V. (1951), "Selective growth stimulating

effects of mouse sarcoma on the sensory and sympathetic nervous system of the chick embryo", *Journal of Experimental Zoology*, Vol. 116 No. 2, pp. 321–361.

Li, E., Bestor, T.H. and Jaenisch, R. (1992), "Targeted mutation of the DNA methyltransferase gene results in embryonic lethality", *Cell*, Vol. 69 No. 6, pp. 915–926.

Li, P., Nijhawan, D., Budihardjo, I., Srinivasula, S.M., Ahmad, M., Alnemri, E.S. and Wang, X. (1997), "Cytochrome c and dATP-dependent formation of Apaf-1/caspase-9 complex initiates an apoptotic protease cascade", *Cell*, Vol. 91 No. 4, pp. 479–489.

Liebl, D.J., Klesse, L.J., Tessarollo, L., Wohlman, T. and Parada, L.F. (2000), "Loss of brain-derived neurotrophic factor-dependent neural crest-derived sensory neurons in neurotrophin-4 mutant mice", *Proceedings of the National Academy of Sciences*, Vol. 97 No. 5, p. 2297 LP-2302.

Liebl, D.J., Tessarollo, L., Palko, M.E. and Parada, L.F. (1997), "Absence of sensory neurons before target innervation in brain-derived neurotrophic factor-, neurotrophin 3-, and TrkC-deficient embryonic mice.", *The Journal of Neuroscience*, Vol. 17 No. 23, pp. 9113–9121.

Lin, M.I., Das, I., Schwartz, G.M., Tsoulfas, P., Mikawa, T. and Hempstead, B.L. (2000), "Trk C Receptor Signaling Regulates Cardiac Myocyte Proliferation during Early Heart Development in Vivo", *Developmental Biology*, Vol. 226 No. 2, pp. 180–191.

Lin, Z., Tann, J.Y., Goh, E.T.H., Kelly, C., Lim, K.B., Gao, J.F. and Ibanez, C.F. (2015), "Structural basis of death domain signaling in the p75 neurotrophin receptor", *ELife*, Vol. 4, p. e11692.

Lindsay, R.M., Thoenen, H. and Barde, Y.-A. (1985), "Placode and neural crest-derived sensory neurons are responsive at early developmental stages to brain-derived neurotrophic factor", *Developmental Biology*, Vol. 112 No. 2, pp. 319–328.

Liu, M., Pereira, F.A., Price, S.D., Chu, M.J., Shope, C., Himes, D., Eatock, R.A., et al. (2000), "Essential role of BETA2/NeuroD1 in development of the vestibular

and auditory systems", *Genes and Development*, Vol. 14 No. 22, pp. 2839–2854.

Liu, Q., Segal, D.J., Ghiara, J.B. and Barbas, C.F. (1997), "Design of polydactyl zinc-finger proteins for unique addressing within complex genomes", *Proceedings of the National Academy of Sciences*, Vol. 94 No. 11, pp. 5525–5530.

Liu, X., Ernfors, P., Wu, H. and Jaenisch, R. (1995), "Sensory but not motor neuron deficits in mice lacking NT4 and BDNF", *Nature*, Vol. 375 No. 6528, pp. 238–241.

Liu, X., Kim, C.N., Yang, J., Jemmerson, R. and Wang, X. (1996), "Induction of apoptotic program in cell-free extracts: Requirement for dATP and cytochrome c", *Cell*, Vol. 86 No. 1, pp. 147–157.

Liu, X., Li, P., Widlak, P., Zou, H., Luo, X., Garrard, W.T. and Wang, X. (1998), "The 40-kDa subunit of DNA fragmentation factor induces DNA fragmentation and chromatin condensation during apoptosis", *Proceedings of the National Academy of Sciences*, Vol. 95 No. 15, pp. 8461–8466.

Liu, X., Zou, H., Slaughter, C. and Wang, X. (1997), "DFF, a heterodimeric protein that functions downstream of caspase-3 to trigger DNA fragmentation during apoptosis", *Cell*, Vol. 89 No. 2, pp. 175–184.

Llambi, F., Causeret, F., Bloch-Gallego, E. and Mehlen, P. (2001), "Netrin-1 acts as a survival factor via its receptors UNC5H and DCC", *The Embo Journal*, Vol. 20 No. 11, pp. 2715–2722.

Lockshin, R.A. and Williams, C.M. (1964), "Programmed cell death—II. Endocrine potentiation of the breakdown of the intersegmental muscles of silkmoths", *Journal of Insect Physiology*, Vol. 10 No. 4, pp. 643–649.

Lyon, M.F. (1961), "Gene action in the X-chromosome of the mouse (mus musculus L.)", *Nature*, Vol. 190 No. 4773, pp. 372–373.

Mah, S.P., Zhong, L.T., Liu, Y., Roghani, A., Edwards, R.H. and Bredesen, D.E. (1993), "The Protooncogene bcl-2 Inhibits Apoptosis in PC12 Cells", *Journal of Neurochemistry*, Vol. 60 No. 3, pp. 1183–1186.

Maisonpierre, P.C., Belluscio, L., Friedman, B., Alderson, R.F., Wiegand, S.J., Furth, M.E., Lindsay, R.M., et al. (1990), "NT-3, BDNF, and NGF in the developing rat nervous system: Parallel as well as reciprocal patterns of expression", *Neuron*, Vol. 5 No. 4, pp. 501–509.

Maisonpierre, P.C., Belluscio, L., Squinto, S., Ip, N.Y., Furth, M.E., Lindsay, R.M. and Yancopoulos, G.D. (1990), "Neurotrophin-3: A neurotrophic factor related to NGF and BDNF", *Science*, Vol. 247 No. 4949, pp. 1446–1451.

Majumdar, S.K., Valdellon, J.A. and Brown, K.A. (2001), "In vitro investigations on the toxicity and cell death induced by tamoxifen on two non-breast cancer cell types", *Journal of Biomedicine and Biotechnology*, Vol. 2001 No. 3, pp. 99–107.

Mak, W., Nesterova, T.B., de Napoles, M., Appanah, R., Yamanaka, S., Otte, A.P. and Brockdorff, N. (2004), "Reactivation of the Paternal X Chromosome in Early Mouse Embryos", *Science*, Vol. 303 No. 5658, pp. 666–669.

Mao, X., Fujiwara, Y., Chapdelaine, A., Yang, H. and Orkin, S.H. (2001), "Activation of EGFP expression by Cre-mediated excision in a new ROSA26 reporter mouse strain", *Blood*, Vol. 97 No. 1, pp. 324–326.

Martin-Zanca, D., Barbacid, M. and Parada, L.F. (1990), "Expression of the trk proto-oncogene is restricted to the sensory cranial and spinal ganglia of neural crest origin in mouse development", *Genes and Development*, Vol. 4 No. 5, pp. 683–694.

Martin, D.P., Schmidt, R.E., DiStefano, P.S., Lowry, O.H., Carter, J.G. and Johnson, E.M.J. (1988), "Inhibitors of protein synthesis and RNA synthesis prevent neuronal death caused by nerve growth factor deprivation.", *The Journal of Cell Biology*, Vol. 106 No. 3, pp. 829–844.

Matsumoto, T., Rauskolb, S., Polack, M., Klose, J., Kolbeck, R., Korte, M. and Barde, Y.A. (2008), "Biosynthesis and processing of endogenous BDNF: CNS neurons store and secrete BDNF, not pro-BDNF", *Nature Neuroscience*, Vol. 11 No. 2, pp. 131–133.

Matsuo, S., Ichikawa, H., Silos-Santiago, I., Arends, J.J.A., Henderson, T.A.,

Kiyomiya, K., Kurebe, M., et al. (1999), "Proprioceptive afferents survive in the masseter muscle of trkC knockout mice", *Neuroscience*, Vol. 95 No. 1, pp. 209–216.

Mattioni, T., Louvion, J.F. and Picard, D. (1994), "Regulation of protein activities by fusion to steroid binding domains.", *Methods in Cell Biology*, Vol. 43, pp. 335–352.

McIlwain, D.R., Berger, T. and Mak, T.W. (2013), "Caspase functions in cell death and disease", *Cold Spring Harbor Perspectives in Biology*, Vol. 5 No. 4, pp. 1–28.

Meakin, S.O. (1997), "A kinase insert isoform of rat TrkA supports nerve growth factor-dependent cell survival but not neurite outgrowth", *Journal of Neurochemistry*, Vol. 69 No. 3, pp. 954–9667.

Mehlen, P., Rabizadeh, S., Snipas, S.J., Assa-Munt, N., Salvesen, G.S. and Bredesen, D.E. (1998), "The DCC gene product induces apoptosis by a mechanism requiring receptor proteolysis", *Nature*, Vol. 395 No. 6704, pp. 801–804.

Mesner, P.W., Winters, T.R. and Green, S.H. (1992), "Nerve growth factor withdrawal-induced cell death in neuronal PC12 cells resembles that in sympathetic neurons", *The Journal of Cell Biology*, Vol. 119 No. 6, pp. 1669–1680.

Milligan, C.E., Oppenheim, R.W. and Schwartz, L.M. (1994), "Motoneurons deprived of trophic support in vitro require new gene expression to undergo programmed cell death", *Journal of Neurobiology*, Vol. 25 No. 8, pp. 1005–1016.

Minichiello, L., Piehl, F., Vazquez, E., Schimmang, T., Hökfelt, T., Represa, J. and Klein, R. (1995), "Differential effects of combined trk receptor mutations on dorsal root ganglion and inner ear sensory neurons", *Development*, Vol. 121 No. 12, pp. 4067–4075.

Mitre, M., Mariga, A. and Chao, M.V. (2017), "Neurotrophin signalling: Novel insights into mechanisms and pathophysiology", *Clinical Science*, Vol. 131 No.

1, pp. 13–23.

Molla Kazemiha, V., Azari, S., Amanzadeh, A., Bonakdar, S., Shojaei Moghadam, M., Habibi Anbouhi, M., Maleki, S., et al. (2011), "Efficiency of Plasmocin™ on various mammalian cell lines infected by mollicutes in comparison with commonly used antibiotics in cell culture: a local experience", *Cytotechnology*, Vol. 63 No. 6, pp. 609–620.

Mori, R., Futamura, M., Tanahashi, T., Tanaka, Y., Matsuhashi, N., Yamaguchi, K. and Yoshida, K. (2017), "5FU resistance caused by reduced fluoro-deoxyuridine monophosphate and its reversal using deoxyuridine", *Oncology Letters*, Vol. 14 No. 3, pp. 3162–3168.

Mowla, S.J., Farhadi, H.F., Pareek, S., Atwal, J.K., Morris, S.J., Seidah, N.G. and Murphyl, R.A. (2001), "Biosynthesis and Post-translational Processing of the Precursor to Brain-derived Neurotrophic Factor", *Journal of Biological Chemistry*, Vol. 276 No. 16, pp. 12660–12666.

Mu, X., Silos-Santiago, I., Carroll, S.L. and Snider, W.D. (1993), "Neurotrophin receptor genes are expressed in distinct patterns in developing dorsal root ganglia.", *The Journal of Neuroscience*, Vol. 13 No. 9, pp. 4029–4041.

Nagatsu, T., Levitt, M. and Udenfriend, S. (1964), "Tyrosine hydroxylase. The initial step in norepinephrine biosynthesis.", *The Journal of Biological Chemistry*, Vol. 239, pp. 2910–2917.

Nagy, A. (1999), "Cre Recombinase: The Universal Reagent for Genome Tailoring", *Genesis*, Vol. 26 No. 2, pp. 99–109.

Narita, M., Shimizu, S., Ito, T., Chittenden, T., Lutz, R.J., Matsuda, H. and Tsujimoto, Y. (1998), "Bax interacts with the permeability transition pore to induce permeability transition and cytochrome c release in isolated mitochondria", *Proceedings of the National Academy of Sciences*, Vol. 95 No. 25, pp. 14681–14686.

Neame, S.J., Rubin, L.L. and Philpott, K.L. (1998), "Blocking Cytochrome c Activity within Intact Neurons Inhibits Apoptosis", *The Journal of Cell Biology*, Vol. 142 No. 6, pp. 1583–1593.

Nikfarjam, L. and Farzaneh, P. (2012), "Prevention and detection of mycoplasma contamination in cell culture", *Cell Journal*, Vol. 13 No. 4, pp. 203–212.

Nikoletopoulou, V., Lickert, H., Frade, J.M., Rencurel, C., Giallonardo, P., Zhang, L., Bibel, M., et al. (2010), "Neurotrophin receptors TrkA and TrkC cause neuronal death whereasTrkB does not", *Nature*, Vol. 467 No. 7311, pp. 59–63.

Nobel Media Ab. (2018a), "The Nobel Prize in Physiology or Medicine 2002."

Nobel Media Ab. (2018b), "The Nobel Prize in Physiology or Medicine 1986."

Nobes, C.D. and Tolkovsky, A.M. (1995), "Neutralizing Anti-p21ras Fabs Suppress Rat Sympathetic Neuron Survival Induced by NGF, LIF, CNTF and cAMP", *European Journal of Neuroscience*, Vol. 7 No. 2, pp. 344–350.

Nolden, L., Edenhofer, F., Haupt, S., Koch, P., Wunderlich, F.T., Siemen, H. and Brustle, O. (2006), "Site-specific recombination in human embryonic stem cells induced by cell-permeant Cre recombinase.", *Nature Methods*, Vol. 3 No. 6, pp. 461–467.

Obermeier, a, Bradshaw, R. a, Seedorf, K., Choidas, A., Schlessinger, J. and Ullrich, A. (1994), "Neuronal differentiation signals are controlled by nerve growth factor receptor/Trk binding sites for SHC and PLC gamma.", *The EMBO Journal*, Vol. 13 No. 7, pp. 1585–1590.

Obermeier, A., Halfter, H., Wiesmüller, K.H., Jung, G., Schlessinger, J. and Ullrich, A. (1993), "Tyrosine 785 is a major determinant of Trk-substrate interaction.", *The EMBO Journal*, Vol. 12 No. 3, pp. 933–41.

Obermeier, A., Lammers, R., Wiesmuller, K.H., Jung, G., Schlessinger, J. and Ullrich, A. (1993), "Identification of Trk binding sites for SHC and phosphatidylinositol 3'- kinase and formation of a multimeric signaling complex", *The Journal of Biological Chemistry*, Vol. 268 No. 31, pp. 22963–22966.

Ogawa, K., Saito, A., Matsui, H., Suzuki, H., Ohtsuka, S., Shimosato, D., Morishita, Y., et al. (2006), "Activin-Nodal signaling is involved in propagation of mouse embryonic stem cells", *Journal of Cell Science*, Vol. 120 No. 1, pp. 55–65.

Ohki, E.C., Tilkins, M.L., Ciccarone, V.C. and Price, P.J. (2001), "Improving the

transfection efficiency of post-mitotic neurons", *Journal of Neuroscience Methods*, Vol. 112 No. 2, pp. 95–99.

Okamoto, I., Otte, A.P., Allis, C.D., Reinberg, D. and Heard, E. (2004), "Epigenetic dynamics of imprinted X inactivation during early mouse development.", *Science*, Vol. 303 No. 5658, pp. 644–9.

Olarerin-George, A.O. and Hogenesch, J.B. (2015), "Assessing the prevalence of mycoplasma contamination in cell culture via a survey of NCBI's RNA-seq archive", *Nucleic Acids Research*, Vol. 43 No. 5, pp. 2535–2542.

Oorschot, D.E. (1989), "Effect of fluorodeoxyuridine on neurons and non-neuronal cells in cerebral explants", *Experimental Brain Research*, Vol. 78 No. 1, pp. 132–138.

Oppenheim, R.W. (1991), "Cell death during development of the nervous system.", *Annual Review of Neuroscience*, Vol. 14, pp. 453–501.

Oppenheim, R.W., Prevette, D., Tytell, M. and Homma, S. (1990), "Naturally occurring and induced neuronal death in the chick embryo in vivo requires protein and RNA synthesis: Evidence for the role of cell death genes", *Developmental Biology*, Vol. 138 No. 1, pp. 104–113.

Oppenheim, R.W., Qin-Wei, Y., Prevette, D. and Yan, Q. (1992), "Brain-derived neurotrophic factor rescues developing avian motoneurons from cell death", *Nature*, Vol. 360 No. 6406, pp. 755–757.

Pascual, M., Rocamora, N., Acsády, L., Freund, T.F. and Soriano, E. (1998), "Expression of nerve growth factor and neurotrophin-3 mRNAs in hippocampal interneurons: Morphological characterization, levels of expression, and colocalization of nerve growth factor and neurotrophin-3", *Journal of Comparative Neurology*, Vol. 395 No. 1, pp. 73–90.

Patrat, C., Okamoto, I., Diabangouaya, P., Vialon, V., Le Baccon, P., Chow, J. and Heard, E. (2009), "Dynamic changes in paternal X-chromosome activity during imprinted X-chromosome inactivation in mice", *Proceedings of the National Academy of Sciences*, Vol. 106 No. 13, pp. 5198–5203.

Peitz, M., Pfannkuche, K., Rajewsky, K. and Edenhofer, F. (2002), "Ability of the

hydrophobic FGF and basic TAT peptides to promote cellular uptake of recombinant Cre recombinase: A tool for efficient genetic engineering of mammalian genomes", *Proceedings of the National Academy of Sciences*, Vol. 99 No. 7, pp. 4489–4494.

Perez-Pinera, P., García-Suarez, O., Germanà, A., Díaz-Esnal, B., de Carlos, F., Silos-Santiago, I., del Valle, M.E., et al. (2008), "Characterization of sensory deficits in TrkB knockout mice", *Neuroscience Letters*, Vol. 433 No. 1, pp. 43–47.

Del Peso, L., González, V.M. and Núñez, G. (1998), "Caenorhabditis elegans EGL-1 disrupts the interaction of CED-9 with CED- 4 and promotes CED-3 activation", *The Journal of Biological Chemistry*, Vol. 273 No. 50, pp. 33495–33500.

Philippidou, P., Valdez, G., Akmentin, W., Bowers, W.J., Federoff, H.J. and Halegoua, S. (2011), "Trk retrograde signaling requires persistent, Pincher-directed endosomes", *Proceedings of the National Academy of Sciences*, Vol. 108 No. 2, pp. 852–857.

Picard, D. (1994), "Regulation of protein function through expression of chimaeric proteins.", *Current Opinion in Biotechnology*, Vol. 5 No. 5, pp. 511–515.

Piñón, L.G., Middelton, G. and Davies, A.M. (1997), "Bcl-2 is required for cranial sensory neuron survival at defined stages of embryonic development.", *Development*, Vol. 124, pp. 4173–4178.

Pirvola, U., Ylikoski, J., Palgi, J., Lehtonen, E., Arumae, U. and Saarma, M. (1992), "Brain-derived neurotrophic factor and neurotrophin 3 mRNAs in the peripheral target fields of developing inner ear ganglia", *Proceedings of the National Academy of Sciences*, Vol. 89 No. 20, pp. 9915–9919.

Radeke, M.J., Misko, T.P., Hsu, C., Herzenberg, L.A. and Shooter, E.M. (1987), "Gene transfer and molecular cloning of the rat nerve growth factor receptor", *Nature*, England, Vol. 325 No. 6105, pp. 593–597.

Raff, M.C. (1992), "Social controls on cell survival and cell death", *Nature*, Vol. 356 No. 63688, pp. 397–400.

Ran, F.A., Hsu, P.D., Wright, J., Agarwala, V., Scott, D.A. and Zhang, F. (2013), "Genome engineering using the CRISPR-Cas9 system.", *Nature Protocols*, Vol. 8 No. 11, pp. 2281–2308.

Rauskolb, S., Zagrebelsky, M., Dreznjak, A., Deogracias, R., Matsumoto, T., Wiese, S., Erne, B., et al. (2010), "Global deprivation of brain-derived neurotrophic factor in the CNS reveals an area-specific requirement for dendritic growth.", *The Journal of Neuroscience*, Vol. 30 No. 5, pp. 1739–1749.

Razin, S. (2006), "The Genus Mycoplasma and Related Genera (Class Mollicutes)", in Dworkin, M., Falkow, S., Rosenberg, E., Schleifer, K.-H. and Stackebrandt, E. (Eds.), *The Prokaryotes: Volume 4: Bacteria: Firmicutes, Cyanobacteria*, Springer US, New York, NY, pp. 836–904.

Rebuzzini, P., Zuccotti, M., Redi, C.A. and Garagna, S. (2015), "Chromosomal Abnormalities in Embryonic and Somatic Stem Cells.", *Cytogenetic and Genome Research*, Vol. 147 No. 1, pp. 1–9.

Renier, N., Wu, Z., Simon, D.J., Yang, J., Ariel, P. and Tessier-Lavigne, M. (2017), "iDISCO: A Simple, Rapid Method to Immunolabel Large Tissue Samples for Volume Imaging", *Cell*, Vol. 159 No. 4, pp. 896–910.

Robinson, M. (1996), "Timing and regulation of trkB and BDNF mRNA expression in placode-derived sensory neurons and their targets", *European Journal of Neuroscience*, Vol. 8 No. 11, pp. 2399–2406.

Rocamora, N., Pascual, M., Sorianol, E., Ac, L., Lecea, L. De and Freund, F. (1996), "Expression of NGF and NT3 mRNAs in Hippocampal Interneurons Innervated by the GABAergic Septohippocampal Pathway", *The Journal of Neuroscience*, Vol. 16 No. 12, pp. 3991–4004.

Rodriguez-Tebar, A., Dechant, G. and Barde, Y.A. (1990), "Binding of brain-derived neurotrophic factor to the nerve growth factor receptor", *Neuron*, Vol. 4 No. 4, pp. 487–492.

Rosenthal, A., Goeddel, D. V., Nguyen, T., Lewis, M., Shih, A., Laramee, G.R., Nikolics, K., et al. (1990), "Primary structure and biological activity of a novel human neurotrophic factor", *Neuron*, Vol. 4 No. 5, pp. 767–773.

Rottem, S. and Barile, M.F. (1993), "Beware of mycoplasmas.", *Trends in Biotechnology*, Vol. 11 No. 4, pp. 143–151.

Roux, P.P. and Barker, P.A. (2002), "Neurotrophin signaling through the p75 neurotrophin receptor", *Progress in Neurobiology*, Vol. 67 No. 3, pp. 203–233.

Sakahira, H., Enari, M. and Nagata, S. (1998), "Cleavage of CAD inhibitor in CAD activation and DNA degradation during apoptosis.", *Nature*, Vol. 391 No. 6662, pp. 96–99.

Saleh, A., Srinivasula, S.M., Acharya, S., Fishel, R. and Alnemri, E.S. (1999), "Cytochrome c and dATP-mediated oligomerization of Apaf-1 is a prerequisite for procaspase-9 activation", *The Journal of Biological Chemistry*, Vol. 274 No. 25, pp. 17941–17945.

Sanchez-Ortiz, E., Yui, D., Song, D., Li, Y., Rubenstein, J.L., Reichardt, L.F. and Parada, L.F. (2012), "TrkA Gene Ablation in Basal Forebrain Results in Dysfunction of the Cholinergic Circuitry", *The Journal of Neuroscience*, Vol. 32 No. 12, pp. 4065–4079.

Von Schack, D., Casademunt, E., Schweigreiter, R., Meyer, M., Bibel, M. and Dechant, G. (2001), "Complete ablation of the neurotrophin receptor p75NTR causes defects both in the nervous and the vascular system", *Nature Neuroscience*, Vol. 4 No. 10, pp. 977–978.

Schatteman, G.C., Gibbs, L., Lanahan, A.A., Claude, P. and Bothwell, M. (1988), "Expression of NGF receptor in the developing and adult primate central nervous system.", *The Journal of Neuroscience*, Vol. 8 No. 3, pp. 860–873.

Schecterson, L.C. and Bothwell, M. (1994), "Neurotrophin and neurotrophin receptor mRNA expression in developing inner ear", *Hearing Research*, Vol. 73 No. 1, pp. 92–100.

Schimmang, T., Alvarez-Bolado, G., Minichiello, L., Vazquez, E., Giraldez, F., Klein, R. and Represa, J. (1997), "Survival of inner ear sensory neurons in trk mutant mice", *Mechanisms of Development*, Vol. 64 No. 1–2, pp. 77–85.

Schimmang, T., Minichiello, L., Vazquez, E., San Jose, I., Giraldez, F., Klein, R. and Represa, J. (1995), "Developing inner ear sensory neurons require TrkB

and TrkC receptors for innervation of their peripheral targets", *Development*, Vol. 121 No. 10, pp. 3381–3391.

Schnedl, W. (1971), "The karyotype of the mouse", *Chromosoma*, Vol. 35 No. 2, pp. 111–116.

Schneider, R. and Schweiger, M. (1991), "A novel modular mosaic of cell adhesion motifs in the extracellular domains of the neurogenic trk and trkB tyrosine kinase receptors", *Oncogene*, Vol. 6 No. 10, pp. 1807–1811.

Schwenk, F., Baron, U. and Rajewsky, K. (1995), "A cre-transgenic mouse strain for the ubiquitous deletion of loxP-flanked gene segments including deletion in germ cells.", *Nucleic Acids Research*, Vol. 23 No. 24, pp. 5080–1.

Scott, J., Selby, M., Urdea, M., Quiroga, M., Bell, G.I. and Rutter, W.J. (1983), "Isolation and nucleotide sequence of a cDNA encoding the precursor of mouse nerve growth factor", *Nature*, Vol. 302 No. 5908, pp. 538–540.

Scott, S.A. and Davies, A.M. (1990), "Inhibition of protein synthesis prevents cell death in sensory and parasympathetic neurons deprived of neurotrophic factor in vitro", *Journal of Neurobiology*, Vol. 21 No. 4, pp. 630–638.

Sehgal, A., Patil, N. and Chao, M. (1988), "A constitutive promoter directs expression of the nerve growth factor receptor gene.", *Molecular and Cellular Biology*, Vol. 8 No. 8, pp. 3160–7.

Seidah, N.G., Benjannet, S., Pareek, S., Chretien, M. and Murphy, R.A. (1996), "Cellular processing of the neurotrophin precursors of NT3 and BDNF by the mammalian proprotein convertases.", *FEBS Letters*, Vol. 379 No. 3, pp. 247–250.

Selby, M.J., Edwards, R., Sharp, F. and Rutter, W.J. (1987), "Mouse nerve growth factor gene: structure and expression.", *Molecular and Cellular Biology*, Vol. 7 No. 9, pp. 3057–64.

Sendtner, M., Holtmann, B., Kolbeck, R., Thoenen, H. and Barde, Y.A. (1992), "Brain-derived neurotrophic factor prevents the death of motoneurons in newborn rats after nerve section", *Nature*, Vol. 360 No. 6406, pp. 757–759.

Seshagiri, S. and Miller, L.K. (1997), "Caenorhabditis elegans CED-4 stimulates

CED-3 processing and CED-3-induced apoptosis.", *Current Biology*, Vol. 7, pp. 455–460.

Shao, Y., Akmentin, W., Toledo-Aral, J.J., Rosenbaum, J., Valdez, G., Cabot, J.B., Hilbush, B.S., et al. (2002), "Pincher, a pinocytic chaperone for nerve growth factor/TrkA signaling endosomes", *The Journal of Cell Biology*, Vol. 157 No. 4, pp. 679–691.

Shelton, D.L. and Reichardt, L.F. (1986), "Studies on the expression of the beta nerve growth factor (NGF) gene in the central nervous system: level and regional distribution of NGF mRNA suggest that NGF functions as a trophic factor for several distinct populations of neurons", *Proceedings of the National Academy of Sciences*, Vol. 83 No. 8, pp. 2714–2718.

Shorey, M.L. (1909), "The effect of the destruction of peripheral areas on the differentiation of the neuroblasts", *Journal of Experimental Zoology*, Vol. 7 No. 1, pp. 25–63.

Silva, J., Barrandon, O., Nichols, J., Kawaguchi, J., Theunissen, T.W. and Smith, A. (2008), "Promotion of reprogramming to ground state pluripotency by signal inhibition", *PLoS Biology*, Vol. 6 No. 10, pp. 2237–2247.

Skaper, S.D., Pollock, M. and Facci, L. (2001), "Mast cells differentially express and release active high molecular weight neurotrophins", *Molecular Brain Research*, Vol. 97 No. 2, pp. 177–185.

Smeyne, R.J., Klein, R., Schnapp, A., Long, L.K., Bryant, S., Lewin, A., Lira, S.A., et al. (1994), "Severe sensory and sympathetic neuropathies in mice carrying a disrupted Trk/NGF receptor gene.", *Nature*, Vol. 368 No. 6468, pp. 246–249.

Smith, A.G. (1991), "Culture and differentiation of embryonic stem cells", *Journal of Tissue Culture Methods*, Vol. 13 No. 2, pp. 89–94.

Smith, A.G., Heath, J.K., Donaldson, D.D., Wong, G.G., Moreau, J., Stahl, M. and Rogers, D. (1988), "Inhibition of pluripotential embryonic stem cell differentiation by purified polypeptides", *Nature*, Vol. 336 No. 6200, pp. 688–690.

Smith, A.G. and Hooper, M.L. (1987), "Buffalo rat liver cells produce a diffusible

activity which inhibits the differentiation of murine embryonal carcinoma and embryonic stem cells", *Developmental Biology*, Vol. 121 No. 1, pp. 1–9.

Sokolova, I.A., Vaughan, A.T.M. and Khodarev, N.N. (1998), "Mycoplasma infection can sensitize host cells to apoptosis through contribution of apoptotic-like endonuclease(s)", *Immunology and Cell Biology*, Vol. 76 No. 6, pp. 526–534.

Soppet, D., Escandon, E., Maragos, J., Middlemas, D.S., Raid, S.W., Blair, J., Burton, L.E., et al. (1991), "The neurotrophic factors brain-derived neurotrophic factor and neurotrophin-3 are ligands for the trkB tyrosine kinase receptor", *Cell*, Vol. 65 No. 5, pp. 895–903.

Soriano, P. (1999), "Generalized lacZ expression with the ROSA26 Cre reporter strain.", *Nature Genetics*, Vol. 21 No. 1, pp. 70–71.

Squinto, S.P., Stitt, T.N., Aldrich, T.H., Davis, S., Blanco, S.M., RadzieJewski, C., Glass, D.J., et al. (1991), "trkB encodes a functional receptor for brain-derived neurotrophic factor and neurotrophin-3 but not nerve growth factor", *Cell*, Vol. 65 No. 5, pp. 885–893.

Stefanis, L., Park, D.S., Yan, C.Y.I., Farinelli, S.E., Troy, C.M., Shelanski, M.L. and Greene, L.A. (1996), "Induction of CPP32-like activity in PC12 cells by withdrawal of trophic support: Dissociation from apoptosis", *The Journal of Biological Chemistry*, Vol. 271 No. 48, pp. 30663–30671.

Stephens, R.M., Loeb, D.M., Copeland, T.D., Pawson, T., Greene, L.A. and Kaplan, D.R. (1994), "Trk receptors use redundant signal transduction pathways involving SHC and PLC-γ1 to mediate NGF responses", *Neuron*, Vol. 12 No. 3, pp. 691–705.

Sterio, D.C. (1984), "The unbiased estimation of number and sizes of arbitrary particles using the disector", *Journal of Microscopy*, Vol. 134 No. 2, pp. 127–136.

Strohmaier, C., Carter, B.D., Urferl, R., Barde, Y.-A. and Dechant2, G. (1996), "A splice variant of the neurotrophin receptor trkB with increased specificity for brain-derived neurotrophic factor", *The EMBO Journal*, Vol. 1513, pp. 3332–

3337.

Sulston, J.E., Schierenberg, E., White, J.G. and Thomson, J.N. (1983), "The embryonic cell lineage of the nematode Caenorhabditis elegans", *Developmental Biology*, Vol. 100 No. 1, pp. 64–119.

Sulston, J.E. and White, J.G. (1980), "Regulation and cell autonomy during postembryonic development of Caenorhabditis elegans", *Developmental Biology*, Vol. 78 No. 2, pp. 577–597.

Sun, L. and Wang, X. (2014), "A new kind of cell suicide: Mechanisms and functions of programmed necrosis", *Trends in Biochemical Sciences*, Vol. 39 No. 12, pp. 587–593.

Suter, U., Heymach, J. V and Shooter, E.M. (1991), "Two conserved domains in the NGF propeptide are necessary and sufficient for the biosynthesis of correctly processed and biologically active NGF.", *The EMBO Journal*, Vol. 10 No. 9, pp. 2395–400.

Svendsen, C.N., Kew, J.N., Staley, K. and Sofroniew, M.V. (1994), "Death of developing septal cholinergic neurons following NGF withdrawal in vitro: protection by protein synthesis inhibition", *The Journal of Neuroscience*, Vol. 14 No. 1, pp. 75–87.

Takagi, N. and Sasaki, M. (1975), "Preferential inactivation of the paternally derived X chromosome in the extraembryonic membranes of the mouse", *Nature*, Vol. 256 No. 5519, pp. 640–642.

Takeuchi, O., Sato, S., Horiuchi, T., Hoshino, K., Takeda, K., Dong, Z., Modlin, R.L., et al. (2002), "Cutting Edge: Role of Toll-Like Receptor 1 in Mediating Immune Response to Microbial Lipoproteins", *The Journal of Immunology*, Vol. 169 No. 1, pp. 10–14.

Tamm, C., Pijuan Galitó, S. and Annerén, C. (2013), "A Comparative Study of Protocols for Mouse Embryonic Stem Cell Culturing", *PLOS ONE*, Vol. 8 No. 12, p. e81156.

Tan, S.-S., Williams, E.A. and Tam, P.P.L. (1993), "X-chromosome inactivation occurs at different times in different tissues of the post-implantation mouse

embryo", *Nature Genetics*, Vol. 3 No. 2, pp. 170–174.

Tauszig-Delamasure, S., Yu, L.-Y., Cabrera, J.R., Bouzas-Rodriguez, J., Mermet-Bouvier, C., Guix, C., Bordeaux, M.-C., et al. (2007), "The TrkC receptor induces apoptosis when the dependence receptor notion meets the neurotrophin paradigm.", *Proceedings of the National Academy of Sciences*, Vol. 104 No. 33, pp. 13361–13366.

Teng, K.K., Felice, S., Kim, T. and Hempstead, B.L. (2010), "Understanding proneurotrophin actions: Recent advances and challenges", *Developmental Neurobiology*, Vol. 70 No. 5, pp. 350–359.

Tessarollo, L. (2004), "NT-3 Replacement with Brain-Derived Neurotrophic Factor Redirects Vestibular Nerve Fibers to the Cochlea", *Journal of Neuroscience*, Vol. 24 No. 10, pp. 2575–2584.

Tessarollo, L., Tsoulfas, P., Donovan, M.J., Palko, M.E., Blair-Flynn, J., Hempstead, B.L. and Parada, L.F. (1997), "Targeted deletion of all isoforms of the trkC gene suggests the use of alternate receptors by its ligand neurotrophin-3 in neuronal development and implicates trkC in normal cardiogenesis.", *Proceedings of the National Academy of Sciences*, Vol. 94 No. 26, pp. 14776–14781.

Tessarollo, L., Vogel, K.S., Palko, M.E., Reid, S.W. and Parada, L.F. (1994), "Targeted mutation in the neurotrophin-3 gene results in loss of muscle sensory neurons.", *Proceedings of the National Academy of Sciences*, Vol. 91 No. 25, pp. 11844–11848.

Theiler, K. (2014), *The House Mouse: Atlas of Embryonic Development*, Springer.

Tian, Y., James, S., Zuo, J., Fritzsch, B. and Beisel, K.W. (2006), "Conditional and inducible gene recombineering in the mouse inner ear", *Brain Research*, Vol. 1091 No. 1, pp. 243–254.

Timmusk, T., Belluardo, N., Metsis, M. and Persson, H. (1993), "Widespread and Developmentally Regulated Expression of Neurotrophin-4 mRNA in Rat Brain and Peripheral Tissues", *European Journal of Neuroscience*, Vol. 5 No. 6, pp. 605–613.

Timmusk, T., Palm, K., Metsis, M., Reintam, T., Paalme, V., Saarma, M. and Persson, H. (1993), "Multiple promoters direct tissue-specific expression of the rat BDNF gene", *Neuron*, Vol. 10 No. 3, pp. 475–489.

Tojo, H., Kaisho, Y., Nakata, M., Matsuoka, K., Kitagawa, M., Abe, T., Takami, K., et al. (1995), "Targeted disruption of the neurotrophin-3 gene with lacZ induces loss of trkC-positive neurons in sensory ganglia but not in spinal cords", *Brain Research*, Vol. 669 No. 2, pp. 163–175.

Trent, C., Tsuing, N. and Horvitz, H.. (1983), "Egg-laying defective mutants of the nematode Caenorhabditis elegans.", *Genetics*, Vol. 104 No. 4, pp. 619–647.

Troy, C.M., Stefanis, L., Prochiantz, A., Greene, L.A. and Shelanski, M.L. (1996), "The contrasting roles of ICE family proteases and interleukin-1 beta in apoptosis induced by trophic factor withdrawal and by copper/zinc superoxide dismutase down-regulation.", *Proceedings of the National Academy of Sciences*, Vol. 93 No. 11, pp. 5635–5640.

Tsujimoto, Y., Cossman, J., Jaffe, E. and Croce, C.M. (1985), "Involvement of the bcl-2 gene in human follicular lymphoma", *Science*, Vol. 228 No. 4706, pp. 1440–1443.

Tucker, K.L., Meyer, M. and Barde, Y. a. (2001), "Neurotrophins are required for nerve growth during development.", *Nature Neuroscience*, Vol. 4 No. 1, pp. 29–37.

Ultsch, M.H., Wiesmann, C., Simmons, L.C., Henrich, J., Yang, M., Reilly, D., Bass, S.H., et al. (1999), "Crystal structures of the neurotrophin-binding domain of TrkA, TrkB and TrkC", *Journal of Molecular Biology*, Vol. 290 No. 1, pp. 149–159.

Urfer, R., Tsoulfas, P., O'Connell, L., Shelton, D.L., Parada, L.F. and Presta, L.G. (1995), "An immunoglobulin-like domain determines the specificity of neurotrophin receptors.", *The EMBO Journal*, Vol. 14 No. 12, pp. 2795–2805.

Valdez, G., Philippidou, P., Rosenbaum, J., Akmentin, W., Shao, Y. and Halegoua, S. (2007), "Trk-signaling endosomes are generated by Rac-dependent macroendocytosis", *Proceedings of the National Academy of Sciences*, Vol. 104

No. 30, pp. 12270–5.

Valenzuela, D.M., Maisonpierre, P.C., Glass, D.J., Rojas, E., Nuñez, L., Kong, Y.,
Gies, D.R., et al. (1993), "Alternative forms of rat TrkC with different
functional capabilities", *Neuron*, Vol. 10 No. 5, pp. 963–974.

Vaux, D.L., Cory, S. and Adams, J.M. (1988), "Bcl-2 gene promotes haemopoietic
cell survival and cooperates with c-myc to immortalize pre-B cells", *Nature*,
Vol. 335 No. 6189, pp. 440–442.

Vaux, D.L. and Korsmeyer, S.J. (1999), "Cell death in development", *Cell*, Vol. 96
No. 2, pp. 245–254.

Wang, Z.Q., Kiefer, F., Urbánek, P. and Wagner, E.F. (1997), "Generation of
completely embryonic stem cell-derived mutant mice using tetraploid blastocyst
injection", *Mechanisms of Development*, Vol. 62 No. 2, pp. 137–145.

Watson, F.L., Porcionatto, M.A., Bhattacharyya, A., Stiles, C.D. and Segal, R.A.
(1999), "TrkA glycosylation regulates receptor localization and activity",
Journal of Neurobiology, Vol. 39 No. 2, pp. 323–336.

Wetmore, C. and Olson, L. (1995), "Neuronal and nonneuronal expression of
neurotrophins and their receptors in sensory and sympathetic ganglia suggest
new intercellular trophic interactions", *Journal of Comparative Neurology*, Vol.
353 No. 1, pp. 143–159.

Wheeler, E.F. and Bothwell, M. (1992), "Spatiotemporal patterns of expression of
NGF and the low-affinity NGF receptor in rat embryos suggest functional roles
in tissue morphogenesis and myogenesis.", *The Journal of Neuroscience*, Vol.
12 No. 3, pp. 930–45.

White, F.A., Keller-Peck, C.R., Knudson, C.M., Korsmeyer, S.J. and Snider, W.D.
(1998), "Widespread elimination of naturally occurring neuronal death in Bax-
deficient mice.", *The Journal of Neuroscience*, Vol. 18 No. 4, pp. 1428–39.

White, K., Grether, M.E., Abrams, J.M., Young, L., Farrell, K. and Steller, H.
(1994), "Genetic control of programmed cell death in Drosophila", *Science*,
Vol. 264 No. 5159, p. 677 LP-683.

Wiesmann, C. and de Vos, A.M. (2001), "Nerve growth factor: structure and

function.", *Cellular and Molecular Life Sciences*, Vol. 58 No. 5–6, pp. 748–759.

Williams, R.L., Hilton, D.J., Pease, S., Willson, T. a, Stewart, C.L., Gearing, D.P., Wagner, E.F., et al. (1988), "Myeloid leukaemia inhibitory factor maintains the developmental potential of embryonic stem cells.", *Nature*, Vol. 336 No. 6200, pp. 684–687.

Wilson, I.A., Niman, H.L., Houghten, R.A., Cherenson, A.R., Connolly, M.L. and Lerner, R.A. (1984), "The structure of an antigenic determinant in a protein", *Cell*, Vol. 37 No. 3, pp. 767–778.

Windisch, J.M., Marksteiner, R. and Schneider, R. (1995), "Nerve growth factor binding site on TrkA mapped to a single 24-amino acid leucine-rich motif", *The Journal of Biological Chemistry*, Vol. 270 No. 47, pp. 28133–28138.

Wolf, B.B., Schuler, M., Echeverri, F. and Green, D.R. (1999), "Caspase-3 Is the Primary Activator of Apoptotic DNA Fragmentation via DNA Fragmentation Factor-45/Inhibitor of Caspase-activated DNase Inactivation", *The Journal of Biological Chemistry*, Vol. 274 No. 43, pp. 30651–30656.

Wright, K.M., Vaughn, A.E. and Deshmukh, M. (2007), "Apoptosome dependent caspase-3 activation pathway is non-redundant and necessary for apoptosis in sympathetic neurons.", *Cell Death and Differentiation*, Vol. 14 No. 3, pp. 625–633.

Wu, C.-Y., Whye, D., Mason, R.W. and Wang, W. (2012), "Efficient Differentiation of Mouse Embryonic Stem Cells into Motor Neurons", *Journal of Visualized Experiments*, No. 64, p. 3813.

Xue, D., Shaham, S. and Horvitz, H.R. (1996), "The Caenorhabditis elegans cell-death protein CED-3 is a cysteine protease with substrate specificities similar to those of the human CPP32 protease", *Genes and Development*, Vol. 10 No. 9, pp. 1073–1083.

Yaar, M., Zhai, S., Pilch, P.F., Doyle, S.M., Eisenhauer, P.B., Fine, R.E. and Gilchrest, B.A. (1997), "Binding of β-amyloid to the p75 neurotrophin receptor induces apoptosis: A possible mechanism for Alzheimer's disease", *Journal of*

Clinical Investigation, Vol. 100 No. 9, pp. 2333–2340.

Yan, H. and Chao, M. V. (1991), "Disruption of cysteine-rich repeats of the p75 nerve growth factor receptor leads to loss of ligand binding", *The Journal of Biological Chemistry*, Vol. 266 No. 18, pp. 12099–12104.

Yan, Q., Johnson, E.M., Bray, G., Aguayo, A. and Aguayo, A. (1988), "An immunohistochemical study of the nerve growth factor receptor in developing rats.", *The Journal of Neuroscience*, Vol. 8 No. 9, pp. 3481–98.

Yang, J., Liu, X., Bhalla, K., Kim, C.N., Ibrado, A.M., Cai, J., Peng, T.I., et al. (1997), "Prevention of apoptosis by Bcl-2: Release of cytochrome c from mitochondria blocked", *Science*, Vol. 275 No. 5303, pp. 1129–1132.

Yao, R. and Cooper, G.M. (1995), "Requirement for phosphatidylinositol-3 kinase in the prevention of apoptosis by nerve growth factor", *Science*, Vol. 267 No. 5206, pp. 2003–2006.

Ying, Q.L. and Smith, A. (2017), "The Art of Capturing Pluripotency: Creating the Right Culture", *Stem Cell Reports*, Vol. 8 No. 6, pp. 1457–1464.

Ylikoski, J., Pirvola, U., Moshnyakov, M., Palgi, J., Arumäe, U. and Saarma, M. (1993), "Expression patterns of neurotrophin and their receptor mRNAs in the rat inner ear", *Hearing Research*, Vol. 65 No. 1–2, pp. 69–78.

Young, L., Sung, J., Stacey, G. and Masters, J.R. (2010), "Detection of Mycoplasma in cell cultures", *Nature Protocols*, Vol. 5 No. 5, pp. 929–934.

Yuan, J. and Horvitz, H.R. (1990), "The Caenorhabditis elegans genes ced-3 and ced-4 act cell autonomously to cause programmed cell death", *Developmental Biology*, Vol. 138 No. 1, pp. 33–41.

Yuan, J., Shaham, S., Ledoux, S., Ellis, H.M. and Horvitz, H.R. (1993), "The C. elegans cell death gene ced-3 encodes a protein similar to mammalian interleukin-1β-converting enzyme", *Cell*, Vol. 75 No. 4, pp. 641–652.

Zakeri, Z. and Lockshin, R.A. (2008), "Cell death: History and future", *Advances in Experimental Medicine and Biology*, Vol. 615, pp. 1–11.

Zambrowicz, B.P., Imamoto, A., Fiering, S., Herzenberg, L.A., Kerr, W.G. and

Soriano, P. (1997), "Disruption of overlapping transcripts in the ROSA geo 26 gene trap strain leads to widespread expression of -galactosidase in mouse embryos and hematopoietic cells", *Proceedings of the National Academy of Sciences*, Vol. 94 No. 8, pp. 3789–3794.

Zhang, M., Cheng, L., Jia, Y., Liu, G., Li, C., Song, S., Bradley, A., et al. (2016), "Aneuploid embryonic stem cells exhibit impaired differentiation and increased neoplastic potential", *The EMBO Journal*, Vol. 35 No. 21, pp. 2285–2300.

Zheng, J., Shen, W.H., Lu, T.J., Zhou, Y., Chen, Q., Wang, Z., Xiang, T., et al. (2008), "Clathrin-dependent endocytosis is required for TrkB-dependent Akt-mediated neuronal protection and dendritic growth", *The Journal of Biological Chemistry*, Vol. 283 No. 19, pp. 13280–13288.

Zheng, M., Jiao, L., Tang, X., Xiang, X., Wan, X., Yan, Y., Li, X., et al. (2017), "Tau haploinsufficiency causes prenatal loss of dopaminergic neurons in the ventral tegmental area and reduction of transcription factor orthodenticle homeobox 2 expression", *FASEB Journal*, Vol. 31 No. 8, pp. 3349–3358.

Zhou, X.F., Chie, E.T. and Rush, R.A. (1998), "Distribution of brain-derived neurotrophic factor in cranial and spinal ganglia", *Experimental Neurology*, Vol. 149 No. 1, pp. 237–242.

Zlotkowski, K., Pierce-Shimomura, J. and Siegel, D. (2013), "Small-Molecule-Mediated Axonal Branching in Caenorhabditis elegans", *ChemBioChem*, Vol. 14 No. 3, pp. 307–310.

Zotti, T., Scudiero, I., Vito, P. and Stilo, R. (2017), "The Emerging Role of TRAF7 in Tumor Development", *Journal of Cellular Physiology*, Vol. 232 No. 6, pp. 1233–1238.

Zou, H., Henzel, W.J., Liu, X., Lutschg, A. and Wang, X. (1997), "Apaf-1, a human protein homologous to C. elegans CED-4, participates in cytochrome c-dependent activation of caspase-3", *Cell*, Vol. 90 No. 3, pp. 405–413.

Zou, H., Li, Y., Liu, X. and Wang, X. (1999), "An APAf-1 · cytochrome C multimeric complex is a functional apoptosome that activates procaspase-9", *The Journal of Biological Chemistry*, Vol. 274 No. 17, pp. 11549–11556.